Effect of Dairy Structures on Gastric Behaviour and Nutrient Digestion Kinetics using a Semi-Dynamic Model

Ana-Isabel Mulet-Cabero

A thesis submitted for the degree of Doctor of Philosophy to the University of East Anglia, for research conducted at the Quadram Institute Bioscience and Teagasc Food Research Centre.

Quadram Institute Bioscience

December 2018

Preface

This thesis was submitted to the University East of Anglia (Norwich, UK) for the degree of Doctor of Philosophy. The work presented herein was undertaken between the former Institute of Food Research (Norwich, UK) from January 2015 to February 2016, Moorepark-Teagasc Food Research Centre (Fermoy, Cork Co., Ireland) from March 2016 to January 2018, the School of Food Science and Nutrition at the University of Leeds (Leeds, UK) from October 2017 to December 2017 and Quadram Institute Bioscience (formerly the Institute of Food Research) from February 2018 to December 2018.

Abstract

Dairy products, due to manufacturing processes, exhibit an array of possible structures at different length scales and are associated with beneficial nutritional and health effects. However, to date there is very little mechanistic understanding of such links. Unravelling the fate of food in the gastrointestinal tract is essential to better understand the health effects of food.

The investigation of different dairy structured matrices was performed using a semi-dynamic model of gastric digestion, developed in this thesis, to simulate the main dynamics of the adult stomach, i.e. gradual gastric acidification, fluid secretion and emptying. It was validated with two dairy matrices obtaining a similar gastric behaviour compared to the corresponding *in vivo* digestion.

The 'fast' and 'slow' digestion kinetics of whey proteins and caseins were shown to be due to their behaviour in the stomach, presenting soluble aggregates and solid, firm coagulation, respectively, which was linked to a higher *ex vivo* Leu absorption at early and late stages of digestion. The gastric restructuring of caseins was modulated by changing the whey protein to casein ratio, addition of lipid, and processing by heating and homogenisation. The most intensive processing resulted in weaker, fragmented coagulation, leading to quicker kinetics of nutrient emptying and rapid protein hydrolysis. The latter was linked to an easier access of pepsin into the weaker structure. The modulation of nutrient digestion kinetics was also obtained by comparing specific dairy macrostructures of semi-solid versus liquid through different gastric behaviours, which could be linked to the satiety responses observed *in vivo*.

This thesis clearly demonstrated the key role of the gastric phase on nutrient bioaccessibility, which can be associated to physiological responses of dairy products. The modulation of gastric behaviour should be further studied and can be exploited to develop food structures with improved and/or tailored biofunctional properties addressing health/nutritional requirements.

Acknowledgements

Firstly, I would like to sincerely thank my supervisors Prof Alan Mackie, Dr André Brodkorb and Prof Pete Wilde for their support and expert guidance as well as motivation and patience throughout my PhD. Their office door was always open whenever I had a question/concern and each one had a key role in different moments of my PhD. I truly think I was very lucky to have them in this process. Secondly, I would like to acknowledge the financial support, this work has funded by the Irish Dairy Levy Research Trust (project number MDDT6261) under Teagasc Walsh Fellowship and BBSRC in the UK (grant BB/J004545/1). The three-month placement at the University of Leeds was funded by the Short-Term Overseas Training Award of the Walsh Fellowship Programme.

My PhD journey gave me the opportunity, apart from performing about 200 gastric digestions, to live in two countries and work with four different lab groups, which allowed me the possibility to meet lovely people who helped me in many ways. I would like to thank everyone who helped me directly or indirectly even though it is not possible to mention every single person in here. From my first year of PhD working in the Mackie's lab at IFR, I would like to acknowledge Neil Rigby for his valuable help in the lab, Balazs Bajka for his support with the confocal and Mike Ridout for training/assistance in several instruments. Outside the lab I would like to mention my Biorefinary guys (Richardo Montull, Ian Wood, Sam Collins and Adam Elliston), I will not forget our breaks full of laughter, and Enri Garcia, who shared a lot of things with me including the passion for cows. I would like to thank Adam Elliston for his valuable help and moral support during the thesis writing and for the rest of my crazy activities I was involved during my PhD. Regarding my period in Ireland, I would like to thank the Brodkorb's group for their support in the lab and I acknowledge Martina O'Brien for her assistance with the LECO and the team of Moorepark Technology Ltd. for their help in the pilot plant. A special thanks to Raul Cabrera, Laura Saez and Bea Mesa, who were my big emotional support there. In my placement at University of Leeds, I am grateful to Amelia Torcello who showed me all about Ussing chambers and Alan Mackie for allowing me to work in his lab (once more). Back in Norwich, in the Wilde group, I would like to thank Louise Salt, Raffaele Colosimo, Kathrin Haider and Romina Bashllari for their moral support and thanks for taking me out of the cell for our Friday's nights out. I would like to acknowledge Shikha Saha for her help with the LC-MS analysis and Grant Calder for his assistance with the confocal, and Perla Troncoso and Marianne Defernez for spending some time with my data. I thank Natalia Perez and Yvonne Gunning for their moral support and attention.

And finally, last but by no means least, I would like to thank my friends and family members back in Spain who have supported me along the way. With special mention to Eric Miguel, my best friend and general life counsellor, because he has always been there through everything with me. I am very grateful to my family, in particular my sister Reyes and brother Ximo for their invaluable support. I would like to express my endless gratitude to my parents, for their continuous encouragement throughout my thesis and my life in general as well as their patience when they had to bear my moments of stress and frustration. Thanks for all the sacrifices that you have made on my behalf. Moltes gràcies papà i mamà, vos vull molt!

<div align="center">Thanks/gracias/gràcies</div>

Outputs from this Project

Peer-reviewed articles:

- **Mulet-Cabero, A. I**., Mackie, A. R., Wilde, P. J., Fenelon, M. A., & Brodkorb, A. (2019). Structural mechanism and kinetics of in vitro gastric digestion are affected by process-induced changes in bovine milk. *Food Hydrocolloids*, *86*, 172-183.

- **Mulet-Cabero, A.-I**., Rigby, N. M., Brodkorb, A., & Mackie, A. R. (2017). Dairy food structures influence the rates of nutrient digestion through different *in vitro* gastric behaviour. *Food Hydrocolloids*, 67, 63-73.

- Ferreira-Lazarte, A., Montilla, A., **Mulet-Cabero, A.-I**., Rigby, N., Olano, A., Mackie, A., & Villamiel, M. (2017). Study on the digestion of milk with prebiotic carbohydrates in a simulated gastrointestinal model. *Journal of Functional Foods*, 33, 149-154.

- **Mulet-Cabero, A. I**, *et al.* (2019). A standardised semi-dynamic *in vitro* digestion method suitable for food–an international consensus (in preparation).

- **Mulet-Cabero, A. I**., Mackie, A. R., Brodkorb, A & Wilde, P. J. (2019). Impact of casein and whey protein ratio and lipid content on *in vitro* digestion and *ex vivo* absorption (in preparation).

- **Mulet-Cabero, A. I**., Mackie, A. R., Brodkorb, A & Wilde, P. J. (2019) Dairy structures and physiological responses: a matter of gastric digestion (in preparation).

Oral presentations in international conferences:

Jun 2018   3rd Food Structure and functionality forum symposium and 3rd IDF symposium on microstructure of dairy products, Montreal, Canada.

Oct 2017   10th NIZO Dairy Conference, Arnhem, The Netherlands.

Apr 2017   5th International Conference on Food Digestion, Rennes, France.

Poster presentations in international conferences:

Nov 2018   32nd EFFoST International Conference, Nantes, France.

Apr 2018   17th Food Colloids Conference, Leeds, UK.

Apr 2017   Society Dairy Technology Spring 2017 Conference, Cork, Ireland. (Best Poster Award)

Dec 2015   44th Annual Food Research Conference, Fermoy, Ireland.

Table of Contents

List of Figures

Figure 7.7 Images of Semi-Solid (A-B) and Liquid (C-D) samples in the initial state (A and C) and after 111.1 min (B) and after 110.3 min (D) of gastric digestion in the semi-dynamic gastric model using pepsin and gastric lipase. Representation of microstructure in the liquid sample before gastric digestion (E) and, the upper cream layer (F) and the bottom aqueous layer (G) after gastric digestion. Proteins and lipids

List of Tables

List of Equations

List of Abbreviations

α-La	α-Lactalbumin
β-Lg	β-Lactoglobulin
AA	Amino Acid
BCAA	Branch Chain Amino Acid
CVD	Cardiovascular Disease
CCK	Cholescystokinin
$d_{3,2}$	Surface-weighted average diameter
$d_{4,3}$	Volume average diameter
DAG	Diacylglycerol
DIAAS	Digestible indispensable AA Score
DGM	Dynamic Gastric Model
EAA	Essential Amino Acid
EC	Exchange Chromatography
EDTA	Ethylene Diamine Tetra Acetic acid
FAMES	Fatty Acid Methyl Esters
FFA	Free Fatty Acid
FID	Flame Ionisation Detector
FCS	Fluorescence Correlation Spectroscopy
FRAP	Fluorescence Recovery after Photobleaching
FTIC	Fluorescein isothiocyanate
GC	Gas Spectrophotometry
GE	Gastric Emptying
GIP	Gastric inhibitory Polypeptide
GI	Gastrointestinal
GLP-1	Glucagon-like-peptide-1

HPLC	High Pressure Liquid Chromatography
HGL	Human Gastric Lipase
HGS	Human Gastric Simulator
HCl	Hydrochloric Acid
IFR	Institute of Food Research
IS	Internal Standard
LDL	Low-density lipoprotein
MRI	Magnetic Resonance Imaging
MS	Mass Spectrophotometry
MFGM	Milk Fat Globule Membrane
MPC	Milk Protein Concentrate
MAG	Monoacylglycerol
MPS	Muscle Protein Synthesis
MW	Molecular weight
$NaHCO_3$	Sodium Bicarbonate
NaCl	Sodium Chloride
NaOH	Sodium Hydroxide
N	Nitrogen
NMR	Nuclear Magnetic Resonance
OPA	o-Phthaldialdehyde
PYY	Peptide YY
PDCAAS	Protein Digestibility -corrected AA score
QIB	Quadram Institute Bioscience
RGE	Rabbit Gastric Extract
RPLC	Reversed Phase Liquid Chromatography
SEM	Scanning Electron Microscopy

SFA	Saturated Fatty Acid
SGF	Simulated Gastric Fluid
SIF	Simulated Intestinal Fluid
SSF	Simulated Salivary Fluid
SMP	Skim Milk Powder
SDS-PAGE	Sodium Dodecyl Sulphate-Polyacrylamide Gel Electrophoresis
TAG	Triacylglycerol
TCA	Trichloracetic acid
UHT	Ultra-High Temperature
UEA	University East of Anglia
UV	Ultraviolet
WPI	Whey Protein Isolate

Amino Acid Symbol	Amino Acid Full Name
Ala	Alanine
Arg	Arginine
Asn	Asparagine
Asp	Aspartic acid
Cys	Cysteine
Gln	Glutamine
Glu	Glutamic acid
Gly	Glycine
His	Histidine
Ile	Isoleucine
Leu	Leucine
Lys	Lysine
Met	Methionine
Phe	Phenylalanine
Thr	Threonine
Trp	Tryptophan
Tyr	Tyrosine
Pro	Proline
Ser	Serine
Val	Valine

xxx

Chapter 1

Introduction and Literature Review

1.1 Introduction

The health properties of foods are conventionally assessed according to their individual nutrient composition. However, there is growing evidence showing that digestion of nutrients and postprandial responses are strongly affected by the structure (or matrix) of food, which is defined as the arrangement of food constituents and their interactions at multiple spatial length scales (Parada *et al.*, 2007), see Figure 1.1. The structure of food either occurs naturally or is created or destroyed by processing and preparation, which might play a critical role in bioaccessibility and bioavailability of nutrients. Bioaccessibility is defined as the amount of ingested nutrient that is available for absorption whereas bioavailability is the proportion of an ingested nutrient that is made available for exerting a defined physiological action in cells (Parada *et al.*, 2007).

Food structure can, then, control physiological responses, for instance, Gebauer *et al.* (2016) showed that the amount of energy absorbed from almonds was dependent on the form in which they were consumed (whole natural almonds; whole roasted almonds; chopped almonds; almond butter). The metabolisable energy measured in healthy volunteers indicated that the whole natural almonds presented the lowest value followed by the whole roasted almonds, chopped almonds and almond butter. Moreover, these values were significantly lower than predicted using Atwater factors, which estimate the energy-yielding substrates, except for the almond butter that was similar. This is one example illustrating that food is more than the sum of its nutrients. However, the rate-determining processes and the underlying mechanisms of the link between food properties and health outcomes remain unclear, which must be addressed by the understanding of how food structures interact within the gastrointestinal (GI) tract (Dupont *et al.*, 2017). This knowledge will provide further insight for the design of future functional foods with specific behaviour of digestion and subsequent physiological outcomes (Norton *et al.*, 2014).
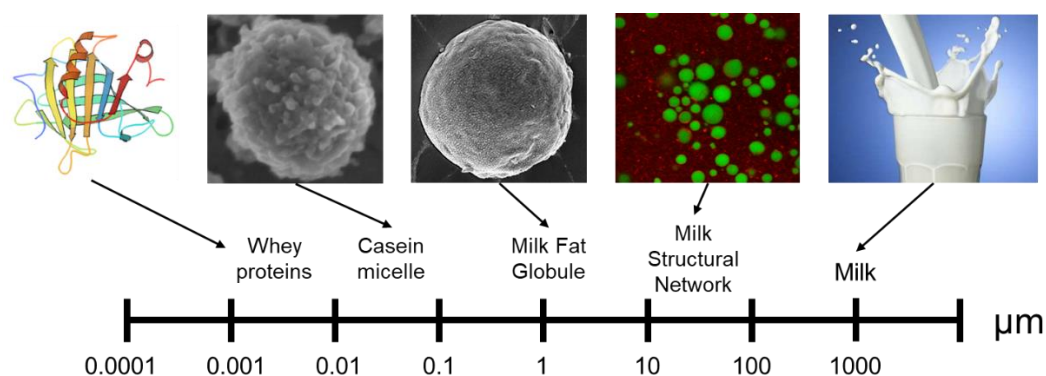
Figure 1.1 Structural elements and relevant length scales of milk, as an example of the concept of food matrix, i.e. the arrangement and interactions of structural elements at multiscales. Electron micrographs of an individual casein micelle and milk fat globule are from Dalgleish *et al.* (2004) and Luo *et al.* (2014), respectively.

Much attention has been paid to strategies to tackle the worldwide obesity problem and, in that context, appetite regulation should be investigated. The main processes governing appetite are satiation and satiety; satiation refers to the feeling of fullness within an eating occasion that leads to meal termination whereas satiety refers to the feeling of fullness for a period until the following eating occasion. These processes are controlled by a combination of neural and humoral signals in response to food in the GI tract. The gastric distension induces neural signalling resulting in short-lasting feeling of satiation and appetite reduction (Janssen *et al.*, 2011). When food enters the small intestine, the nutrient composition is sensed, and hormones are secreted. The main appetite related gut hormones are cholecystokinin (CCK), peptide YY (PYY) and glucagon-like peptide-1 (GLP-1), which can modulate satiety by reducing appetite and altering GI processes. For instance, the presence of mainly lipid and protein in the duodenum is known to stimulate CCK, which in turn, slows gastric emptying (GE) and reduce appetite (Karhunen *et al.*, 2008). This duodenal feedback is mainly controlled by the caloric density of digesta, therefore sufficient nutrients need to be emptied to modulate a given gastric volume. However, the persistence of this effect depends on the hormone, and macronutrient type and source. Therefore, the satiety signals need to be prolonged to induce that effect of satiety and fullness for longer, which could be obtained by the slow nutrient breakdown and might benefit obese/overweight people. Furthermore, more efficient nutrient release, in particular protein, would be useful for athletes; depending on sport characteristics, fast protein digestion and uptake are needed for strength training and fast recovery, whereas more constant amino acid absorption is sought for endurance exercise. In the same way, elderly individuals will benefit from foods with fast amino acid uptake to enhance muscle synthesis, counteracting sarcopenia. Hence, different strategies need to be

developed in order to optimise kinetics of nutrient release and uptake to tailor nutritional needs (Norton *et al.*, 2014). Moreover, proteins have been recognised to have a higher satiating power than lipids and carbohydrates (Veldhorst *et al.*, 2008), and this effect differs depending on the source of protein (Anderson *et al.*, 2004).

The physico-chemical characteristics of food components and the whole matrix impact how individual components interact and behave within the GI tract. Research has mainly focussed on the small intestine digestion in order to control nutrient digestion using different mechanisms such as the ileal break (Maljaars *et al.*, 2008) by manipulating interfacial composition of fat droplets for instance, that alters the access to enzymes and bile and might slow the release of lipid.

However, possibly having a more significant impact, the stomach can play a key role in controlling the rate of nutrient absorption and subsequent physiological responses. A schematic diagram illustrating this approach is displayed in Figure 1.2. There are several complex processes occurring in the gastric compartment: enzymatic (pepsin and gastric lipase), physical (e.g. muscular contractions) and chemical (e.g. pH decrease and ionic composition). The behaviour of food structures will depend on their physico-chemical properties in the gastric environment, which might cause changes to the initial structure altering the food's functional characteristics. Several types of colloidal behaviour might be observed depending on the stability of the structure. Golding *et al.* (2011) showed that colloidal structures can be tailored to exert different behaviour under the acidic conditions of the stomach. The properties of food structure adopted in the stomach will profoundly impact gastric disintegration and the rate of GE, i.e. gastric contents gradually delivered into the duodenum. Marciani *et al.* (2007) showed that gastric acid-unstable emulsions led to the formation of an intragastric oil layer to be formed on top of the chyme in the stomach. This accelerated GE of the aqueous phase followed by a slow emptying of the intragastric oil layer. This contrasted to the slow GE after the ingestion of gastric acid stable emulsions. Then, due to differences in the rate of delivery of nutrients to the duodenum, they might be absorbed and metabolised at different rates, altering hormonal secretion and physiological responses. For instance, the slower GE of the acid stable emulsion in the study by Marciani *et al.* (2007) study led to a greater secretion of CCK and greater satiety. A slow GE has been also shown to help diabetics by reducing peaks in lipemia (Rayner *et al.*, 2001). Therefore, control of GE by intragastric behaviour of digesta can be essential for ensuring optimal digestion addressed to specific physiological responses. This approach should be further studied and exploited to design healthier food structures in the future.
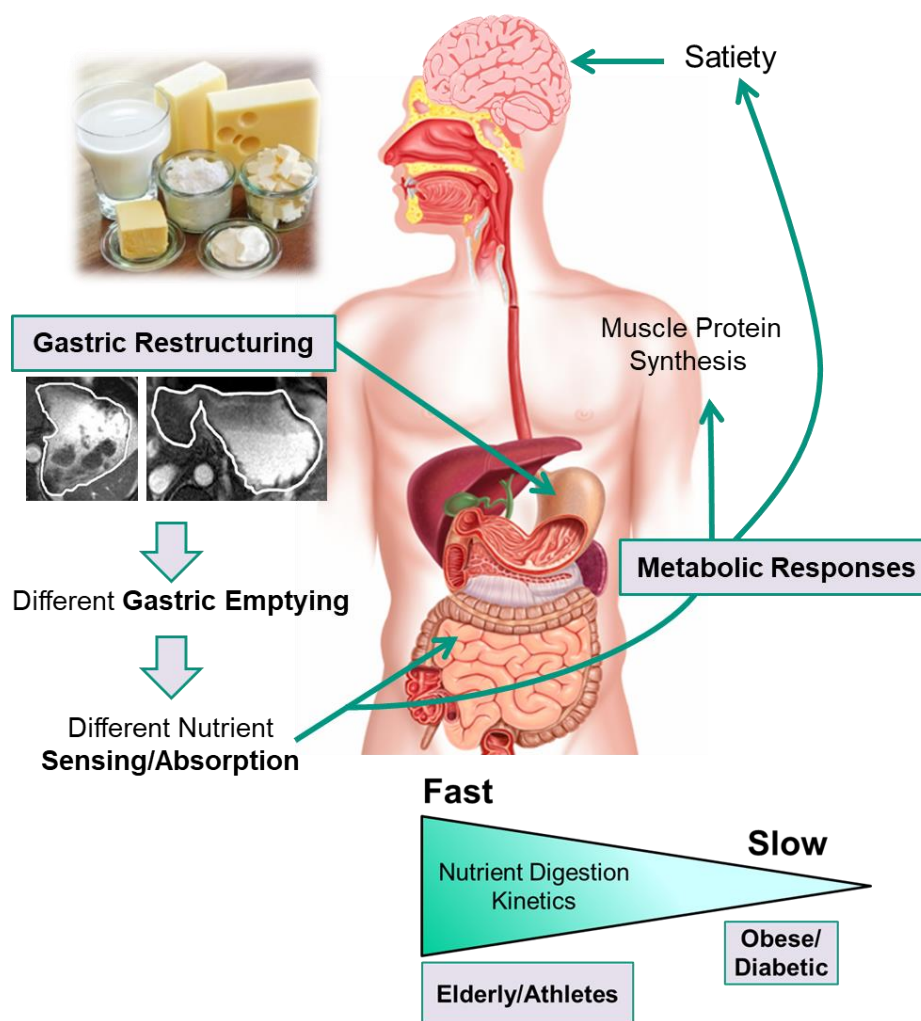
Figure 1.2 Schematic representation of the approach showing the role of gastric digestion in controlling nutrient delivery and absorption by the restructuring of food in the gastric conditions. This might, subsequently, exert different physiological responses that can be helpful to specific population groups. Images of the stomach by magnetic resonance imaging of are from Mackie *et al.* (2013).

To achieve this, a deep understanding of the mechanisms of food breakdown in the stomach is critical. This research should progress further in the light of the development of sophisticated *in vivo* techniques such as magnetic resonance imaging. Despite the gold standard for investigating nutrient digestion being the human body, there are ethical and economic reasons that constrain its use. *In vitro* models are widely used, and they are mainly classified into static and dynamic. Sophisticated dynamic models can simulate the dynamics of stomach physiology, but they are also expensive and restrictive. One example is the Human Gastric Simulator (HGS) developed at the Riddet Institute (Kong *et al.*, 2010). In contrast, static models (Minekus *et al.*, 2014) are cheap and simple to use but are less suitable to simulate complex gastric conditions, so they are mainly used to investigate the bioaccessibility of nutrients with less consideration of the structural changes during gastric digestion.

Therefore, there is a need to develop a simple, intermediate model that provides the advantages of both *in vitro* model types. The approach of a semi-dynamic gastric model was developed and used in this thesis. This model can achieve digestive properties comparable to *in vivo* behaviours in a more accessible way, although it remains impossible to perfectly simulate human physiological conditions. Nevertheless, these more sophisticated *in vitro* approaches can provide additional knowledge regarding the physico-chemical mechanisms underpinning the *in vivo* findings.

Dairy products are consumed widely and constitute an important part of our diet due to their nutritional value. The manufacturing processes affect the macronutrient organisation and texture providing an array of possible structures at different length scales, which consequently might modulate the kinetics of product disintegration and nutrient release in the GI tract. There is some research on absorption and physiological responses in milk and dairy products. For example, Lacroix *et al.* (2008) showed that the heat treatment of ultra-high temperature (UHT) in milk led to faster nitrogen delivery, compared to pasteurised milk. Also, Boirie *et al.* (1997) showed fast and slow absorption rates of whey proteins and caseins, respectively, although caseins were reported to be more susceptible to enzymatic proteolysis than whey proteins at molecular level (Macierzanka *et al.*, 2009). The gastric phase has often been overlooked in relation to food digestion and health implications. In some studies, it has been suggested that the physiological responses obtained are related to gastric digestion but it has hardly been investigated. Therefore, there are key gaps in the literature about the structural changes and nutrient emptying kinetics during gastric digestion of dairy matrices. Also, the study of complex foods, in which different types of nutrients coexist is challenging since these nutrients might play synergistic or competitive roles, which makes the outcomes of digestion even more difficult to interpret.

This literature review therefore aims to illustrate how the physiological responses and patterns of digestion observed following consumption of dairy products with different structures might be linked to gastric digestion and the need for its further study. Dairy products and their impact on health, and their main constituents will be briefly discussed together with a general explanation of GI tract and nutrient digestion. This literature review chapter will focus on assessing how dairy structures at several length scales affect nutrient bioaccessibility and bioavailability kinetics leading to different metabolic effects, in light of gastric digestion. In that view, only *in vivo* studies and *in vitro* studies using dynamic and semi-dynamic models are considered. Static *in vitro* methods will not be included because they are not able to provide accurate

kinetic data of nutrient digestion. This chapter only includes dairy structures from bovine origin, so it does not include milk from other animal sources.

1.2 General Implications of Dairy Consumption for Nutrition

Milk and dairy products have been widely recognised as excellent nutritional sources, containing proteins, lipids, carbohydrates, vitamins and minerals, in particular, calcium. The composition of milk, on average, is 87% water, 4% to 5% carbohydrate, 3% to 4% of protein and lipid, 0.8% minerals and 0.1% vitamins (Pereira, 2014). Dairy foods are the major contributors of dietary saturated fatty acids (SFA) and the evidence linking those fatty acids with cardiovascular diseases (CVD), through the increase of blood lipids in particular low-density liopoprotein (Griffin, 2017), has partly resulted in the reduction of dairy consumption, by 13.7% between 2003 and 2013 in the UK (Defra family food survey, AHDB Dairy, 2015). Nevertheles, there is a paradox in the fact that increasing evidence has shown the consistent neutral or even benefitial associations between dairy food consumption and CVD as shown in meta-analyses prospective cohort studies (Givens, 2017), and several other diseases (Thorning *et al.*, 2016). A multinational cohort study in 21 countries from five continents was recently published showing that the consumption of dairy products (milk, yogurt and cheese) was associated with lower risk of mortality and CVD (Dehghan *et al.*, 2018).

This discrepancy is probably due to the generalised approach of evaluating the health benefits of a food according to its individual components rather than the matrix and then, the health benefits of dairy products are probably due to a synergistic effect between the various components when consumed as a whole. Therefore, when investigating the health effects of dairy products, the whole matrix and its specific structure has to be considered (Thorning *et al.*, 2017). Indeed, Panahi *et al.* (2014) showed, using isovolumetric preloads, the effect of whole milk and its individual macronutrients. The response of postprandial glycemia in whole milk was 56% lower than the sum of the glycemic responses for each macronutrient.

Furthermore, milk proteins are classified as high-quality proteins considering human amino acid (AA) requirements and digestibility. They have high true digestibility and postprandial protein utilization of 95-96% and 74%, respectively (Bos *et al.*, 1999). In fact, milk proteins are frequently considered the best protein source taking into account the conventional measurement methods for protein value of essential amino acid score and protein-digestibility corrected amino acid score (Schaafsma, 2000). The AA profile is different between the two main milk proteins;

whey proteins are especially riched in branched chain amino acids (BCAAs), i.e., Leu, Ile, and Val as well as Lys, compared to caseins (Gorissen *et al.*, 2018). Milk proteins can be generally considered as a better source of protein compared to plant proteins since the later proteins are less digestible and deficient in one or more essential amino acids (EAAs) and their Leu content is 6-8%, compared to 10-13% in dairy proteins (Gorissen *et al.*, 2018). The EAAs, in particular BCAAs, are important since they excert a key role in muscle protein synthesis (Wolfe, 2002). Moreover, the high levels of Leu, in particular in whey proteins, induce the stimulation of glucose-dependent insulin-tropic polypeptide (GIP) (Nilsson *et al.*, 2004). This hormone increases insulin response and lowers blood glucose, which might be beneficial for type-2 diabetics. Milk protein ingestion has been suggested to have benefits on cardiometabolic health (Fekete *et al.*, 2016). Moreover, milk proteins have important biological functions, casein micelle carries calcium and phosphate for efficient absorption. Several peptides from milk proteins have been reported to exert certain functions such as antihypertensive, opoid-like activity and antithrombotic properties (Fekete *et al.*, 2015; Jauhiainen *et al.*, 2007).

1.3 Composition and Structure of Dairy Constituents

1.3.1 Milk Proteins

Bovine milk usually contains about 3-4% protein, which varies depending on the lactation period, animal breed and seasonality among other factors. The main proteins in milk are caseins and whey proteins, accounting for approximately 80% and 20% of bovine milk protein respectively.

1.3.1.1 Caseins

There are four different casein proteins: α_{s1}-, α_{s2}-, β- and κ-casein, in a ratio of 4 : 1 : 4 : 1, respectively and ranging in molecular mass from about 20 to 25 kDa (Fox *et al.*, 1998). Caseins are insoluble at pH 4.6 (isoelectric point of the caseins), are relatively hydrophobic molecules that are comparatively low in sulfur-containing AAs (i.e. Cys and Met) and contained high levels of phosphate group. α_{s2}- and κ-caseins have two Cys residues per molecule, and high levels of Pro. It is mainly due to the latter feature that the caseins have fairly little secondary (α-helix or β-sheet) and tertiary structures showing a relatively open and flexible structure (Fox *et al.*, 1998). Their low level of secondary structure is of high importance since it is readily susceptible to proteolysis but not easily denatured (Guo *et al.*, 1995). Also, caseins

can exhibit good emulsifying properties because of their open, flexible structure and uneven distribution of polar AAs.

Caseins are associated into supramolecular colloidal particles, called casein micelles, having an average diameter of 120 nm (Fox *et al.*, 1998). The structure of the casein micelle is still a subject of discussion, in particular the internal part. Two of the most persistent models proposed for casein micellar structure are the sub-micelle and nanocluster models (Dalgleish *et al.*, 2012) (see Figure 1.3) but there are some common characteristics. Casein micelles contain colloidal calcium phosphate and κ-casein faces the aqueous phase. κ-casein provides the stability of casein micelles due to steric effects of the protruding "hair" from the C-terminal regions of κ-casein sausing repulsion between micelles thus preventing aggregation. This is also helped by the electrostatic repulsions due to the negative surface potential of -20 mV at native pH of milk. The disposition of calcium phosphate in the micelle plays an important role in the micelle properties; without the colloidal calcium phosphate, the transport of high calcium concentrations in a soluble form would not be possible at pH conditions of milk and milk could not be coagulated by rennet. A further description of the casein structure is given in a review by Fox *et al.* (2008).
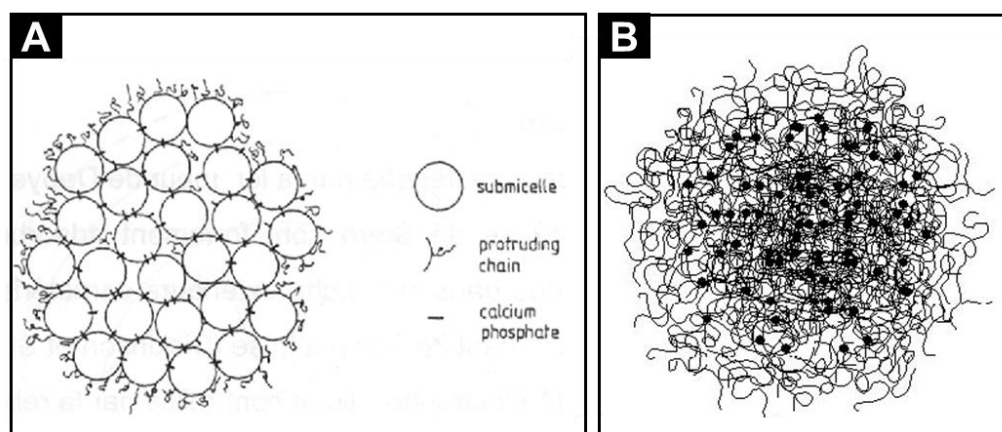
Figure 1.3 Schematic representation of the structure of casein micelle based on A) sub-micelle model and B) nanocluster model (Adapted from De Kruif *et al.* (2012)).

1.3.1.2 Whey Proteins

Whey proteins are globular proteins comprised of β-lactoglobulin (β-Lg), α-lactalbumin (α-La), bovine serum albumin, lactoferrin and immunoglobulins. β-Lg is the major whey protein in bovine milk (about 50% of the total whey proteins) with a molecular mass of 18 kDa and α-La represents about 20% of the whey proteins of bovine milk and has a molecular mass of 14 kDa (Walstra *et al.*, 1984). In contrast to caseins, whey proteins are soluble at pH 4.6 and are rich in sulphur-containing AAs. β-Lg contains five Cys residues, four are involved in disulphide linkages (-S-S-) and

one is free (-SH) but buried inside the native form of the protein, which becomes exposed on denaturation (e.g. by heating). This can result in the formation of sulphydryl–disulphide interactions with other β-lg molecules or κ-casein. Denaturation occurs at temperatures above 70°C (de la Fuente *et al.*, 2002). The main feature of whey proteins is the possession of high levels of secondary, tertiary and, in most cases, quaternary structures, which is pH-dependent.

β-Lg has shown binding and carrier function to fatty acids as well as hydrophobic compounds such as retinol, and antioxidant capacities, whereas lactoferrin is crutial element in iron absorption (Mills *et al.*, 2011).

1.3.2 Milk Lipids

Bovine milk typically contains 3-4% lipids but levels vary widely depending on breed, seasonality and animal feed among many other factors (Pereira, 2014). Lipids in milk are in globules surrounded by a trilayer, called milk fat globule membrane (MFGM) that consists of phospholipids, cholesterol, glycoproteins and enzymes (Lopez, 2011). The presence of the MFGM helps stabilise the lipids against the processes of flocculation, coalescence and creaming as well as protecting the milk fat from lipolysis (Lopez, 2005). However, the MFGM is dynamic and fragile and can be damaged easily by processing operations. The lipid globules in milk range in size from about 0.2 to 15 μm with a mean diameter of about 4 μm. The structure of milk fat has been extensively reviewed by Michalski (2009).

Triacylglycerols (TAG) represent 97-98% of the fat in milk, having a complex mixture of saturated, monosaturated, polysaturated and trans fatty acids which accounts for approximately 70%, 25%, 2.3% and 2.7%, respectively (Månsson, 2008). Within SFAs, the most abundant are C16:0 (30%), C14:0 (11%), and C18:0 (12%) (Pereira, 2014). Milk contains a group of octadecadienoic isomers (cis-9, trans-11, and the trans-10, cis-12) derived from linoleic acid that has been reported to provide health benefits in the cardiovascular system and immune function (Bhattacharya *et al.*, 2006).

1.3.3 Formation of Dairy Structures

A vast range of dairy products originate from milk following processing, for instance, fermented products such as yogurt, sour cream and some cheeses, and butter, which possess different structural organisation (Figure 1.4). Farming of milk started around 10,000 BC during the "agricultural revolution" when the nomadic tribes changed and settled in communities. Soon after, the apparition of products like cheese, yogurt and

butter occurred by accident due to the transport of milk in bottles made from sheep or goat skin and stomach. Since then, a great variety of liquid milk (usually pasteurised and homogenised) e.g. whole, semi-skimmed and skimmed milk, cheeses and other products have been developed. Likewise, various powders obtained from milk or whey proteins (e.g., casein, caseinates, whey protein concentrate and whey protein isolate) are important food ingredients and consumer products. The processing conditions will not only vary the physico-chemical properties such as pH and rheological properties but the macronutrient organisation at the different length scales.
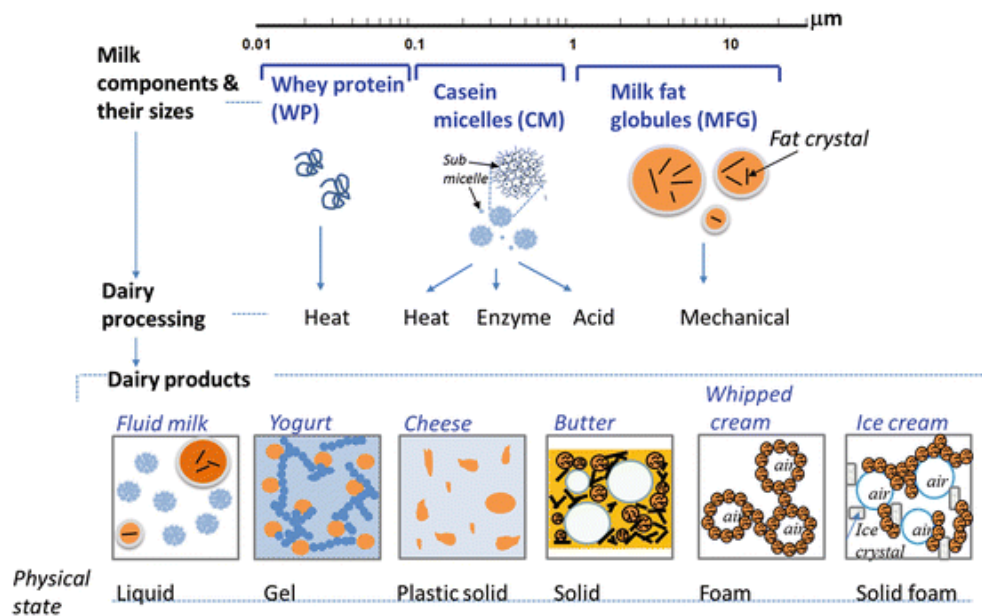
Figure 1.4 Schematic representation of the main dairy products produced by milk processing showing the changes in matrix structure (image taken from Truong *et al.* (2016)).

Some of the most common processes used in the dairy industry are homogenisation and heat treatment. More detailed information about these processes can be found in other reviews (Michalski *et al.*, 2006; Singh, 2004).

Heat treatment is applied to food in order to ensure microbial stability. The most common heat treatments applied to milk are pasteurisation, that consists of heating at 70-90°C for ≥ 15 s, and ultra-high temperature (UHT) sterilization involving heating at 135-150°C for a few seconds. Heat treatment has been reported to induce several changes in the protein constituents, including the denaturation and aggregation of whey proteins, in particular β-Lg (de la Fuente *et al.*, 2002). Heat-denatured β-Lg interacts with κ-casein on the surface of the casein micelle via hydrophobic interactions and disulfide bond formation (Sharma *et al.*, 1993). The extent of denaturation of whey proteins in UHT-treated milk is much higher than that in pasteurised milk (Douglas *et al.*, 1981). Therefore, the level of protein aggregation is

higher in UHT-treated milk compared to pasteurised milk. Moreover, the pH for coagulation of unheated and heated milk is about 5 and 5.3 respectively (Donato *et al.*, 2007). Heat also causes reorganization in the casein micelles (Dalgleish *et al.*, 2012) and induce an alteration of the mineral equilibrium of the milk by decreasing soluble calcium (Schreiber, 2001). This can impair the functionality of the casein micelle and subsequently alter casein coagulation (Guinee *et al.*, 1997), which may affect nutrient digestion kinetics. Heated milk, in particular at UHT conditions, is sensitive to glycosylation, through the Maillard reaction, due to its content of lactose that can react with amine groups in protein, often from Lys, from caseins and, therefore, this might reduce the availability of Lys (Rolls *et al.*, 1973) but it has little effect on the net protein utilization. The effect of Maillard reactions in milk was reviewed by van Boekel (1998) showing that the optimum pH for the Maillard reaction is between 8 and 10, which is not relevant to dairy products, and the amount of Maillard products measured in UHT-treated milk was 0.6-0.9 mmol/L.

Homogenisation is used by the dairy industry to reduce the size of fat globules in milk and creams, in order to reduce creaming and coalescence during long shelf-storage. In milk, this reduction is usually from an average size of 3-5 µm to below 1 µm (Michalski *et al.*, 2006). Homogenisation disrupts the MFGM and reduces the fat globule size and causes also the disruption of casein micelles (Lodaite *et al.*, 2009). This, therefore leads to the formation of a new interface on the fat globules, which mainly consists of adsorbed milk proteins and native MFGM fragments (Lopez, 2005; Sharma *et al.*, 1993). The effect of homogenization on dairy products has been extensively reviewed by Michalski *et al.* (2006). Homogenisation increases the total surface area of lipid droplets, which has relevance in nutrient digestion and will be described in this work. There are other physicochemical properties that are altered such as ζ-potential, which might also influence the colloidal stability and physico-chemical behaviour during digestion in the GI tract.

1.4 Human Gastrointestinal Tract

In this section an overview of the upper gastrointestinal (GI) physiology is presented. The gastric digestion will be explained in more detail since it constitutes an important part of this work.

Human digestion is a complex multistage process during which ingested food is broken down into the basic nutrient constituents, which enables effective absorption by the small intestine enterocyte and can then be used by the body for growth, cell maintenance, and energy (Guerra *et al.*, 2012). Ingested food undergoes a number

of mechanical and biochemical processes during its passage through the different compartments of the GI tract, starting from the mouth, and continuing in the stomach and small intestine. Figure 1.5 illustrates the main processes occurring in each compartment.

Mouth
Mastication, high shear
pH 5-7, 37°C
Transit time: 10-120 s
Salivary α-amylase, salts, mucin

Stomach
Storage, mixing, peristalsis
pH 1-6, 37°C
Transit time: 1-4 hr
Pepsin, gastric lipase, HCl, salts

Small intestine
Peristalsis
pH 6-7.5, 37°C
Transit time: 2-5 hr
Pancreatin, bile, salts
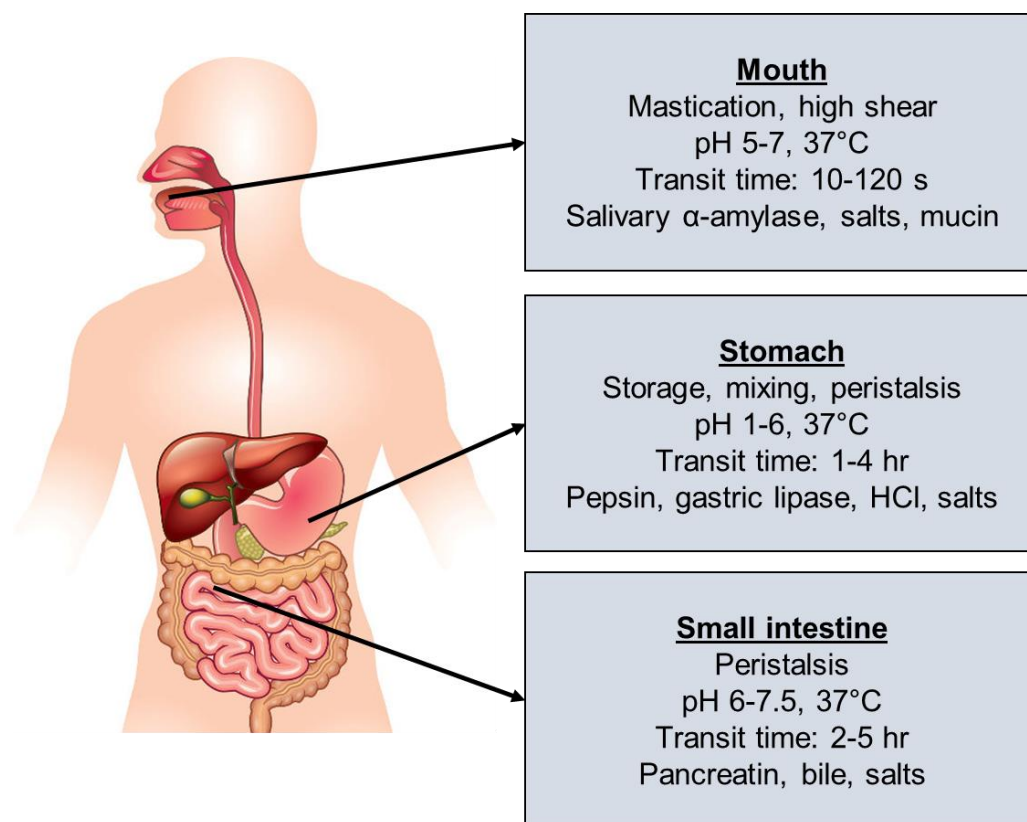
Figure 1.5 Schematic representation of the major physiological factors that take place during digestion in the upper GI tract.

The digestion of food starts in the oral cavity, in which food undergoes complex physico-chemical processes due to mastication and salivation (Chen, 2009). Food is mixed with salivary secretion containing salivary α-amylase, mucin and salts, with moderate change in pH. The time of residence of food in the mouth depends on the properties of food and varies between individuals. For solid food, this process forms a bolus that enables the food to be swallowed and enter the stomach through the oesophagus. In the gastric compartment, food is mixed with the gastric secretions consisting of HCl, salts and enzymes (pepsin and gastric lipase), and it is subjected to mechanical processes due to peristaltic waves. The digesta from the stomach (i.e. chyme) gradually enters the small intestine in a process called gastric emptying. The pH of food increases to pH 6-7.5 due to the secretion of $NaHCO_3$. Chyme is mixed with pancreatic enzymes (trypsin, chymotrypsin, carboxypeptidases, pancreatic lipase and pancreatic amylase), coenzymes and bile salts, which are secreted by the pancreas, gall bladder and liver. The major nutrient absorption occurs in the small

intestine via the mucosa, which is formed into villi and microvilli to increase the surface area. These are lined with enterocytes, i.e. nutrient absorbing cells.

1.4.1 Gastric Physiology

The description of gastric physiology has been reviewed in detail in other works (Kong *et al.*, 2008; Malagelada *et al.*, 1989), and a description of the main features is provided as follows.

After oral processing, a bolus is formed and enters the stomach, which is divided into four sections i.e. fundus, body, antrum and pylorus (see Figure 1.6) with different functionality. The fundus and body act as a gastric reservoir whereas particle disintegration and mixing occur in the antrum. The pylorus acts like a sieve between the stomach and the duodenum, only particles smaller than 2-3 mm can pass through it during the fed state (Hellström *et al.*, 2006; Newton, 2010). The time of residence of food in the stomach is also highly variable, ranged from 30 min to 4 hours (Lin *et al.*, 2005), which depends on the food properties such as caloric content and rheological properties.

In the stomach, the ingested food is mixed with gastric secretions to produce a mixture called chyme. The gastric juice is secreted gradually during digestion and contains mainly hydrochloric acid (HCl) and the enzymes gastric lipase and pepsinogen (an active precursor that is converted into the proteolytic enzyme pepsin upon contact with acid). This secretion can be influence by the physical state of meal; for instance, Malagelada *et al.* (1979), showed that a solid-liquid meal resulted in greater gastric secretions compared to the same meal in homogenised form. The gastric pH differs from the fasted to the fed state and during gastric digestion. The pH value of fasted condition is below 2 and increases after the ingestion of food, which depends on composition, pH, quantity and consistency of meal (Calbet *et al.*, 2004; Dressman *et al.*, 1990; Malagelada *et al.*, 1979). Then, the pH decreases gradually until it reaches values below 2, restoring the basal state (Malagelada *et al.*, 1976). The rate of change in pH is as a consequence of the progressive secretion of HCl as well as the decrease of buffering capacity of the content (mainly representing food protein) by gastric emptying. Ionic strength and osmolality are other physicochemical gastric factors to consider. In general, the ionic strength and osmolality of a fasted stated are about 100 mmol/L and 190 mOsm/kg, respectively (Kalantzi *et al.*, 2006) and the major ions present are: Na^+, K^+, Ca^{2+} and Cl^-.
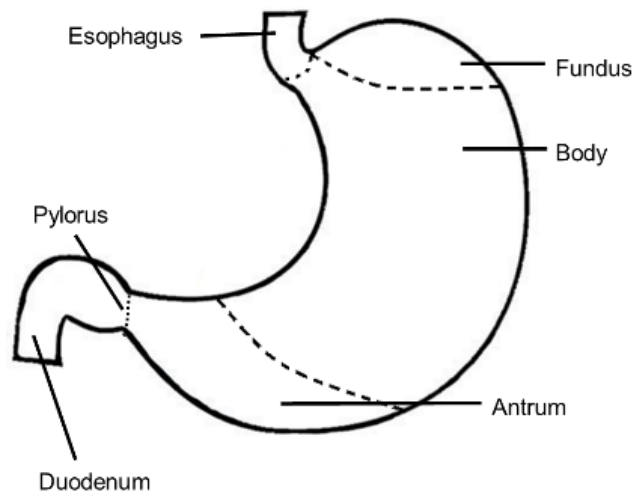
Figure 1.6 Schematic diagram of the stomach and its main parts.

The muscular contractions of the stomach wall mix, shear and force the chyme towards the pylorus. These contractions are spread from the fundus to the pylorus being more vigorous and creating higher shear forces in the antrum, resulting in a homogenous chyme at the bottom part in contrast to the non-homogenous digesta located within the fundus (Pal *et al.*, 2004). In the antrum, the disintegration of solids mainly occurs in a mechanism of propulsion-grinding-retropulsion, until the particles acquire the proper size to be emptied (Schulze, 2006; Schwizer *et al.*, 2006). There are three main types of mechanisms for the disintegration of particles: fragmentation, erosion and degradation. Fragmentation involves the breakdown of larger particles into smaller ones, erosion is the damage of surface food and degradation is related to the action of enzymes and acid (Kong *et al.*, 2008). As a result of these peristaltic antral contractions, chyme is released through the pyloric sphincter into the duodenum resulting in the last step of the food processing in the stomach, so called gastric emptying.

1.4.2 Gastric Emptying and Food Properties

Gastric emptying (GE) depends on several food properties such as consistency (Malagelada *et al.*, 1979; Santangelo *et al.*, 1998), viscosity (Marciani *et al.*, 2001), nutrient composition (Goetze *et al.*, 2007), caloric density (Calbet *et al.*, 1997; Hunt *et al.*, 1975; Kwiatek *et al.*, 2009; Sauter *et al.*, 2011), particle size (Holt *et al.*, 1982) and volume (Hunt *et al.*, 1985; Kwiatek *et al.*, 2009; Moore *et al.*, 1981). For instance, Malagelada *et al.* (1979) showed that the time of GE was shorter when a meal was consumed in a homogenised form instead of a solid-liquid state, however the emptying rate of the solid-liquid meal was faster for the first hour, probably due to an

initial emptying of the liquid part. The intestinal feedback mechanisms are able to control GE rate with respect of the duodenum, which is the major control mechanism for GE by stimulating a negative feedback pathway. The duodenum contains receptors that sense the presence of nutrients and stimulates the secretion of gut hormones, which slows down emptying by reducing the antral contractions (Janssen *et al.*, 2011). This modulation of antral peristalsis controls the volume of chyme that is received from the stomach (Wren *et al.*, 2007) and ensures that the optimal amount of chyme is delivered to the duodenum to allow it to be fully digested and absorbed in the small intestine.

It is generally accepted that liquid meals empty from the stomach according to zero-order or first-order kinetics. In contrast, solid meals have shown a biphasic pattern consisting of a lag phase during which little emptying occurs related to the time solids achieve a suitable particle size, followed by a linear emptying phase (Schulze, 2006; Siegel *et al.*, 1988). However, the importance of this lag-phase is still controversial since its identification and duration is highly variable, depending on meal properties, e.g. meal viscosity and particle size (Hellström *et al.*, 2006; Urbain *et al.*, 1989) as well as methodology and inherent intervariability. For instance, Moore *et al.* (1981) showed, using a double-isotope technique for measuring solid and liquid components, that the solid phase followed a linear GE whereas the liquid phase was curvilinear with an initial rapid GE. Nevertheless, it seems apparent that liquid meals empty with a shorter half time emptying compared to solid meals, which could be related to the time for breaking down larger particles to obtain the particle size that can pass through the pylorus. This is considering that there are no changes in the physical state of the liquid during the gastric phase. Indeed, the intragastric behaviour of the ingested food might also influence the GE profile. For instance, phase separation in the stomach can lead to the layering of lipid on the top, which contributed to an initial rapid GE, shown by Marciani *et al.* (2008). Similarly, Steingoetter *et al.* (2015) showed that the gastric acid unstable emulsion exhibited biphasic and faster emptying profile than the gastric stable emulsion. The Elashoff's power exponential curve modelling GE has been well described by Elashoff *et al.* (1982) and some computer programmes for dynamic models use that equation for controlling chyme transit.

1.5 Methodology for Studying Gastric Digestion

1.5.1 *In Vivo* Methodology for Gastric Digestion Monitoring

The use of some advanced techniques in combination with computational modelling (Ferrua *et al.*, 2015) has helped to gain more insight into the complex study of gastric digestion dynamics *in vivo*. A more detailed description of the techniques used for GI motor assessment can be found in Dinning *et al.* (2010) and Szarka *et al.* (2009).

The classical methods to measure gastric motility require the insertion of a barostat or manometer into the stomach, which may alter the normal gastric function. Some methods to monitor volumes in the stomach include scintigraphy, in which there is administration of a radionuclide isotope and has low spatial resolution and cannot measure the volume of the total meal including secretions (Feinle *et al.*, 1999). Ultrasound has better resolution but cannot measure volumes in the body and fundus accurately because of air-fluid interfaces (Szarka *et al.*, 2009). Breath test is another non-invasive technique that allows the determination of GE indirectly. This assesses the rate of transit and uptake of ^{13}C labelled substrate by the metabolic conversion of ^{13}C in the liver into ^{13}CO$_2$ which is exhaled in the breath and detected using mass spectrometer (Sanaka *et al.*, 2008). Another method is a wireless capsule (Iddan *et al.*, 2000), in which the gastric behaviour of meal can be followed while the camera is in the stomach. The images are obtained by using a lens of short focal length and transmitted using ultra high frequency- band radio telemetry. Some wireless capsules can also track the pH and some motility factors of the GI tract (Kloetzer *et al.*, 2010). Recently, some non-invasive techniques of visualisation and imaging have increasingly been used. One of the most effective and used systems is magnetic resonance imaging (MRI), which has the capability to simultaneously measure gastric volume, gastric motility, gastric secretions and gastric emptying (Marciani, 2011). MRI overcomes some of the limitations of other non-invasive techniques and allows high-resolution imaging of the spatial distribution of the intraluminal ingested food (Schwizer *et al.*, 1994). Its sensitivity to proton changes allows the discrimination between the water and the lipid components of a meal. For instance, MRI helped establish the importance of the acid stability in the stomach (Marciani *et al.*, 2008) and the impact of the meal viscosity (Marciani *et al.*, 2001). Bluemel *et al.* (2015) found low concordance between breath test and MRI when using isocaloric and isovolumetric meals differing in casein content. The results indicated that the properties and intragastric processes of the test meal led to the differences between

the methods. The authors recommended validation by imagining methods prior the ^{13}C-acetate breath test to allow for the correct interpretation of the derived GE data.

Regarding invasive techniques, endoscopy by nasogastric intubation offers the possibility to aspirate samples from the gastric digesta and analyse them. This technique, in contrast to the non-invasive techniques, focussed on the characterisation of the physico-chemical properties of the digesta in the gastric environment. This can be combined with imaging by using a tube with lens systems and fibre optic.

Both invasive and non-invasive techniques are often applied in combination with clinical assessment of blood testing for hormonal responses and plasma amino acid and triacylglycerol uptake.

1.5.2 *In Vitro* Methodology for Investigating Gastric Digestion

The *in vitro* models to simulate the digestion in the GI tract are mainly classified into static and dynamic. The static model is the simplest but most used system and it is the harmonised static protocol (Minekus *et al.*, 2014), developed by the INFOGEST COST Action, which offers the possibility to apply a protocol with digestion parameters by consensus that can be compared. The related gastric phase involves hydrolysis by pepsin at constant pH 3 for 2 hours while applying sufficient stirring to mix at 37°C. Static *in* vitro models can be useful in predicting the overall nutrient hydrolysis and end-points values of the digestion *in vivo* (Egger *et al.*, 2017). A comprehensive review about the correlation between *in vitro* and *in vivo* data on macro- and micro-nutrients is given by Bohn *et al.* (2017). However, this correlation is not feasible when investigating the structural changes and nutrient breakdown kinetics that occur in response to dynamic changes in gastric digestion conditions.

On the other hand, dynamic models are designed to mimic the gastric dynamics in terms of physical and/or chemical environment, in particular the gradual secretion of gastric fluids and peristaltic contractions. Examples of this model are the Human Gastric Simulator (HGS), described in Kong *et al.* (2010), the Dynamic Gastric Model (DGM) developed at the Institute of Food Research (UK), described in Thuenemann *et al.* (2015), and the multicompartment models of TNO Gastro-Intestinal Model (TIM) developed in TNO Triskelion (The Netherlands) described in Minekus (2015), DIDGI-system from INRA (France) detailed in Ménard *et al.* (2015) and the SIMGI model developed in CSIC, Spain (Barroso *et al.*, 2015). A comprehensive review of developments in dynamic systems for *in vitro* analysis of digestion can be found in Dupont *et al.* (2018). Since the HGS will be referred to on several occasions

throughout the thesis, a brief description of the main features is given as follows and referred by Kong *et al.* (2010). The simulated stomach of HGS consists of a cylindrical latex chamber as shown in Figure 1.7. The contractions waves of the stomach are mimicked using Teflon rollers that squeeze the flexible wall of the simulated stomach periodically using an increasing amplitude which provides a vigorous mixing in the bottom part, which was validated by assessing the pressure exerted on a rubber bulb when compared to the mechanical forces observed *in vivo*. GE is simulated by a peristaltic pump connected to the bottom part typically using a rate of 3 mL/min and a mesh bag with pore size of 1.5 mm is used to simulate the sieving effect of the pylorus. The digestive secretions are delivered following a steady secretion rate that can be adjusted from 0.03 to 8.2 mL/min using a peristaltic pump, typically 2.5 mL/min is used.
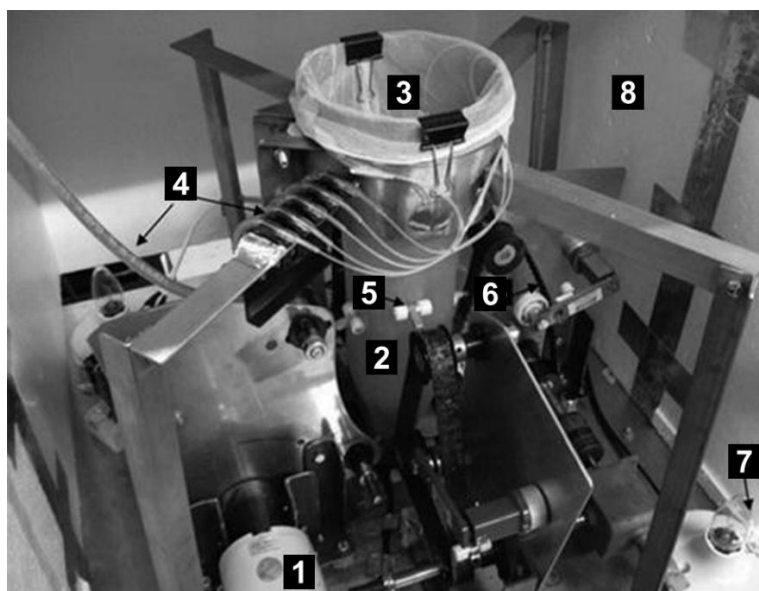
Figure 1.7. Human Gastric Simulator. (1) Motor (2) Gastric compartment (3) Mesh bag (4) Simulating secretion tubes (5) Teflon roller set (6) Conveying belt (7) Insulated chamber. From Kong *et al.* (2010).

1.6 Digestion and Absorption of Nutrients

1.6.1 Digestion and Absorption of Proteins

Figure 1.8 shows a schematic diagram of the process of digestion and absorption of proteins. The digestion of proteins starts in the stomach by pepsin. Pepsinogen is secreted by chief cells in the gastric mucosa and it is autoactivated by gastric acid. Pepsin is an endopeptidase with a higher specificity for cleaving peptide bonds in which the carboxyl group is provided by Tyr, Phe, Trp, and Leu (Goodman, 2010). Then the native (or partially degraded) proteins found in food are broken down

into a mixture of large polypeptides, smaller oligopeptides, and some free amino acids (AAs) (Erickson *et al.*, 1990). Pepsin can partially digest 10-15% dietary protein in the stomach (Goodman, 2010) and it has its optimum pH at 2 (Piper *et al.*, 1965).

These protein products are further digested in the small intestine by other proteases, i.e. trypsin, chymotrypsin and elastase, which are serine proteases secreted in the pancreas. Trypsin predominantly cleaves the peptide bonds next to Lys and Arg, chymotrypsin cleaves peptide bonds adjacent to hydrophobic AAs (Tyr, Trp, Phe, Met and Leu) and elastase cleaves peptide bonds adjacent to Ala, Gly and Ser (Goodman, 2010). There are exopeptidases, called carboxypeptidases, that cleaves the carboxyl ends of the peptide chains to remove AAs. Therefore, the intestinal proteolysis is highly efficient resulting in a mixture of free AAs and oligopeptides (2-6 AAs) that account for approximately 40% and 60%, respectively, of the total α-amino nitrogen (Erickson *et al.*, 1990). Some peptides are further hydrolysed by aminopeptidases located on the brush border membranes. Therefore, the joint action of the gastric, intestinal and brush border proteolysis provides the availability of free AAs, di- and tri-peptides allowing their transport across the brush border membrane. There are different carrier mechanisms for the intracellular transport of AAs, di- and tri-peptides but they are mostly Na^+ dependent (Hinsberger *et al.*, 2004). The AA transporters have been defined by these two main functional criteria: type of AA transported (acidic, neutral or zwitterionic, or basic) and transport mechanism used (facilitated diffusion or secondary active transport) (Goodman, 2010).

The rate and extent of protein digestion is strongly depended on the accessibility of the cleavage sites to enzymes and side-chain flexibility of the substrate, which is governed by the structure of protein. Macierzanka *et al.* (2009), showed that β-Lg was resistant to pepsinolysis due to the compact globular structure compared to the loose structure of β-casein. However, the degree of proteolysis in β-Lg was increased when emulsified with oil, which was due to the partial unfolding of the β-Lg secondary structure improving accessibility to pepsin. Other types of processing such as heat treatment can lead to chemical modification and aggregation, depending on the temperature and time of exposure, which, in turn, will affect protein digestion. For instance, the heating at UHT conditions increased the rate of proteolysis of whey proteins (Miranda *et al.*, 1987), due to the unfolding of the structure, which exposes the cleavage sites and enhances then the accessibility of enzymes. Similarly, the heat treatments at 62.5-78°C resulted in an increase of proteolysis susceptibility of β-Lg after 10 min of hydrolysis using trypsin and chymotrypsin (Stănciuc *et al.*, 2008). This was obtained at pH 7, however, there was a decrease in degree of hydrolysis at pH

7.5, due to probably the formation of covalent aggregates between the β-Lg monomers presents at that pH that may hide the cleavage sites for the enzymes. Moreover, milk protein digestion was slower and lower when in gel matrices compared to that in liquid matrices (Barbé *et al.*, 2013). Other factors that affect protein hydrolysis are the lipid interaction with the proteins and the presence of physiological surfactants, i.e. bile acids and phospholipids (Mackie *et al.*, 2010). Gass *et al.* (2007) showed that bile salts displaced proteins and increase proteolysis.Therefore, the structure of proteins at the different length scales can impact the rate and extent of proteolysis.

1.6.2 Digestion and Absorption of Lipids

A schematic diagram of the process of digestion and absorption of lipids is shown in Figure 1.8. Lipids in food are mainly found as triacylglycerols (TAG) and their digestion starts in the stomach by gastric lipase, accounting for 10-40% overall lipolysis (Armand, 2007). Human gastric lipase is secreted by the chief cells located in the fundic mucosa of the stomach. Gastric lipase has been reported to preferentially cleave at sn-3 position of the ester bond of TAG resulting in sn-1,2 diacylglycerol (DAG) and free fatty acids (FFA) (Michalski *et al.*, 2013). Lipids are further digested in the small intestine by the action of lipases and esterases, i.e. pancreatic lipase, cholesterol esterase and phospholipase, with the presence of colipase and bile salts. The intestinal lipolysis contributes to 40-70% of the overall lipid hydrolysis (Armand, 2007). Pancreatic lipase acts at the surface of the lipid particle and hydrolyses fatty acids at the sn-1/ 3 positions of the glycerol backbone and produces FFAs and 2-monoacylglycerol (MAG). Colipase absorbs to the TAG surface and interacts with lipase and bile salts to allow the TAG to enter the active site of the lipase enzyme, facilitating the digestion. Colipase also prevents the inactivation of lipase by the bile salts. The products of dietary lipid breakdown are solubilized by the formation of mixed micelles with bile salts and phospholipids, which pass through the enterocyte membrane (Mu *et al.*, 2004). In the enterocyte, the FFAs and 2-MAG become protonated and leave the mixed micelles and they are re-synthesized into TAGs (Goodman, 2010). These TAGs bind with lipoproteins forming chylomicrons that allow the transport of lipids to the body's cells via the lymphatic system and then to the systemic circulation .
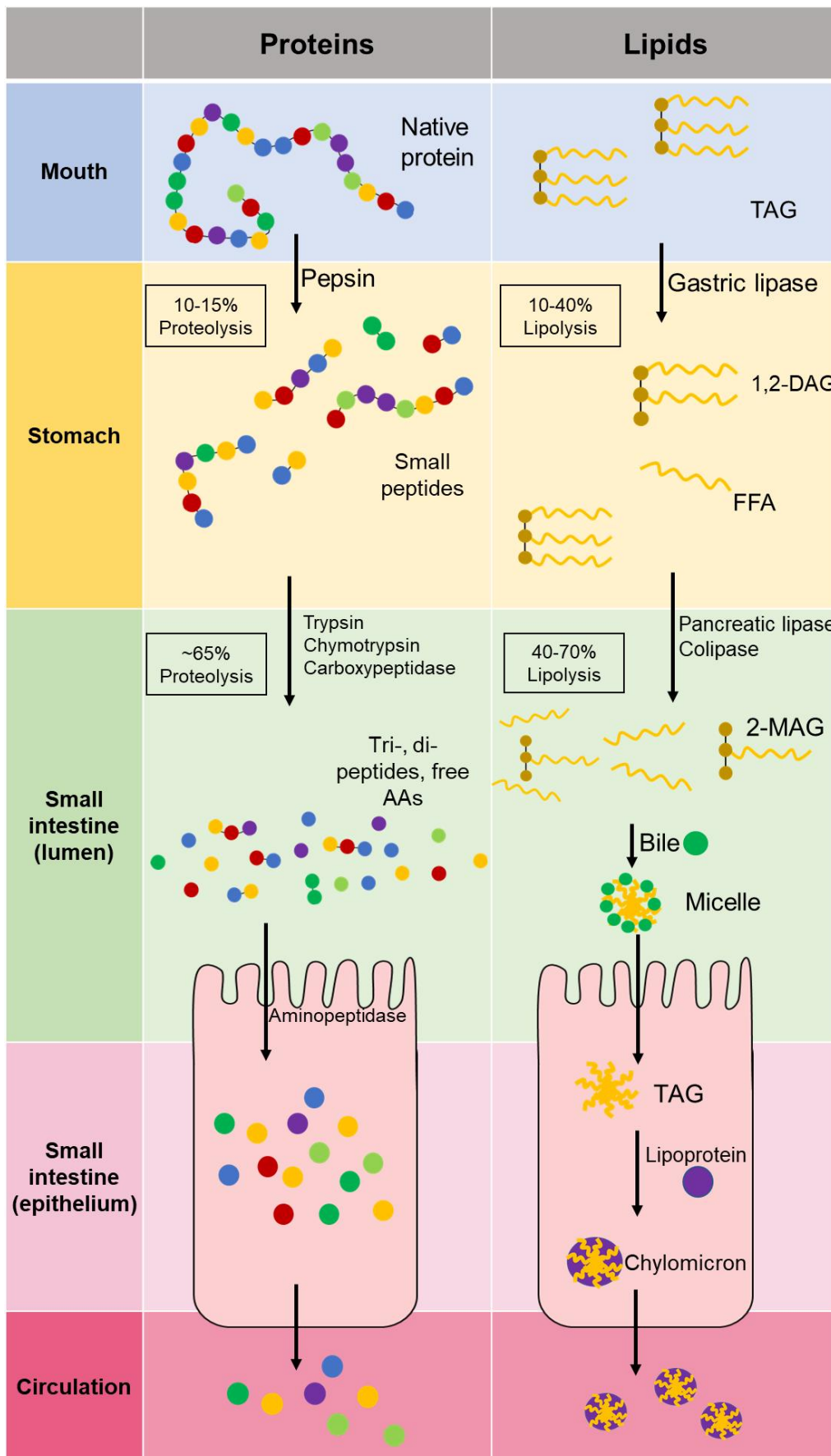
Figure 1.8 Schematic diagram for both proteins and lipids of the processes of digestion in mouth, stomach and intestine, and the process of absorption through the epithelium

1.7 Effect of Dairy Proteins on Digestion and Physiological Responses

1.7.1 Dairy Proteins and Bioaccessibility

The nature of dairy proteins in terms of their molecular structure and physico-chemical properties, as described above, has a strong impact on gastric and intestinal digestion which subsequently affects the bioaccessibility of nutrients. In general, it is assumed that casein coagulates in the acid conditions of the stomach whereas whey proteins remain relatively soluble. Despite the fact that there are several indirect indications suggesting this behaviour occurs, no direct visual evidence of the restructuring of casein occurring in the human stomach has been reported so far. Some studies reported the markedly different GE and digestion kinetics between the main milk proteins (Mahé *et al.*, 1991; Mahé *et al.*, 1996). However, there are contradictory studies in which no differences in GE for the different milk proteins were found (Calbet *et al.*, 2004; Lang *et al.*, 1998). In the latter studies, sodium or calcium caseinate was used whereas milk or micellar casein were digested in those studies where the GE was different. Therefore, the state of the casein and its processing history seems to strongly influence its digestion behaviour in the stomach. Caseins in the micellar state are coagulated by pepsin (Tam *et al.*, 1972) and low pH (Dalgleish *et al.*, 2012). This contrasts to caseinate, i.e. a mixture of caseins with the calcium phosphate removed, which does not have the same micellar-type structure and is not coagulated by pepsin. In this chapter, studies using casein in micellar form will be mainly discussed because it is the most relevant structural form found in natural dairy products.

In that context, Miranda *et al.* (1981) showed in rats that the rate of GE in skimmed milk was slower compared with that of a mixture of denatured caseins and the proteolysis in the stomach was much lower in the skimmed milk reporting that α_{s1}-casein and β-casein were almost undergraded and κ-casein was converted into para-κ-casein.

The distinct rate and composition of the products delivered to the small intestine after the ingestion of different milk proteins suggest a different time of residence and behaviour in the stomach. Mahé *et al.* (1996) investigated the digestion kinetics of intrinsically labelled ^{15}N β-Lg and casein drinks, which were fed to healthy young volunteers. The effluents from the jejunum were collected by a nasal tube and their protein contents and flow rate were assessed. The jejunal flow rate peaked in the first

20 min after β-Lg digestion, which was present mostly in the intact form. In contrast, casein was more slowly recovered in the jejunum in a more degraded form. These results were supported by a more recent human study (Boutrou *et al.*, 2013) where the authors found that, after casein ingestion, the delivery of dietary protein in the jejunum was progressive for 6 hours and in the form of medium size-peptides (750-1,050 Da). In contrast, the ingestion of whey protein induced the release of larger-size peptides (1,050-1,800 Da) and was completed after 3 hours. The authors suggested that the coagulation of casein could lead to a slower rate of emptying compared to a more rapid emptying of the whey proteins in solution. Therefore, casein coagula could be more exposed to pepsin hydrolysis leading to the emptying of more degraded products.

1.7.2 Dairy Proteins and, Absorption and Protein Metabolic Utilization

The distinct pattern of protein digestion in the GI tract has been reflected in different rates of AA absorption, which might modulate the postprandial metabolism of whole body protein synthesis, breakdown and oxidation in the liver. Boirie *et al.* (1997) performed a study on young healthy subjects using intrinsically ^{13}C-Leu labelled whey protein and micellar casein drinks, which were matched for Leu content but were not isonitrogenous. The postprandial whole-body Leu balance, considered as an index of protein deposition, was assessed by tracing samples from blood and breath. The plasma AA appearance, i.e. aminoacidemia, was fast, high and transitory after whey protein drink ingestion, which led to an increase in whole body protein synthesis (68%) but no support in whole body protein breakdown. In contrast, the ingestion of a casein drink resulted in a lower, slower and prolonged release of AAs. This was associated with a markedly higher inhibition of whole protein breakdown (34% for 7 hours), but just slight stimulation of whole protein synthesis (31%) compared to whey protein drink. However, the Leu balance was positive for the casein drink over 7 hours, promoting protein deposition whereas no effect was provided from whey protein drink. The authors classified, in relation to that postprandial behaviour, whey proteins and casein as 'fast' and 'slow' digested proteins respectively, which has been widely considered in the literature. In the same line, Lacroix *et al.* (2006a) showed in healthy volunteers that the aminoacidemia for the first hour in whey proteins ingestion was rapid and high followed by a decrease reaching values below the baseline of total plasma AAs after 3 hours, which resulted in hypoaminoacidemia. The dietary nitrogen was labelled using ^{15}N labelling and the kinetics of protein utilization were followed during 8 hours in plasma and urinary urea. The observed

plasma AA rate matched with the higher rate and transfer of dietary N to urea after whey protein intake compared to casein ingestion. In this study, a milk protein drink containing 20:80 ratio of whey proteins:caseins was also studied and there was no significant difference in the dietary nitrogen utilization when compared to casein drink. This might be attributed to the profound effect of coagulation in the stomach. In this line, the behaviour of blends with different ratios of whey proteins and caseins could be interesting to investigate.

Caseins and whey proteins have different AA composition, the main difference is a higher Leu content in whey proteins. One might think that the different AA composition of the protein sources, not the protein digestion kinetics, might induce different dietary nitrogen postprandial metabolism. Also, a different nitrogen content could affect postprandial balance. This was addressed in a study by Dangin *et al.* (2001). Casein and whey protein drinks were matched in AA composition and nitrogen contents but designed to have different digestion rates. The fast-digested drinks were whey protein and casein hydrolysate, and the slow-digested drinks were caseins and whey proteins consumed at repeated times during digestion. In accordance with the previous studies illustrated, they showed that fast-digested drinks induced rapid, pronounced and transient increase of aminoacidemia, which led to high and immediate stimulation of protein synthesis. In contrast, slow-digested drinks induced moderated and prolonged aminoacidemia over 4-5 hours resulting in the inhibition of protein breakdown and no effect in protein synthesis. Also, the possible effect of insulin inhibiting hydrolysis was refuted because no increase in insulin level was observed. Similarly, Bos *et al.* (2003) demonstrated that the availability of AAs by digestion kinetics was the main driver for protein metabolism by using milk protein compared to soy protein. The ingestion of the latter protein resulted in a higher and earlier (2.5 hours) AA peak in plasma compared with milk proteins (3.9 hours), which was linked to a lower postpandrial nitrogen retention of soy protein showing significantly higher urea production within the first 2 hours.

The inclusion of other nutrients in the protein matrix might affect protein utilization. Gaudichon *et al.* (1999), investigated whether the addition of sucrose or milk fat affected the net postprandial protein utilization of milk protein. Sucrose, but not fat, significantly reduced the postprandial transfer of [^{15}N]-milk nitrogen to urea, which could be mainly due to a delayed GE of the meal because of the higher energy density. Nevertheless, the total amount of dietary nitrogen recovered over an eight-hour period after meal ingestion was not different. The absence of any effect in the presence of fat was unexpected because the energy density was similar to that of the sucrose meal and the authors suggested that lipid may have separated and formed a

layer on top of the meal in the stomach and emptied after the aqueous phase of the meal. However, having similar behaviour to the control milk protein sample, fat could be entrapped in the coagulum possibly formed in the stomach.

Mariotti *et al.* (2015) investigated the effect of caseins and whey proteins in TAG response in a mixed high-fat meal using a crossover design in healthy overweight men. The authors showed that caseins, compared to whey proteins, markedly reduced postprandial TAG and formation of plasma chylomicrons, which was suggested to be caused by low solubility and phase separation of casein in gastric conditions. This contrasts with other studies showing whey proteins to be more efficient in lowering effects on blood lipids (Mortensen *et al.*, 2009; Pal *et al.*, 2010). Therefore, there is a gap in understanding the influence of other nutrients included in the food matrix on metabolic effects, which should be studied considering the digestive kinetics and gastric behaviour.

1.7.3 Dairy Proteins and Skeletal Muscle Mass

Muscle mass maintenance is regulated by the balance between muscle protein breakdown and synthesis rates, which has been dependent on physical activity and food intake. The postprandial muscle protein synthetic response to feeding is regulated on factors including dietary protein amount, source and digestion, AA absorption and uptake by muscle and intramyocellular signalling (Gorissen *et al.*, 2015). Muscle protein synthesis (MPS) is of particular interest to athletes, active people and the elderly. Ageing can result in a diminished muscle protein synthetic response after protein intake, which is often accompanied with the progressive decline of skeletal muscle mass, known as sarcopenia. Some studies have shown that faster digestion of whey proteins resulted in an enhancement of MPS responses in elderly men (Burd *et al.*, 2012; Dangin *et al.*, 2003; Pennings *et al.*, 2011; West *et al.*, 2011), in elderly men after resistance exercise (Burd *et al.*, 2012) and also in young men at rest and after resistance exercise (Tang *et al.*, 2009). In general, it has been shown that the specific pattern in plasma aminoacidemia after the consumption of whey proteins, i.e. rapid and pronounced AA peak, was the main driver. Moreover, a strong correlation was reported between plasma Leu levels and muscle protein accretion (Pennings *et al.*, 2011). The stimulation of MPS is driven primarily by essential AAs (Volpi *et al.*, 2003), from which Leu has been reported as the main signal (Drummond *et al.*, 2008). Therefore, a direct comparison of the effects of the absorption rates of these two proteins related to MPS is conflicted by their differing AA contents. In healthy men after resistance exercise, whey proteins ingested as a single bolus was compared to the same amount of protein but taken in repeated small

drinks, which aimed to simulate slower digested protein (West *et al.*, 2011). The authors showed that whey proteins consumed as a bolus caused a rapid and greater increase in aminoacidemia, which was reflected in a greater stimulation in MPS response at an early stage (1-3 hours) compared to the whey protein consumed repeated times (3-5 hours). They concluded that the pattern of aminoacidemia, not the net AA exposure, was the main driver for the effect in skeletal muscle. These results were supported by other studies using casein and casein hydrolysate (Pennings *et al.*, 2011).

However, these findings are in contrast to other studies (Churchward-Venne *et al.*, 2015; Dideriksen *et al.*, 2011; Reitelseder *et al.*, 2011). Reitelseder *et al.* (2011) in young men and Dideriksen *et al.* (2011) in older men and women demonstrating that ingestion of whey proteins compared with calcium caseinate resulted in similar rates of MPS. As mentioned previously, the selection of the casein source is critical. The increased solubility of casein salt might increase the rate of digestion and speed the resultant aminoacidemia. Moreover, the timing of the synthetic measurements (i.e. 4 versus 6 hours of recovery) and/or the tracer infused (i.e. [^{13}C] Leu *vs* [^{13}C] Phe) may account for the contrasting findings.

The ingestion of other macronutrients together with dairy proteins is another factor to consider in relation to MPS (Churchward-Venne *et al.*, 2015; Gorissen *et al.*, 2014). Co-ingestion of carbohydrates with casein resulted in no differences in muscle synthetic response in both young and elderly men (Gorissen *et al.*, 2014). However, this resulted in a delay of protein digestion and absorption, attributed to the decrease of GE rate. In contrast, other studies showed a greater AA uptake into peripheral tissues in resting subjects when milk proteins were combined with lipid and sucrose (Mariotti *et al.*, 2000). Elliot *et al.* (2006) showed that milk ingested as a whole food stimulated net MPS following resistance exercise, suggesting that its consumption would be suitable during recovery. Interestingly, the uptake of AAs, based on Thr and Phe, was greater for whole milk compared to fat-free milk. However, the reason of this outcome was not clear for the authors suggesting that the extra energy could help the N balance process. Therefore, further work should be performed in investigating the role of lipid in AA uptake.

1.7.4 Dairy Proteins, Satiety and Food Intake

The ingestion of protein stimulates the release of gut hormones involved in appetite and food intake regulation, such as CCK, GLP-1, PYY and insulin (Anderson *et al.*, 2004). Whey proteins might be considered to have a greater effect on satiety

compared to caseins since a higher content of branched chain AAs can greatly stimulate insulin secretion (Nilsson *et al.*, 2004). However there is no consistent evidence supporting one milk protein to be more satiating than the other (Bendtsen *et al.*, 2013). Hall *et al.* (2003) investigated in healthy lean volunteers the appetite responses of whey proteins and casein drinks containing both lipid and carbohydrate with their total energy matched. The authors found that a whey-based drink was satiating for 180 min after ingestion according to the appetite subjective score and was more efficient at decreasing energy intake in an *ad libitum* lunch, served 90 min after ingestion, than a casein drink. The secretion of the most important hormones in the role of satiety, i.e. CCK and GLP-1, increased by 60% and 65% respectively after whey proteins ingestion compared to caseins. Similarly, Veldhorst *et al.* (2009) reported a decrease in appetite after, in particular, 20 min of consumption of 15 g of whey proteins (as a part of a standard breakfast) compared to casein or soy protein, which was in accordance to the higher concentration of GLP-1 and insulin observed following whey protein consumption. Accordingly, Luhovyy *et al.* (2007) showed that whey proteins greatly suppressed food intake more quickly, i.e. at 90 min compared to the latter time of 150 min observed in casein after meal consumption. In contrast, casein consumption was reported to induce a greater satiety promoting effect than whey proteins in a study by Acheson *et al.* (2011), in which subjective appetite sensations were measured for 330 min. This was supported by Alfenas *et al.* (2010) with normal weight subjects, in which casein consumption led to a daily lower energy intake with 7-day supplementation compared to whey protein. Calbet *et al.* (2004) did not find significant differences in the hormonal secretion of GLP-1 and PYY when the casein and whey proteins were compared with their hydrolysates. The variability of results can be explained by the protein source, quantity and time of measurements used in the studies. Overall, it seems that fast digested protein could have a greater satiety promoting power in the short term in contrast to the long-term effect shown by the slow digested protein of casein. Then the different digestion and subsequent AA absorption rate of casein and whey proteins might affect the secretion of GI hormones and subsequent satiety and food intake.

The ingestion of milk as a whole was more effective for decreasing satiety and reducing food intake than consuming the isocaloric drinks containing casein or whey proteins alone (Lorenzen *et al.*, 2012), which could be as the result of a greater increase of CCK and GLP-1 (Diepvens *et al.*, 2008). Moreover, milk consumption has been reported to promote satiety and decrease food intake when compared to other drinks such as fruit juice (Dove *et al.*, 2009).

In this section, we showed evidence of how the single milk proteins affect the physiological functions differently after their digestion. Casein and whey proteins have been categorised as slow and fast protein respectively according to their plasma AA appearance rate. Several studies have shown that the different aminoacidemia patterns, rather than protein composition, have a profound effect on protein metabolism, in particular protein synthetic response of skeletal muscle. Despite the fact that it is widely suggested that gastric digestion could be the main driver for these outcomes, there is still no direct evidence. As far as it is known, there is no *in vivo* study showing the changes in gastric behaviour during the digestion of the main dairy proteins.

1.8 Dairy Microstructure and Digestion, Absorption and Physiological Responses

1.8.1 Dairy Microstructure Induced by Heat Processing

Structural and functional modifications of milk proteins following heating have been extensively reported (de la Fuente *et al.*, 2002; Singh, 2004). However, the impact of heat treatments on the digestion of milk proteins has been much less studied and it is still subject of debate. A lot of attention has been paid to the nutritional quality of dairy protein after heat treatments. There is a belief that heat treatment negatively affects protein quality and claims have been made that raw milk is more nutritious and more easily digested than heat treated milk. The main chemical modifications to milk proteins during heating are denaturation of whey proteins, in particular β-Lg, casein-whey protein interactions and glycosylation by Maillard reaction. Despite the significant biochemical alterations induced by heat, some studies have shown no impairment of digestibility (Efigênia *et al.*, 1997; Rutherfurd *et al.*, 2005), and nitrogen availability (Lacroix *et al.*, 2006b) after pasteurisation and UHT treatment in rats.

From our knowledge, there is only one study in humans assessing the nutritional impact of milk heat treatment. Lacroix *et al.* (2008) compared the treatments of pasteurisation (72°C for 20 s) and UHT (140°C for 5 s) with non-heated milk. The kinetics of postprandial utilization of dietary nitrogen for the transfer into serum protein and AA, body urea and urinary urea over 8 hours were significantly faster for UHT milk compared to pasteurised milk and non-heated milk, which had a similar protein metabolic pattern. This shows that the digestive kinetics were more rapid after UHT milk ingestion. There were no firm conclusions regarding the mechanisms behind this observation. The rapid nitrogen utilization could be induced by a rapid GE due to

different structural changes in the stomach but the authors also suggested that possible Lys damage following processing could also promote the higher deamination level.

The faster nitrogen utilisation in highly heat treated milk might be due to faster gastric digestion. Miranda *et al.* (1987), using a rat model, compared skimmed milk samples heated using UHT and autoclaved (120°C for 20 min) conditions with non-heated skimmed milk. The heat treatment, in particular autoclaved, accelerated the GE rate of total nitrogen and casein hydrolysis. This contrasts to the work by Barbé *et al.* (2013), in mini-pigs, in which a higher mean retention time in the stomach of heated skimmed milk (90°C, 10 min) was observed when compared to a non-heated system. However, in the latter study, they used chromium to measure the gastro-duodenal transit, which does not represent the solid phase of any coagulum formed in the stomach. In general, there is limited research on the GE rate of heated milk samples to draw any firm conclusions.

However, a faster GE induced by heating might be more in accordance with some evidence showing reduced milk protein coagulation in the stomach. The study by Kaufmann (1984), using mini-pigs, appears to be the only *in vivo* study reporting visually that heat treatment modifies the structure of the coagulum formed in the gastric compartment. This study also demonstrated the restructuring of milk in the stomach, whereby the coagulum formed with UHT sterilized milk in the stomach was less firm and had crumbly structure compared to pasteurised milk and more so with raw milk. Moreover, Meisel *et al.* (1984) reported a significant effect of UHT treatment on acidification and protein emptying during gastric digestion. The pH at 360 min of gastric digestion was 4.32 and 1.80 for raw and UHT+homogenised milk, respectively. The protein content in chyme after 360 min digestion was approximately 75% in raw milk compared to 25% in UHT+homogenised milk. This could potentially be related to the differences in pepsin activity found. The analysis of the chyme at 360 min showed that pepsin activity was approximately 1,000 U/g protein in raw milk in contrast to the approximate value of 33,000 U/g protein measured in UHT+homogenised milk.

Similarly, using the *in vitro* model HGS, Ye *et al.* (2016a) showed the formation of different structures of the coagula formed in the simulated stomach between unheated and heated skimmed milk (90°C for 20 min). Unheated milk formed a dense, solid structure with small pores in contrast to the loose and particulate structure of the heated milk. This coagulation behaviour was not affected by the presence of milk fat as shown in the digestion of whole milk under the same conditions (Ye *et al.*, 2016b). In unheated milk, casein hydrolysis slowed down and mainly occurred at the surface of the coagulum compared to the inner part, indicating slower pepsin diffusion into the

matrix. In contrast, the loose, particulate structure of the heated milk enhanced pepsin diffusion, since more breakdown products were observed. Caseins were also degraded with digestion time in whole milk, showing that the presence of fat did not significantly change the protein network structure obtained during gastric digestion for the same concentration and milk processing conditions. Gastric behaviour also had an impact on the composition of nutrient emptying, such that whey proteins were preferentially emptied in unheated milk since they were not involved in the formation of the coagulum (Ye *et al.*, 2016a). This contrasts to the small amounts of caseins and almost no intact whey proteins that were firstly emptied in heated milk. The rate of release of fat globules from the coagulum was also influenced by the matrix structure. In whole milk, fat globules were entrapped in the protein matrix but fat globules of unheated milk were distributed more evenly within the matrix compared to those in heated milk (Ye *et al.*, 2016b). This seemed to affect the release of lipid from the coagula, which was faster in heated milk. Therefore, this study demonstrated the significant influence of heat treatment on the gastric digestion behaviour and nutrient digestion kinetics of milk. However, the heating conditions of this study (90°C for 20 min) were not comparable to those used conventionally in the milk industry, which might have different effects on changes in the protein molecular structure.

As pointed out in the previous studies, pepsin seems to play a key role in the disintegration of protein matrices in the gastric digesta. Aggregation induced by heat treatment might limit or modify the accessibility to some cleavage sites by digestive enzymes, which might affect the peptides released during digestion. There is very little research in this aspect on *in vivo* systems. Barbé *et al.* (2014b), using mini-pigs, compared the release of peptides into the duodenum from raw or heated (90°C, 10 min) skimmed milk. The number of peptides identified was slightly lower in heated milk compared to the non-heated sample. However, β- and α_{s1}-caseins, which are very similar in their sequence length and abundance in milk, produced a different number of peptides. The number of peptides deriving from α_{s1}-casein was less abundant than β-casein, showing more resistance to proteolysis probably due to differences in secondary structure and phosphorylation. This contrasts to Sánchez-Rivera *et al.* (2015), using the same samples but digested in the dynamic gastric model available in INRA (France), that found a higher resistance of β-casein regions to digestion compared to other caseins. The latter results were in accordance with the study performed by Dupont *et al.* (2010) using an infant *in vitro* static digestion. Moreover, Sánchez-Rivera *et al.* (2015) found rapid hydrolysis of caseins after just 4 min in non-heated milk whereas intact caseins were visible for up to 50 min in heated milk, which was assessed by SDS-PAGE. The authors suggested that heat induced aggregation between caseins and whey proteins might be the cause of this behaviour.

However, this is opposite to the results reported above with other dynamic gastric models. It seems that the gastric colloidal behaviour was completely different, unfortunately there was no reference to that in the study by Sánchez-Rivera *et al.* (2015). This highlights the need for full characterisation of the structure and behaviour of the matrices and also the physical and chemical environments of the dynamic models that could induce differences in the coagulation and digestion behaviour.

As illustrated, there are still conflicting results regarding casein digestion, as this appears to be sensitive to the matrix structure, which in turn is very sensitive to the environmental conditions and processing. However, the effect of heat on whey protein digestion is much simpler and more generally accepted. Native β-Lg is resistant to pepsin digestion while heating β-Lg promotes its hydrolysis. Temperatures above 75°C denature whey proteins, in particular β-Lg which unfolds and exposes hydrophobic groups. This susceptibility to proteolysis has been seen in several digestion systems; mini-pigs (Barbé *et al.*, 2013), dynamic gastric model (Ye *et al.*, 2016a) and static digestion model (Islam *et al.*, 2017). However, as far as it is known, there are no published human studies investigating this effect.

1.8.2 Dairy Microstructure Induced by Homogenisation Processing

Homogenization is another common process used in the dairy industry. Homogenisation induces very high shear rates to reduce the size of the lipid droplets, which changes the microstructure and can have an impact on nutrient digestion. Studies of the effect of droplet size on dairy nutrient digestion have been mainly performed using *in vitro* static models in particular with regard to lipolysis in infant formula and human milk (Bourlieu *et al.*, 2015). It is generally believed that the reduction in droplet size following homogenisation enhances lipid digestion because of the overall larger interface area available for lipase action. However, other factors such as protein matrix and droplet interfacial composition play an important role and it is complex to distinguish the main driver of the digestion outcomes (Garcia *et al.*, 2014).

To our knowledge, the effect of homogenisation of a milk matrix on the digestive kinetics has not been studied in adult humans to date. However, *in vitro* systems have been used to get some understanding of this relationship. Ye *et al.* (2017) using the HGS, reported very similar gastric behaviour in terms of pH and timing of coagulation when homogenised milk was compared to non-homogenised milk. The structure of the coagula in homogenised milk was more fragmented than raw milk but this effect

was much less profound than observed with heat treatment, and it did not affect the pattern of protein digestion.

The structure of the protein network in which lipid droplets are embedded seems to be a critical factor in the hydrolysis rates of lipid as previously stated. Guo *et al.* (2014) investigated the effect of the droplet size in whey protein emulsion gels in the oral and gastric compartments The different droplet size (1, 6 and 12 µm) induced a different initial gel structure; the 1 µm-droplet gel appeared to be evenly distributed and bound to the protein network compared to the 12 µm-droplet gel, which had a lower fracture force modulus. The 6 µm-droplet gel presented an intermediate structure. The oral breakdown of these samples in a human mouth showed significant coalescence and release of oil droplets for the biggest droplet size (Guo *et al.*, 2014). The gel boluses were mimicked in the *in vitro* study followed by gastric digestion using the HGS (Guo *et al.*, 2014). The initial gel structure strongly influenced its disintegration during the gastric phase, resulting in significant break down of particles and coalescence during digestion for the 6 µm- and 12 µm-droplet gels, which caused the creaming observed after 300 min of gastric digestion. In contrast, the oil droplets of the 1 µm-droplet gel bolus largely remained within the protein matrix during gastric digestion. Moreover, the hydrolysis rate of whey proteins was higher in 12 µm-droplet gel. This could be attributed to the loose protein structure induced to the higher droplet size, which could promote the access to pepsin to the cleavage sites.

The effect of the droplet size in relation to colloidal stability in gastric environment has been less studied which can be attributed to the limitations of *in vitro* systems, in particular static models. Some clinical studies have shown a significant impact of emulsion droplet size and intragastric stability not only on nutrient delivery and absorption (Golding *et al.*, 2011; Marciani *et al.*, 2007) but also on satiety (Marciani *et al.*, 2008), and subsequent regulation of energy intake (Hussein *et al.*, 2015). In general, emulsions that were stable in the gastric environment emptied more slowly from the stomach, which was regulated by hormonal feedback from the duodenum. Steingoetter *et al.* (2015). reported that a reduction in droplet size by two orders of magnitude (0.3 versus 52 µm diameter) delayed GE by 38 min for acid-stable emulsions in a human trial. Moreover, smaller droplet diameter (0.7 µm) emulsions facilitated lipid digestion of TAG in the stomach (20-37%) and proximal small intestine (57-73%), compared to lipid droplet size of 10 µm (7-16% in gastric and 37-46% in duodenum) due to the larger surface area (Armand *et al.*, 1999), suggesting an increase in fatty acid sensing. Nutrient sensing was linked to hormonal response feedback mediated in particular by CCK (Ledeboer *et al.*, 1995; Seimon *et al.*, 2009), which enhances the perception of satiety and reduced subsequent energy

intake. These human studies demonstrated that the gastric stability and particle size of food emulsions greatly impacts the transit of lipids throughout the GI tract and might further influence satiety and food intake. Unfortunately, these studies did not include any dairy based ingredients or it was not the focus of the study. This highlights the gap of knowledge in understanding the physiological response to consumption of dairy structures.

Regarding dairy-based systems, Peters *et al.* (2014) studied the effect of droplet size (3 versus 0.1 µm) in a milk shake. They did not find any significant effect in CCK released, satiety and food intake for 180 min after drink ingestion. This is in contrast to the significant enhancement in satiety for the smaller size droplets observed by Maljaars *et al.* (2012). In the latter study, the same milk shake but without lipid was orally administered and the lipid droplets were infused directly to the small intestine. In the Peters *et al.* (2014) study the sample including protein could potentially coagulate in the stomach entrapping the lipid droplets, which could delay or change the effect on satiety that was expected. Unfortunately, the gastric behaviour was not investigated in the study. Again, this illustrates the crucial importance of studying the gastric phase and the importance of the effect of the matrix within which the components of interest are arranged.

Droplet size is also thought to influence food intake behaviour as previously mentioned. However, the study of satiety is quite complex because it also involves cognitive factors as well as physiological factors. Lett *et al.* (2016b) aimed to modulate satiation and satiety by controlling oil droplet size ($d_{4,3}$ of 2 versus 50 µm) of an emulsion (1% wt sodium caseinate and 15% wt sunflower oil). This aimed to enhance satiety using small droplet size by increasing the perception of creaminess via enhancing hedonic appeal. They did not find significant differences in sensory characteristics, which contrasts with their previous study (Lett *et al.*, 2016a). However, interestingly, the smaller droplet size within an emulsion preload resulted in a significant reduction in food intake (62.4 kcal) at a subsequent *ad libitum* meal. The authors did not find any conclusive primary mechanism responsible for this effect on satiety, but it is likely from earlier discussions, that this difference in droplet size would affect the lipid profile emptied from the stomach, and the subsequent feedback and control of gastric emptying could influence satiety. This highlights the complexity of investigating appetite behaviour because of the multiple physiological and sensory factors involved, referred to as the "satiety cascade".

The literature reviewed in this section illustrated the significant effect of dairy processing by heating and droplet size modulation on nutrient digestion kinetics. However, the underlying mechanisms are not fully understood. Regarding heat

processing, only drastic temperatures seem to have significant effects on protein bioavailability as reported by the increase of N availability and utilisation in the body after high heat treatment in humans. There is evidence suggesting that gastric digestion play a critical role, however physiologically relevant gastric models and samples that reflect commercial conditions need to be used. The important role of pepsin, and the mechanisms by which it controls this process needs to be further investigated. The diffusion of pepsin into the structures formed in the stomach has rarely been studied, but this would help to further understand the precise mechanisms controlling protein digestion in the stomach, and how this affects the nutrient absorption kinetics. Also, the effect of heat on casein digestion is still controversial and needs further investigation taking into account the digestion model and heating conditions. Moreover, there are no reports about the effect of heat treatment on satiety in dairy products.

Homogenisation has been observed to cause a profound effect on milk gastric behaviour *in vitro* but it needs confirmation in humans. It is generally accepted that lipolysis is enhanced by reduction of droplet size, however, the physical properties of protein networks and their interactions with lipid droplets seem to play a critical role and also needs to be studied in this context. This is required not only in process engineered structures but also those induced in the gastric environment. Therefore, the effect of droplet size should be investigated in a food matrix to assess the gastric colloidal behaviour that will impact not only on lipid absorption rate but physiological responses such as satiety.

1.9 Dairy Macrostructures and Digestion, Absorption and Physiological Responses

1.9.1 Liquid *vs* (Semi)Solid Structures and Digestion

The processing procedures applied to milk can induce different physical structures of semi-solid and solid texture such as yogurt and cheese, showing different rheology that might influence nutrient release and absorption. Scanff *et al.* (1990) showed, using calves, that casein in milk was retained for a long time in the stomach after coagulation and released later in the form of small and large peptides. By contrast, in yogurt, caseins were emptied constantly from the stomach in both intact and degraded forms. In humans, Mahé *et al.* (1994) compared the digesta of proximal jejunum and terminal ileum between milk and yogurt. They found, in milk, an early emptying of whey proteins, which remained in solution whereas casein

coagulated. In contrast, the greater viscosity of yogurt provided a more delayed and regular release of nitrogen into the duodenum compared to milk. This was suggested to be due to the different gastric emptying pattern, the gastric half emptying time (measured using ^{14}C-PEG-4000) was shorter in milk (35 min) than in yogurt (60 min). However, this did not affect the overall extensive digestion of milk proteins from both matrices; approximately 91% of N was absorbed between the stomach and the terminal ileum in 240 min. These outcomes were supported by Gaudichon *et al.* (1995) in humans and mini-pigs (Gaudichon *et al.*, 1994), in which the dependence of liquid to solid ratio of the gastric digesta in GE was highlighted. The viscosity of yogurt also influenced the postprandial lipid profile in humans by delaying the peak in plasma TAG whereas milk provided a lower but more long-lasting rise of TAG in plasma (Sanggaard *et al.*, 2004). Interestingly, Mahé *et al.* (1994) reported, in humans, that the absorption of calcium in the duodenum was significantly higher after ingestion of yogurt (67%) compared to that of milk (44%), probably due to a higher casein availability in yogurt. This shows that the effect of intestinal delivery rates does not only affect macronutrients but micronutrients as well.

Using similar macrostructures, Barbé *et al.* (2013) compared the effect of unheated skimmed milk and its correspondent gel produced using rennet in mini-pigs. The gel matrix ingestion induced significantly lower and prolonged Leu levels in plasma throughout a 7-hour period after meal ingestion, whereas the liquid structure peaked after 30 min of meal ingestion. It was suggested that the gel structure could slow down proteolysis and AA absorption, which could be reflected physiologically. However, the levels of the GI hormones measured in this study, CCK and Ghrelin, did not present any significant difference between the matrices over a 4-hour period after meal ingestion. Despite the different AA uptake rate that was obtained, the authors found no significant differences in the mean retention time in the stomach. The measurement was based on chromium-EDTA, which is a non-hydrolysable and non-absorbable marker of the liquid phase, which might not be representative of the entire gastric phase contents of the heterogeneous structures formed in the stomach. The effect of these matrices (milk liquid versus gel) was further studied in relation to the pattern of peptides released into the duodenum at different times using mini-pigs (Barbé *et al.*, 2014b). The authors reported that the food matrix did not affect the accessibility of enzymes to the cleavage sites as seen, due to the identification of the same peptides over the digestion time but the structure had a great impact on the quantity of identified peptides. The gel structure presented lower amounts of free AAs but higher number of peptides, when compared to the matrix ingested in a liquid state, even though the latter was supposed to coagulate in the stomach. The mechanisms behind these results were not clearly identified, which illustrates the difficulty of

interpretation of results in a system with several contributory factors, such as matrix structure, gastric restructuring and emptying and enzyme accessibility. The mechanisms behind the results of these dairy structures were investigated by mathematical modelling, which accounted for the main digestive events including gastric behaviours of coagulation and syneresis in the stomach (Le Feunteun *et al.*, 2014). It was shown that the gastric retention controlled by the physico-chemical properties of the matrices was the limiting step explaining the differences in the mini-pig data. Importantly, the gastric phase was determined to have the crucial, rate-limiting effect in explaining the kinetics of AA absorption observed *in vivo*.

1.9.2 Liquid *vs* (Semi)Solid Structures, and Appetite

Only a few studies have investigated the impact of the physical structure of dairy matrices in relation to appetite. Sanggaard *et al.* (2004), did not find any difference in appetite sensation, measured by visual analogue scale, and insulin and glucose between yogurt and whole milk in eight healthy men, despite the significant slower rate of GE observed after yogurt consumption. However, the level of GIP was twice higher in yogurt between 30 and 120 min but the measured gut hormones remained elevated for longer time after milk ingestion, in agreement with the postprandial lipid profile. The rapid first emptying of whey proteins and the subsequent slow emptying of the casein coagulum might counteract the effect of viscosity in the yogurt with the more homogenous nutrient emptying and lead to similar appetite sensations. Dougkas *et al.* (2012) studied the effect of three isocaloric dairy products (semi-skimmed milk, yogurt and cheese) consumed as a snack on appetite and subsequent *ab libitum* lunch energy intake in overweight men. The yogurt intake reduced the rating of hunger of 8 and 10% compared with cheese and milk, repectively, whereas they did not present any difference in the overall energy intake or the satiety hormones of ghrelin, PYY and insulin. Similarly, Mackie *et al.* (2013) compared two isocaloric samples (same lipid, protein and carbohydrate content) with a different physical structure. The liquid sample was a milk protein-stabilised emulsion and the semi-solid sample was a mixture of grated cheese and yogurt. The authors showed a different behaviour in the stomach using MRI; the semi-solid matrix presented sedimentation whereas liquid matrix presented creaming. The semi-solid sample promoted greater fullness over the three-hour study, which was linked to the volume of the gastric contents remaining by the slower GE rate over the first hour. However, the effective reduction of hunger of the semi-solid meal was not reflected in the plasma CCK level, which was lower over the first hour and then similar for both meals. This shows that the rationale of the satiety biomarkers does not always guarantee high perceived

satiety, since there is not a mathematical association (Veldhorst *et al.*, 2008). As occurs in many clinical studies, a complete understanding of the underlying mechanisms of the physiological responses in combination with the fate of digestion is difficult. For instance, the evaluation of the nutrient delivery during gastric digestion could provide useful information to shed light on the *in vivo* observations. This could more conveniently be performed in suitable *in vitro* systems. Therefore, the approach of combining the strengths of *in vivo* and *in vitro* models could provide more relevant data in order to understand the mechanisms linking food structure and physiological responses.

Currently, there are no conclusive results of the impact of dairy products on appetite and energy intake, and research of the satiating power of solid versus liquid matrix remains inconsistent (Almiron-Roig *et al.*, 2003). The potential for dairy products to help individuals control body weight needs further investigation, which should importantly include the study of the behaviour in the stomach. Also, the study of the rate of GE usually provides contradictory outcomes when compared to the rate of nutrient absorption; most of the labelled substrates used only reflect the behaviour of the liquid phase of the digesta so it is important to understand the structural changes of the whole food matrix within the stomach.

1.9.3 (Semi)Solid Structures with Different Textures

Protein gel texture induced by processing might affect disintegration kinetics during gastric digestion and subsequent AA bioavailability. Guo *et al.* (2015) used the HGS to study the gastric disintegration between two whey protein emulsion gels, i.e. hard gel (69.9 N hardness) and soft gel (19.2 N hardness). Prior to the gastric digestion simulation, the samples went through an oral phase simulating the bolus obtained in an *in vivo* study (Guo *et al.*, 2013). In the gastric phase, the soft gel disintegrated faster than the hard gel, suggesting that the main mechanism of disintegration for hard gel was abrasion whereas soft gel presented both abrasion and fragmentation during gastric digestion. The disintegration in the stomach was accelerated by the action of pepsin, in particular after 180 min of digestion for the soft gel. This could be attributed to the weakly crosslinked protein structure observed in the soft gel, compared to the intimately linked protein matrix of the hard gel, which could hamper pepsin accessibility. However, the rate of hydrolysis measured by SDS-PAGE did not present significant differences, but it could have an impact on the type of peptide released. The behaviour of the gastric disintegration had a significant impact on the GE, which was related to the retention of solids in the HGS as a function of time. The GE was faster in soft gel after 180 min of digestion whereas the gastric

content retention before 120 min in soft gel was higher, which was attributed to a larger particles size of the original bolus (Guo *et al.*, 2013). This shows the relevant importance of the oral phase in the process of gastric disintegration. The rate of GE between the matrices was almost the same at the end of gastric digestion (300 min) indicating that slower emptying of the soft gel at the beginning of digestion due to particle size of bolus was compensated by the more rapid disintegration due to easier hydrolysis by pepsin. Similarly, a recent study using pigs investigated the effect of viscosity in yogurt on GE by gama scintigraphy and protein digestion using the dynamic model DIDGI® (Ménard *et al.*, 2018). The low and high viscosity yogurt with the same nutrient composition but different viscosity (2.2 versus 0.3 Pa·s) were compared a control yogurt with lower protein and fiber content, and intermediate viscosity (1.3 Pa·s). The authors showed that the enrichment of protein and fibre slowed down GE whereas the viscosity seemed not to be a controlling parameter in emptying since low and high viscosity yogurts presented no significant difference. However, since the control yogurt differed in both nutrient composition and viscosity, it is not possible to draw any conclusive outcome. Moreover, the pepsin hydrolysis of whey proteins was higher in the high viscosity yogurt compared to the low viscosity sample, which was suggested by the authors to be due to the different behaviour observed when entering the small intestine.

The mode of gelation applied might affect the protein network structure of the gel. Barbé *et al.* (2014a), using mini-pigs, compared the gel structure obtained from skimmed milk powder using rennet (cheese model) and acidification (yogurt model) coagulation. The rennet gel led to lower levels of milk protein, in particular casein, released in the duodenum. The Leu level in plasma was also significantly lower throughout a 7-hour period after rennet gel ingestion compared to the acid gel. The authors linked these results with a possible formation of a more compact chyme of rennet gel in the stomach. They observed, using a dynamic gastric model, that the acid gel formed with no apparent syneresis in contrast to the extensive syneresis observed in the rennet gel. The hardness of rennet gel could imply a longer gastric retention time. However, the measured mean residence time in the stomach based on chromium-EDTA did not show any difference between the two matrices. Again, this measurement may not be representative of the difficult analysis of heterogenous systems. The different bioavailability of AAs could then be attributed to the different starting pH of the meals; the acidity of the acid gel (pH 4.0) could favour pepsin hydrolysis compared to the rennet gel (pH 6.6). There was no significant difference in the postprandial CCK level whereas the level of ghrelin was significant lower in the rennet gel compared to the acid gel, which might potentially enhance satiation and be

linked with a higher gastric distension. This shows the complexity of linking structuring in the stomach, GE, nutrient absorption and physiological responses.

When lipid is included in the food matrix, the protein matrix is not only important for protein digestion but might also affect lipid digestion in the intestine. Guo *et al.* (2015) studied, in whey protein emulsion gels (hard versus soft), the effect of gastric disintegration using HGS on lipid bioaccessibility during a simulated intestinal digestion. The gastric digesta at 60 and 240 min were used for *in vitro* intestinal digestion performed for 150 min. The size of the gel particles was reduced after 60 min of gastric digestion in both samples but the initial rate of lipolysis of the soft gel was significantly higher than the hard gel, even though the solid content of that digesta was lower. At 240 min, the digesta from the soft gel consisted of individual oil droplets as well as smaller particles, compared to the hard gel in which most of the oil droplets remained within the protein network. This study indicated that protein network modulates the release of oil droplets and can limit the access to the droplet's surface by pancreatic lipases.

Examples of dairy products in which oil droplets are dispersed in a solid protein matrix are yogurt and cheese. The influence of the protein matrix on the release of lipids might impact absorption and lipaemia, which can have potential effects on risk markers of cardiovascular diseases. Drouin-Chartier *et al.* (2017) compared the lipid absorption from hard and soft cheeses and butter, matched in total calories and macronutrient content. There were no differences in serum TAG, FFA and apoB-48 in the incremental area under the curve over 8 hours. However, it seemed that the soft cheese induced greater increase in TAG concentration at 2 hours and attenuated the low dense lipoprotein of apoB-48 compared to the firm cheese. These results showed that the physical structure may not necessarily influence the overall magnitude of postprandial lipemia but more importantly the timing and magnitude of the TAG peak value. This could be related to the protein network and lipid droplet arrangement within the cheese matrix. The authors suggested that the homogenised lipid droplets in soft cheese are enclosed in a loose protein gel, which causes easier access for both pepsin and gastric lipase in the stomach. Moreover, the lipid droplets were smaller, giving the food an overall larger surface area, which might facilitate lipolysis. Interestingly, they did not find any differences between hard cheese and butter. This could be attributed to a limited availability of the nutrients; hard cheese could take longer to be disintegrated in the stomach and the formation of layering could be possible in the case of butter delaying the delivery of lipid. Similar results were obtained in a study comparing milk, butter and mozzarella-cheese (Clemente *et al.*, 2003). There was no significant difference in the average of postprandial plasma

TAG but in the peak time (315, 277 and 225 min for butter, mozzarella and milk respectively). This contrasts with the GE rate, using ultrasonographic measurements of the antrum-pylorus section, in which mozzarella cheese presented a faster emptying compared to milk and butter. This study showed that GE might not play a critical role in modulating postprandial lipids in blood, using this specific methodology. However, it should also be noted that the study was performed with type 2 diabetic patients, which could modify the outcome when compared with healthy subjects. It is important to note that lipemia can be affected by other factors such as fatty acid composition (degree of saturation and length of fatty acid chain) and the properties of the lipid droplet interface.

There are some studies suggesting that the consumption of fat in cheese form has different effect on blood lipids by reducing low density lipoprotein cholesterol, when compared to the same amount of fat consumed in butter form (Hjerpsted *et al.*, 2011; Tholstrup *et al.*, 2004). Indeed, Feeney *et al.* (2018) showed that dairy fat in form of cheese lower the total cholesterol levels compared with that of equal amount of fat, casein and calcium content in different matrices, suggesting the synergistic effect of the constients in the cheese matrix. The role of calcium in the fat absorption has been seen one important factor controlling the metabolic responses observed (Thorning *et al.*, 2016) but this has to be proven in humans and, in general, more research is needed to understand the role of the food matrix on gastric digestion and lipaemia, and metabolic effects, which should be in the context of the lipid/protein organisation and interaction and their behaviour in the gastric compartment.

In conclusion, this section illustrated that dairy products with different physical structures can affect the rates of nutrient hydrolysis as well as absorption, which is mainly driven by the physico-chemical effect of the structure on gastric digestion. It seems that solid and semi-solid dairy structures have slower digestion than liquid meals. However, the restructuring of liquid meals in the stomach through, for instance coagulation and phase separation, should also be considered. Moreover, factors of the initial food matrix such as hardness, viscosity and pH are also relevant for the breakdown of the food, and how these properties evolve within the GI tract are crucial in nutrient digestion. For instance, studying the rheological properties of the chyme during gastric digestion could provide valuable information about the effect on gastric digestion time. Protein digestion is usually overlooked when assessing lipid digestion in complex matrices. However, research has shown that disintegration of a protein matrix in the stomach is crucial for lipid accessibility and subsequent digestion. This is important not only for the initial design of structures but also the structures that can be formed within the gastric compartment. It has been evident from the literature that

there is a complex relationship between structuring in the stomach, the content and rate of nutrients emptied from the stomach and the rate of nutrient absorption. This could be due to the methodology used for measuring GE and also the characterisation of the food matrix. It is difficult to assess both absorption of nutrients and bioaccessibility in relation to gastric behaviour. For that, using both *in vivo* and relevant *in vitro* gastric digestion systems could be an interesting approach to gain more insight into the mechanisms of nutrient digestion. There is currently no evidence of how the different physical dairy structures can influence nitrogen metabolism, and also, more research on satiety responses is needed. Moreover, some research in cheese (Fang *et al.*, 2016; Lamothe *et al.*, 2012) has shown that lipid digestion rates can depend on the hardness, cohesiveness and elasticity of the cheese type, which constitutes an important factor in gastric disintegration. However, these studies applied an *in vitro* static model for digestion and there are no clinical studies showing this influence.

1.10 Research aims

This thesis tackled the hypothesis that dairy structures exhibit different physiological responses through the impact of gastric behaviour resulting in different kinetics of nutrient digestion. The work described aimed at gaining fundamental insights in this new direction of understanding the behaviour of food structures in the stomach for controlling nutrient digestion. Milk and dairy products are widely consumed and are associated with several physiological effects, but the mechanistic understanding of this association is lacking. Dairy matrices cover a wide array of structural levels from macrostructures to microstructures to the molecular level of the milk proteins. Research literature has suggested that milk and dairy structures might have a profound effect on gastric digestion, but better evidence is required. The work described in this thesis was carried out at the Quadram Institute Bioscience (the former Institute of Food Research) in Norwich (UK), Teagasc Food Research Center in Fermoy (Ireland) and the School of Food Sciences and Nutrition at University of Leeds in Leeds (UK).

The main objectives of this research were as follows.

- To develop an *in vitro* model that could closely simulate the dynamic processes of the human stomach, i.e. an intermediate model between the static and fully dynamic models, which could apply the strengths of both systems. This work has been described in Chapter 3.

- To determine the gastric behaviour of whey proteins and caseins and different blends, and the possible impact on intestinal digestion and absorption of nutrients. Then, to understand the key limiting factors controlling the rate of absorption of milk proteins (e.g. gastric emptying, luminal hydrolysis, AAs mucosal absorption). Also, to investigate whether lipid inclusion in milk protein matrices affects gastric restructuring and the possible influence on intestinal digestion and absorption of nutrients. This work has been detailed in Chapter 4.

- To evaluate the effect of processing of milk under controlled and commercial conditions (UHT, pasteurisation and homogenisation) on the gastric behaviour and nutrient digestion kinetics. This work has been described in Chapter 5.

- To determine the mechanisms by which pepsin acts during the gastric digestion of commercial milk samples. This work has been shown in Chapter 6.

- To validate the *in vivo-in vitro* correlation approach by identifying the mechanisms of physiological responses observed in dairy macrostructures, which could also allow investigation of the efficacy and usefulness of the developed semi-dynamic model. This work has been described in Chapter 7.

Chapter 2

General Materials and Methods

2.1 Materials

The common materials used in most experiments are included in this chapter. The materials specific to each chapter have been included in the corresponding chapter.

2.1.1 Chemicals

Pepsin from porcine gastric mucosa (lyophilized powder), pancreatin from porcine pancreas (8x USP specifications), bovine bile (dried, unfractionated) were obtained from Sigma-Aldrich Chemical Co. (St. Louis, MO, USA). The enzyme activities and bile salt concentration were measured according to the assays detailed in Minekus *et al.* (2014). Purified Milli-Q® water was used. The electrophoresis reagents were obtained from Invitrogen™ (Life Technologies Corp., CA, USA). All other chemicals used in different experiments were of standard analytical grade and purchased from Sigma-Aldrich Chemical Co., unless otherwise specified and used without further purification.

2.2 Methods

This section presents the common methods for most of the experiments used in this thesis. It provides a description of the basic, general principles behind each method and instrument. Also, the general protocol is described when a method was applied in more than one chapter. Any modifications of the general protocol are detailed in the methods section of the corresponding experimental study chapter.

2.2.1 Emulsion Processing

An important part of this project was the use of emulsions as the starting material. Both naturally occurring such as milk or produced using milk proteins and lipids. For that, a brief explanation of how they are formed in relation to the instruments that were used is provided.

An emulsion is defined as a colloidal dispersion of liquid droplets in a liquid continuous phase. In food systems, oil-in-water (O/W) and water-in-oil (W/O) emulsions are the two main types of emulsions. In O/W emulsions, oil is dispersed as finely droplets in the continuous phase of water (Dickinson, 1992) and milk is an example of this type of system.

In an emulsion, an interfacial layer between the different phases is formed in which surface-active compounds can be arranged in order to prevent the emulsion instability. An unstable emulsion can lead to changes in the structure or size distribution of droplets. Common processes of instability in emulsions are: creaming, sedimentation, flocculation, coalescence and phase separation (see Figure 2.1). Biochemical factors such as pH, salt concentration and enzyme hydrolysis can induce those changes. Therefore, the instability processes might occur in the gastrointestinal tract (McClements *et al.*, 2010).
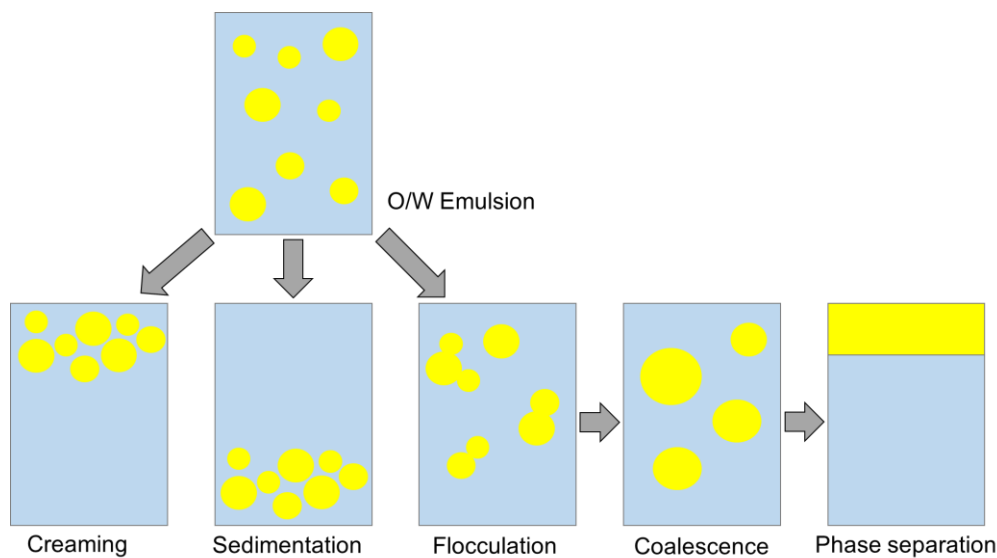
Figure 2.1 Schematic representation of the main mechanisms of instability of an oil-in-water (O/W) emulsion, i.e. creaming sedimentation, flocculation, coalescence and phase separation. (Yellow and blue represent lipid and water phases, respectively).

The most commonly used emulsifiers in food systems are proteins, polysaccharides and small molecule surfactants (Dickinson, 2013). An emulsifier is an amphiphilic molecule and is effective firstly when it adsorbs to the surface of the droplet and reduces the interfacial tension of the emulsion droplet interface. Secondly, it forms a protective layer surrounding the droplets providing stability against coalescence and flocculation via electrostatic and steric stabilization mechanisms (Dickinson, 1992).

An emulsion cannot be formed spontaneously (except for microemulsions which are a special case) therefore mechanical energy approaches are normally needed in order to break up the lipid phase obtaining a homogenous dispersion of oil droplets with diameters usually ranging between 0.1 and 100 µm. The three main approaches to create emulsions are: pressure (e.g. high-pressure valve homogeniser), mechanical (e.g. high-shear mixer) and ultrasonic homogenisation. Food emulsions are usually prepared using a range of methods (Walstra *et al.*, 1997), which depends

mainly on the nature of starting material, size and properties of emulsion droplets. The most commonly used device in the food industry is a high-pressure valve homogeniser because it can offer effective control of size distribution of the resultant emulsion. The homogenisers used in the project were high-pressure valve type with both one or two stages. A premix step is necessary previous to the homogenisation step, but it was not required when milk was used since it is already an emulsion. In Chapter 4, a one-stage homogeniser, APV 1000 (SPX Flow Technology North Carolina, USA) (see Figure 2.2) was used for processing the dispersions of milk protein solution and some lipid. In the case of Chapter 5, a two-stage homogeniser was used in milk processing, which is generally used to manufacture dairy products because of its ability to effectively minimize droplet size. When homogenisation was applied in combination with heat treatment, a tubular heat exchanger MicroThermics® (MicroThermics®, NC, USA) with in-line homogeniser was used, Model NS 2006H (Niro Soavi, Parma, Italy) (see Figure 2.3). An independent 2-stage homogeniser, Gaulin Labor, Lab 60 type (APV Gaulin GmbH, Lubeck, Germany) (see Figure 2.4) was used when homogenisation was applied separately. This was just due to practical convenience and their basic operating conditions are the same. In general, in a two-stage homogeniser, the first stage is used to force the system through a small orifice, between a valve and seat, at a high pressure (See Figure 2.5). During this stage, there is dramatic reduction in lipid droplet size due to shear stress, inertial forces and cavitation (Michalski *et al.*, 2006). In the second stage, the homogenization pressure is lowered to disperse the possible lipid droplet aggregates that could be formed at the first stage and it helps to maintain backpressure. The specific settings used are described in the corresponding chapters.

Figure 2.2 Lab scale one-stage valve homogeniser, APV 1000 (SPX Flow Technology, North Carolina, USA).

Figure 2.3 MicroThermics® tubular heat exchanger (MicroThermics®, NC, U.S.A). using an in-line two-stage valve homogeniser, Model NS 2006H (Niro Soavi, Parma, Italy).

Figure 2.4 Two-stage homogeniser, Gaulin Labor, Lab 60 type (APV Gaulin GmbH, Lubeck, Germany).
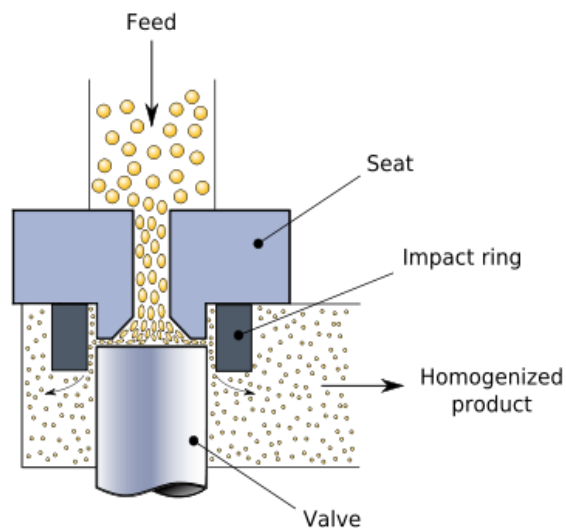
Figure 2.5 Schematic representation of the homogenisation mechanism by high-pressure valve approach.

2.2.2 *In Vitro* Digestion and *ex Vivo* Nutrient Transport

In vitro digestion experiments are very useful to investigate the effect of food structure and composition on digestion. The following methods describe the different *in vitro* systems used for the simulation of gastrointestinal (GI) digestion.

2.2.2.1 *In Vitro* Gastric Digestion

The gastric phase was simulated using a semi-dynamic gastric model, which was developed during this project. Details about the model are described in a separate chapter (Chapter 3). The general protocol was as follows.

The oral phase was simulated before the gastric digestion. 20 g of sample was mixed with a volume of the oral mixture containing 79.9% SSF (1.25x) prepared according to Minekus *et al.* (2014),19.6% MilliQ® water and 0.5% $CaCl_2(H_2O)_2$ (0.3 mol/L). The volume of this oral mixture corresponded to the total solids content of the sample (previously measured using CEM Smart Trac System-5 (CEM Corp., Matthews, N.C., U.S.A.). The mixing was performed using a rotator (SB3 Model, Stuart, Bibby Scientific, UK) at 30 rpm for 2 min. The temperature was kept at 37°C using an incubator (BF56, Binder GmbH, Germany).

The resulting mixture was then put through the gastric digestion using a reaction vessel for the simulation of the stomach, which was a v-form glass vessel (5-70 mL titration vessel, Metrohm, Switzerland) with thermostat jacket (37°C). The sample from the oral phase was placed in the reaction vessel after the addition of the basal volume, which consisted of the 10% of the constituents of SGF (1.25x), MilliQ® water, HCl (1.5 mol/L) and $CaCl_2(H_2O)_2$ (0.3 mol/L) from the total volume of the gastric mixture. The total gastric mixture contained 80% SGF (1.25x), 7.78% MilliQ® water, 8.7% HCl (1.5 mol/L) and 3.48% pepsin and 0.04% $CaCl_2(H_2O)_2$ (0.3 mol/L). Two solutions were added at a constant rate, which depended on the corresponding gastric time: (1) the simulated gastric electrolyte mixture containing the 90% of the constituents of SGF (1.25x), MilliQ® water, HCl (1.5 mol/L) and $CaCl_2(H_2O)_2$ (0.3 mol/L) from the total volume of the gastric mixture and (2) 0.8 mL pepsin solution (made with MilliQ® water). The simulated gastric electrolyte mixture of SGF (1.25x), HCl, water and $CaCl_2(H_2O)_2$ was delivered by a dosing device of an automatic titrator (brand specified in each chapter) and the enzyme solution was delivered by a syringe pump (brand specified in each chapter). A 3D action shaker (Mini-gyro rocker, SSM3 Model, Stuart, Barloworld Scientific limited, UK) set at 35 rpm was used for agitating the vessel.

Gastric emptying (GE) was simulated by taking five aliquots, as the general protocol, referred to as GE1-5 in the text. Aliquots were taken from the bottom of the vessel using a laboratory tool (specified in each chapter) that had an inner diameter of approximately 2 mm. The pH was measured and a sufficient volume of NaOH (2 mol/L) was added to the samples to increase the pH above 7, inhibiting pepsin activity.

Finally, samples were snap-frozen in liquid nitrogen and stored at -20°C for further analyses.

The simulation of the emptying was based on caloric density, as the general protocol. A linear GE rate of 2 kcal/min, which is considered the average caloric content that is emptied *in vivo* in a regulated manner by the antrum for an average food volume of 500 mL (Hunt *et al.*, 1985) was used and scaled down for this reduced-volume system (20 mL of sample).

2.2.2.2 *In Vitro* Small Intestinal Digestion

Small intestinal digestion was performed following the standardised static INFOGEST protocol (Minekus *et al.*, 2014), including the preparation of simulated intestinal fluid (SIF) and proportions added of the rest of the intestinal phase components. However, the current procedure was performed individually in each GE aliquot from the gastric digestion in order to assess the kinetics of nutrient digestion in the small intestine. This methodology will be illustrated and explained further in Chapter 3 and the corresponding experimental chapters. The general protocol was as follows.

The simulation of the intestinal phase was performed using the individual GE aliquots. The protocol was performed according to the standardised procedure of Minekus *et al.* (2014). The amounts of pancreatin solution, bile salt and $CaCl_2$ $(H_2O)_2$ were adjusted in each case depending on the gastric aliquot volume in order to get a final activity/concentration of 100 U/mL (based on trypsin), 10 mmol/L and 0.6 mmol/L, respectively. Samples were placed in a rotator (SB3 Model, Stuart, Bibby Scientific, UK) at 40 rpm within an incubator (BF56, Binder GmbH, Germany) to keep the temperature at 37°C. Aliquots (volume and time specified in each chapter) were taken, mixed with inhibitor (0.1 mol/L phenylmethylsulfonyl fluoride), snap-frozen using liquid nitrogen and stored at -20°C for further analyses.

2.2.2.3 *Ex Vivo* Absorption

The Ussing chamber methodology was applied to study absorption of amino acids by *ex vivo* murine small intestinal tissue. The principles of the technique have been described in this section since it is not widely used. The detailed protocol has been described in Chapter 4.

The Ussing chamber was developed by Hans Ussing in 1951 to investigate the ion transport across frog skin. Its application has increased to include measuring the transport of electrolytes for instance. However, it has not often been used to study a

food-related system on health. In Chapter 4, the Ussing chamber methodology was used to assess the absorption of amino acids across murine small intestinal tissue after gastric digestion and *in situ* intestinal digestion (See Figure 2.6). However, this technique could be also used to study the transport of other nutrients such as glucose, fatty acids and vitamins across a range of animal species intestinal tissues, including rat, pig and human (Geraedts *et al.*, 2012; Neirinckx *et al.*, 2010). It can be also used to study other functionalities of epithelia tissue, e.g. protective and secretory.
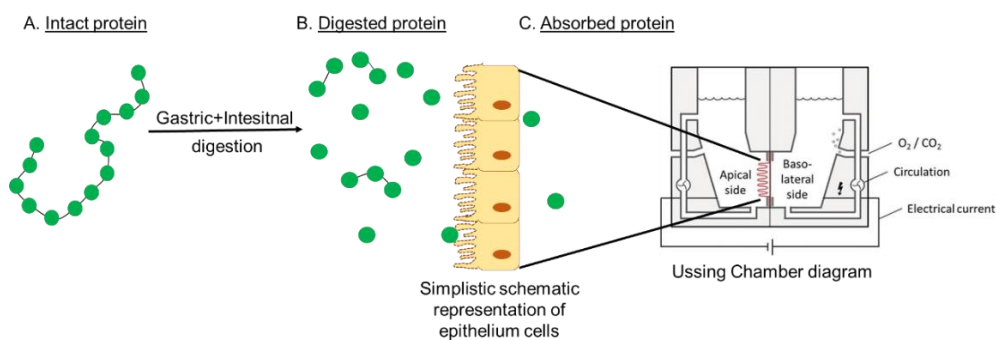
Figure 2.6 Schematic representation of the use of Ussing Chamber technique to study protein absorption after gastric and intestinal digestion. A tissue section of intestinal epithelium containing epithelium cells separates the apical and basolateral sides of the Ussing chamber. (Ussing chamber diagram from Verhoeckx *et al.* (2015)).

The *ex vivo* methodology of the Ussing chamber provides a better representation of the *in vivo* situation, when compared to the most used epithelial Caco-2-cells, since the use of intestinal tissue segments offers the morphological and physiological features of the intestinal wall, including the multicellular conglomeration and presence of the mucus layer. This allows the direct measurement of nutrient uptake. Moreover, it is a simpler and, less expensive and restrictive than the *in vivo* approach. However, some of the weaknesses are, the relatively low throughput to get an interpretation of the complex physiological system and dependence on the optimal function of the intestine section preparation. Also, the viability and integrity of the tissue is limited, and it is more difficult than other *in vitro* systems to compare results due to inter-individual variability among animals (Neirinckx *et al.*, 2010). Tissue from animals is usually used since the availability of healthy human tissue is very limited, so data is extrapolated.

The basic design of an Ussing chamber (Figure 2.7) consists mainly of a U-shaped chamber, perfusion system and electrical circuitry. The chamber consists of two halves, between which the tissue is placed in a removable slider with pins. This separates the two halves of the chambers; the mucosal membrane, also named apical side, is orientated to one chamber half, whereas the serosal membrane, also named basolateral side, is facing the other half-chamber. The size of the chamber/slider

depends on the origin of the tissue being used. The electrical circuitry consists of four electrodes (two Ag-AgCl electrodes for voltage and two Ag electrodes for current) in each chamber connected by means of an agar-bridge. There is a continuous flow of gas (95% O_2/ 5% CO_2 mixture) that causes bubbles. This allows the circulation and oxygenation of buffer/sample throughout the system. The system is held at 37°C by means of water jacket heating. Further description of the methodology can be found in Hug (2001).
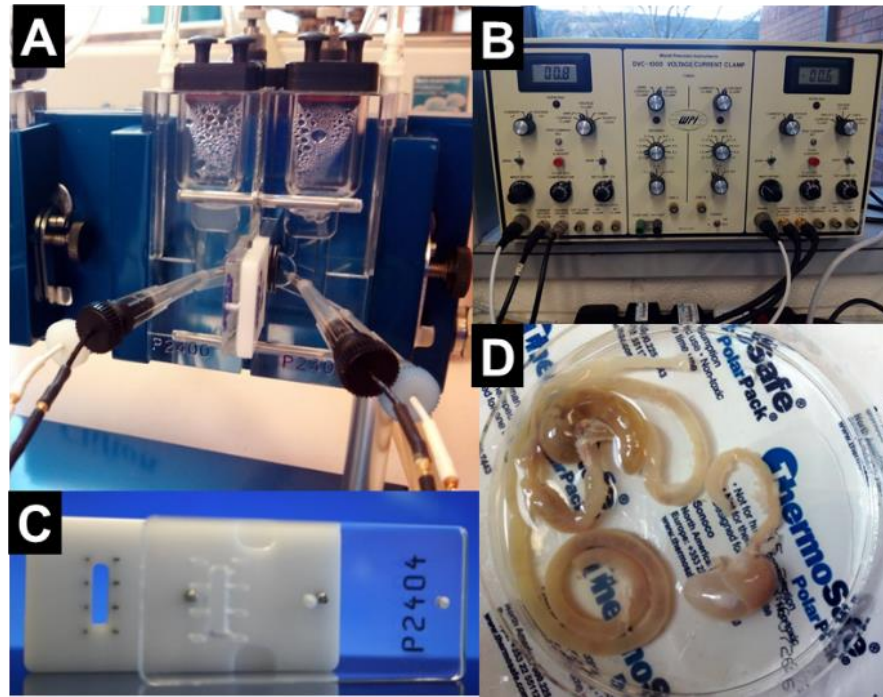
Figure 2.7 (A) The setup of the Ussing chamber and (B) the electrical system. (C) A slider used for mounting a section of murine intestine and (D) an example of the murine digestive tract used for dissecting a section.

The principle underlying the use of Ussing chamber stems from the polarity and tightness of epithelia allowing the active transport of the nutrients. The asymmetric distribution of proteins across both apical and basolateral membranes generates this polarity. The disposition and permeability of tight junctions, which hold the cells together, determine the resistance known as transepithelial resistance and integrity of the tissue. The transepithelial resistance is monitored during the experiment, which can be calculated by knowing the voltage and the transepithelial current from the voltage clamp. The resistance is normalised per unit area.

2.2.3 Physical Properties Analysis

The analysis of some physical properties of the dairy systems were determined to provide better understanding of the digestion behaviour. Particle size analysis,

rheology and microscopy imaging were applied, and their general principles and methodologies have been described in this section.

2.2.3.1 Particle Size Analysis

Emulsion droplet diameter was determined by laser light diffraction (or static light scattering) using a Mastersizer instrument (Malvern Instruments Ltd., Worcestershire, UK), see Figure 2.8. It reports size as equivalent spheres, which is a universal concept across laser diffraction instruments. Laser diffraction measures particle size distribution by measuring the angular variation in the intensity of light scattered as a laser beam passes through a dispersed particulate sample. Smaller particles scatter light at wider angles and the intensity of the light is lower, compared to larger particles. Then, the angular scattering pattern is dependent on the particle size distribution of the sample. Laser diffraction requires a model that accurately defines the light scattering pattern of all particles. Mie theory has been found to be more accurate over a wider range of sizes, this theory calculates the particle size distribution, assuming a volume-equivalent sphere model. It is valid for all wavelengths and size of particles. The application of Mie's theory requires the knowledge of three optical properties, i.e. the refractive index of both dispersant and the sample material and the absorption of the sample material. These properties were found in the database of the instrument. As part of the size distribution data, there are size distribution statistics that can be automatically obtained through the instrument software, i.e. mean, median and mode. The mean is an average particle diameter and depends on the parameter that is weighted. The two most important weighed mean values are $d_{3,2}$ and $d_{4,3}$ mean diameter. $d_{3,2}$ is the surface area weighted mean, referred to the diameter of a sphere having the same surface area as the particle. $d_{4,3}$ is the volume weighted mean referred to the average diameter of spheres with equivalent volume. Therefore the latter is sensitive to the presence of large particles and $d_{3,2}$ is sensitive to the presence of small particles.

Figure 2.8 Mastersizer 3000 equipped with a 300 RF lens with a wet dispersion unit (Hydro MV), supplied by Malvern Instruments Ltd, Worcestershire, UK.

The general protocol used was as follows.

The particle size distribution and average lipid droplet diameter of initial and digested samples were determined using a laser-light diffraction unit (Mastersizer 3000, Malvern Instruments Ltd, Worcestershire, UK) equipped with a 300 RF lens and a wet dispersion unit (Hydro MV). A volume of initial and digested samples was added in the instrument to reach ~10% laser obscuration. The size distribution was obtained using polydisperse analysis, while droplet size measurements were recorded as surface area weighted ($d_{3,2}$) and volume weighted ($d_{4,3}$) means, where $d_{3,2}$ is defined as $\sum n_i d_i^3 / n_i d_i^2$ and $d_{4,3}$ is defined as $\sum n_i d_i^4 / n_i d_i^3$, where n_i is the number of particles with diameter d_i. Each measurement was carried out in triplicate.

2.2.3.2 Rheological Properties Analysis

Rheology is the study of flow and deformation (viscosity) of materials. Viscosity refers to the resistance of a fluid to flow and is the force per unit area applied to the material, directly proportional to stress. When a force is applied to a material, it will react and undergo either deformation (strain) or flow (strain rate). Properties of a material such as particle size and interaction between the different constituents in the matrix will influence the flow/deformation behaviour. A rheometer is a precision instrument that contains the material of interest in a geometric configuration, controls the environment around it, and applies and measures wide ranges of stress and measures the resultant strain and strain rate.

In this thesis, rheology was used with the aim to quantify the viscoelastic properties of the coagulum formed during the gastric phase. This coagulum was considered to have gel-like behaviour, which has the ability to behave as a solid while retaining many of the characteristics of the liquid components. Strain tests have been used for studying the behaviour of food gels (Tabilo-Munizaga *et al.*, 2005), which are generally categorised by small- and large- deformation strain testing.

In small-deformation strain testing, a minimal amount of strain or stress is applied to measure the rheological behaviour, preventing or minimising damage to the sample. Gels have viscoelastic properties therefore a dynamic oscillatory shear test can be applied. This test has been reported to be useful for studying the nature of the protein matrix (Tunick, 2011). The main dynamic tests are frequency sweep, amplitude sweep, temperature sweep and time sweep. In these tests, different moduli can be determined. G' value is a measure of the energy stored in the sample during the deformation process, representing the elastic behaviour of a sample. To the contrary, G'' value is a measure of the deformation energy that is dissipated or lost through flow of the sample representing the viscous behaviour of a sample. Also, the complex modulus, G*, can be calculated combining G' and G'' and is a measure of the deformation of the sample. Oscillatory tests were performed in the study referred to in Chapter 5 using the rheometer AR 2000 (TA Instruments, Crawley, UK) illustrated in the Figure 2.9.

Figure 2.9 AR 2000 EX Rheometer supplied by TA Instruments, Crawley, UK.

The measurement of these fundamental rheological properties in the coagulum was not an easy task since the sample was highly structured and some sort of manual deformation was needed to adapt its size to the gap of the geometry. Therefore, large-deformation test was also used in an attempt to improve the analysis (Chapter 4).

Large-deformation approach refers to deforming a sample to an extent at which the food matrix is damaged or fractured. This is usually correlated with sensory evaluation in the food industry. Tests of compression, tension and torsion can be performed to determine different values and patterns of gel fracture properties and are widely used in both solids and semi-solids by the food industry. One type of large-deformation methodology, penetration test, was used in the study related to Chapter 4. Figure 2.10 A shows the texture analyser TA.XT Plus (Stable Micro Systems, Surrey, UK) that was used for the test. In this test, a cylindrical probe penetrates the sample up to a required depth and data in terms of gel strength can be obtained from the force applied and the distance of penetration. Figure 2.10 B shows a typical curve obtained in this test. The gel strength is provided by the maximum value of the force obtained.
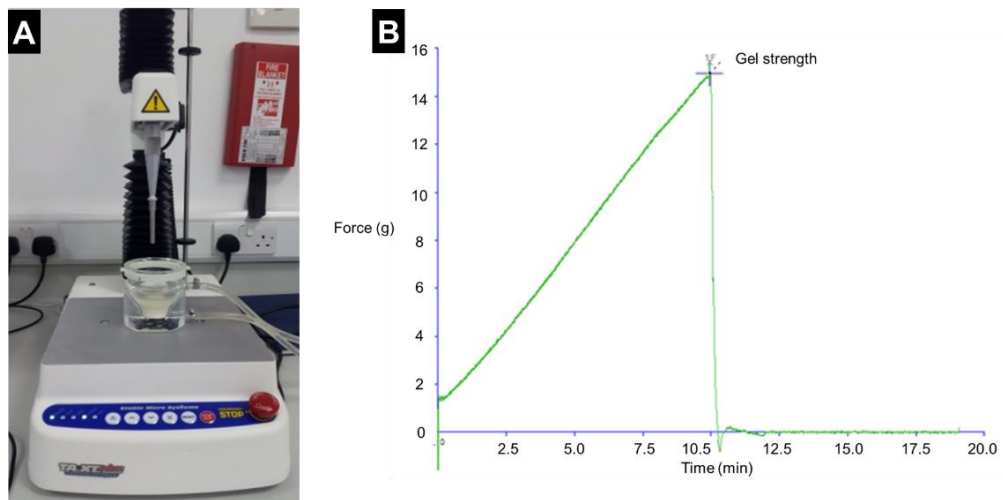
Figure 2.10 (A)Texture analyser TA.XT Plus supplied by Stable Micro Systems, Surrey, UK. (B) Typical curve obtained in the penetration test that was performed.

2.2.3.3 Confocal Laser Scanning Microscopy

The microstructure of the samples studied in this thesis was visualised by confocal laser scanning microscopy (CLSM). This technique is based on wide-field fluorescence microscopy, which uses the fluorescence of the samples both naturally occurring or by the additions of dyes that can bind with the compounds of interest. The instrument is typically composed of a laser light source, dichroic mirror, filters and detection system. The first filter selects the light which will excite the fluorophores

contained in the sample and emitted fluorescent light passed through a second filter. Much of the light collected by the objective to form an image comes from the regions above and below the selected focal plane, reducing the contrast and sharpness of the final image. A confocal microscope is a high-resolution fluorescence microscope that eliminates the out-of-focus light by the inclusion of two pinhole apertures positioned at the focal planes of the objective. It not only removes out-of-focus-light from the image but also the light scattered from within the optical instrument itself. Consequently, it offers an increase of contrast and signal-to-noise in the final image. Therefore, confocal microscopy offers two main advantages, elimination or reduction of the background and ability to provide time-series of 3D images with high resolution.

Confocal microscopy was used in this project in order to assess the structure and interaction between protein and lipid in both initial sample and during gastric digestion. The general protocol is described as follows.

The microstructure of the initial and digested samples was observed using a confocal microscope (brand specified in each chapter). Figure 2.11 shows two of the confocal microscopes used in the thesis. The images were taken using both 20 x and 63 x oil-immersion objectives and simultaneous dual-channel imaging, He–Ne laser (excitation wavelength at 633 nm) and an Argon laser (excitation wavelength at 488 nm). A mixture of two dyes was used, which consisted of 0.1% Fast green FCF solution (in water) to detect protein and 0.1% Nile red solution (in propanediol) to detect the lipid phase (proportions are described in each chapter).
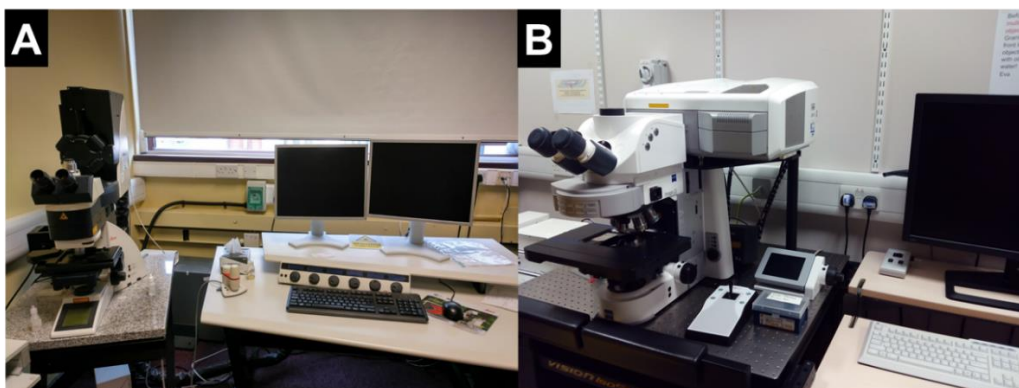
Figure 2.11 Confocal scanning laser microscopes, (A) Model Leica TCS SP5, supplied by Leica Microsystems, Baden-Württemberg, Germany and (B) Zeiss LSM 780 confocal (Carl Zeiss, Inc.)

2.2.4 Protein Analysis

Protein analysis constitutes an important part of this project. The aim was to assess the kinetics of protein emptying and breakdown, in particular, during gastric

digestion. The following methods describe the techniques used in this project to assess the composition and concentration of proteins.

2.2.4.1 Total Nitrogen Analyser

A total nitrogen analyser, LECO FP628 (LECO Corp., St. Joseph, MI, USA), see Figure 2.12, was used to determine the total protein content in initial and digested samples. This is based on the combustion Dumas method, an international standardised method for the determination of the total nitrogen content. The sample is combusted at high temperature (950-1,050°C) in a pure oxygen atmosphere and the combustion products (including N_2 and NOx) are then collected in a vessel (ballast) for equilibration. The homogenised gases are swept by a helium carrier gas and, CO_2 and H_2O are removed by sorbents (Lecosorb / Anhydrone). The NOx gases are passed through a copper tube that reduces the NOx to N_2 and removes excess oxygen. Then, N_2 is measured with a thermal conductivity detector and its content is calculated by taking into account the mass of the sample injected. The total nitrogen value is converted into total protein by using a nitrogen conversion factor suitable for the protein nature, which is determined according to the amount of nitrogen in the protein amino acid sequence. The nitrogen conversion factor established for milk proteins is 6.38 (FAO, 2003).

Figure 2.12 LECO FP628 Nitrogen analyser supplied by LECO Corp., St. Joseph, MI, USA.

The Dumas method offers several advantages over the other international standard method for total nitrogen analysis, Kjeldahl method, since it provides shorter analysis times, easier operation and improved safety. Both methods have similar precision and no differences were found when they were applied in dairy products (Wiles *et al.*, 1998).

The general procedure followed for the analysis of total protein content is described as follows.

The protein content of the initial sample and emptied digesta was determined using a LECO FP628 Protein analyser (LECO Corp., St. Joseph, MI, USA). Prior to the analysis, blank and drift corrections were performed. At least five blanks were analysed, until three consecutive blanks had a stable value with a standard deviation of less than 0.002% and the last three consecutive values were used for the blank correction. EDTA is typically used as a reference standard to interpret the detector response as % nitrogen (the theoretical N concentration for EDTA is 9.586%). At least four EDTA standards were run until three consecutive values have a relative standard deviation of 0.2% or less and the last three consecutive values were used to calculate the drift factor correction. For the test samples, about 0.2 g of sample was weighed in tin foil cups (LECO Corp.), sealed and placed in the instrument's loader. A conversion factor of 6.38 was used to obtain the protein content from the nitrogen content.

2.2.4.2 Sodium Dodecyl Sulphate-Polyacrylamide Gel Electrophoresis

Sodium dodecyl sulphate-polyacrylamide gel electrophoresis (SDS-PAGE) was performed to determine the intact and hydrolysed protein and the nature of the protein, in this case caseins and whey proteins.

SDS-PAGE is a widely used method for separating proteins according to their molecular weight. Figure 2.13 illustrates the principles of this technique. A reducing agent such as dithiothreitol or mercaptoethanol is added to break the protein disulphide bonds. SDS is an anionic detergent that unfolds and charges proteins negatively by binding to the protein molecules proportionally to the length of the protein, achieving the same charge to mass ratio. Then, the mobility of the protein through the polycrylamide gel, which differs in pore size according to the state of crosslinking, depends on the molecular weight of the protein. An electric field is applied to move the charged molecules, the ones with small molecular weight migrate more rapidly through the gel than larger molecules. This methodology is helpful for relatively large peptides, but the resolution of SDS gel is usually low for small peptides
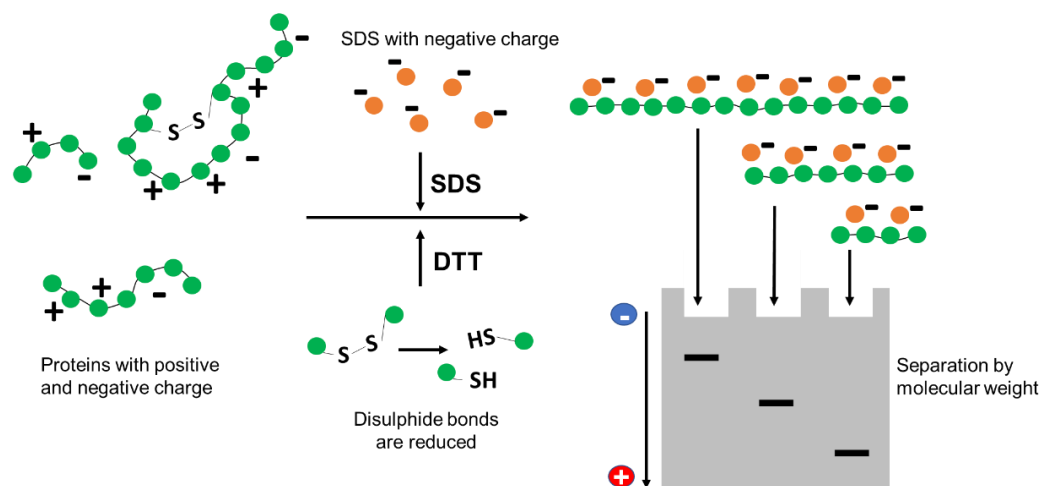
Figure 2.13 Schematic representation of SDS-PAGE procedure for protein separation.

The general protocol used in the project is described as follows.

SDS-PAGE was performed on the initial and digested samples during gastric phase. The electrophoresis was performed using the XCell SureLock™ Mini-Cell. 4-12% polyacrylamide NuPAGE Novex Bis-Tris 12-well precast gels (Invitrogen, Life Technologies Corp., CA, USA) were used according to the manufacturer's instructions. This type of gel is capable of resolving proteins in the range of 200-2.5 kDa. Running buffer consisted of 50 mL NuPAGE MES buffer (2-(N-morpholino) ethanesulfonic acid) and 950 mL water. A volume of 65 µL sample was mixed with 10 µL 10x NuPAGE reducing agent and 25 µL NuPAGE LDS sample buffer. The mixture was heated at 70°C for 10 min. 10 µL of the mixture was loaded onto the gel. The electrophoresis settings were 200 V (350 mA) for 35 min. After the run, gel was removed from the cassette, a fixing solution (50% methanol and 10% acetic acid in v/v) was applied to the gels for at least 2 hours before staining with Coomassie Blue. Mark 12™ Unstained Standard (Invitrogen, Life Technologies Corp., CA, USA) was used as a molecular weight marker.

2.2.4.3 o-Phthalaldehyde Spectrophotometric Assay

Protein hydrolysis occurs during the gastrointestinal digestion by proteases, releasing peptide fragments with amino group ends. It is important to measure the extent of hydrolysis, which relates to the number of peptide bonds cleaved during a hydrolytic process. The production of protein hydrolysates is limited by enzyme activity but also protein attributes and, structural and physico-chemical changes in the course of digestion.

There is no absolute protein assay for assessing protein hydrolysis, each method has different advantages and limitations. The most well-known methods for the determination of degree of hydrolysis in food proteins are pH-stat technique, the trinitro-benzene-sulfonic acid (TNBS) method and o-phthalaldehyde (OPA) method. OPA method was selected on the basis of its sensitivity, convenience and environmental safety, compared to other spectrophotometry assays (Nielsen *et al.*, 2001). The OPA assay has been reported to be useful for the evaluation of the progress of hydrolysis during digestion of milk proteins (Church *et al.*, 1983).

The OPA assay is based on the reaction between primary amino groups and OPA chemical in presence of SH-compound such as dithiothreitol or β-mercaptoethanol. This forms a compound that absorbs at 340 nm (Figure 2.14), which is evaluated by spectrophotometry and the absorbance is proportional to the concentration of free amino groups. This assay is based on the assumption that a free amino group and a free carboxyl group are released every time a peptide bond is hydrolysed.
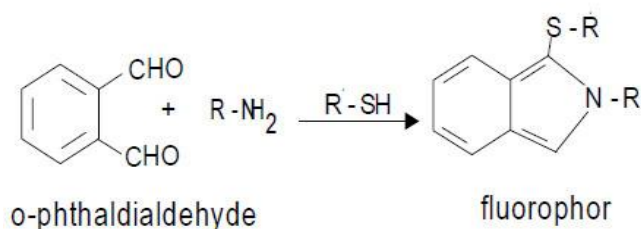
Figure 2.14 Representation of OPA reaction in a molecular level.

Standard solutions were used for quantitation. A calibration curve was created by plotting the absorbance at 340 nm of each standard concentration versus the known concentration of the standards. Leu was selected as the standard since the absorption of OPA after reacting with Leu was found very close to the average response of other amino acids (Nielsen *et al.*, 2001).

The application of this assay requires a clear sample without interference from insoluble material or particles causing light scattering. The samples analysed by OPA assay were therefore pre-treated as follows.

Addition of trichloroacetic acid (TCA) at 3.12% final concentration to sample, causes the precipitation of insoluble protein that could interfere in the further analysis. Then, the samples were centrifuge at 10,000 g for 30 min at room temperature and the supernatant was filtered using a syringe filter of PVDF 0.45 µm membrane (Millex-GV, Millipore). The use of TCA in protein hydrolysed samples prior to quantitative

analysis has been widely used (Flanagan *et al.*, 2003). Therefore, the extent of proteolysis was determined from the TCA-soluble protein fraction, which consists of small peptides and amino acid residues (Rowland, 1938).

The levels of free R-NH$_2$ groups were determined using the OPA spectrophotometric assay in micro-titre plates based on the protocol described in Nielsen *et al.* (2001) with some modifications. OPA reagent consisted of 3.81 g sodium tetraborate decahydrate dissolved in approximately 80 mL water. Once dissolved, 0.088 g dithiothreitol and 0.1 g SDS were added. Then, 0.080 g OPA dissolved in 2-4 mL ethanol was placed in the solution that was finally made up to 100 mL with Milli-Q® water.

Different concentrations of standard Leu solution (made with phosphate buffer solution) ranged from 0 to 10 mmol/L were used to obtain a calibration curve. 10 µL of standard/sample was placed into each well and mixed with 200 µL of OPA reagent. The reaction was allowed to proceed for 15 min, then the absorbance was measured at 340 nm using a microplate reader (brand specified in each chapter).

2.2.4.4 Amino Acid Analysis

Amino acids (AAs) are the basic monomeric units of the protein molecule, which are readily available to diffuse across the intestinal wall. Once absorbed, they are involved in a range of physiological functions. Therefore, AAs analysis is important to understand the implications of the food matrix on protein disintegration and the potential effects on health. The analysis of AAs was performed using ion-exchange chromatography and reversed phase chromatography coupled to tandem mass spectrometry, independently. These techniques were applied in the study related to Chapter 4. In this section the fundamentals of these techniques are explained, and the details of the protocols have been described in the corresponding chapter.

There is no official standardised method for analysis of AAs in foods. However, the most commonly used methods for separating and quantifying free AAs include the liquid chromatography technique of ion exchange chromatography (EC), reversed phase liquid chromatography (RPLC), gas chromatography (GC) and capillary electrophoresis, coupled to UV absorbance or fluorescence. These techniques are included in the group of column chromatography. In this, analytes in a mobile phase are separated because their different affinities for the stationary phase of the column. The interactions of the analytes with the stationary phase determine the migration time, which are based on properties such as charge and size. After being separated

by the column, the concentration of each of the analytes is determined by a suitable detector.

AAs are highly polar compounds and, therefore, their chemical derivatization may be required for chromatographic separation to improve separation and detection, which can be applied by a pre- or post-column step. In the derivatization process, a reagent is used to react with the amino group. The most common derivatization reagents are ninhydrin, *o*-phthalaldehyde, 6-aminoquinoyl-*N*-hydroxysuccinimidyl carbamate, 2,5-dioxopyrrolidin-1-yl-2(4-methylpiperazin-1-yl) acetate and N-metyl-N-trimethylsilyltrifluoroacetamide (Gilani *et al.*, 2008). Derivation of AAs in GC is also required, improving the volatility and thermal stability of analytes. The most employed procedure is silylation. GC analysis provides good resolving power, the limit of detection reported was 0.03-12 µmol/L (Kaspar *et al.*, 2008). However, this derivatization is sensitive to moisture and not all the AAs derivatives are stable.

The technique of cation EC has been widely used followed by post-column derivatization with ninhydrin and ultraviolet detection. The analyser Jeol JLC-500/V AminoTac™ (see Figure 2.15), based on the cation EC technique, was used in this thesis for the analysis of AAs in samples after *in vitro* gastric and intestinal digestion. The stationary phase consisted of highly polymerised resin that separates compounds by differences in their overall charge, charge density, and surface charge distribution, at particular pH and temperature. The analyte molecules are retained on the column based on ionic interactions. The stationary phase surface contains ionic functional groups of opposite charge that interact with analyte ions. For proteins, their surface charge on the molecules, which binds to cation exchanger should be net positive. Thus, to get binding of a specific protein, the pH should be below the isoelectric point of that protein. This method also incorporates a post-column reaction of ninhydrin with free AAs, so the results can be detected in the visible range. The reaction of ninhydrin with AAs containing a primary amine generates a derivative that can be absorbed at 570 nm and secondary amines forms a product absorbing at 440 nm. The linearity ranges, typically, from 5-2,500 µmol/L. The disadvantages of the method are the long runtime and the instability of ninhydrin. An example of the chromatogram obtained for a standard solution is illustrated in Figure 2.16.

Figure 2.15 Jeol JLC-500/V AminoTac™ amino acid analyser supplied by Joel Ltd., Herts, UK.
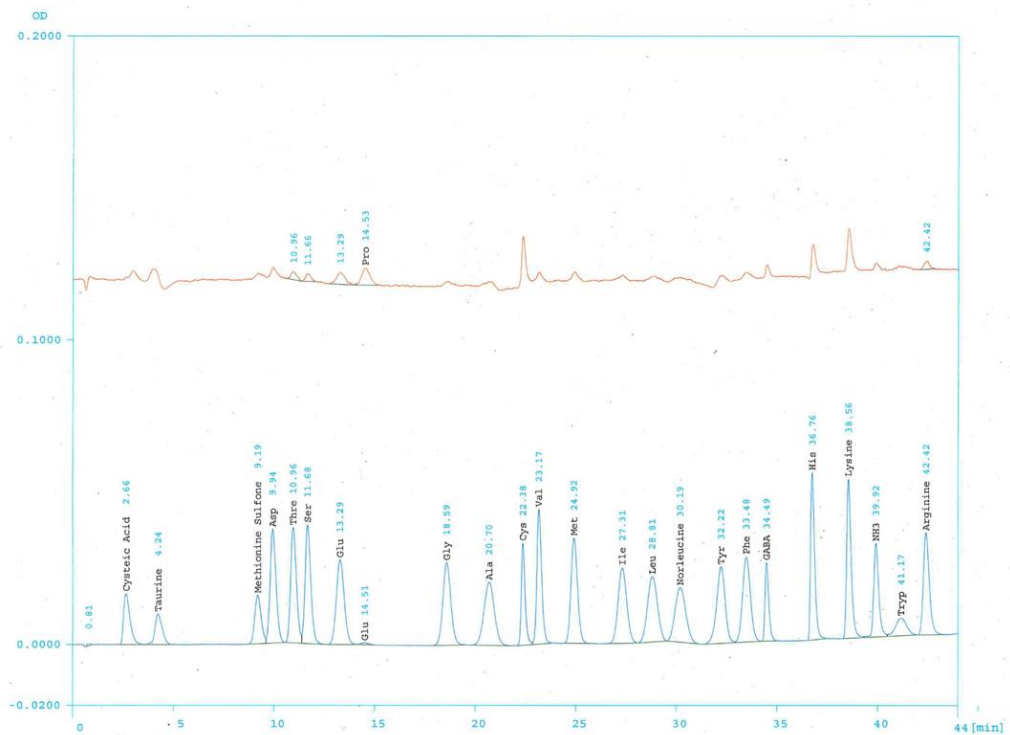
Figure 2.16 Chromatogram of the separation of each amino acid in a standard solution using cation EC.

RPLC has been increasingly used, compared to ion EC. This technique separates molecules based on their hydrophobicity. RPLC uses a hydrophobic stationary phase and a hydrophilic mobile phase. The stationary phase is commonly composed of porous silica particles linked to alkyl chains (typically C8 and C18). C18 packed columns are typically used for the separation of small or low hydrophobic proteins (≤10 kDa).

95

Liquid chromatography techniques that are coupled to an optical detector have low limit of quantification, 5 μmol/L (Kaspar *et al.*, 2008). However, they still offer low specificity, when compared to mass spectrophotometry (MS). (Kaspar *et al.*, 2008). MS is a technique that ionizes analytes, separating the ions based on their mass-to-charge (m/z) ratio and detects them. The selectivity of the quantification is increased by the use of tandem MS (MS/MS). The principle of MS/MS is that a sample is ionized by an ion source and separated by m/z ratio in the first mass analyser. The ions of *m/z* value of interest are selected and fragmented generating fragment ions, which are separated and recorded by the second mass analyser. MS/MS offers high accuracy and sensitivity. Another advantage is that derivatization is not needed. However, it can be subject to matrix effects, which could be addressed by the use of stable-isotope-labelled internal standards. In this project, the use of a technique for AA analysis with high sensitivity was needed in the samples obtained from Ussing chamber (Chapter 4). For that, LC and electrospray ionization MS/MS, Agilent 6490 triple quadrupole MS equipped with an Agilent 1290 HPLC system (Agilent Technologies, Santa Clara, CA, USA) (see Figure 2.17) was used using labelled standards.
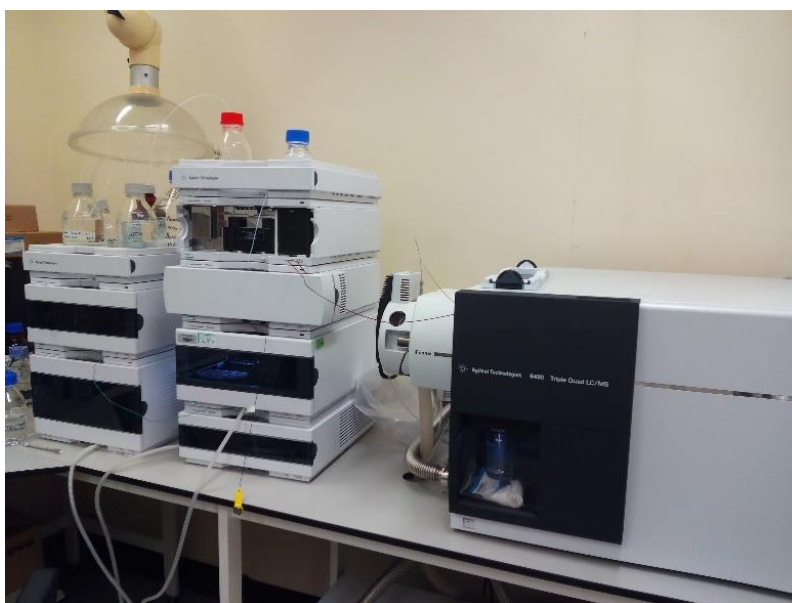
Figure 2.17 Agilent 6490 triple quadrupole MS equipped with an Agilent 1290 HPLC system supplied by Agilent Technologies, Santa Clara, CA, USA.

2.2.5 Lipid Analysis

The following methods describe the techniques used in this project to assess the composition and concentration of lipids.

2.2.5.1 Total Lipid Analyser

The lipid content of the initial sample and emptied digesta was measured using a CEM Smart Trac 5 System® (CEM Corp., Matthews, N.C., U.S.A.), see Figure 2.18. The method consists of a microwave-drying step followed by nuclear magnetic resonance (NMR) analysis. Moisture is evaporated from the sample using microwave energy and weight loss is determined by electronic balance readings before and after drying. Microwave drying is an AOAC-approved reference method (Method 985.14). Then, lipids are determined on the basis of NMR analysis.

Figure 2.18 CEM Smart Trac System-5 supplied by CEM Corp., Matthews, N.C., USA.

The NMR technique incorporated into the CEM Smart Trac System® is based on low-resolution time domain NMR, which is commonly used for lipid analysis. It uses a low field strength that is not designed to correct the inhomogenity of the magnetic field. This implies that the differences in the electronic structure of molecules obtained using high-resolution NMR cannot be detected. Figure 2.19 illustrates the basic principles of low-resolution NMR. This technology aligns the hydrogen protons of the sample to the magnetic field. Then it sends pulses of radiofrequency energy for very short periods through the sample, which causes a stronger field in which the hydrogen atoms are aligned. Following the pulse, the atoms return to equilibrium orientation emitting a signal known as a free induction decay or transverse relaxation time, which is measured. The induction decay relates to realignment of the protons in response to the pulsing. Therefore, differences in the signal of rate of decay are used to differentiate constituents in the analysed matrix. Removal of water in the sample is

needed since the protons of water cannot be distinguished from those of lipid. After drying, the main constituents of food that contain significant amounts of protons are lipid, protein, and carbohydrate, which present differences in the induction decay times and the instrument is able to differentiate. Both protein and carbohydrate in dried foods exhibit transverse relaxation times that are very short and the signal from these substances decays very rapidly. However, for lipid the transverse relaxation times are considerably longer and thus the signal decays relatively slowly. Therefore, the signal obtained using this technique will be directly proportional to the number of protons associated to lipid, which will be proportional to the lipid content of the sample. This method is recognized as an AOAC peer verified method.

A. A sample is placed in the magnetic field

B. Hydrogen atoms align to the magnetic field

C. An RF pulse forces atoms to align temporarily

D. The atoms relax and the instruments interprets the signal
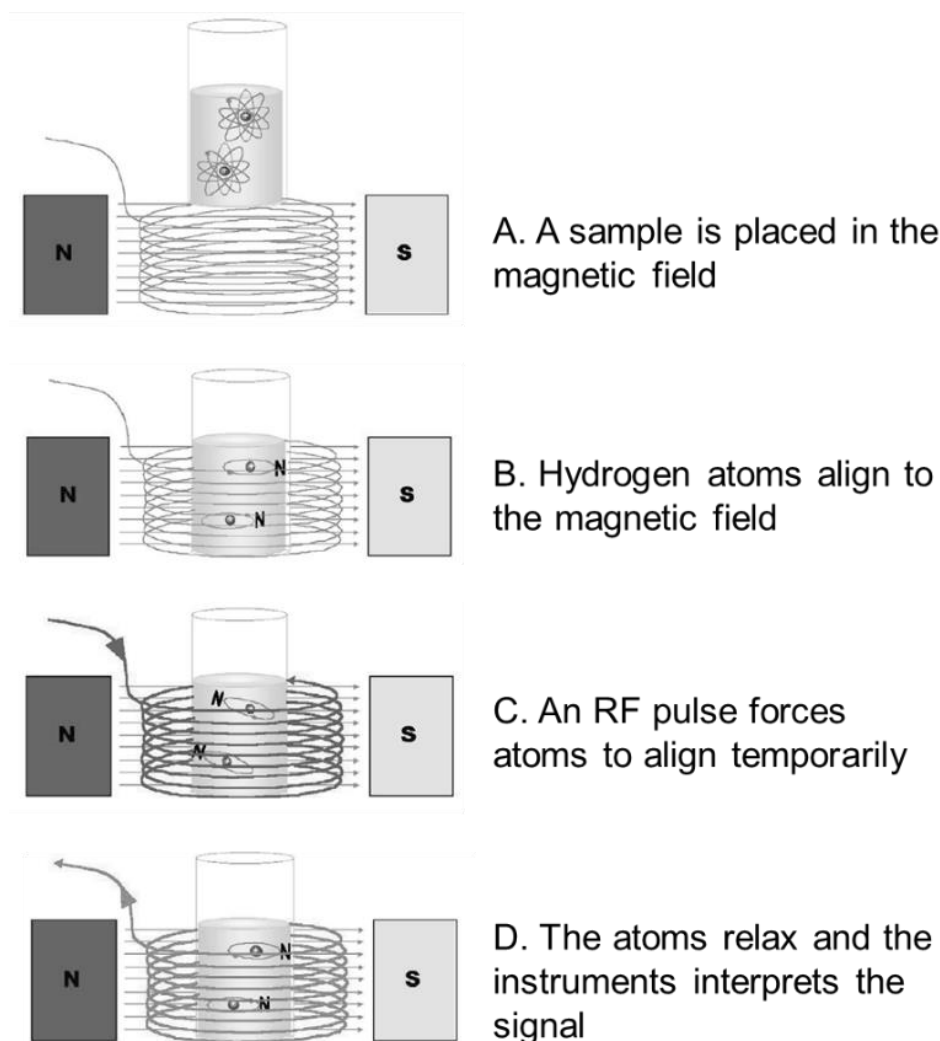
Figure 2.19 Schematic representation of the principle of NMR for the determination of lipid content (adapted from the web site cem.com).

This methodology has been used for the analysis of lipid in dairy products (Cartwright *et al.*, 2005). The advantages to use this methodology are the speed of the analysis and elimination of the problems associated to the solvent extraction methods.

The general protocol is described as follows and it is illustrated in Figure 2.20.
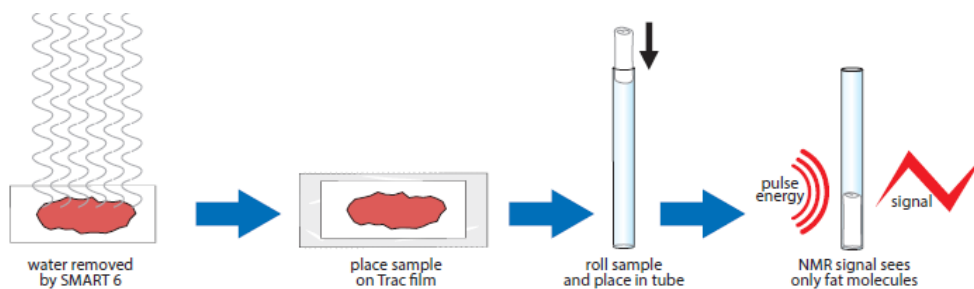
Figure 2.20 Schematic representation of the protocol for the determination of lipid content (taken from the web site cem.com)

Initial and digested aliquots from gastric phase were used. A homogenised sample was obtained by warming to 40°C to disperse the lipid and using an ultraTurrax® homogeniser at 7,500 rpm for ~ 30 s. Approximately 2 g of sample was placed on a glass fibre pad (CEM Corp.) and dried in the CEM Smart Trac 5 System® by microwave drying. After drying, the sample (including the glass fiber pad) was placed on a sheet of Teflon film (CEM Corp.), rolled into a cylindrical shape and placed into a special Teflon tube (CEM Corp.) fitted for the instrument (Figure 2.20). The tube containing the sample was placed into the NMR chamber of the CEM Smart Trac 5 System®. The settings of the NMR pulse generator were as follows: Pulse power 250 W nominal; pulse times variable in 100 ns increments; transmit and receive phases selectable 0, 90, 180, and 270°; nominal 90° pulse times 4 ms (18 mm probe). Magnet: permanent, thermally stabilized, 0.47 T (20 MHz), homogeneity >10 ppm. Signal detection: dual channel (quadrature) detection with programmable low-pass filtering, programmable data acquisition rate up to 4 MHz per pair of points. Moisture and fat results are displayed by the instrument as a percentage (g/100 g).

2.2.5.2 Gas Chromatography-Mass Spectrophotometry

The use of gas chromatography (GC) coupled to MS was used in order to quantify the lipid hydrolysis by analysing each lipid compound in both initial and digested samples.

The matrix of these samples consisted of a mixture of lipid, protein and carbohydrates. In order to avoid any interference, isolation of the lipid prior to analysis was required. Solvent extraction techniques are one of the most commonly used methods for lipid extraction. Lipids are soluble in organic solvents, i.e. chloroform, and insoluble in water. Therefore, lipid components can be separated in foods from water soluble components, such as proteins and carbohydrates. The lipid part of samples consisted of a mixture of mainly triacylglycercols, diacylglycercols,

monoacylglycercols and free fatty acids. The separation among the lipid compounds will depend on the polarity of the solvent compared to that of the lipid species. Hydrophobic lipids such as triacyglycerols are more soluble in non-polar solvents whereas diglycerides and monoglycerides have both hydrophobic and hydrophilic moieties and short chain fatty acids (C1-C4) are very hydrophilic compounds.

The extracted samples can then be analysed. Chromatography techniques, e.g. thin layer chromatography and GC are usually applied to determine the lipid profile of food samples. GC coupled to a mass spectrophotometer was used in the study referred in Chapter 7, using 7890B GC System equipped with 5977A mass spectrometry detector (Agilent Technologies, USA) (Figure 2.21). In GC, the sample is volatilized and injected into a column. The sample is transported by a mobile phase of inert gas and the different elution occurs due to the different interaction with the stationary phase of the column. However, some lipid compounds are not very volatile, such as triacylglycerols. For this reason, lipid samples were treated to obtained fatty acid methyl esters (FAMEs), increasing their volatility. Fatty acids in foods vary in chain length, degree of unsaturation and position on the glycerol molecule and the lipid fraction then consists of a complex mixture of different molecules. The compounds elute at different times depending on their polarity (chain length and degree of saturation) and boiling point, the fatty acids with the lowest boiling point and/or the most polar had the shortest retention time. After the separation of the molecules in the column, they are broken down into ionized fragments using electron or chemical ionization sources. The compounds can be then identified by comparing their retention times with those obtained from standards. MS is a powerful technique that provides the identification and quantification of the chemical structure of these molecules that it would be more difficult with the use of GC only. The most standard procedure for ionization is electron ionization, the molecules are bombarded with free electrons emitted from a filament. These fragmented ions are then separated based on their different mass-to-charge ratio by a mass analyser. Finally, the signal of the separated ions is amplified and transmitted by a detector, obtaining mass spectra data. An example of the chromatogram obtained using the standards is shown in Figure 2.22.

Figure 2.21 7890B Gas Chromatography System equipped with a model 7694 autosampler and 5977A mass spectrometry detector (Agilent Technologies, USA).

In this system of analysis, an internal standard should be used to normalise or correct for sample-to-sample preparation variance and standard to sample matrix differences. The internal standard chosen should not be naturally present in the sample matrix.
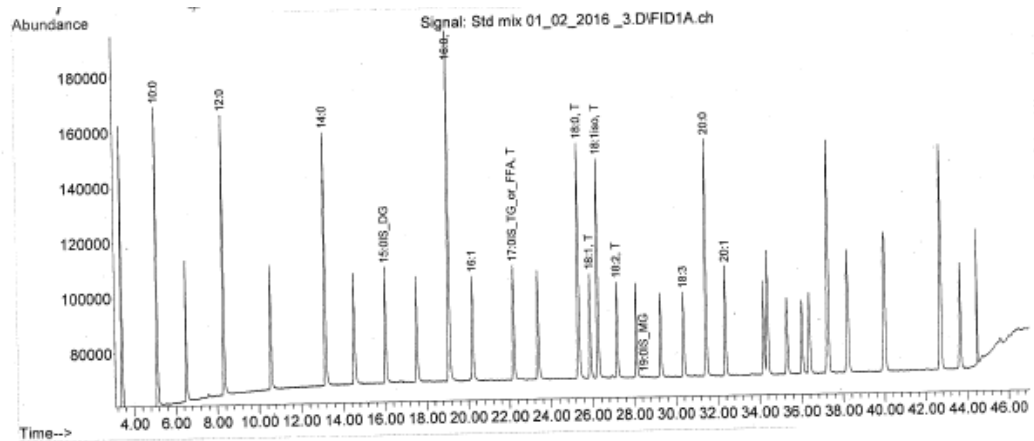
Figure 2.22 Example of chromatogram obtained in a lipid standard mix by GC-MS

Chapter 3

Development of a Semi-Dynamic *in Vitro* Digestion Model

3.1 Introduction

There is growing interest in investigating the fate of food in the gastrointestinal (GI) tract in light of understanding the impact of food on human health. The gastric phase is central to understand the connection between food structure and rates of nutrient release and, in turn, digestion and absorption in the small intestine. There are several types of dynamic process occurring in the stomach, e.g. enzymatic, chemical and physical, described in Chapter 1, which are relevant to understand the behaviour of food structure.

The study of food digestion *in vivo*, in particular in humans, is the reference methodology. However there can be issues regarding time, cost, ethics, invasive sampling and high inter-individual variability. For this reason, *in vitro* models are widely used since they can overcome those issues as well as allowing more detailed information to be obtained and improving reproducibility having greater control of the experimental conditions. These models allow the determination of nutrient bioaccessibility and they are usually performed as preliminary tests to produce evidence for future health claims to be further investigated in human studies. The most used type of *in vitro* model in the literature is the static method, often consisting of a series of stages simulating the different digestive compartments in which conditions remain constant. An internationally harmonised protocol for static simulation of digestion in the upper GI tract of adults has been developed by the COST Action INFOGEST (Minekus *et al.*, 2014). In this, the pH is set constant at pH 3 for the gastric digestion time of 2 hours, under these conditions pepsin activity is optimum resulting in overestimation of protein hydrolysis. Moreover, the structural changes and different colloidal behaviours that might occur in the stomach affecting nutrient breakdown and delivery cannot be simulated. For instance, several studies using a static digestion reported fast hydrolysis of caseins (Egger *et al.*, 2016; Islam *et al.*, 2017; Tunick *et al.*, 2016) whereas caseins have shown slow protein absorption *in vivo* (Boirie *et al.*, 1997; Dangin *et al.*, 2001; Mahé *et al.*, 1996). This is suggested to be due to the formation of coagula in the gastric compartment, which is not observed in static studies.

The static *in vitro* model has been seen as a useful tool for assessing end-point values, however it cannot provide kinetic data about nutrient digestion and structural changes because the complexity of the gastric dynamics is not simulated (Bohn *et al.*, 2017). Another *in vitro* model, the dynamic model, is able to mimic the biochemical and mechanical aspects of the human stomach however they are complex, time-consuming and expensive to use since their use involves large amounts of enzymes.

In addition, dynamic models are often commercially run and are often not available to food researchers. Therefore, there was the need of an intermediate model that could provide the advantages of the two models, a system that could provide more realistic trends about nutrient digestion while taking into account the relevant *in vivo* gastric secretion and emptying, and yet could easily be used in laboratories without specialist facilities.

A semi-dynamic gastric model was developed in this thesis to obtain better physiological relevance in the kinetics of gastric digestion compared to the static model but without the constrictions of cost and access, and the use of large samples needed in fully dynamic models. The features are the simulation of the main gastric dynamics of gradual acidification, fluid and enzyme secretion and emptying. Using *in vivo* data on gastric volume changes during digestion (Mackie *et al.*, 2013), this model has been reported to closely simulate the behaviour observed in the human stomach by magnetic resonance imaging (Chapter 7), allowing the determination of the underlying mechanisms leading to the physiological responses observed in humans.

In this chapter the main steps in the development of the model are described, with particular consideration of the dynamic pH profile and gastric emptying (GE). This chapter presents the final outcomes and design of the model based on the aims of developing a simpler, cheaper, more accessible model that had a higher throughput than fully dynamic models yet gives a more accurate insight into gastric processing than current static models. It builds upon the standardised outcomes of the static INFOGEST protocol (Minekus *et al.*, 2014). The results of this thesis will be the basis for an international consensus method published in 2019, with a detailed description of the experimental parameters and commercially available equipment so that the method can be easily reproduced in any laboratory worldwide.

3.2 Materials and Methods

3.2.1 Materials

Skimmed milk power (SMP), from Fonterra, New Zealand, was used in most of the trial experiments performed. The enzymes were provided by Sigma Aldrich (St Louis, Mo, USA). Enzyme activities were determined based on the assays detailed in Minekus *et al.* (2014). The α-amylase of oral phase was not included in any experiment because starch was not present in the matrix, however it should be included when starch is present. Porcine pepsin activity was based on bovine blood haemoglobin as a substrate (one unit will produce a ΔA280 of 0.001 per minute at pH

2.0 and 37°C) measured as TCA-soluble products. Porcine pancreatin was used and the trypsin activity was considered, which was based on p-toluene-sulfonyl-L-arginine methyl ester, TAME, (one unit hydrolyses 1 µmol of TAME per minute at 25°C, pH 8.1). The concentration of bile salts (bovine origin) was measure using a commercial kit (DiaSys Diagnostic System GmbH, Germany). The reagents and protocol for the digestive fluids i.e. salivary, gastric and intestinal simulated fluids were according to Minekus *et al.* (2014), and detailed below.

3.2.2 Preparation of Simulated Digestion Fluids

The preparation of the stock solutions for the simulated salivary fluid (SSF) is detailed in Table 3.1. The stock solution was made up with water to 400 mL, obtaining 1.25x concentrated solution. The addition of enzymes, Ca^{2+} solution and water will result in the correct electrolyte concentration (1x) in the final digestion mixture. This aims to reach the concentration of 0.75 mmol/L of Ca^{2+} (using $CaCl_2(H_2O)_2$) in the final digestion mixture.

Table 3.1 Preparation of the simulated salivary fluid (SSF), 1.25x concentrated, for the simulation of the oral phase.

Constituent	Stock concentration ($mol \cdot L^{-1}$)	Volume of stock (mL)	Concentration in SSF ($mmol \cdot L^{-1}$)
KCl	0.5	15.1	15.1
KH_2PO_4	0.5	3.7	3.7
$NaHCO_3$	1	6.8	13.6
NaCl	2	-	-
$MgCl_2(H_2O)_6$	0.15	0.5	0.15
$(NH_4)_2CO_3$	0.5	0.06	0.06

The solution was adjusted to pH 7 using 1 mol/L HCl and made up with distilled water to 400 mL. The solution was stored at 4°C up to one week.

The preparation of the stock solutions for the simulated gastric fluid (SGF) is detailed in Table 3.2. The stock solution was made up with water to 400 mL, obtaining 1.25x concentrated solution. The addition of enzymes, Ca^{2+} solution, HCl and water will result in the correct electrolyte concentration (1x) in the final digestion mixture. This aims to reach the concentration of 0.075 mmol/L of Ca^{2+} (using $CaCl_2(H_2O)_2$) and pepsin activity of 2,000 U/mL in the final digestion mixture.

Table 3.2 Preparation of simulated gastric fluid (SGF), 1.25x concentrated, for the simulation of the gastric phase.

Constituent	Stock concentration (mol·L^{-1})	Volume of stock (mL)	Concentration in SGF (mmol·L^{-1})
KCl	0.5	6.9	6.9
KH$_2$PO$_4$	0.5	0.9	0.9
NaHCO$_3$	1	12.5	25
NaCl	2	11.8	47.2
MgCl$_2$(H$_2$O)$_6$	0.15	0.4	0.1
(NH$_4$)$_2$CO$_3$	0.5	0.5	0.5

The solution was adjusted to pH 7 using 2 mol/L HCl and made up with distilled water to 400 mL. The solution was stored at 4°C up to one week.

The preparation of the stock solutions for the simulated intestinal fluid (SIF) is detailed in Table 3.3. The stock solution was made up with water to 400 mL, obtaining 1.25x concentrated solution. The addition of enzymes, Ca^{2+} solution, bile and water will result in the correct electrolyte concentration (1x) in the final digestion mixture. This aims to reach the concentration of 0.3 mmol/L of Ca^{2+} (using CaCl$_2$(H$_2$O)$_2$) and pancreatin activity of 100 U/mL (based on trypsin activity) and bile concentration of 10 mmol/L in the final digestion mixture.

Table 3.3 Preparation of simulated intestinal fluid (SIF), 1.25x concentrated, for the simulation of the intestinal phase.

Constituent	Stock concentration (mol·L^{-1})	Volume of stock (mL)	Concentration in SIF (mmol·L^{-1})
KCl	0.5	6.8	6.8
KH$_2$PO$_4$	0.5	0.8	0.8
NaHCO$_3$	1	42.5	85
NaCl	2	9.6	38.4
MgCl$_2$(H$_2$O)$_6$	0.15	1.1	0.33
(NH$_4$)$_2$CO$_3$	0.5	-	-

The solution was adjusted to pH 7 using 2 mol/L HCl and made up with distilled water to 400 mL. The solution was stored at 4°C up to one week.

A solution of 0.3 mol/L CaCl$_2$(H$_2$O)$_2$ was also prepared but added separately.

3.2.3 Semi-Dynamic Gastric Model Equipment

Figure 3.1 shows the typical set up for the semi-dynamic gastric model and the functional parts are individually illustrated in Table 3.4. The auto-titrator (including pH probe and dosing device), vessel with thermostat water jacket and vessel lid with openings were purchased from Metrohm Ltd (Switzerland), circulating water bath was from VWR, twin syringe infusion pump was from Harvard Apparatus PHD Ultra Syringe Pump, orbital shaker (Stuart mini gyro-rocker, SSM3) was provided by Stuart, Barloworld Scientific limited, UK. Plastic tubing to connect end of syringe with vessel

lid was made in-house and the tubing from the dosing device to the vessel was from Metrohm Ltd.
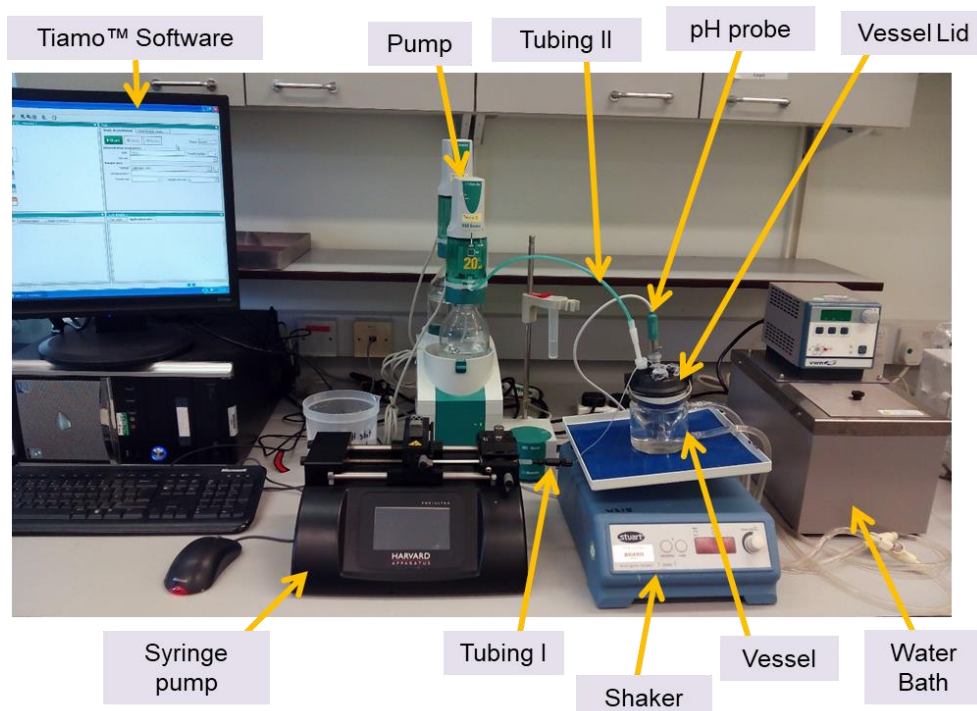
Figure 3.1. Set up of the semi-dynamic gastric model.

Table 3.4. Description of the parts of the semi-dynamic gastric model.

Image of Model Part	Generic Name	Functions
	pH electrode	Records pH within the simulated stomach (reaction vessel). Since a pH curve is previously determined its use is not required in every digestion
	Pump (Dosing device)	Delivers the simulated electrolyte gastric mixture containing the electrolytes and acid at a defined rate. The delivery rate is programmed using the software Tiamo™ (Metrohm)
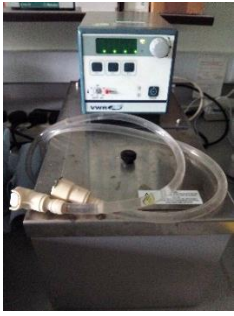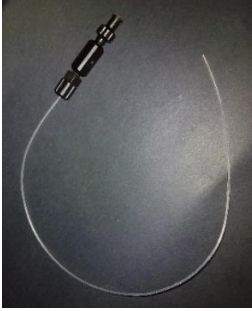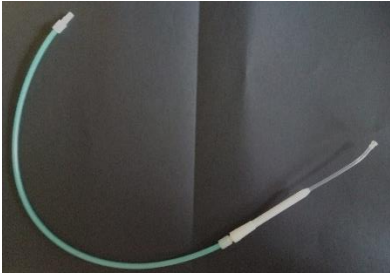
Image of Model Part	Generic Name	Functions
	Syringe pump	Delivers the enzyme solution. The delivery rate is programmed manually in the pump
	Reaction vessel	Holds the food to be digested simulating the stomach. It is made of glass and water jacketed to keep the temperature at 37°C. The vessel that was used in the studies of this thesis had an outer diameter of 78 mm, height of 82 mm and volume of 5-70 mL
	Vessel Lid	Holds the tubing and pH probe. Allows the sealing of the vessel and the emptying
	Shaker	Moves gently the vessel resulting in gentle mixing of the gastric contents. It is usually set at 35 rpm

Image of Model Part	Generic Name	Functions
	Water bath	Heats water at 37°C, which is circulated through the vessel
	Tubing I	Connects the syringe containing the enzyme solution with the vessel, allowing accurate delivery of small volumes. It is held by the lid of the reaction vessel
	Tubing II	Connects the pump (dosing device from Metrohm) containing the simulated electrolyte gastric mixture with the vessel, allowing accurate delivery. It is held by the lid of the reaction vessel

3.3 Results

3.3.1 Oral Phase

The oral phase remains essentially the same as the INFOGEST static protocol (Minekus *et al.*, 2014) but the 1:1 ratio of salivary fluids to food was calculated based on the dry weight of food proportion instead of the volume of food. This is mainly designed for solid/semi-solid foods in order to obtain paste-like consistency simulating the formation of a bolus. The amount of saliva secreted in relation to the amount and type of food ingested is highly variable, the values typically can range from 0.05 to 0.5 g saliva/g food (Watanabe *et al.*, 1988). Therefore, the proportion of saliva added with the dry matter content can provide more relevant relation.

3.3.2 Development of a Dynamic Gastric pH Profile

The dynamic pH curve observed in the human stomach was the principal parameter to be simulated. For that, SMP was used in first trials as a food model. This dynamic profile is one of the main changes from the static model. The latter provides the constant pH profile during gastric digestion as illustrated in Figure 3.2. The initial pH of the sample was 6.5, after the addition of HCl the pH dropped drastically to pH 3 and was constant during the gastric digestion time.
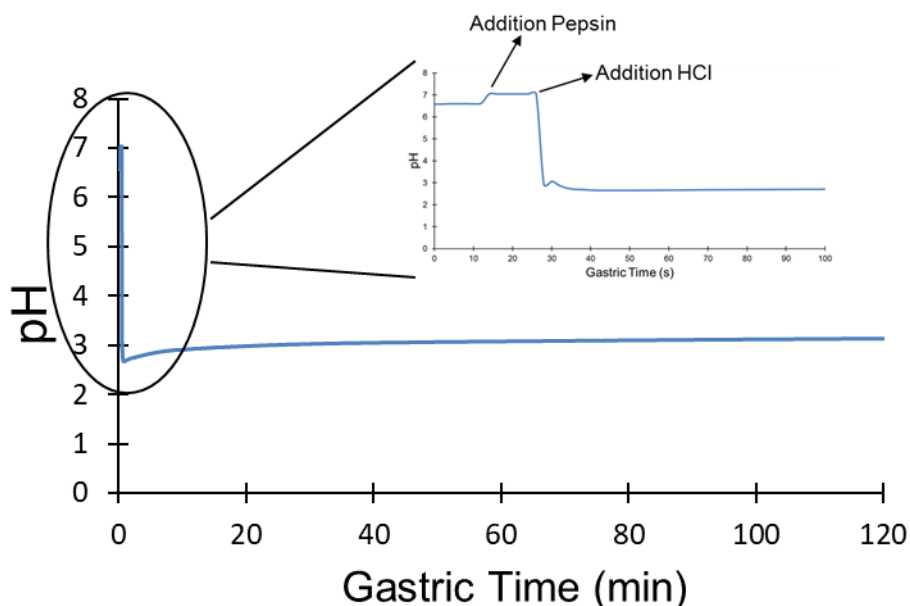
Figure 3.2 Example of a pH curve of gastric digestion under static model conditions and a zoom of the curve during the first 100 seconds of digestion.

The first approach to obtain a dynamic pH profile was to create a curve with set pH endpoints using a method in the pH titrator's software (Tiamo™). The method was optimised by modifying the parameters of titration in particular the minimum and maximum rate of addition of HCl. The best approximation is illustrated in Figure 3.3 using 9.5% SMP dissolved in phosphate buffer without the addition of digestive fluids. The pH value at the end of the acidification was 2 and the average pH was approximately 3.5.
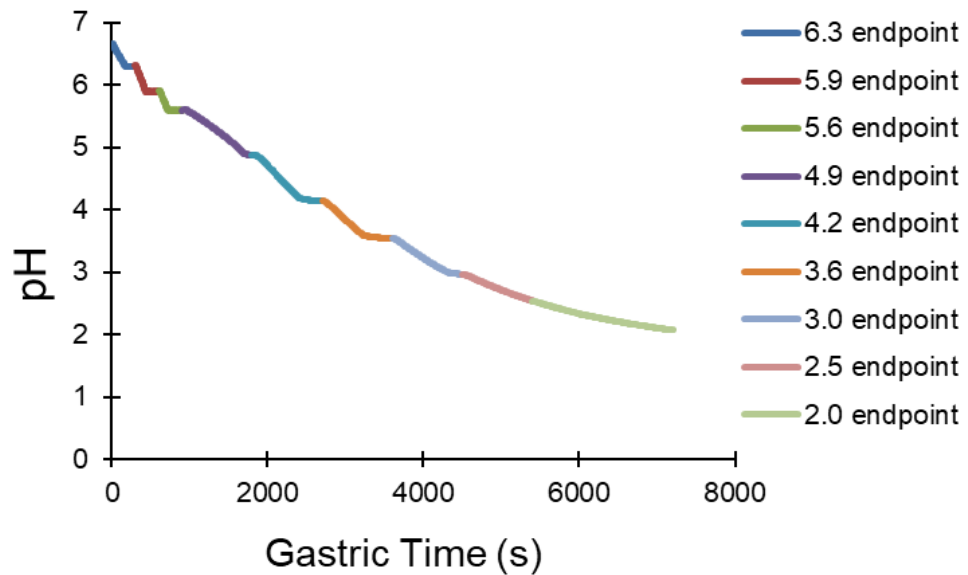
Figure 3.3 Programmed pH curve for 9.5% SMP in phosphate buffer adding 0.5 mol/L HCl. Note: a magnetic stirrer was used as mixing system.

The next step was to test the previous programmed method using simulated digestive fluids, both salivary and gastric, including the addition of pepsin to reach a final activity of 2,000 U/mL by means of the dosing device following a constant rate of 0.0083 mL/min. For this trial, 5 mL of 9.5% SMP was mixed with 5 mL SSF. Then, the sample was placed in the vessel and 10 mL of SGF at pH 7 was added. Gastric digestion was carried out for 2 hours at 37°C and using magnetic stirring at 225 rpm meanwhile pepsin solution was added at constant rate of 0.0083 mL/min. Samples (0.5 mL) were taken during the digestion at 5, 10, 15, 30, 60, 90 and 120 min and mixed with 50 μL NaHCO₃ to raise the pH in order to stop pepsin activity. The pH profile together with the curve of HCl addition can be seen in Figure 3.4. In this case, there was slower pH decrease compared with the previous trial and the final pH value did not reach pH 2, which could be due to the buffering action of pepsin.
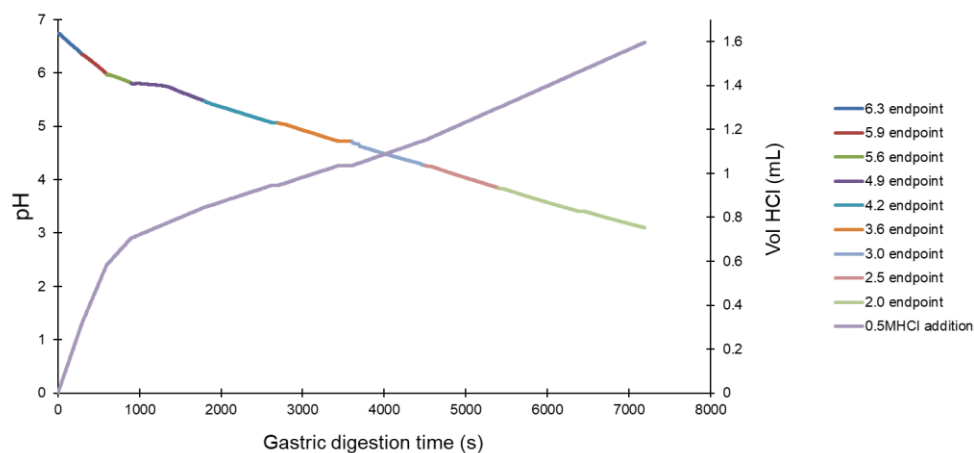
Figure 3.4 Programmed pH curve with different endpoints using 9.5% SMP including oral and gastric phases. Pepsin solution was prepared at 2,000 U/mL (in final volume) and delivered by means of a dosing device following a constant rate of 0.0083 mL/min. The solution 0.5 mol/L HCl was added by another dosing device.

Regarding gastric behaviour, some precipitation was visible at around 30 min, which gradually dissolved resulting in a clear solution (Figure 3.5 A). In contrast, no visible formation of precipitate was observed during the static digestion Figure 3.5 B. The SDS-PAGE of digestion using both static and dynamic pH profile can be seen in Figure 3.6. In the dynamic pH profile there was progressive casein hydrolysis compared to the static method, in which the bands of casein were not visible after 5 min.
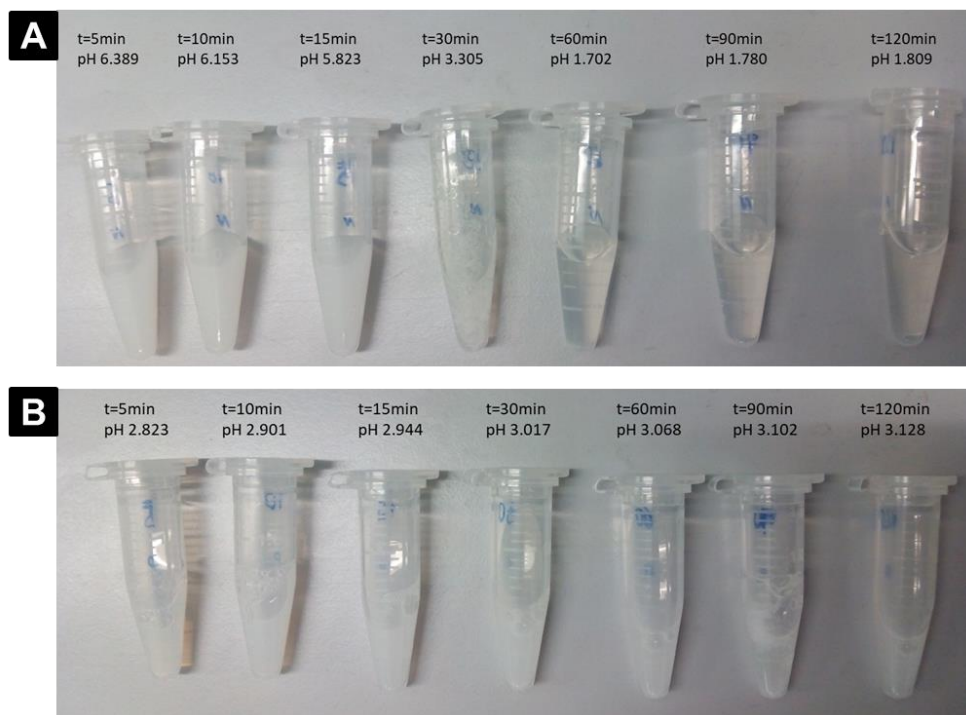
Figure 3.5 Behaviour during gastric digestion of SMP in (A) dynamic pH and (B) static pH.
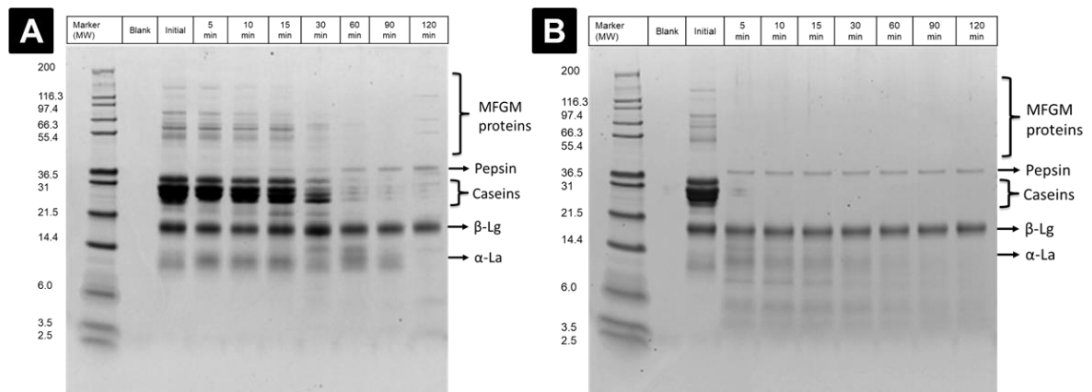
Figure 3.6 SDS-PAGE of the samples taken during gastric digestion in (A) dynamic pH and (B) static pH.

The amount of food, mainly protein, will determine the amount of acid to add because it affects the buffering capacity, which can be observed in Figure 3.7 with different concentrations of SMP (20, 10 and 5%) using the pH programmed curve with fixed endpoints. This suggests that the buffer capacity of the protein is directly proportional to concentration, therefore, the higher buffering capacity results in less changes in the pH value.
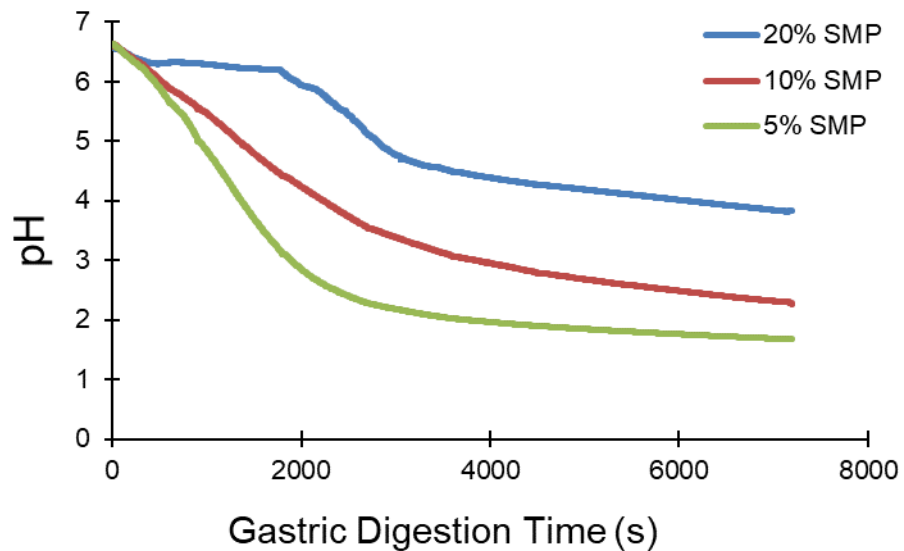
Figure 3.7 pH profile, in dynamic conditions, of different concentrations of SMP (20, 10 and 5%).

The approach of designing a pH curve with multiple endpoints is time consuming because it needs optimisation depending of those parameters, which is not convenient practically. Therefore another approach was tested, this is to measure the volume of acid needed in order to reach a pH value of 2 and an average pH of about 3, and deliver that volume at constant rate for the duration of the gastric phase.

This experiment can be performed prior the actual digestion without considering the addition of enzyme and performing gastric emptying. Therefore this excludes two opposing factors adding the enzymes will increase the buffering capacity of the system while the emptying will lower it. Then, a test digestion considering these two aspects can be tested to check the pH curve. This approach is illustrated in Figure 3.8 for the sample of 20% SMP.
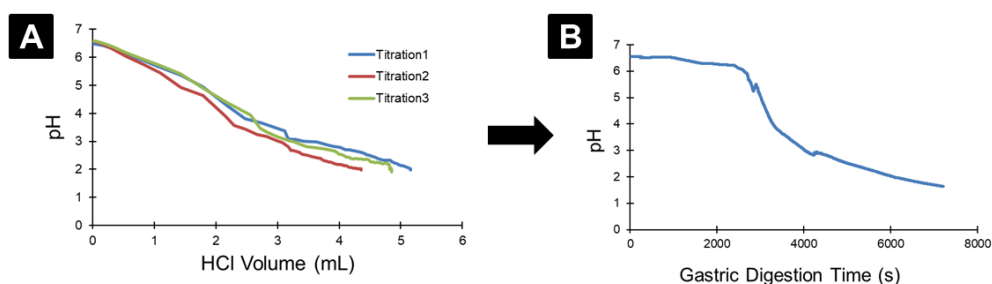
Figure 3.8 In a sample of 20% SMP, (A) three measurements of the volume of HCl needed to reach pH 2, (B) pH curve using a constant delivery of the measured volume of HCl during gastric digestion time.

The pH profile was further improved by the simulation of the basal state of the stomach, in which the gastric residue pH is below 2 and results in a rapid initial lowering of the food immediately after entering the stomach. This was achieved by adding 10% of the required acid in the gastric reaction vessel before placing the food to be digested. Then, the remaining 90% was gradually delivered during the total gastric phase time.

3.3.3 Gastric Mixing System

The initial experiments were performed using a magnetic stirrer inside of the simulated stomach, i.e. reaction vessel. However, this altered the structural changes and could prevent the formation of colloidal structures. Therefore, other types of mixing systems were tested, e.g. orbital shaker. The objective was to obtain some gentle mixing between the gastric secretions and the food inside of the vessel. Figure 3.9 shows the pH curves comparing the mixing systems of magnetic stirrer and the orbital shaking system using a 10% SMP solution, showing that the end values of pH were similar. After two hours of gastric digestion, using the orbital shaker, there was a white clot remaining (Figure 3.10) whereas a clear solution was obtained when magnetic stirrer was used. The incorporation of glass balls (4 balls of 4.5 mm diameter) at the bottom of the vessel when using the orbital shaker aimed to provide a more vigorous mixing at the bottom simulating the higher shear that occurs in the antral part of the stomach. This approach did not work because the balls became

entrapped in the coagulum formed during the gastric behavior, which made their movement impossible.
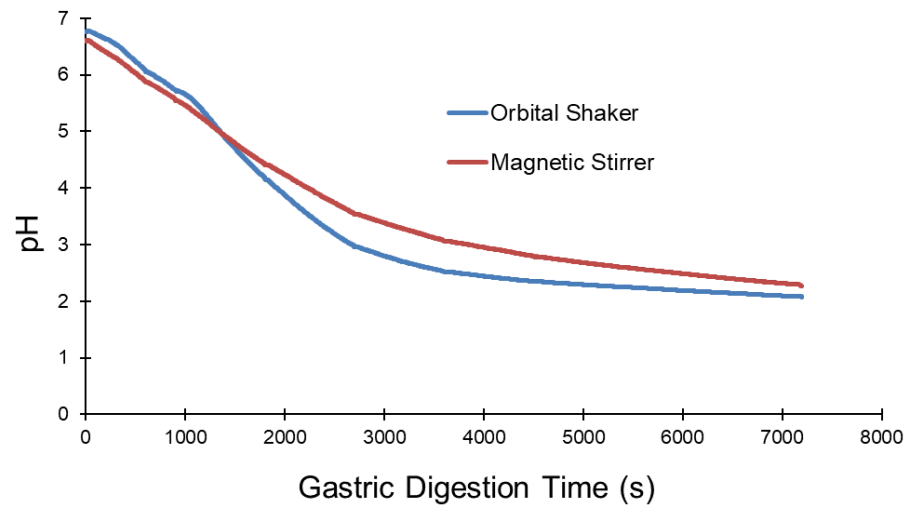
Figure 3.9 pH profile of 10% SMP using an orbital shaker and a magnetic stirrer inside of the vessel.
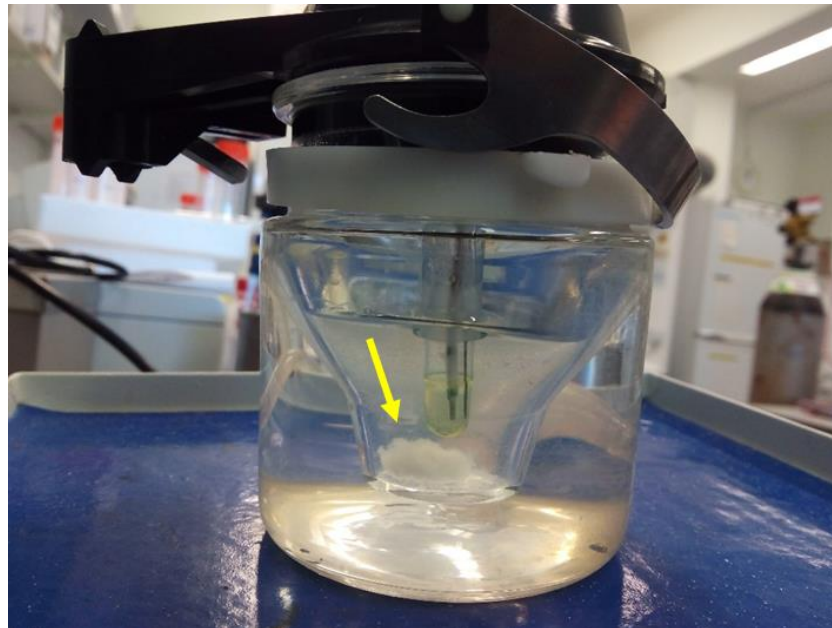
Figure 3.10 Behaviour of 10% SMP after 2 hours of gastric digestion using an orbital shaker as mixing system. Yellow arrow pointing the clot on the bottom of the vessel.

Another type of mixing was tried in the study relating to Chapter 5, mixing inside of the vessel using a 50-mL syringe with plastic tubing. This consisted of pulling in and then pushing out the digesta from the vessel using the syringe. This aimed to take an accurate volume calculated from gastric emptying at each emptied point. The mixing was performed initially before each gastric emptying point. However, this resulted in excessive mixing that disrupted the colloidal structures that developed during the gastric phase (see Figure 3.11), which could alter the simulated nutrient

115

content emptied from the stomach to the duodenum. However, this mixing was applied at early stage of digestion which seemed to provide better results without affecting the later intragastric behavior.
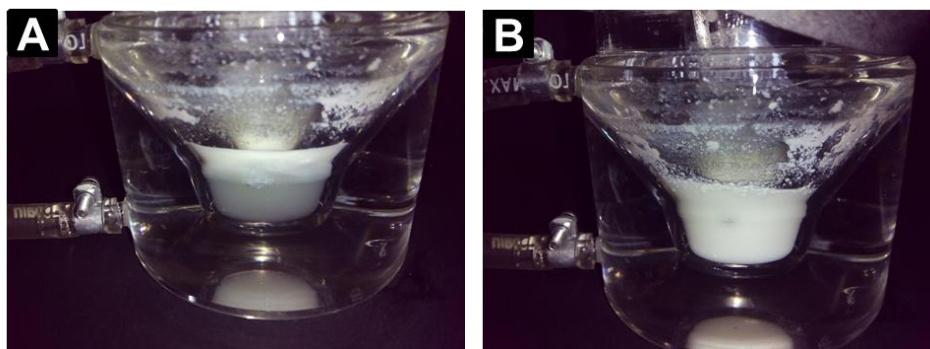
Figure 3.11 Gastric behaviour of a sample (UHT+homogenisation milk) used in Chapter 5, (A) before mixing with syringe and (B) after mixing with syringe.

3.3.4 Gastric Secretions and Gastric Emptying

An example of the calculations for the volume of each gastric fluid used in the semi-dynamic model can be seen in Table 3.5. The oral phase is simulated before the gastric digestion. In this example, 20 g of sample is mixed with a volume of the oral mixture containing 79.9% SSF (1.25x), 19.6% MilliQ® water and 0.5% $CaCl_2(H_2O)_2$ (0.3 mol/L), which corresponds to the total solids content of the sample (3 mL in this example). This mixture is placed in the reaction vessel after the addition of the basal volume, which consists of the 10% of the constituents of SGF (1.25x), MilliQ® water, HCl (1.5 mol/L) and $CaCl_2(H_2O)_2$ (0.3 mol/L) from the total volume of the gastric mixture. The total gastric mixture contained 80% SGF (1.25x), 7.78% MilliQ® water, 8.7% HCl (1.5 mol/L) and 3.48% pepsin and 0.04% $CaCl_2(H_2O)_2$ (0.3 mol/L). Two solutions are added at a constant rate, which depends on the corresponding gastric time, in this example 200 min: (1) the simulated gastric electrolyte mixture containing the 90% of SGF (1.25x), MilliQ® water, HCl (1.5 mol/L) and $CaCl_2(H_2O)_2$ (0.3 mol/L) from the total volume of the gastric mixture and (2) 0.8 mL pepsin solution. The simulated gastric electrolyte mixture of SGF (1.25x), HCl, water and $CaCl_2(H_2O)_2$ was delivered by a dosing device of an automatic titrator and the enzyme solution can be delivered by a syringe pump.

Table 3.5 Example of the parameters used in the semi-dynamic model. Example of 20 g food having 3 g of dry weight and nutrient composition of 5% lipid 3.8% protein, 5% carbohydrate. The energy content is 0.8 kcal/mL calculated using the Atwater factors of 9 kcal/g for fat and 4 kcal/g for protein and carbohydrates. The gastric emptying was scaled down from the considered *in vivo* emptying average of 2 kcal/min in a 500 mL meal (Hunt *et al.*, 1985) . Then, the gastric half time (t$_{1/2}$) was considered to be the same. A volume of 1.5 mL of 2 mol/L HCl is needed to reach pH 2. Five gastric emptied aliquots are taken during the gastric digestion. The density was set at 1 g/cm^3.

A. Food Sample (example)						
Food volume (g)	20					
Energy content (kcal/mL)	0.8					
Total solids (g)	3.0					
B. Gastric Emptying and Total Digestion Time						
	in Vitro	*in Vivo*				
Food volume (mL)	20.00	500.00				
Gastric volume (Oral +basal) at t=0 (mL)	25.30	550.00				
Energy content of food (kcal)	16.00	400.00				
Energy emptying rate (kcal/min)	0.08	2.00				
Volume emptying rate (mL/min) (Emptied in 5 steps of 9.2 mL every 40 min)	0.13	2.75				
Gastric halftime, t$_{1/2}$ (min)	100.0	100.0				
Total digestion time (min)	200.0					
C. Oral and Gastric Digestion						

	Oral Phase		**Gastric phase**				
Compound	**Total Oral Mixture (mL)**	**Total Oral Mixture (%)**	**Total Gastric Mixture (mL)**	**Total Gastric Mixture (%)**	**Basal (mL)**	**Simulated Gastric Electrolyte Mixture (mL). Rate 0.1 mL/min**	**Pepsin Solution (mL). Rate 0.004 mL/min**
SSF (1.25x)	2.40	79.90	-	-	-	-	-
CaCl$_2$(H$_2$O)$_2$ (0.3 mol/L)	0.01	0.50	0.01	0.04	0.001	0.01	-
MilliQ® Water	0.59	19.6	1.79	7.78	0.18	1.61	-
SGF (1.25x)	-	-	18.40	80.0	1.84	16.56	-
HCl (1.5 mol/L)	-	-	2	8.7	0.20	1.80	-
Pepsin solution (2,000 U/mL final)	-	-	0.8	3.48	-	-	0.8
Total	3.00	100	23	100	2.22	19.98	0.8

There are some *in vivo* studies providing data about gastric emptying (GE) rates, i.e. the volume and time in which chyme is delivered from the stomach to the small intestine. This information can be used and applied to the semi-dynamic model by downscaling the volume, about 25 times, since the model is design for smaller volumes than used in human studies. However, this information is only available for a very limited range of foods. Therefore, the GE was based on the caloric density of food, one of the main factors controlling GE (Calbet *et al.*, 1997; Hunt *et al.*, 1985; Kwiatek *et al.*, 2009; Moran *et al.*, 1999; Sauter *et al.*, 2011), the constant rate of 2 kcal/min and 500 mL of volume was used as reference of a standard meal size. The information about the caloric content or the nutrient composition of the sample can be measured or calculated theoretically by applying the standard Atwater factors (1 g of lipid yields 9 kcal, 1 g of protein yields 4 kcal and 1 g of carbohydrates yields 4 kcal).

Table 3.5 shows an example of the calculations regarding GE. In this example, it can be assumed that a 500 g meal is digested, using only a Y g sample. In this case Y= 20. Assuming a scale of 20g / 500g = 0.04 for the rates calculated. Using a constant emptying rate of 2 kcal/min, a 20 g meal with 3 g dry weight with a calorie density of 0.8 kcal/mL would empty at 2 * 0.04 = 0.08 kcal/min. However, both the oral secretions and gastric secretions also need to be taken into account. Thus, the total volume entering the stomach from the oral phase is 20 g of food + 3 mL oral secretion. Then there will be 23 mL of gastric secretion making a total of 46 mL to be emptied. As already described the caloric emptying rate is 0.08 kcal/min and the total calories is 20 g * 0.8 kcal/g = 16 kcal leading to an emptying time of 16/0.08 = 200 minutes. Therefore the total emptying rate will be 46/200 = 0.23 mL/min. If we decide to empty in 5 stages then each stage will need to remove 46/5 = 9.2 mL, which occurs after every 40 minutes.

Regarding the practicalities of the gastric emptying, the aliquots are taken from the bottom of the vessel, simulating the portion of food that would be ready to be delivered into the duodenum, by using lab tools with an opening diameter of approximately 2 mm. Some of the lab tools that were tested and used are pipette tip, serological pipette and syringe with embedded plastic tubing (see Figure 3.12). This was different in some studies of the thesis according to the practical development and the handling of the complex samples.
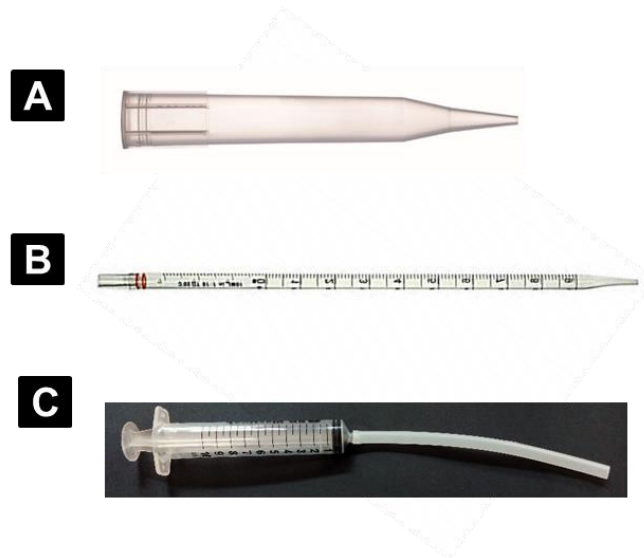
Figure 3.12 Different lab tools that were used to simulate the gastric emptying, (A) pipette tip, (B) serological pipette and (C) plastic syringe with attached tubing (in-house made).

3.3.5 Intestinal Phase

The intestinal phase remains essentially the same as the INFOGEST static protocol (Minekus *et al.*, 2014) but with chyme emptied from the gastric phase being digested separately in parallel, i.e. each emptied aliquot goes through as intestinal digestion, as illustrated in Figure 3.13. Therefore, regarding the volume of the intestinal phase, the volume of the SIF (1x), including pancreatin solution and bile salts, was added according to the proportions based on the INFOGEST static protocol (Minekus *et al.*, 2014).
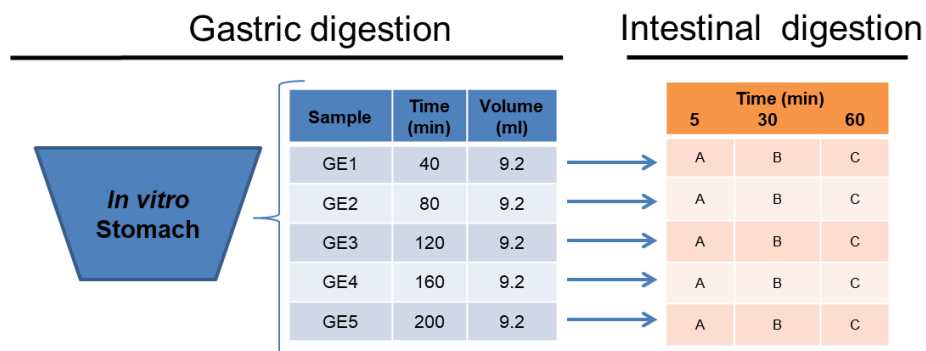
Figure 3.13 Schematic diagram of gastric digestion using the semi-dynamic model having five gastric emptying points (GE) and the subsequent intestinal digestion of each gastric emptied aliquot, during which several aliquots can be taken during time (e.g. after 5, 30 and 60 min of intestinal digestion).

3.4 Discussion

The developed method was built on the basis of the harmonised static digestion INFOGEST (Minekus *et al.*, 2014) regarding digestive fluid composition and the consideration of the dynamic addition of enzymes and reagents, which has been developed further in order to better simulate the stomach dynamics to obtain more physiologically relevant data about nutrient digestion kinetics and structural changes during gastric digestion.

3.4.1 Shape/Geometry of Simulated Stomach

The human stomach has a J-shape however the construction or purchase of this kind of vessel can be difficult. Therefore the reaction vessel selected for this model has a vertical cylinder with V-form alignment, which has been adopted by other dynamic models such as Human Gastric Simulator (HGS) and Dynamic Gastric Model (DGM). This allows the formation of structures driven by colloidal behaviour such as phase separation, as might occur *in vivo*. However, the limitation is that with this arrangement gravity could influence sedimentation and then the particle sieving. The maximum capacity of the vessel used in the experiments presented in this thesis was 70 mL, and typically the initial food volume of 20 mL was selected providing accurate results. This relatively small volume is convenient in terms of handling and also cost, because the use of relatively small amounts of enzymes needed.

Furthermore, the transparent wall of the vessel allows the visual observation and continuous monitoring in real-time and allows photography and video recording. This contrasts with other dynamic models such as HGS, having an opaque gastric compartment. Moreover, the vessel is thermostatically controlled by a circulating water jacket, which allows the simulation of the normal body temperature (37°C) and it can be fully closed during gastric time, except when emptying is applied.

3.4.2 Gastric Mixing

One of the main strengths of this semi-dynamic model is the simulation of the gentle mixing occurring in the fundus/body part of the stomach by using an orbital shaker. This allowed some mixing of the fluids added with the food, in particular to disperse the acid solution in the vessel and, at the same time, provided a non-homogenous chyme. Some studies have shown that the contents in the stomach are poorly mixed contradicting the traditional idea of a complete and rapid intragastric homogenisation of food (Ferrua *et al.*, 2010; Marciani *et al.*, 2001). Therefore, the

model provides much better simulation of *in vivo* conditions than the static model in which high shear is used. As suggested in Figure 3.10, the use of a magnetic stirrer inside of the vessel was observed to disrupt the matrix or/and any possible colloidal interactions occurring during digestion as a consequence of the change in pH, ionic strength and enzymic hydrolysis.

However, the model does not simulate the rather complex mechanical forces of high shear and mixing occurring in the antrum, which is better mimicked by most fully dynamic models. The mixing system has been reconsidered in the harmonised semi-dynamic model INFOGEST protocol (in preparation), in which a paddle type stirrer (see Figure 3.14) placed in the lowest possible part of the reaction vessel and using very low speed (e.g. 10 rpm) could provide a better mixing in that bottom part allowing easier emptying and mimicking better the homogenous chyme of that area. This might be more convenient for systems with complex nature and/or samples in which the consistency changes drastically during the gastric phase. It is clear that this mixing will not provide the same level of simulation than that in dynamic models. Nevertheless, the aim of this semi-dynamic model was not to design another complex dynamic model but to achieve a simpler, more accessible version whilst achieving similar results.

Figure 3.14 Examples of the paddle stirrers that can be used in the semi-dynamic model, the dimensions of which will depend on the geometry of the reaction vessel and they can be 3D printed.

3.4.3 Gastric Secretions

The extent and rate of the gastric juice secretion *in vivo* is subject to complex regulatory control mechanisms for the optimal digestion of nutrients, which will depend on the volume, consistency and nutrient content of ingested food (Armand *et al.*, 1995; Flourie *et al.*, 1985; Malagelada *et al.*, 1979) as well as having a high degree of inter subject variability. For instance, Malagelada *et al.* (1979) reported that the addition of gastric acid and pepsin was maximum within the first 60 min and greater for a solid-liquid meal compared to the same meal in a homogenised form. In this model, the gastric secretions were intended to obtain a final ratio of oral phase content (containing the sample) to total gastric mixture of 1:1 (v/v), which is based on the INFOGEST static digestion (Minekus *et al.*, 2014). The secretions were programmed to be delivered at constant rate during the total gastric time, which is the same approach used in the HGS. This is a simplistic approach compared to *in vivo*, but convenient to use in the laboratory. Some dynamic systems are better at mimicking those non-linear variations, for instance, the digestive secretions in the DGM are programmed to change in response to the acidification and volume of the meal.

The initial addition of 10% simulated gastric electrolyte mixture in the vessel aimed to simulate the basal (fasted) content in the stomach that lowers the pH of food entering from the mouth. The volume of gastric secretion in the fasted state varies among subjects but it is typically 10-50 mL (Fidler *et al.*, 2009; Goetze *et al.*, 2009; Koziolek *et al.*, 2013) considering a standard meal size of 500 mL, then it was convenient to take 50 mL as the average fasted level of secretion. Thus 10% of the required acid was added to the basal secretion in the gastric reaction vessel at the start of the gastric phase and the remaining 90% was gradually delivered with the electrolytes during the total gastric phase time. This may not be completely representative of the situation *in vivo*, but is a simpler methodology to implement in the laboratory.

It is important to note that the secretions were delivered by plastic tubes (see Table 3.4) that were located on the walls of the vessel at approximately 4 mm from the bottom, therefore the solutions were always in contact with the digesta. This simulates the secretions that are produced by the stomach wall and mixed with the meal creating a non-homogeneous gradient. Also, the delivery of acid and enzyme was performed through separate pump systems to avoid the auto degradation of the enzyme.

3.4.4 Dynamic pH Profile

The pH in the human stomach is highly variable. Changes in the pH strongly affect the activity of the digestive enzyme and influence the possible structural changes within the digested food. One of the aims in the development of this model was to closely simulate the dynamic pH changes occurring in the human stomach which depends on the properties of food, in particular the buffering capacity. Typically, the pH in healthy subjects is around 2 under fasted conditions due to the basal residue, which is homogenous within the stomach (McLauchlan *et al.*, 1989). This basal acidity leads to a rapid lowering of the pH of the ingested food, which is simulated by the addition of the aforementioned 10% simulated gastric secretion in the reaction vessel before the start of the *in vitro* gastric digestion. This will drop the pH of food as soon as it is added to the simulated stomach. After meal consumption, the pH increases rapidly up to values of pH 7 or that of the food, after which the pH decreases gradually back to 2 over 2 hours as an average time (Dressman *et al.*, 1990; Malagelada *et al.*, 1976). The pH values as well as the duration of these processes depend on the food properties, e.g. the initial pH, buffering capacity, composition, and quantity of the food ingested. The decrease of pH during gastric digestion is not only due to the secretion of HCl but also the emptying of the chyme, which reduced both the amount of digested food in the stomach and its buffering capacity.

The determination of the volume of acid needed to reach pH 2 and the delivery of the acid at a constant rate was the simplest and most effective approach. Gastric acidification can be monitored in real-time by a pH electrode immersed in the solution. However, it is important to note that there could be fluctuations in the pH inside the vessel due to the heterogeneity of the sample, the limiting mixing and the emptying performed during the digestion as illustrated in Figure 3.15. Nevertheless, this provided close simulation of the stomach environment, in which the acid distribution is not homogenous, leading to pH gradients (Hila *et al.*, 2006). In particular, McLauchlan *et al.* (1989) showed significant differences between the fundus and the antral regions during fed conditions when the pH values were recorded over 24 hours. The pH values of the emptied aliquots taken from the bottom were also measured, which were different from the pH values of the digesta inside the vessel (Figure 3.16).
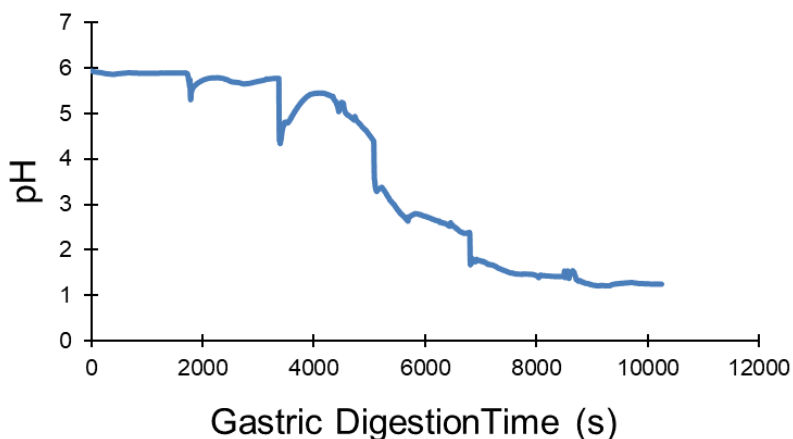
Figure 3.15 Example of the fluctuations in pH recording measured in the reaction vessel. The pH record was performed using the pH electrode attached to the pH titrator (Titrando, Metrohm). This graph corresponds to a sample of raw milk used in Chapter 5.
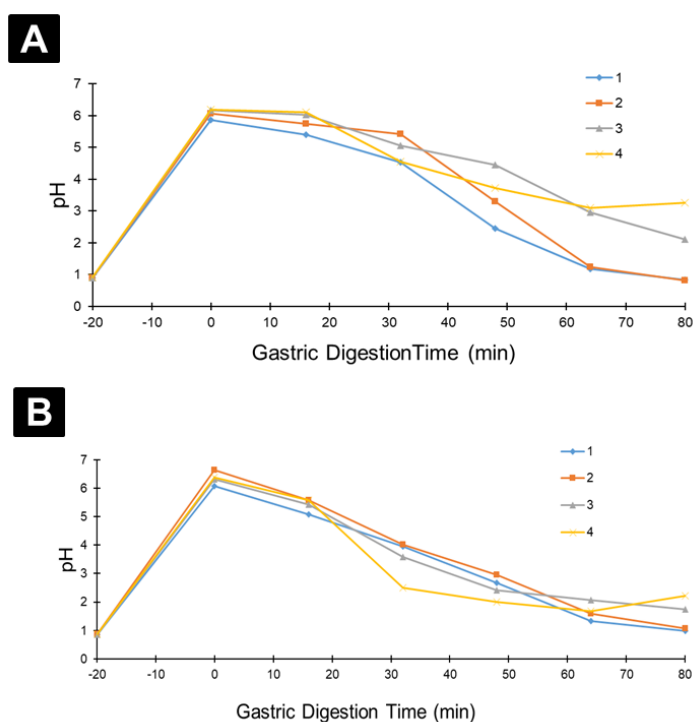
Figure 3.16 Example of the pH profile of some samples (used in Chapter 4), (A) values obtained from inside the simulated stomach by the pH probe attached to the pH titrator and (B) pH values from the emptied aliquots using an external pH meter after the step of mixing with Ultraturrax homogeniser.

3.4.5 Gastric Emptying

The regulation of GE is a complex process which is regulated by factors including gut hormones and properties of food, e.g. viscosity, consistency, volume,

particle size and caloric density. There is some evidence that the caloric density may be the main factor in regulating the rate of GE, a high caloric density inducing slower/longer GE (Calbet *et al.*, 1997; Moran *et al.*, 1999). The caloric content delivered to the duodenum is regulated so the nutrient delivery rate, maintained by a feedback through the release of hormones, in a range from 0.5 to 8 kcal/min (Calbet *et al.*, 1997; Hunt *et al.*, 1975). This depends on the time range over which this rate is calculated and the physical state of the gastric content, having an average rate of 2-3 kcal/min. Brener *et al.* (1983) reported a constant caloric delivery rate of 2.1 kcal/min, similar to Costill *et al.* (1974) and Hunt *et al.* (1985) who reported the mean rate of caloric emptying of 2.5 kcal/min and Sauter *et al.* (2011) reporting 1.9 kcal/min. Moreover, there are studies showing that the type of calories does not seem to play a critical role (Calbet *et al.*, 1997; Hunt *et al.*, 1975; McHugh *et al.*, 1979). The increase in meal volume can also increase GE (Moore *et al.*, 1981) but the semi-dynamic model assumes a fixed volume of 500 mL which was scaled down to be more practical. Furthermore, the physical state of meal (solid or liquid) has been shown to influence the GE behaviour (Camilleri *et al.*, 1985; Malagelada *et al.*, 1979). The emptying for liquids is more rapid following first order exponential kinetics compared to solid meals in which a biphasic emptying behaviour has been observed. Also, the different colloidal behaviour in the stomach has been shown to induce changes in emptying profile (Marciani *et al.*, 2007; Steingoetter *et al.*, 2015).

This complex system of multiple variables cannot be simulated in a simple model, therefore the most convenient approach was to consider a linear rate of emptying of 2 kcal/min as an average, which seems a good approximation due to the ability of the antrum and pylorus to maintain a relatively constant emptying rate. Similarly, in the DGM, the duration of the gastric phase is based on the caloric content of the sample. Nevertheless, the semi-dynamic model can also be applied if the information of the GE (volume and time) from clinical studies is known.

The semi-dynamic gastric model also provides the option of selecting the number of aliquots to be emptied. Since the aim of the model is to provide kinetic data, a minimum of 3 points should be considered. As shown in the rest of the chapters, an emptying protocol using five GE points was performed leading to a balance between the quality and quantity of data and a practical workload.

The gastric sieving created by the pylorus (Thomas, 2006) is simulated by using a 2 mm diameter orifice in the selected lab tool used for sampling (e.g. tip, serological pipette, syringe), see Figure 3.12. It is important to note that by introducing this factor, the delay in the delivery of solid particles can be more closely simulated to the situation *in vivo*. There were some cases in which there was some residue remaining

at the end of the simulated digestion, this was usually collected together with the last GE point simulating the housekeeper wave that fully empties the human stomach at the end of the gastric phase (Meyer *et al.*, 1988). Also, it is important to note the loss of sample through the emptying process, which will largely depend on the complexity of the studied sample, and the properties of any structures that they form, some examples are illustrated in Figure 3.17. This is the main reason for considering the weight of initial food and the collected aliquots instead of volume.
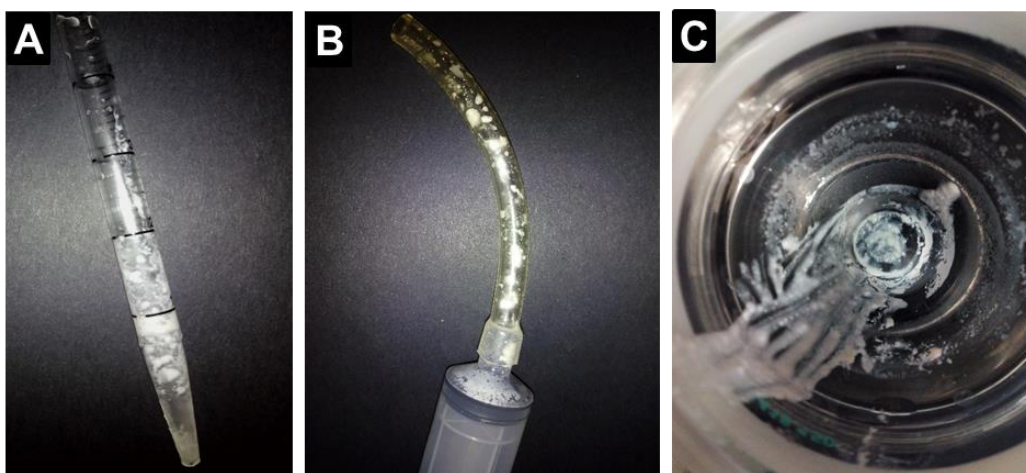
Figure 3.17 Examples of the sample losses during gastric digestion experiments in (A) serological pipette, (B) tubing of plastic syringe and (C) reaction vessel.

3.4.6 Gastric Lipase

The inclusion of gastric lipase in the *in vitro* gastric digestion is still under debate although there is evidence showing its relevant contribution to not only gastric but intestinal digestion. Gastric lipolysis accounts for 10-40% of the overall lipid digestion mainly by hydrolysing triacylglycerol into diacylglycerol and contributes up to 7.5% to the duodenal lipolysis of triacylglycerol (Carriere *et al.*, 1993). Most of the studies in this thesis have been performed without the addition of gastric lipase because the human gastric lipase (HGL) or suitable alternatives were not commercially available or expensive. This was in accordance to the recommendation of the harmonised static model INFOGEST (Minekus *et al.*, 2014). However, rabbit gastric extract (RGE) was used in the study related to Chapter 7. The gastric lipase from RGE has been suggested as a potential substitute for the HGL because it has similar activities and specificities to those of HGL. It has specificity for the sn-3 position of triacylglycerol and an optimum pH range from 5 to 3.5 (Carriere *et al.*, 1991). It is important to note that the RGE contains both gastric lipase and pepsin, therefore the activity of both enzymes should be measured. If the pepsin activity in the RGE is not enough in order to reach the final activity required (4,000 U/mL in total gastric mixture), this should be

supplemented with pepsin from porcine origin as performed in Chapter 7. The delivery of RGE solution can be performed in the semi-dynamic gastric model by the addition of another syringe pump or a dual channel syringe pump.

3.4.7 Applicability of the Semi-Dynamic Model

The semi-dynamic model can provide valuable data about the extent and rate of nutrient digestion and in particular it allows the study of the impact of the food matrix, through structural changes occurring in the stomach, on nutrient bioaccessibility. In a collaboration with the Spanish research institution, Consejo Superior de Investigaciones Cientificas (CSIC), in Madrid, Ferreira-Lazarte *et al.* (2017) used this model with some modifications to study the effect of prebiotic carbohydrates on the gastric digestion of milk proteins. Importantly, efforts by the INFOGEST network have been put into the development of a harmonised version of this protocol that will provide its use internationally. A consensus manuscript, largely based on the semi-dynamic model developed during this thesis and described in this chapter, is currently being prepared and a publication including a detailed protocol will be released soon. The flow diagram that will be presented in this manuscript is illustrated in Figure 3.18. Moreover, an inter-laboratory trial on the digestion of SMP using this model is planned within the INFOGEST network, in a similar way that the inter-laboratory trial for the static digestion model was performed (Egger *et al.*, 2016).
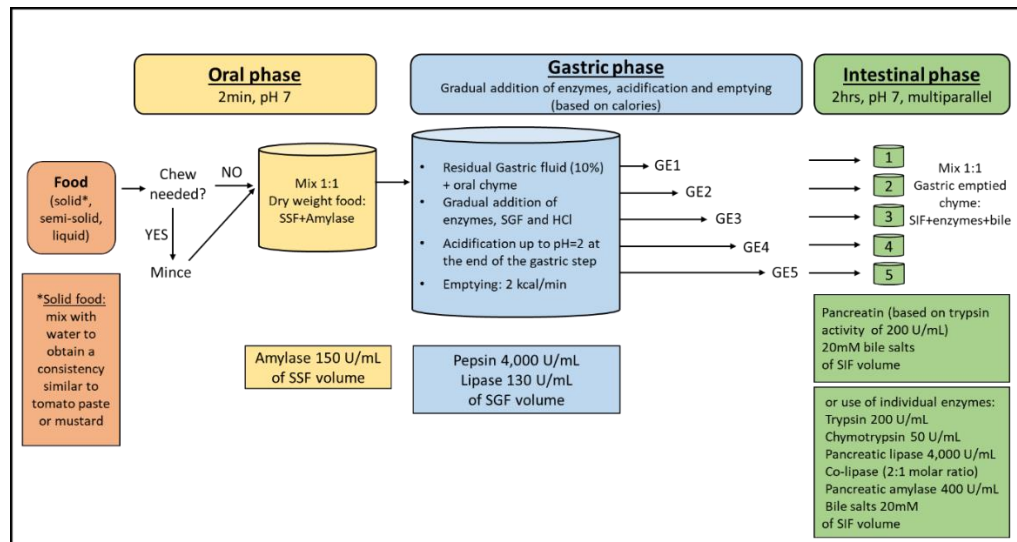
Figure 3.18. Overview and flow diagram of the simulated semi-dynamic *in vitro* digestion method included in the consensus manuscript within the INFOGEST network that will be published.

It is important to highlight the limitations and difficulties of an *in vitro* model of digestion. Firstly, since one of the main aims was to develop a relatively simple,

accessible model that could be used in most laboratories, the mixing consists of a basic stirring system that is not realistically able to simulate the peristalsis occurring in the stomach. Nevertheless, it reflects more closely the levels of mixing in the stomach compared to a static model. In the same line, dynamic GE sampling is used, based on caloric content using the simple approach of the linear GE rate of 2 kcal/min, which is not altered, for instance, by the physical state of the food and the colloidal behaviour within the stomach. Moreover, it does not simulate the oral and intestinal phases as dynamic process. Furthermore, regarding analysis, it is not possible to know the contribution of protease in the protein content/protein hydrolysis analysis because the amount of enzyme that is intact or hydrolysed is uncertain. Also, it is more complex and subjective to handle the samples with regards to the GE and the data obtained can be more complex to analyse and difficult to interpret.

3.5 Conclusion

Gastric digestion is one of the most important steps for fully understanding the mechanisms of the kinetics of nutrient digestion, particularly for real food, i.e. heterogenous and structured foods. Therefore, it is imperative to use relevant *in vitro* models that can simulate more closely the gastric environment, particularly where the structure of the food influences digestion rate. The semi-dynamic model developed in this thesis can provide more physiologically relevant data in relation to structural changes of food and nutrient digestion kinetics in an accessible way in terms of cost and practical simplicity. Nevertheless, it is rather difficult to simulate the overall physiological conditions in the same precision as it occurs in the human stomach, so it is important to recognise and account for its limitations. The work of this chapter has significantly contributed to the development of the harmonised protocol and a related manuscript has been currently prepared by the INFOGEST network, which will be published in 2019 to provide laboratories across the world the opportunity to use this model.

Chapter 4

Impact of Dairy Proteins and Lipid formulation on *in Vitro* Digestion and *ex Vivo* Absorption

4.1 Introduction

There is a growing demand and interest in functional food products, addressed to the needs of specific populations in order to optimise nutrition and provide more effective ways of maintaining wellbeing. For instance, the current greater longevity, causing the growth in population of elderly people aged 80 years and over, has resulted in considering the relevance of products addressed to healthy aging. This might help to prevent and/or attenuate sarcopenia, which is a condition of the progressive loss of skeletal muscle mass with aging, and it is attributed to an imbalance between muscle protein synthesis (MPS) and breakdown. Food intake and physical activity are the main stimuli for MPS. With regards to diet, consumption of proteins/amino acids, in particular Leu, have been seen to be the main stimuli of the net protein synthesis (Tipton *et al.*, 1999). Apart from protein composition, the amino acid (AA) availability is significantly driven by the rate of protein digestion, a major factor for protein deposition (Dangin *et al.*, 2001). Different patterns of postprandial aminoacidemia resulted in different body protein synthesis, breakdown and oxidation (Boirie *et al.*, 1997). Therefore, this should be considered as a strategy to exploit in order to achieve specific uptakes and physiological responses that might benefit specific population groups.

Milk proteins are considered a high quality protein source taking into account the essential AA score and protein-digestibility corrected amino acid score (Schaafsma, 2000). Moreover, they are generally considered a superior source of protein compared to plant proteins since the latter are less digestible and deficient in one or more essential AAs and their Leu content is 6-8%, compared to 10-13% in dairy proteins (Gorissen *et al.*, 2018). The main milk proteins, i.e. caseins and whey proteins, have been reported to show different postprandial protein kinetics in humans, which affect the whole body protein metabolism (Boirie *et al.*, 1997). The ingestion of whey proteins resulted in a high, rapid and transient increased in plasma AAs promoting protein synthesis without supporting protein breakdown. In contrast, caseins induced a low, slow and prolonged aminoacidemia profile, which inhibited body protein breakdown. The Leu balance was positive for the casein drink over 7 hours, promoting protein deposition whereas no effect was provided from whey protein drink. From this study, whey proteins and caseins were labelled as 'fast' and 'slow' proteins, respectively, as analogy to the carbohydrate metabolism. Some studies have shown that faster digestion of whey proteins resulted in an enhancement of MPS responses in elderly men (Dangin *et al.*, 2003; Pennings *et al.*, 2011; West *et al.*, 2011) and in elderly men after resistance exercise (Burd *et al.*, 2012). The coingestion of other macronutrients with dairy proteins is another factor to consider

that may affect the metabolic responses. Elliot *et al.* (2006) showed the uptake of AAs, based on Thr and Phe, was greater for whole milk compared to fat-free milk.

However, the underlying mechanisms of this link between protein structure and metabolic responses are not well understood. The main milk proteins have different physico-chemical properties, which are governed by their structure. Caseins have a relatively open and flexible conformation forming ordered structures known as casein micelles and are insoluble at pH 4.7. In contrast, whey proteins have globular, compact structure and are soluble under acidic conditions. Food is subjected to several digestive conditions within the gastrointestinal (GI) tract and the physico-chemical properties of food will determine the changes in the different compartments. Therefore, it is important to understand the interactions of food structures within the GI tract to underpin the health effects, but this information is still scarce.

There are some studies suggesting the gastric phase as the limiting factor of some of the metabolic effects observed however its study has been rarely undertaken. Boirie *et al.* (1997) suggested that the slow AA absorption behaviour of casein was due to the coagulation that might occur in the human stomach, which could result in a longer gastric emptying (GE), delaying the digesta that is delivered into the small intestine in contrast to the whey proteins that remain soluble and can enter the small intestine rapidly. Investigation of the food behaviour in the human stomach is complex and requires advanced techniques such as magnetic resonance imaging or invasive techniques, which have restrictions in terms of cost and ethics. For that, *in vitro* models are usually used to investigate the mechanisms controlling nutrient digestion within the GI tract. However, static models do not simulate the dynamics of digestion in the stomach that are of relevance, in particular in milk proteins. For example, in contrast to what has been suggested *in vivo*, caseins were reported to be digested rapidly using a static model (Egger *et al.*, 2017). Therefore, a semi-dynamic model was developed and used in the present study to simulate the main dynamics of the human stomach including gradual pH decrease and progressive gastric juice secretion and emptying.

In this study the hypothesis that the different rates of absorption of the main milk proteins were governed by the behaviour adopted within the gastric conditions was tested. Also, the strategy of controlling nutrient uptake by the different rates of nutrient bioaccessibility was studied. For that, formulations differing in the ratio of whey proteins and caseins were tested and the influence of the inclusion of lipid in the protein matrix was also studied. Therefore, the aim of this study was to investigate

the influence of the native protein structure on the gastric behaviour that could potentially result in different physiological responses.

4.2 Materials and Methods

4.2.1 Materials

Whey protein isolate (WPI), BiPRO, was purchased from Davisco, Foods international INC, USA. The protein content was 88.48% (w/w) of dry powder measured by the Kjeldahl method in duplicate (in-house analytical service). Milk protein concentrate (MPC), Solmiko® MPC 80, was obtained from Glanbia Ingredients, Ireland. The protein content was 79.23% (w/w) of dry powder measured by the Kjeldahl method in duplicate (in-house analytical service). Rapeseed oil was purchased from a local supermarket (Tesco, Ireland). Deuterated Leu (5,5,5-D3, 99%), D10 Ile (D10, 98%) and Val (D8, 98%) were purchased from from Cambridge Isotope Laboratories, Inc. (CK Isotopes Ltd., Leicestershire, UK).

4.2.2 Methods

An overview of the experimental planning for this study is illustrated in Figure 4.1.
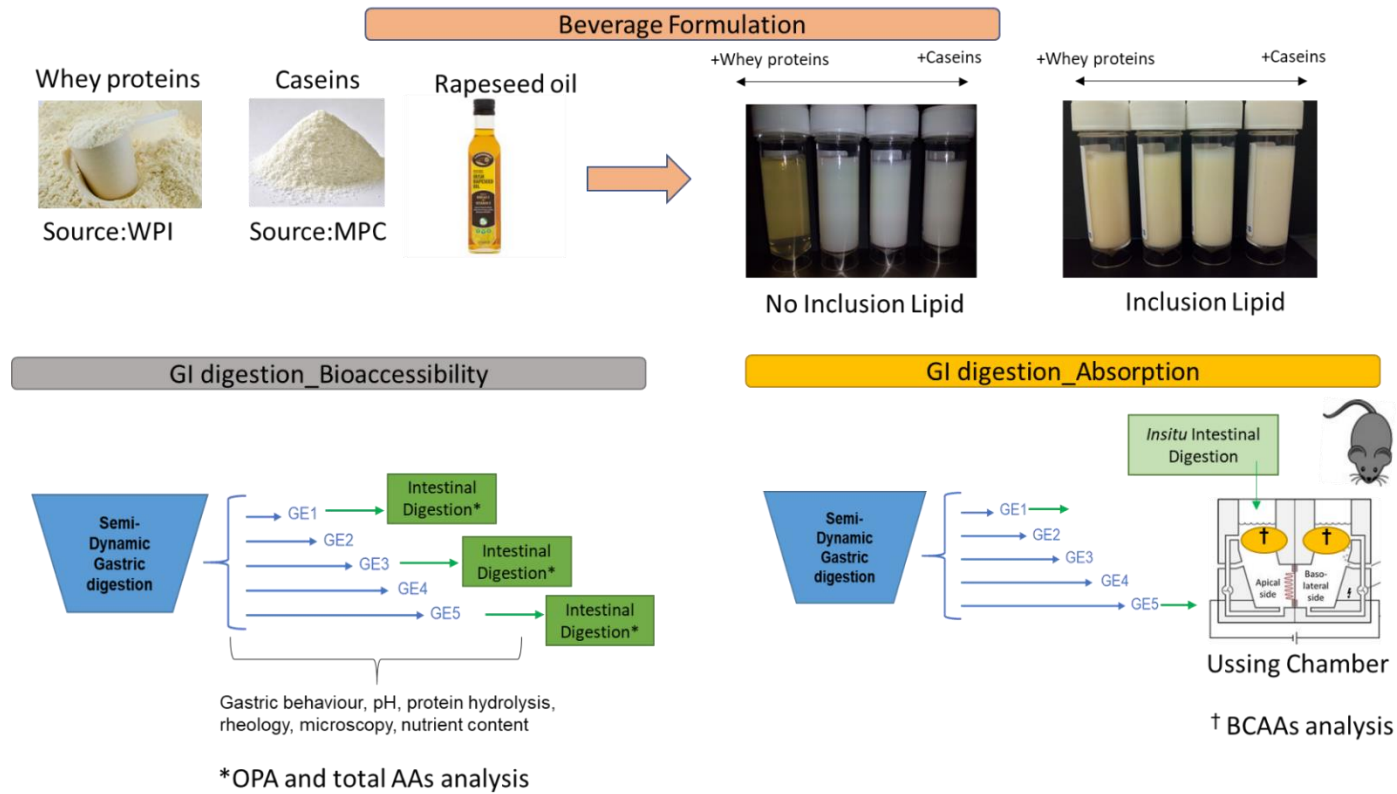
Figure 4.1 Schematic representation of the experimental work for Chapter 4.

4.2.2.1 Preparation of Samples

Table 4.1 shows the content of protein, lipid and total solids of the studied samples as protein solutions and emulsions. The protein solutions referred to 0C:100W and 80C:20W were prepared at 8% (w/w) protein. The 0C:100W was prepared by dissolving WPI powder in water using a mixer (IKA Ecrostar, mix speed 700 rpm) with a paddle stirrer for 2 hours at room temperature. The sample 80C:20W was prepared by dissolving MPC in water using a mixer (IKA Ecrostar, mix speed 700 rpm) with a paddle stirrer for 2 hours at 50°C (using a water bath). Then, an amount of NaN$_3$ was added (0.02% in the final solution) as anti-microbial agent and the solutions were stored overnight at 4°C for rehydration. The samples 20C:80W and 50C:50W were prepared freshly by mixing different amounts of 0C:100W and 80C:20W. The 20C:80W sample was prepared by mixing 75% (w/w) of 0C:100W and 25% (w/w) of 80C:20W. The sample 50C:50W was prepared by mixing 37.5% (w/w) 0C:100W and 62.5% (w/w) 80C:20W. The pH of the samples was adjusted at pH 7 using NaOH (2 mol/L).

Samples with lipid inclusion were prepared starting with the preparation of 0C:100W and 80C:20W at 10% protein (w/w) following the same protocol described previously. Then, the samples 20C:80W and 50C:50W were prepared in the same manner as described before. Each stock protein solution was mixed with 2% rapeseed oil and water in order to achieve a final protein concentration of 8% (w/w). These emulsion samples were named as follows: (0C:100W)2%, (80C:20W)2%, (50C:50W)2% and (20C:80W)2%. The protein solution of 50C:50W was also used to obtained emulsions containing 4% and 8% rapeseed oil. The coarse emulsions were prepared using an Ultra-Turrax (T25 digital, IKA, Germany) at 10,000 rpm for 1 min. Then, they were processed using a homogeniser (APV 1000, SPX Flow Technology, Charlotte, North Carolina, USA) at 200 bar with 3 passes. The pH of the samples was adjusted at pH 7 using NaOH (2 mol/L).

Table 4.1 Compositional description of the studied samples.

| Sample | Protein composition %(w/w) Theoretical[1] | | Added Lipid % (w/w) | Total solids % (measured[2]) |
	Caseins	Whey proteins		
0C:100W	0%	8%	0	8.58 ± 0.08
20C: 80W	1.8%	6.4%	0	8.96 ± 0.08
50C:50W	4%	4%	0	9.47 ± 0.04
80C: 20W	6.4%	1.8%	0	9.83 ± 0.06
(0C:100W)2%	0%	8%	2	10.45 ± 0.02
(20C: 80W)2%	1.8%	6.4%	2	10.68 ± 0.06
(50C:50W)2%	4%	4%	2	11.19 ± 0.04
(80C: 20W)2%	6.4%	1.8%	2	11.71 ± 0.03
(50C:50W)4%	4%	4%	4	12.98 ± 0.01
(50C:50W)8%	4%	4%	8	16.67 ± 0.05

[1]The content of whey proteins and caseins was based on the theoretical content of 80% caseins and 20% whey proteins in the MPC that was used. [2]The total solid content was measured using CEM Smart Trac System-5 (CEM Corp., Matthews, N.C., U.S.A.). Values are the mean ± standard deviation of two independent duplicates.

The droplet size was measured using a laser-light diffraction unit (Mastersizer, Malvern Instruments Ltd, Worcestershire, UK) as described in section 2.2.3.1. The optical parameters chosen were a particle and dispersant (water) refractive index of 1.47 and 1.33, respectively. The absorbance value of the lipid globules was 0.001. The mean values (n = 6) of $d_{4,3}$ were 0.73 ± 0.08 µm, 0.53 ± 0.03 µm, 0.34 ± 0.02 µm and 0.29 ± 0.04 µm for the samples (0C:100W)2%, (20C:80W)2%, (50C:50W)2% and (80C:20W)2%, respectively. The mean values (n = 3) of $d_{4,3}$ were 0.47 ± 0.06 µm and 0.62 ± 0.04 µm for (50C:50W)4% and (50C:50W)8%, respectively.

4.2.2.2 *In Vitro* Digestion Protocol

4.2.2.2.1 *In Vitro* Gastric Digestion by the Semi-Dynamic Model

The simulation of the adult GI digestion was done by the semi-dynamic model previously detailed in Chapter 3 and using the protocol described in section 2.2.2.1 with some modifications.

The oral phase was simulated before the gastric digestion. 20 g of sample was mixed with a volume of the oral mixture containing 79.9% SSF (1.25x),19.6% MilliQ®

water and 0.5% $CaCl_2(H_2O)_2$ (0.3 mol/L). The volume of the oral mixture corresponded to the content of total solids of the sample (Table 4.1) in 20 g. The volume of the oral mixture varied slightly between samples, ranging from 1.72 to 3.33 mL due to the difference of the total solid concentration in the analysed samples. The mixing was performed using a rotator (SB3 Model, Stuart, Bibby Scientific, UK) at 30 rpm for 2 min. The temperature was kept at 37°C using an incubator (BF56, Binder GmbH, Germany).

The resulting mixture was then put through the gastric digestion using a reaction vessel, which was a v-form glass vessel (5-70 mL titration vessel, Metrohm, Switzerland) with thermostat jacket (37°C). The sample from the oral phase was placed in the reaction vessel after the addition of the basal volume, which consisted of the 10% of the constituents of SGF (1.25x), MilliQ® water, HCl (1.5 mol/L) and $CaCl_2(H_2O)_2$ (0.3 mol/L) from the total volume of the gastric mixture. The total gastric mixture contained 80% SGF (1.25x), 7% MilliQ® water, 8.7% HCl (1.5 mol/L) and 3.48% pepsin and 0.04% $CaCl_2(H_2O)_2$ (0.3 mol/L). Two solutions were added at a constant rate, which depended on the corresponding gastric time: (1) the simulated gastric electrolyte mixture containing the 90% of the constituents of SGF (1.25x), MilliQ® water, HCl (1.5 mol/L) and $CaCl_2(H_2O)_2$ (0.3 mol/L) from the total volume of the gastric mixture and (2) 0.8 mL pepsin solution (made with MilliQ® water). The simulated gastric electrolyte mixture of SGF (1.25x), HCl, water and $CaCl_2(H_2O)_2$ was delivered by a dosing device (800 Dosino, Metrohm, Switzerland) of an automatic titrator (842 Titrando, Metrohm, Switzerland) and the enzyme solution was delivered by a syringe pump (Legato, Kd Scientific, USA). A 3D action shaker (Mini-gyro rocker, SSM3 Model, Stuart, Barloworld Scientific limited, UK) at 35 rpm was used for agitating the vessel. Since the amount of oral mixture was slightly different between the samples due to their composition, the amount of gastric mixture added was accordingly (see Table 4.2).

Table 4.2 Total volume of both oral and gastric mixture added in the simulated digestion of each sample.

Samples	Total Oral Mixture (mL)[a]	Gastric Fluids Secretions		
		Total Gastric Mixture (mL)[b]	Delivery Rate of Simulated Gastric Electrolyte Mixture (mL/min)[c]	Delivery Rate of pepsin solution (µL/min)[d]
0C:100W	1.72	21.72	0.24	10.0
20C: 80W	1.79	21.79	0.24	10.0
50C:50W	1.89	21.89	0.24	10.0
80C: 20W	1.97	21.97	0.24	10.0
(0C:100W)2%	2.09	22.09	0.15	6.40
(20C: 80W)2%	2.14	22.14	0.15	6.40
(50C:50W)2%	2.24	22.24	0.15	6.40
(80C: 20W)2%	2.34	22.34	0.15	6.40
(50C:50W)4%	2.60	22.60	0.12	4.70
(50C:50W)8%	3.33	23.33	0.08	3.08

[a]The total oral mixture referred to a mixture of 79.9% SSF (1.25x concentrated), 19.6% MilliQ® water and 0.5% $CaCl_2(H_2O)_2$ (0.3 mol/L). [b]The total gastric mixture contained 80% SGF (1.25x concentrated), 7.78% MilliQ® water and 0.04% $CaCl_2(H_2O)_2$ (0.3 mol/L), 8.7% HCl (1.5 mol/L) and 3.48% pepsin solution. [C] The simulated gastric electrolyte mixture represented the 90% of the total gastric mixture of the constituents of SGF (1.25x), MilliQ® water, $CaCl_2(H_2O)_2$ (0.3 mol/L) and HCl (1.5 mol/L). This was delivered through a dosing device of an automatic titrator, which was programmed according to the total time of digestion and the remaining 10% was firstly added in the reaction vessel to simulate the basal state. [d]The volume of 0.8 mL of pepsin solution was added in the gastric digestion of each sample, which was delivered during the corresponding total gastric digestion time.

Gastric emptying (GE) was simulated by taking five aliquots, referred to as GE1-5 in the text. Samples were taken from the bottom of the vessel using a 10 mL plastic syringe (BD Plastipak, Ireland), the aperture of which had an inner diameter of 2.5 mm with a plastic tube attached (3.6 mm inner diameter). It is important to note that in some cases there was some residue left in the last GE point that could not be taken using that syringe; this was taken using a spatula and included in the last point. The pH was measured and a sufficient volume of NaOH (2 mol/L) was added to the samples to increase the pH above 7, inhibiting pepsin activity. Finally, samples were snap-frozen in liquid nitrogen and stored at -20°C until subsequent intestinal digestion. A separate gastric digestion was performed in order to study the gastric restructuring and nutrient delivery. An aliquot (250 µL) of these GE aliquots was used for microscopy. Then, the sample was mixed using a homogeniser (T10 basic Ultra-Turrax®, IKA®, Germany) at approximately 30,000 rpm for 30 s to obtain a homogenous sample for the corresponding analyses.

The simulation of the emptying was based on caloric density. A linear GE rate of 2 kcal/min, which is considered the average caloric content that is emptied *in vivo*

in a regulated manner by the antrum for an average food volume of 500 mL (Hunt *et al.*, 1985), was used and scaled down for this reduced-volume system. This implied that the volume and time of each emptying point differed between protein solutions and emulsions due variations in the caloric content (see Table 4.3).

Table 4.3 Time (min) at which gastric emptying (GE) was applied in the samples, based on their caloric content. Five emptying points were used.

	Gastric emptying time (min)				
	GE1	**GE2**	**GE3**	**GE4**	**GE5**
0C:100W	16	32	48	68	80
20C: 80W	16	32	48	68	80
50C:50W	16	32	48	68	80
80C: 20W	16	32	48	68	80
(0C:100W)2%	25	50	75	100	125
(20C: 80W)2%	25	50	75	100	125
(50C:50W)2%	25	50	75	100	125
(80C: 20W)2%	25	50	75	100	125
(50C:50W)4%	34	68	102	136	170
(50C:50W)8%	52	104	156	208	260

4.2.2.2.2 Small Intestinal *in Vitro* Digestion

The simulation of the intestinal phase was performed on the GE1, GE3 and GE5 aliquots of each sample. The protocol was performed according to the standardised procedure Minekus *et al.* (2014). The amounts of pancreatin solution, bile solution and $CaCl_2(H_2O)_2$ were adjusted in each case depending on the gastric sample volume in order to get a trypsin activity of 100 U/mL, and the concentrations of 10 mmol/L bile and 0.6 mmol/L $CaCl_2(H_2O)_2$ in the final digestion mixture. Samples were placed in a rotator (SB3 Model, Stuart, Bibby Scientific, UK) at 40 rpm using an incubator (BF56, Binder GmbH, Germany) to keep the temperature at 37°C. The digestion was performed for 30 min, except in the case of the GE5 aliquot, in which the duration was 120 min. One aliquot (2 mL) was taken after 30 min and 120 min (only in GE5 samples), mixed with 20 µL of inhibitor (0.1 mol/L PMSF) and snap-frozen using liquid nitrogen for subsequent analyses.

4.2.2.2.3 *Ex Vivo* Absorption by Ussing Chamber Technique

The Ussing chamber methodology was used to investigate the kinetics of AA absorption of different milk protein-based formulation. A further description of this technique can be seen in section 2.2.2.3. This technique was applied in selected samples previously digested using the semi-dynamic gastric model. These were the first and last GE points, i.e. GE1 and GE5 points of each sample, using two replicates from individual gastric digestions. Therefore, two independent samples of each GE point and sample were used.

4.2.2.2.4 Intestinal Tissue Samples

All animal protocols were approved by local ethical review committees and conformed to relevant national guidelines (University of Leeds, Leeds, UK). Intestinal tissue sections were obtained from 6 to 8-week-old male/female mice (strain C578L/6). The animals had free access to water and usual meal any time before the collection. Mice were euthanized by cervical dislocation. The whole length of the digestive tract was collected and transported in a tube containing 10 mmol/L glucose solution in an ice-cold bag.

4.2.2.2.5 Ussing Chamber Set up and Sampling

A jejunum section was taken and cut longitudinally along the mesenteric attachment. The section was washed with 10 mmol/L glucose solution and most of the muscular layer was stripped away with fine forceps. The tissue segment was mounted on the slider (P2404, Physiologic Instruments), which was placed in an Ussing chamber (EM-CSYS-4 system EasyMount with P2400 chamber). Up to three segments from each animal were used. The active epithelial surface area of each segment was 0.25 cm^2.

Both sides of the Ussing chambers were filled with Ringer solution containing 120 mmol/L NaCl, 3 mmol/L KCl, 23 mmol/L NaHCO$_3$, 0.5 mmol/L MgCl$_2$, 1.25 mmol/L CaCl$_2$ and 10 mmol/L mannitol, according to Brighton *et al.* (2015). The apical and basolateral sides were filled with Ringer solution with 10 mmol/L mannitol and 10 mmol/L glucose, respectively. The system was maintained at 37°C with continuous bubbling using 5% CO$_2$/95% O$_2$ (v/v).

The voltage and resistance were continuously monitored to evaluate the viability of the tissue using DVC-1000 (WPI Instruments) multichannel computer-controlled voltage clamp unit. This was performed with the use of Ag/AgCl electrodes and 150

mmol/L NaCl agarose (previously prepared). The recordings were collected using Spike2 8.08 software.

After the slider with the tissue was placed in the Ussing chamber, the system was allowed to equilibrate for 30 min. During this period, the voltage and resistance values were monitored over time. After the equilibration, the solutions from both sides were removed. The apical side was refilled with the sample and the basolateral side was refilled with 1 mL of fresh Ringer solution containing 10 mmol/L glucose.

The sample placed in the apical side of the Ussing chamber was aimed to simulate an *in situ* intestinal digestion while diffusion took place. For that, an aliquot from gastric digestion was quickly mixed with bile solution, water, $CaCl_2(H_2O)_2$ and pancreatin solution. The proportions used were according to the standardised INFOGEST static protocol for small intestinal digestion (Minekus *et al.*, 2014), in order to achieve 100 U/mL of pancreatin (based on trypsin activity), 0.6 mmol/L $CaCl_2(H_2O)_2$ and 10 mmol/L of bile, in the final digestion mixture. A volume of this mixture was mixed with Ringer solution (10x concentrated) and mannitol (100 mmol/L) to achieve a final concentration of 10 mmol/L in the sample that was finally placed in the apical side of the Ussing chamber.

An aliquot of 100 μL was taken from both apical and basolateral at 5, 30 and 60 min and the same volume was replaced with fresh Ringer solution containing 10 mmol/L mannitol and glucose accordingly. The aliquots collected were mixed with 100 μL of 24% TCA to stop protease activity and stored at -20°C for further analysis. During the experiment, both voltage and current values were monitored every 10 min and the resistance was calculated. At the end of the experiment, a mixture of foskolin and 3-isobutyl-1-methylxanthine was added (final concentration of 10 μmol/L and 100 μmol/L, respectively) to both apical and basolateral sides, which should cause a substantial increase in potential difference if the integrity of the tissue is satisfactory. Experiments that did not show a clear increase were repeated. Two Ussing chambers were used simultaneously each experimental day using the tissue sections of one mouse. The two GE points, i.e. GE1 and GE5 of each sample were usually assessed each day.

4.2.2.3 Confocal Laser Scanning Microscopy

The microstructure of the initial and the emptied aliquots from the semi-dynamic gastric digestion was observed by confocal laser scanning microscopy (CLSM) using a Leica TCS SP5 microscope (Leica Microsystems, Baden-Württemberg, Germany), as described in section 2.2.3.3. A dye mixture of Fast green FCF solution (0.1% made

with water) and Nile red (0.1% made with propanediol) solution at 1:3 proportion was used. 250 µL of initial/digested sample was gently mixed with 25 µL of mixed dye.

4.2.2.4 Texture Analysis of Gastric Digesta

Some indication of the consistency with regards to the strength of the coagulum formed during semi-dynamic gastric digestion was assessed using a texture analyser (TA.XT Plus, Stable Micro Systems). For that, additional gastric digestions were performed but stopping the run at GE2 time and the vessel of reaction was immediately placed in the texture analyser instrument. The digesta was compressed by a cylindrical stainless-steel probe (6 mm diameter) until the distance of the probe inside the coagulum was 10 mm. The test was run at a speed of 1.0 mm/s and the trigger force was 1 g. Five measurements were made for the same digesta sample and three independent gastric digestions were performed. The value of strength, i.e. the maximum force, in each measurement was obtained from the force-time curve of the texture profile (see section 2.2.3.2).

4.2.2.5 Total Protein and Lipid Content Analysis

The protein and lipid content of the initial sample and the emptied aliquots was determined using a LECO FP628 Protein analyser and CEM Smart Trac System-5 and a SMART Trac Rapid Fat Analyzer, respectively. Details of these techniques have been described in sections 2.2.4.1 and 2.2.5.1. Each sample was measured twice and each measurement was carried out in in three independent replicates.

4.2.2.6 Quantification of Protein Hydrolysis

The spectrophotometric assay o-phthalaldehyde (OPA) described in 2.2.4.3 was used for the quantification of the free amino groups released during digestion. The absorbance was measured at 340 nm using a multi-mode microplate reader, Synergy™ HT (BioTek® Instruments, Inc., Winooski, VT). Each sample was measured twice and each measurement was carried out in three independent replicates.

4.2.2.7 Protein Identification in Emptied Digesta

Sodium dodecyl sulphate-polyacrylamine gel electrophoresis (SDS-PAGE) which is described in the section 2.2.4.2 was used to determine protein composition. SDS-PAGE was performed on the initial and digested samples previously diluted (1:100) with water.

4.2.2.8 Cation Exchange Chromatography for Amino Acid Analysis

The analysis was performed on samples from the semi-dynamic gastric (G1, G3 and G5) and static intestinal digestion (G1I, G3I, G5I and G5I120). The samples were pretreated before AAs analysis. An aliquot of sample (750 µL) was mixed with 750 µL 24% (w/v) TCA, which removed higher molecular weight proteins from the matrix. Then, the mixture was centrifuged at 14,000 rpm for 10 min. Ninhydrin derivatization with norvaline was used as an internal standard. The analysis was performed using a Jeol JLC-500/V AminoTac™ amino acid analyser fitted with a Jeol Na$^+$ high-performance cation-exchange column (Joel Ltd., Garden city, Herts, UK). The chromatography analysis was performed by Anne Marie McAuliffe from the Technical Services Lab in Moorepark Teagasc Food Research Centre (Ireland). Further details of this method can be seen in the section 2.2.4.4.

4.2.2.9 Liquid Chromatography coupled to Tandem Mass Spectrophotometry for Amino Acid Analysis

The branch chain AAs (BCAAs), i.e. Leu, Ile and Val, were detected and quantified by LC-MS/MS (described in the section 2.2.4.4) on the samples from the Ussing chamber experiments, both apical and basolateral sides.

A mixture of Leu, Ile and Val standard was used for the calibration ranging from 0.31 to 10 µmol/L. Internal standard consisted of 5 µmol/L of each Leu (5,5,5-D3, 99%), D10 Ile (D10, 98%) and Val (D8, 98%). 10 µL of this internal standard was added to 50 µL of each concentration standard or sample. After centrifugation (13,300 rpm, 4°C for 10 min), sample was transfer to HPLC vials for LC-MS/MS analysis. Agilent 6490 Triple Quad MS mass spectrometer equipped with an Agilent 1290 HPLC system (Agilent Technologies, Santa Clara, CA, USA) was used. The method for the separation of amino acids was adapted from Nemkov *et al.* (2015). The LC flow rate was 0.78 mL/min. The column used for the analysis was Phenomenex Kinetex XB-C18 2.6 µm (150 x 4.6 mm) column. The column temperature and auto sampler were maintained at 25°C and 4°C, respectively. 1 µL was used for the injection volume. The samples were analysed using 0.1% formic acid in water (mobile phase A) and 0.1% formic acid in 100% acetonitrile (mobile phase B). The isocratic elution was 5% mobile phase B and 95% mobile phase B. The run time was 6 min.

The 6490 MS/MS system was equipped with an electrospray ionization (ESI) source operated in positive-ion detection mode. Nitrogen gas was used for nebulation, desolvation, and collision. The analytes were monitored in multiple-reaction monitoring (MRM) mode. The MRM precursor, product ions and collision energy were

optimized by Agilent optimizer software. The transitions of precursor ions to product ions (*m/z)* and some optimized MS operating parameters of the analyte are described in Appendix A. The source parameters were: gas temperature of 200°C with a gas flow of 16 L/min, a sheath gas temperature of 300°C with a sheath gas flow of 11 L/min, a nebuliser pressure of 50 psi and capillary voltage of 3500 V for positive polarity, Nozzle Voltage 1000 V. The iFunnel parameters were: high pressure radio frequency of 150 V and low-pressure radio frequency of 60 V. The LC eluent flow was sprayed into the mass spectrometer interface without splitting. Identification was achieved based on retention time of authentic amino acid standards and product ions.

The quantification was done by the MassHunter Quantitative B.06 Workstation software (Agilent Technologies, CA, US). Calibration curves were obtained by using authentic standards (Leu, Ile and Val) containing deuterated Leu, Ile and Val mixture as internal standard. The ratio of analyte and internal standard peak area was plotted against the corresponding concentration (0-10 µmol/L) to obtain the calibration curve. In the analysed samples, the peak area ratio (peak area of analyte/peak area of the internal standard). was calculated and applied to the calibration curve to obtain the concentration of each AA.

4.2.3 Statistical Analysis

The results were expressed as mean ± standard deviation of three independent replicates unless otherwise stated. To identify differences in normally distributed results within groups during gastric digestion, one-way ANOVA was applied. Where overall significant interaction was observed ($p < 0.05$), the means of individual formulations were compared using Tukey's post hoc test. Statistical analyses were performed using GraphPad Prism software (Prism 5 for Windows, Version 5.04).

4.3 Results

4.3.1 Gastric pH of the Emptied Digesta

The pH of the emptied gastric aliquots during the semi-dynamic gastric digestion from all the samples is shown in Figure 4.2. In general, they followed a predefined curve, in which there was a low pH before the gastric digestion simulating the basal stage, then the pH increased up to values around 6 and decreased progressively during gastric digestion reaching values of about 2. There were significant differences, in

particular in the case of the sample 80C:20W, in which the pH was lower at 32 min compared to the other samples (Figure 4.2 A). Also, the samples containing higher casein content, i.e. 50C:50W and 80C:20W, had slight pH increase at the end of the digestion. A similar trend was observed in the samples when 2% lipid was added (Figure 4.2 B), although the profile of the sample (50C:50W)2% was more similar to the samples containing higher content in whey proteins, in particular in the end point. Figure 4.2 C compares the effect of lipid in samples with the same protein composition, i.e. C:W ratio of 1. It can be observed that the pH decrease in (50C:50W)8% was lower and slower during the gastric digestion time when compared to the other samples, in particular when lipid was not included. This could be partly due to the longer residence time, having lower secretion rate, in the simulated stomach as observed in Figure 4.2 D, giving it more chance to be mixed.
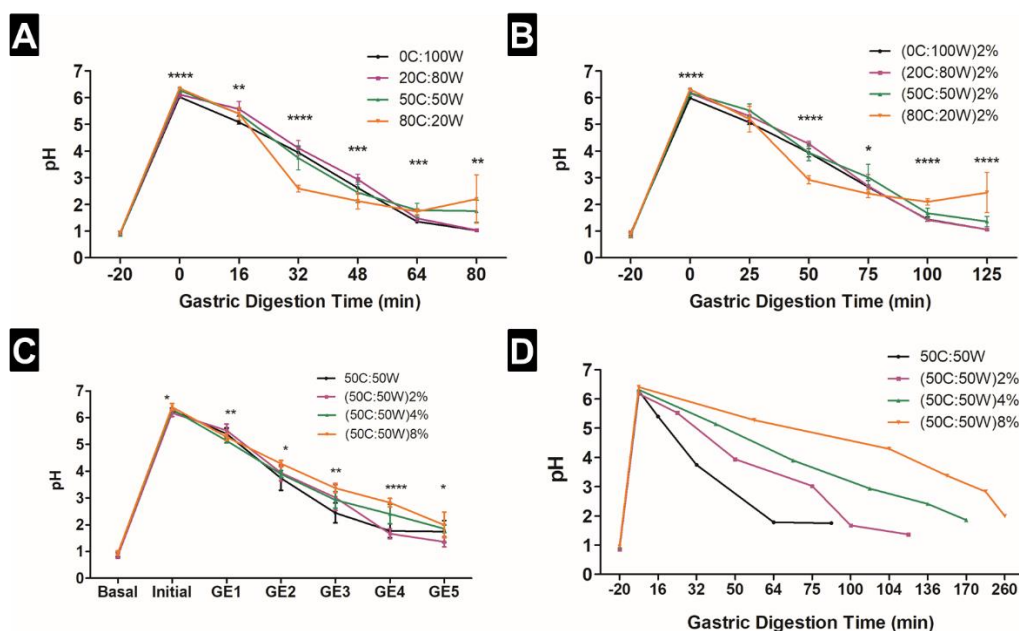
Figure 4.2. Change in pH during gastric digestion using the semi-dynamic model, measured in the emptied aliquots, of (A) protein solution samples, (B) emulsion samples with 2% lipid, (C) samples with C:W ratio of 1 (i.e. formulation 50C:50W) containing 0%, 2%, 4% and 8% lipid in the emptied aliquots expressed as function of the GE points, and (D) same pH values than in graph (C) but expressed as function of the actual gastric digestion time. Gastric digestion time is as indicated in A, B and D graphs and the time before the start of the digestion (-20 min) corresponds to the basal stage. In C, the pH values are referred to the basal stage (before gastric digestion), initial (t=0, sample including oral phase and basal volumes) and the different GE samples (GE1-GE5) corresponding to each gastric emptying (GE) point. The time values are displayed in Table 4.3. Values are presented as means ± SD (n=6). Significance difference in pH between samples in each GE point was determined by one-way ANOVA, $p \leq 0.05$ (*), $p \leq 0.01$ (**), $p \leq 0.001$ (***) and $p \leq 0.0001$ (*****).

4.3.2 Gastric Behaviour

Figure 4.3 shows the gastric behaviour of the protein solution samples at the corresponding time points of GE1, GE3 and GE5. In general, all the samples

presented protein aggregation within the first 10 min of gastric digestion. However, the aggregates in samples 0C:100W and 20C:80W that were initially dispersed within the vessel were progressively solubilised. During digestion time, they tended to form a layer in the bottom part of the vessel with a clear top part, resulting in a completely clear solution at the end of the gastric digestion. The extent of this aggregation was visually larger in the case of 20C:80W as seen in Figure 4.3 F, and the clear solution was obtained later on in the gastric digestion when compared to the 0C:100W sample. In contrast, the initial aggregates formed within the vessel in the samples 50C:50W and 80C:20W were insoluble, which led to the formation of firm and compact coagula located at the bottom of the vessel, similar to mozzarella cheese in texture, and a clear layer at the top part. However, according to visual observations, the formation of that compact coagula in the case of 50C:50W tended to be slightly later and having a more particulate consistency compared with the sample 80C:20W. The digesta of the samples obtained at the corresponding GE2 time displayed in a petri dish can be observed in Figure 4.3 M-P, illustrating the range of structures obtained in the gastric phase.
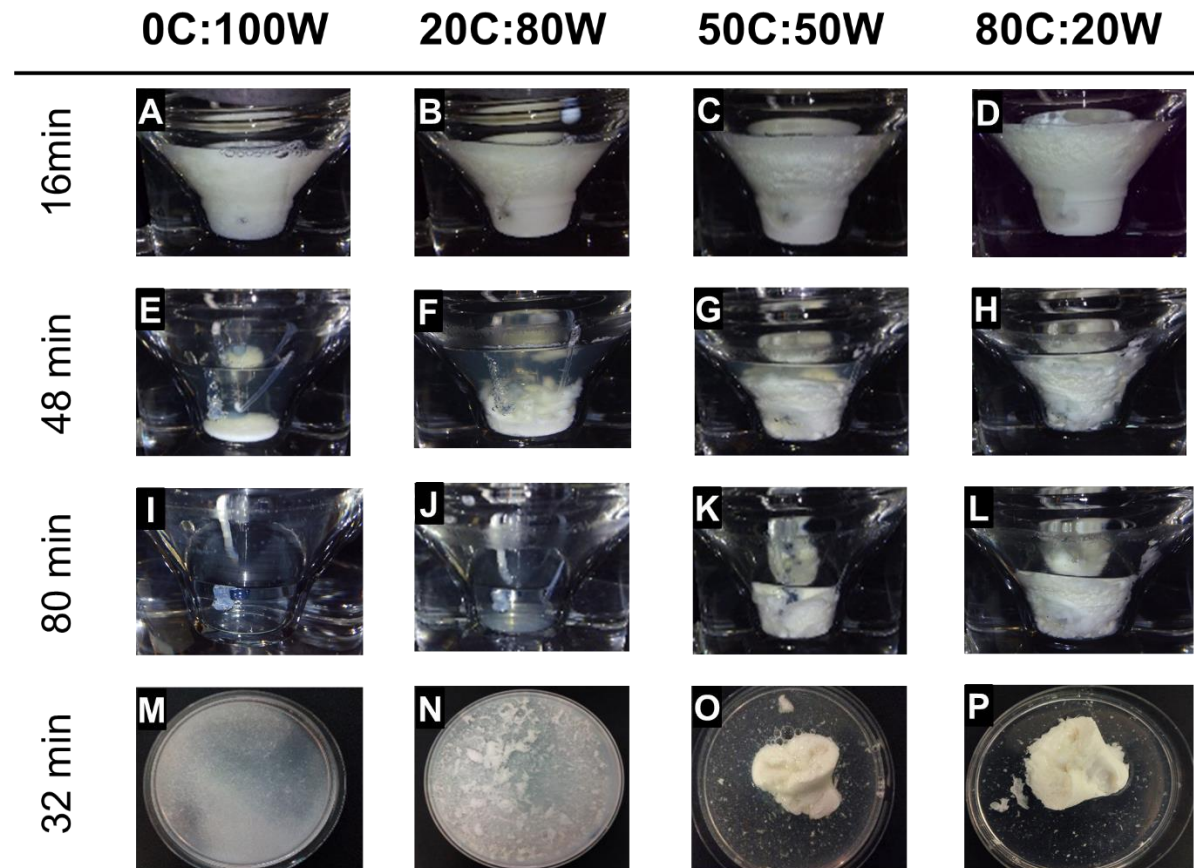
Figure 4.3 Gastric behaviour of the protein solution samples displayed in the vessel of the gastric model at 16, 48 and 80 min, corresponding to the GE1, GE3 and GE5 time points, respectively. Figures from M to P correspond to the gastric behaviour displayed in a petri dish at 32 min (GE2 time point). The images correspond to the behaviour immediately before emptying.

Similar gastric behaviour was observed in the samples when 2% lipid was included, which is illustrated in Figure 4.4. There was visible protein aggregation within the first 10 min of gastric behaviour, similar to the behaviour observed in the protein solution samples. The aggregates in the samples (0C:100W)2% and (20C:80W)2% were being dissipated during the progress of gastric digestion, resulting in the formation of cloudy and clear layers at the bottom and top, respectively. However, in the emulsion (20C:80W)2%, the aggregates were more persistent as seen in Figure 4.4 F and the height of the cloudy layer was larger at the end of the digestion. This contrasted to the behaviour of the samples with higher casein content, i.e. (50C:50W)2% and (80C:20W)2%, which resulted in compact coagulation with a clear layer at the top of the vessel after the initial protein aggregation. However, according to visual observations, the compact coagula was formed earlier in the sample (50C:50W)2% and it was more particulate with a softer consistency, having a larger serum layer in the top of the reaction vessel, when compared to the sample (80C:20W)2%. The closer visualisation of the digesta obtained at the corresponding GE2 time (see Figure 4.4 M-P) illustrates that the inclusion of lipid reduced the firmness of the coagulum, in particular for (50C:50W)2%. Also, the aggregates formed in (20C:80W)2% were smaller compared to those obtained when lipid was not added.
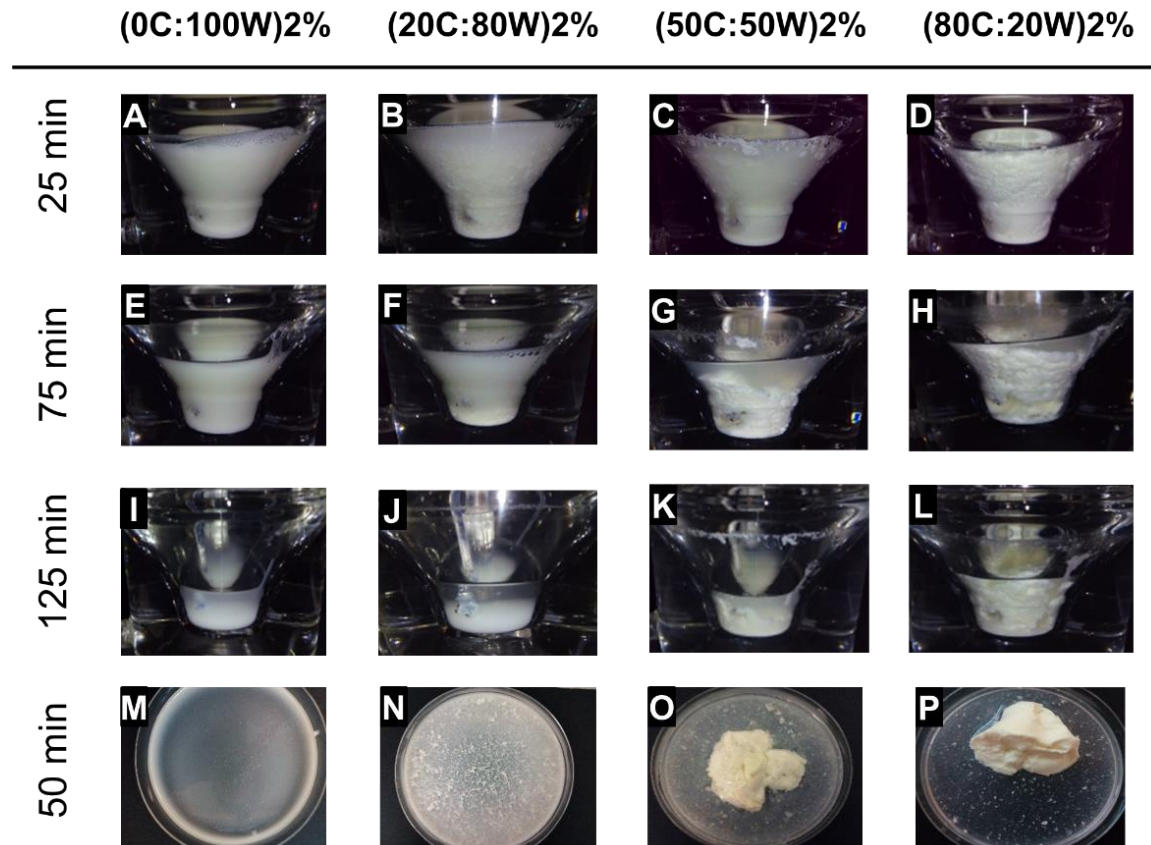
Figure 4.4 Gastric behaviour of the emulsion samples displayed in the vessel of the gastric model at 25, 75 and 125 min, corresponding to the GE1, GE3 and GE5 time points, respectively. Figures from M to P correspond to the gastric behaviour displayed in a petri dish at 50 min (GE2 time point). The images correspond to the behaviour immediately before emptying.

The increase of lipid in the formulation within the same protein C:W ratio of 1, i.e. formulation 50C:50W, did not visibly affect the behaviour during the gastric digestion (Figure 4.5) when compared with the corresponding sample without lipid. However, it was observed that the inclusion of lipid reduced the firmness of the coagulum, in particular for the sample with the highest lipid content. Indeed, more particulate coagula with a tendency to cream could be seen in the case of (50C:50W)8% (see Figure 4.5 F). The reduced firmness could be seen in the digesta at GE2 time displayed in Figure 4.5 H, showing the greater number of particles of different sizes, when compared with the same digesta without lipid (Figure 4.3 O).
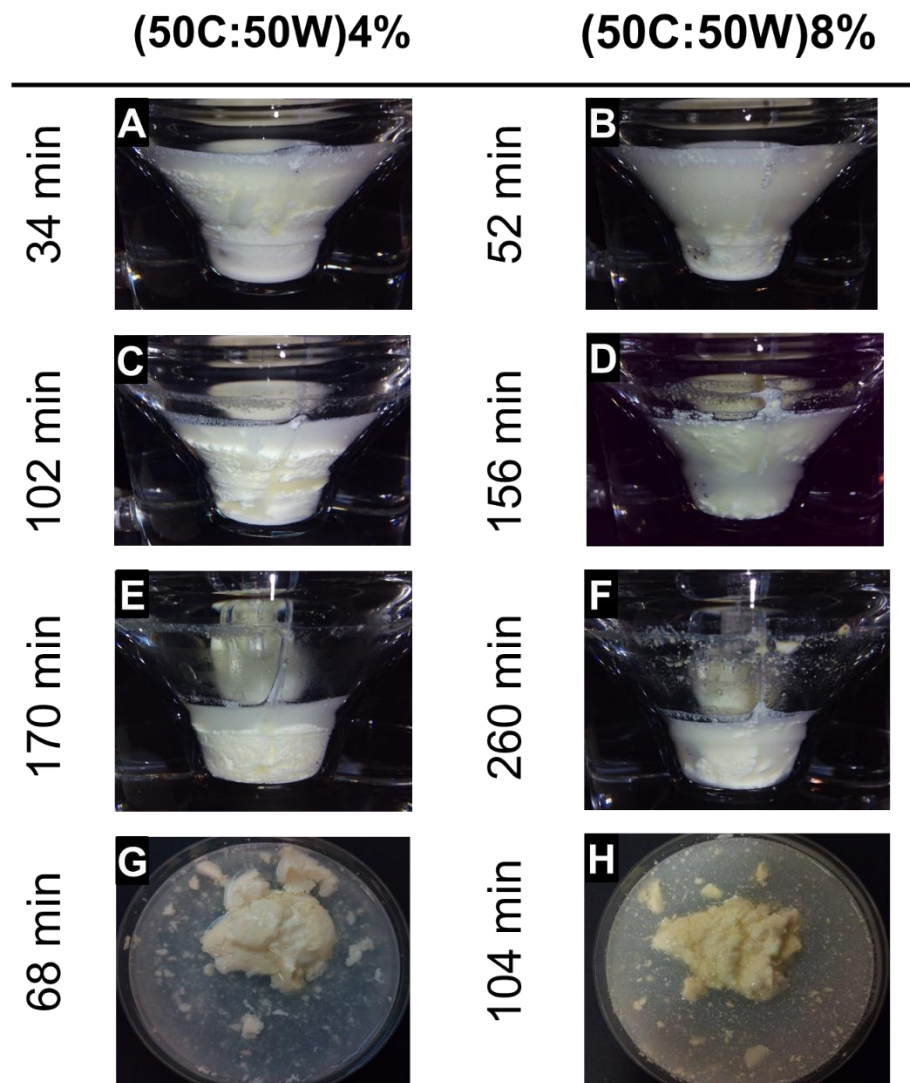
Figure 4.5 Gastric behaviour of emulsion samples with higher lipid content (4% and 8%) displayed in the vessel of the gastric model at GE1, GE3 and GE5 points. Figures G and H correspond to the gastric behaviour displayed in a petri dish at 68 and 104 min (GE2 time point). The images correspond to the behaviour immediately before emptying.

4.3.3 Consistency of the Gastric Coagula

The strength of the coagula was tested in the samples in which these structures were formed, i.e. 50C:50W, 80C:20W, (50C:50W)2%, (80C:20W)2%, (50C:50W)4% and (50C:50W)8% and the analysis was performed on the digesta corresponding to GE2 time (Figure 4.6). However, the value corresponding to the sample (50C:50W)8% could not be measured because the strength of the coagula was below the limit of the detection of the instrument. From the compression test, the sample 80C:20W presented the highest value of force accounting for 22.8 g whereas the weakest coagula were obtained in the sample with the highest lipid content tested, i.e. (50C:50W)4%, resulted in a value of 2.25 g. The results showed that the addition of lipid significantly affected the strength of the milk sample (80C:20W) coagula, more than for the samples containing C:W ratio of 1, i.e. 50C:50W.

Figure 4.6 B shows that there was a greater extent of decrease in coagula consistency in the samples with C:W ratio of 4 when lipid was added compared to the samples with C:W ratio of 1, in which the decline of the coagula strength was much less strongly affected.
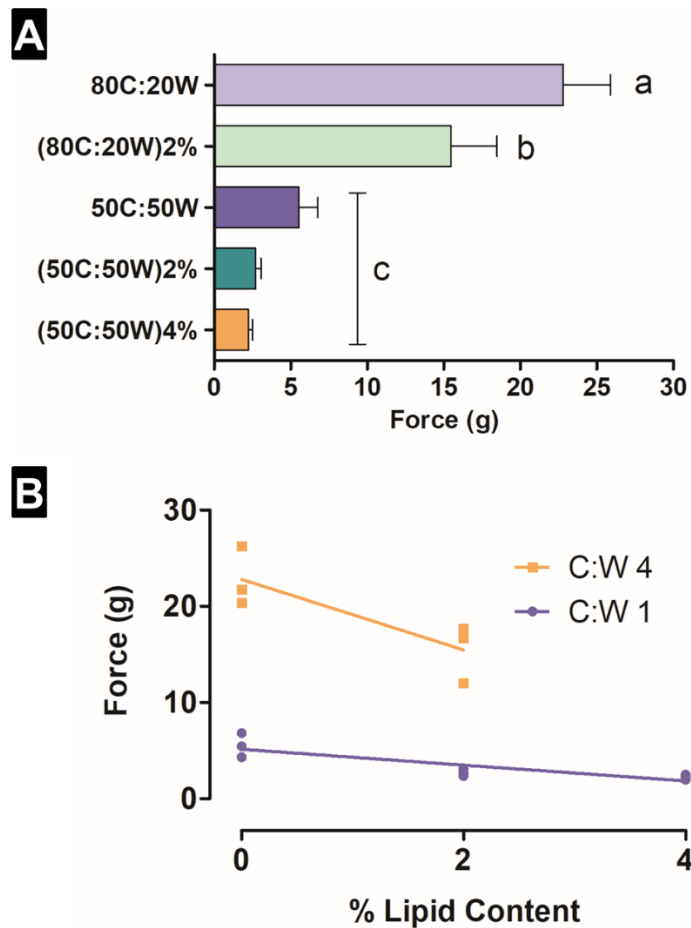
Figure 4.6 (A) Strength, based on the force (g), of the coagula obtained at GE2 time of the samples in which this solid structure was formed during gastric digestion. Each data point is the mean and error bars represent standard deviation of five measurements in three independent replicates. The means of the five groups were significantly different ($p < 0.0001$) based on one-way ANOVA test. Tukey's multiple comparison test showed significant differences ($p < 0.05$) between each group with different superscript letters (a, b, c). (B) Impact of the lipid inclusion on the consistency (strength) of the coagula, based on the force (g), of the coagula obtained at GE2 time of the samples in which this solid structure could be formed during gastric digestion. The samples are based on the protein ratio (C:W) of 1 and 4. Each data point is the mean of five measurements in an independent replicate, having three replicates for each sample.

4.3.4 Nutrient Delivery from the *in Vitro* Stomach

The nutrient content, both protein and lipid, was analysed in each gastric emptied aliquot simulating the nutrients that were delivered from the stomach to the small intestine during the gastric digestion. Figure 4.7 A shows the protein content in each GE point in the four main formulations with and without the addition of 2% lipid. In general, there was a similar protein content (about 8%) in GE1 in all the samples. However, there were significant differences ($p < 0.05$) between the samples in GE2, GE3 and GE5. In general, the formulations with higher whey protein contents (i.e. 0C:100W and 20C:80W) were different to the formulations with the same or higher

casein content (i.e. 50C:50W and 80C:20W), in particular at GE5 accounting for 14.14 and 17.25% w/w protein respectively. In GE2 and GE3, the protein released was higher in formulations 0C:100W and 20C:80W than that in formulations 50C:50W and 80C:20W whereas an opposite trend could be observed in GE5. Moreover, the pattern of the nutrient released of the formulations was not influenced by the inclusion of 2% lipid, with the exception to the formulation (50C:50W)2% at GE5 that presented significant differences ($p < 0.05$). Comparing the different inclusions of lipid in the same C:W ratio of 1 (Figure 4.7 B), the protein delivery was relatively constant during the first four GE points and then there was a slight increase. There were significant differences in GE1 and, in particular, GE5, in which the protein content for the non lipid added sample (i.e. 50C:50W) was higher than the rest, which could be related to the higher extent of coagulation.
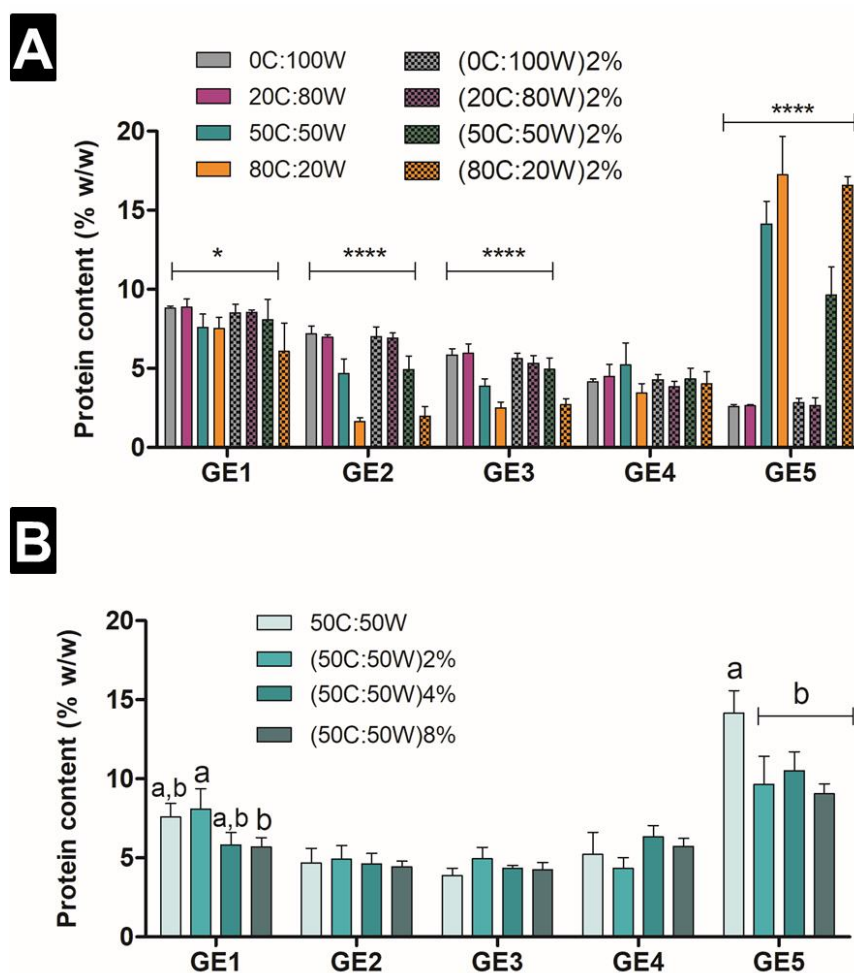
Figure 4.7 The protein content (w/w, %) of the gastric emptying points (GE1-GE5) of (A) protein solution and emulsion samples, and (B) comparison of the different lipid inclusion in the same protein composition matrix, C:W ratio of 1. Values are presented as means ± SD (n=3). The values were corrected by the different gastric dilution in each point. Mean values within a column with different superscript letters (a, b, c) were significantly different ($p < 0.05$).

The pattern of lipid delivery for the emulsion samples with 2% lipid (Figure 4.8 A) showed similar delivery of lipid in GE1 but a different progression during the gastric digestion time, in particular at GE2 and GE5. In GE2, the lipid delivery was higher in the samples (0C:100W)2% and (20C:80W)2% accounting for 1.60 and 1.76% respectively when compared to (50C:50W)2% and (80C:20W)2% representing 0.59 and 0.22% (w/w) lipid, respectively. In contrast, a higher lipid delivery was observed in GE5 for (50C:50W)2% and (80C:20W)2% accounting for 4.43 and 4.84% (w/w) lipid, respectively, suggesting the involvement of lipid in the protein coagulum. Figure 4.8 B shows the comparison of the different lipid concentrations using the same protein formulation, C:W ratio of 1. In general, the pattern of lipid delivery was similar to the pattern of protein delivery in the 50C:50W sample alone (Figure 4.7), thus the pattern of lipid delivery was controlled by or linked to the protein composition.
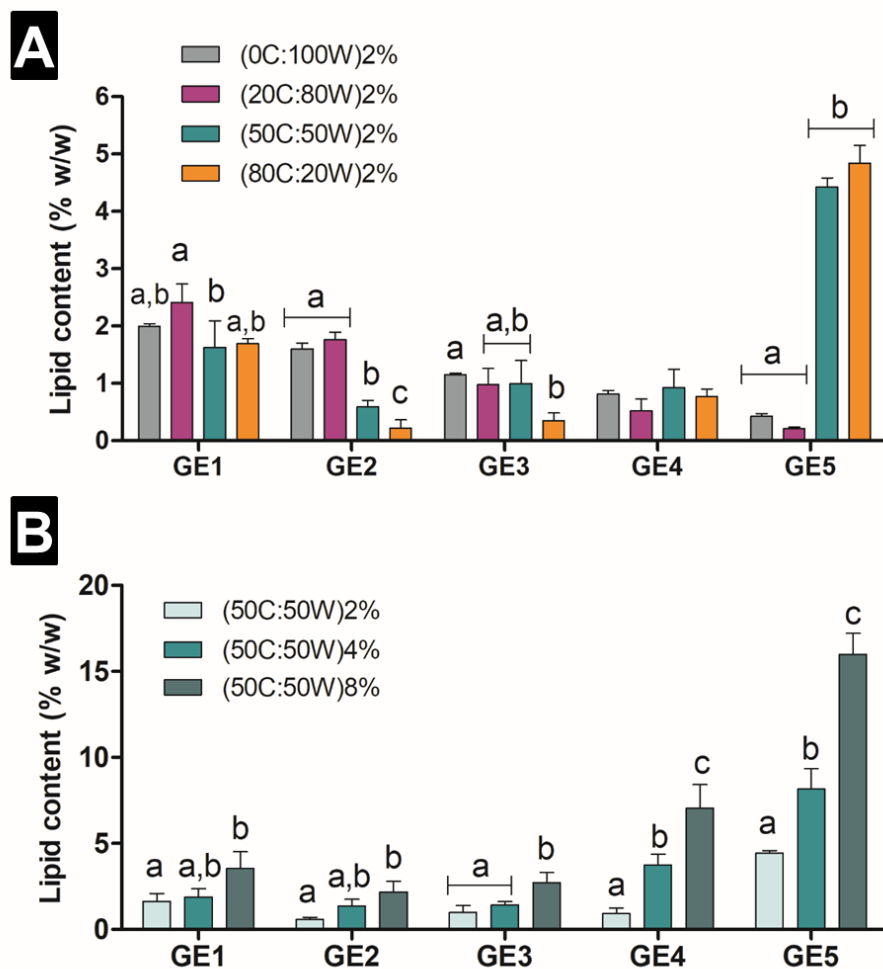
Figure 4.8 The lipid content (w/w, %) of the gastric emptying points (GE1-GE5) of (A) emulsion samples of 2% lipid, and (B) comparison of the different lipid inclusion in the same protein composition matrix, C:W ratio of 1. Values are presented as means ± SD (n=3). The values were corrected by the different gastric dilution in each point. Mean values within a column with different superscript letters (a, b, c) were significantly different (p < 0.05).

The trends of protein delivery are displayed in Figure 4.9. The formulations with higher whey protein contents (C:W ratio of 0 and 0.25) presented a remarkably similar trend, showing the highest protein delivery in GE1 and gradually decreasing during gastric digestion with the lowest amount of protein delivered at GE5, regardless of lipid addition. In contrast, the formulation with the highest casein content (C:W ratio of 4) showed the lowest protein delivery at the early stages of gastric digestion, in particular in GE2, increasing in GE4 and significantly higher in GE5. An intermediate pattern between these two extreme behaviours was found in the formulation with a C:W ratio of 1, in which there was a more constant protein delivery for a longer gastric digestion time, from GE1 to GE4. However, using this protein ratio, the inclusion of 2% lipid resulted in a lower protein concentration emptied in GE5. The theoretical curve of protein delivery was calculated, which assumes that the protein concentration is purely due to the dilution from the gastric digestion and the protein distribution is considered homogenous in the digesta. This shows a continuous linear delivery of protein through gastric digestion due to the gradual dilution by the gastric secretions, which is similar to that observed for the samples with higher whey protein content.
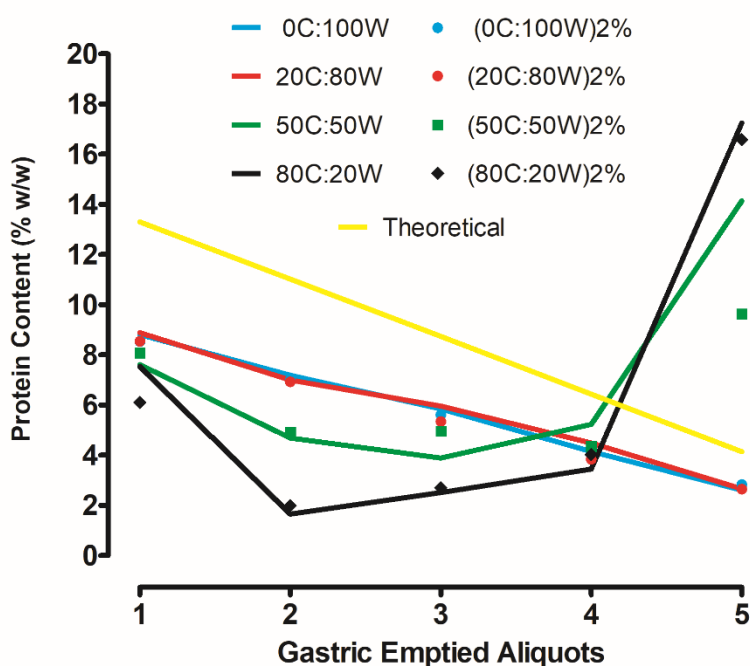
Figure 4.9 Trends of protein delivery during gastric digestion comparing milk protein ratios, and the theoretical curve of protein delivery.

4.3.5 Microstructure of Gastric Emptied Aliquots

Figure 4.10, Figure 4.11 and Figure 4.12 show the microstructure observed using CLSM in the samples before digestion, and the aliquots that were emptied at GE1, GE3 and GE5. With regards to the protein solution samples (Figure 4.10), there

were differences in the structure of the protein aggregation observed at GE1 (16 min); the emptied aliquot of 0C:100W (Figure 4.10 E) showed an open structure in contrast to the more compact protein network found in the aliquot of 80C:20W (Figure 4.10 H). The protein structuring of the emptied aliquots 0C:100W and 20C:80W was reduced with time, resulting in almost no protein particles at GE5 (80 min) (Figure 4.10 N and M). This contrasted with the 50C:50W and 80C:20W aliquots, which showed solid structured matrix, in particular in the case of the 80C:20W sample (Figure 4.10 P). This microstructural behaviour was similar to that observed in the emulsions in which 2% of lipid was included and the lipid droplets seemed to be embedded into the protein matrix since there was not, in general, evidence of creaming. However, both (50C:50W)2% and (80C:20W)2% aliquots at GE5 time (Figure 4.11 O, P) seemed to have a more particulate structure when compared to the corresponding samples without lipid (Figure 4.10 O, P). The increase of lipid content in the samples of (50C:50W)4% and (50C:50W)8% (Figure 4.12) did not show differences in the structures at the first GE points when compared to the corresponding samples with less or no lipid added. However, at the end of gastric digestion, they developed a crumbly structure, having protein particles of different sizes as well as free lipid droplets (Figure 4.12 G and H).
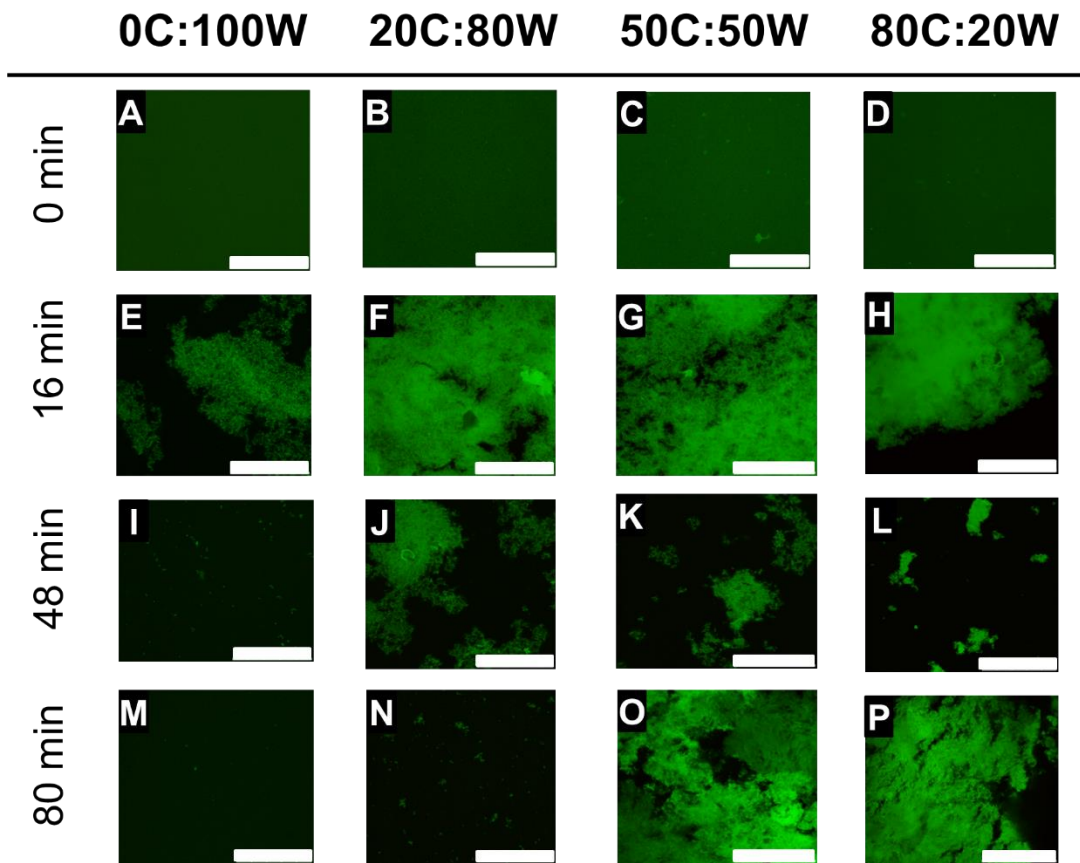
Figure 4.10 Examples of confocal microscopy images of the protein solution samples before digestion (0 min) and, at 16 min (GE1), 48 min (GE3) and 80 min (GE5) of gastric digestion in the gastric emptied aliquots. Green shows the protein. The scale bar corresponds to 100 µm.
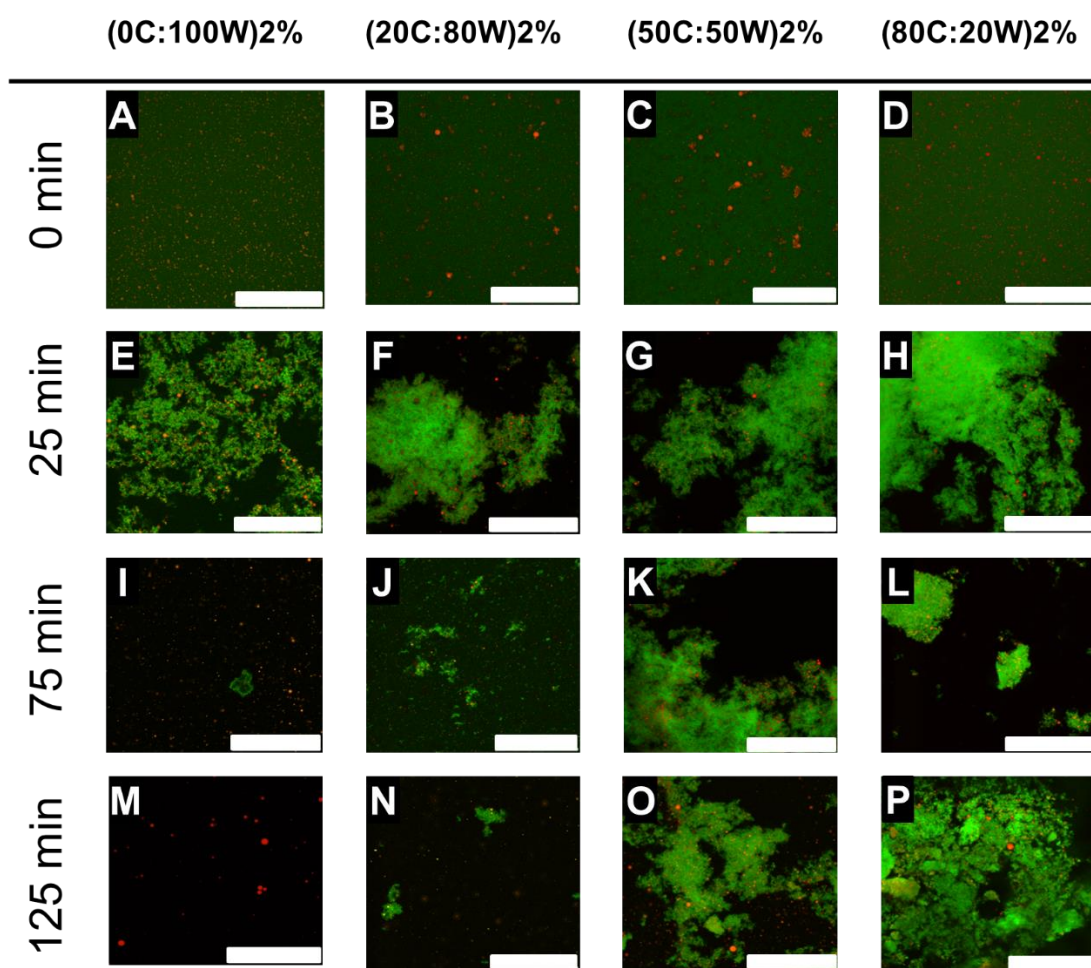
Figure 4.11 Examples of confocal microscopy images of the emulsion samples before digestion (0 min) and, at 25 min (GE1), 75 min (GE3) and125 min (GE5) of gastric digestion in the gastric emptied aliquots. Green shows the protein and red shows the lipid. The scale bar corresponds to 100 μm, except N in which it corresponds to 50 μm.
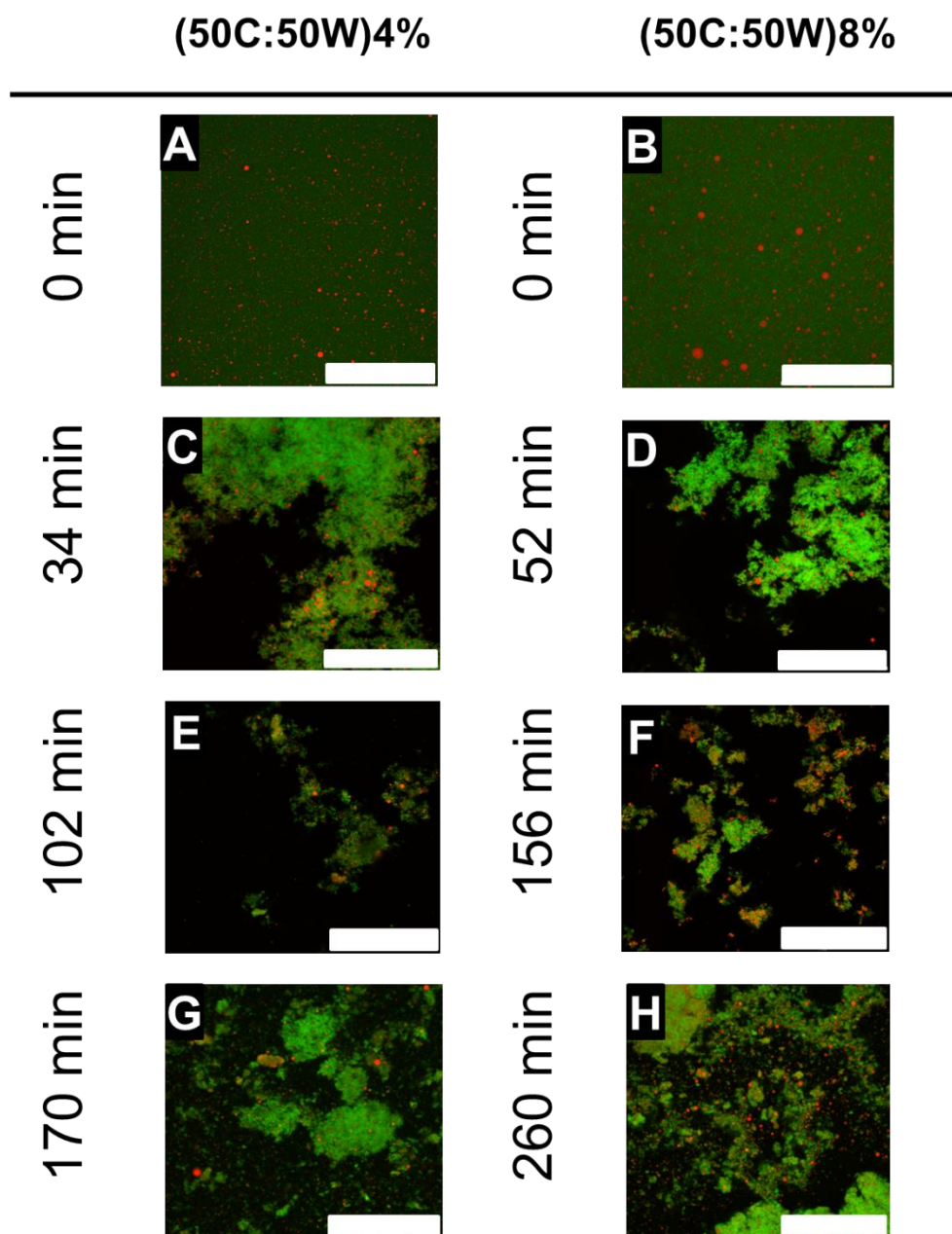
Figure 4.12 Examples of confocal microscopy images of the 50C:50W emulsion samples containing higher lipid content (4% and 8%) before digestion (0 min) and, at GE1, GE3 and GE5 in the gastric emptied aliquots. Green shows the protein and red shows the lipid. The scale bar corresponds to 100 μm.

4.3.6 Protein Composition of Gastric Emptied Aliquots

The protein composition of the gastric emptied aliquots was also studied by SDS-PAGE, illustrating qualitatively the composition of the main milk proteins that reach the small intestine (Figure 4.13). The bands of the main milk protein, casein and whey proteins, in the samples before digestion (referred to I) did reflect the different protein formulation in relation to C:W ratio. For instance, the sample 0C:100W showed higher band intensity in whey proteins in contrast to 80C:20W, in

which the whey proteins bands were weaker and the caseins bands had stronger intensity. The intensity of the β-Lg band in the samples 0C:100W and 20C:80W gradually decreased during gastric digestion (Figure 4.13 A), which can be attributed to the continuously emptying and dilution of the digesta, whereas a higher intensity of β-Lg was found in the sample 80C:20W at the end of the digestion with lower intensity in the intermediate times of digestion. Interestingly, β-Lg seemed to be delivered continuously throughout the gastric phase in the sample with the protein C:W ratio of 1 when compared with the sample of C:W ratio of 4. The band of α-La was present in the three first GE points, after which it was not detected anymore, with the exception of the sample 80C:20W, in which it was present in the two first GE points, with some evidence of its presence in GE5. The pattern for caseins differed depending on their concentration. The sample 20C:80W presented the caseins bands in the first three GE points and thereafter no bands were detectable. In contrast, in the samples 50C:50W and 80C:20W, the caseins were detectable in the first emptying points, in particular GE1 and GE2 points but they were almost not observed in GE3 and GE4 points, and they could be observed in the last emptying point (GE5), showing a higher intensity in the case of 80C:20W. Similar trends were observed when 2% lipid was added in the protein formulations (Figure 4.13 B). However, the casein bands seemed to be weaker, in particular in the case of (50C:50W)2% and (80C:20W)2% at GE5, showing a more constant and lower content of caseins during gastric digestion. The increase of lipid at the levels of 4% and 8% did not cause significant changes in the SDS-PAGE pattern observed in the emulsion using 2% in the 50C:50W sample (Figure 4.13 C), except that the casein bands in GE2 appeared to be weaker in (50C:50W)4% and (50C:50W)8%. It is important to note that pepsin band could not be detected, which was probably due to the dilution applied to the samples (1:100) in order to obtain distinct bands of the main milk proteins on the SDS PAGE gels.
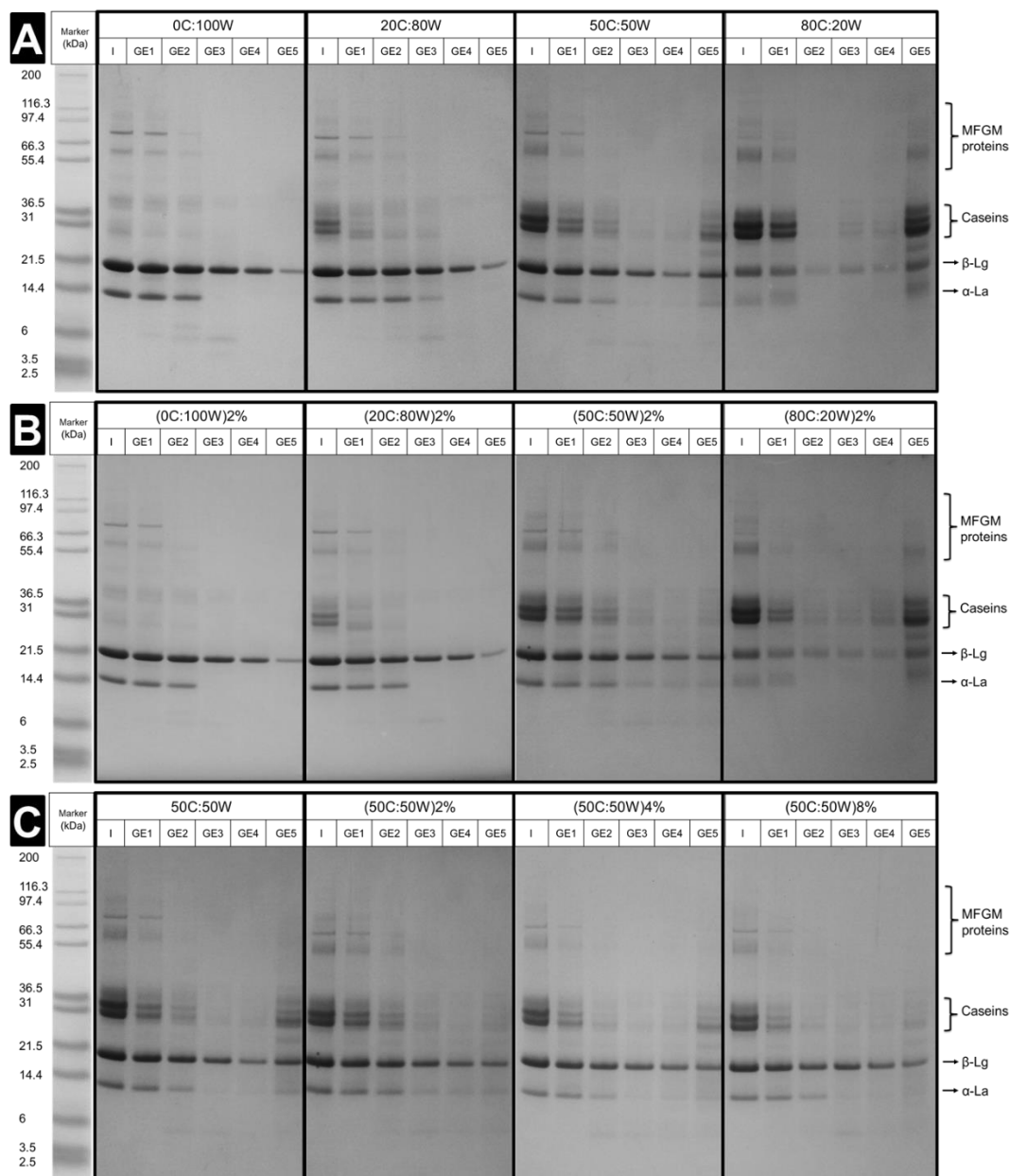
Figure 4.13 SDS-PAGE (under reducing conditions) of (A) protein solution samples, (B) emulsion samples with 2% lipid and (C) samples with the C:W ratio of 1 (i.e. 50C:50W) with 0%, 2%, 4% and 8% lipid. The emptied aliquots at the corresponding GE points (GE1-GE5) were analysed together with the initial sample (I), referred to before digestion and a molecular weight marker. The samples are labelled in the figure accordingly. Samples were diluted (1:100) with water.

4.3.7 Protein Hydrolysis during GI Digestion

The level of free amino groups (R-NH$_2$), obtained using OPA assay, represents an indication of the degree of protein hydrolysis. Figure 4.14 shows the levels of free amino groups of all the formulations in the G1, G3 and G5 points, and in the corresponding intestinal digestions for 30 min and 120 min (in the case of G5 point). There was a substantial increase in protein hydrolysis from the gastric to the small intestinal phase in all the measured GE points. The major difference among the

protein solution formulations can be observed in the G5 point after intestinal digestion for both 30 min and 120 min (Figure 4.14 A), in which the formulations of 0C:100W and 20C:80W presented the lowest concentration of free amino groups compared to 50C:50W and 80C:20W. There were similar amounts of amino groups released in G1I and G3I. Regarding the emulsions with the addition of 2% lipid (Figure 4.14 B), the pattern was similar but the formulation (80C:20W)2% seemed to present a lower concentration of amino groups in G1 and G3 after intestinal digestion for 30 min showing significant differences between (0C:100W)2% and (80C:20W)2% in G1I. In general, the inclusion of different lipid concentrations in the same protein formulation does not seem to modify the protein hydrolysis (Figure 4.14 C). However, there were some significant differences in G5I120 between the samples 50C:50W and (50C:50W)8%.
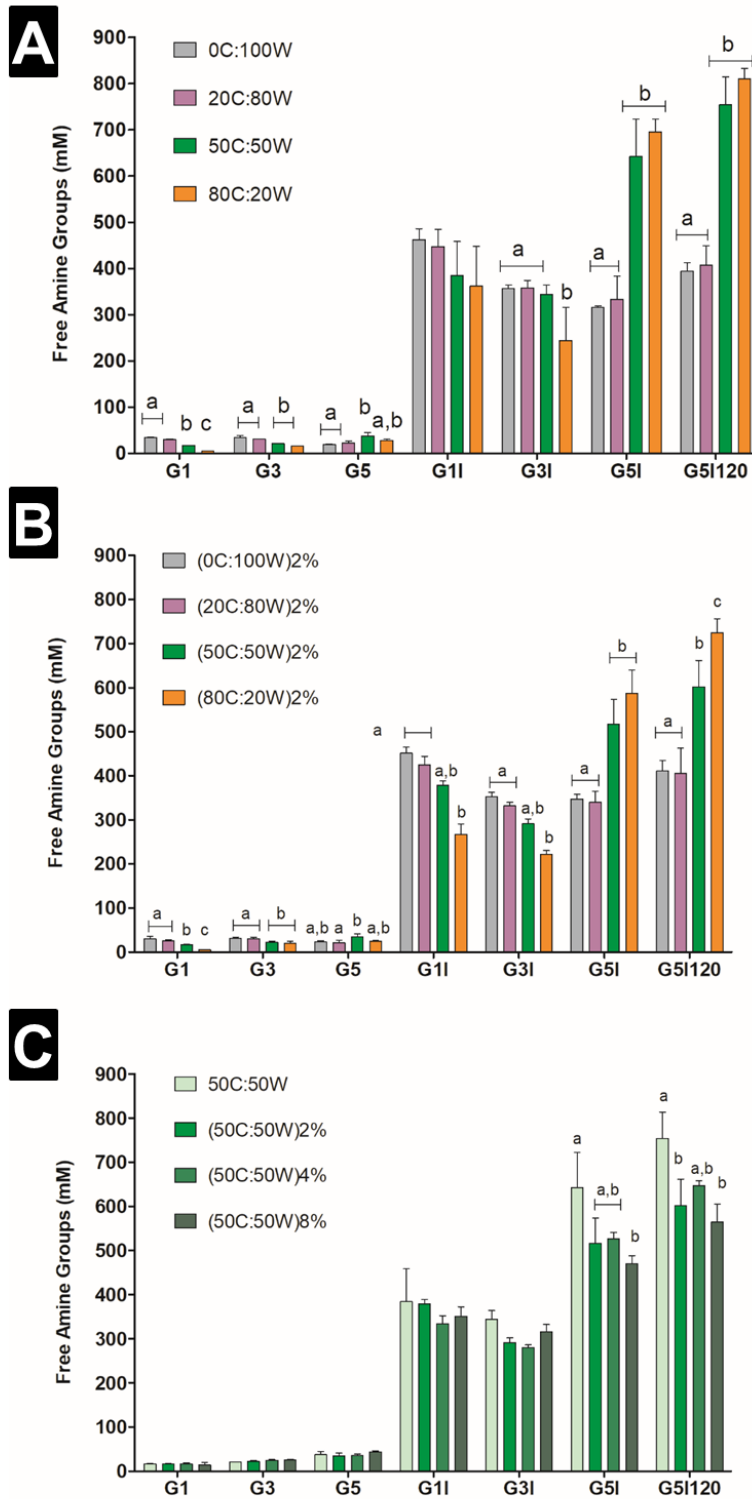
Figure 4.14 Concentration of free amino groups in the gastric emptying points (G1, G3 and G5) and their respective intestinal digestion for 30 min (G1I, G3I and G5I) and for 120 min in G5 (i.e. G5I120) of (A) protein solution samples, (B) emulsion samples with 2% lipid, and (C) comparison of the different lipid inclusion (0, 2,,4, and 8%) in the same protein composition matrix, C:W ratio of 1. Values are presented as means ± SD (n=3). The values were corrected by the different gastric dilution in each point. Mean values within a column with different superscript letters (a, b, c) were significantly different ($p < 0.05$).

In relation to protein digestion, the individual AAs were also analysed (see Appendix B) and the total AAs concentration of the four protein formulations with and without the 2% lipid inclusion is represented in Figure 4.15. Similar to the results obtained using OPA assay, there was a substantial increase in AA levels from the gastric to the small intestinal phase. The concentration of total AAs during the intestinal phase was relatively constant in the formulations of 0C:100W and 20C:80W, regardless the inclusion of lipid. This differed with the gradual increase of AAs level during intestinal digestion in the formulations of 50C:50W and 80C:20W, regardless lipid addition, starting from concentrations of about 1,300 mg/mL at G1I to reaching levels of about 3,000 mg/mL.
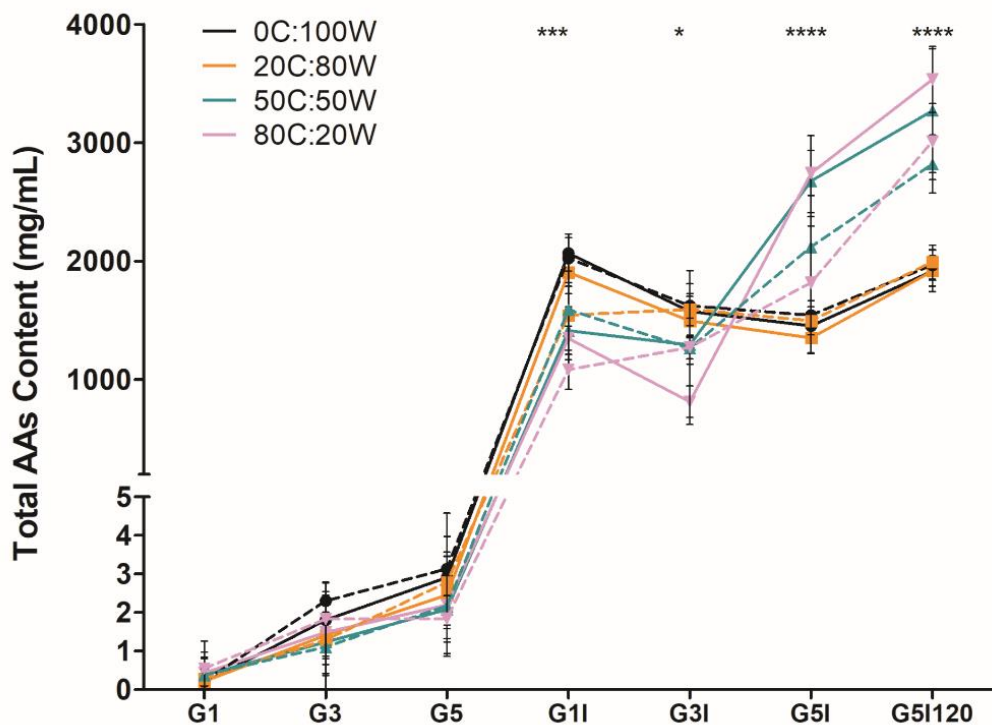
Figure 4.15 Total AAs content (mg/mL) in the gastric emptied aliquots G1, G3 and G5, and their respective small intestinal digestion for 30 min (G1I, G3I and G5I), and the intestinal digestion of G5 for 120 min (G5I120). The protein solution and the emulsion (2% lipid) samples are represented in solid line and broken line, respectively. Values are presented as means ± SD (n=3). The values were corrected by the different gastric dilution in each point. Significance difference in AAs content between samples in each GE point was determined by one-way ANOVA, $p \leq 0.05$ (*), $p \leq 0.01$ (**), $p \leq 0.001$ (***) and $p \leq 0.0001$ (*****).

4.3.8 Bioaccessibility and Absorption of AAs

The concentration of total branched-chain amino acids (BCAAs) and Leu, Ile and Val, independently, for all the samples at both GE1 and GE5 in the apical and basolateral sides of the Ussing chamber can be seen in Appendix C and the representation of Leu trends is displayed in Figure 4.16. The determination in the

apical side represents the Leu content that was digested and became accessible whereas the determination in the basolateral side represents the Leu content that was able to be transported across the intestinal wall and thus available to be metabolised and used for physiological functions. In general, the Leu concentration in all the samples in both GE points increased during small intestinal digestion, showing the progressive breakdown of the protein, liberating AAs and increasing their absorption. However, the rate and extent of these processes were different between the samples. In GE1, the protein solution samples in the absence of lipid (Figure 4.16 A), showed similar Leu concentration in the apical side at 5 min of intestinal digestion. However, the sample 0C:100W showed the most rapid increase in Leu concentration whereas the lowest rate was found in the sample 80C:20W. After 60 min of intestinal digestion, the highest apical Leu concentration was found in the sample 0C:100W followed by 20C:80W, 50C:50W and 80C:20W, accounting for 396.04, 280.83, 257.15 and 210.30 µg/mL, respectively. These patterns were related to the Leu concentration that was absorbed (basolateral concentrations), the highest rate of Leu absorption was observed in 0C:100W whereas the samples 50C:50W and 80C:20W presented the slowest rate with a similar pattern. The order of the samples according the Leu concentration analysed after 60 min of intestinal digestion was the same than in the apical side, i.e. 0C:100W following by 20C:80W, 50C:50W and 80C:20W, accounting for 20.97, 16.17, 13.15 and 11.72 µg/mL respectively. However, there were not significant differences in the intestinal digestion time points among the samples. The patterns observed in GE1 differed from those obtained in GE5 with the same samples (Figure 4.16 a). With regards to apical side, the samples 50C:50W and 80C:20W presented a higher Leu concentration than 0C:100W and 20C:80W after 5 min of intestinal digestion. There was a slight increase in Leu concentration during intestinal digestion in the samples 0C:100W and 20C:80W, which accounted for 87.59 and 108.71 µg/mL respectively at 60 min of intestinal digestion. Despite the low Leu release in those samples, there was still some Leu absorption during the intestinal phase, representing 8.77 and 12.95 µg/mL for 0C:100W and 20C:80W respectively after 60 min of digestion. This contrasts to the rapid rate of Leu accessibility in. the samples 50C:50W and 80C:20W showing 301.24 and 368.72 µg/mL respectively at the end of the intestinal digestion. This was reflected in a higher absorbed Leu obtained in the basolateral side, accounting for 16.78 and 18.25 µg/mL for the samples 50C:50W and 80C:20W, respectively.
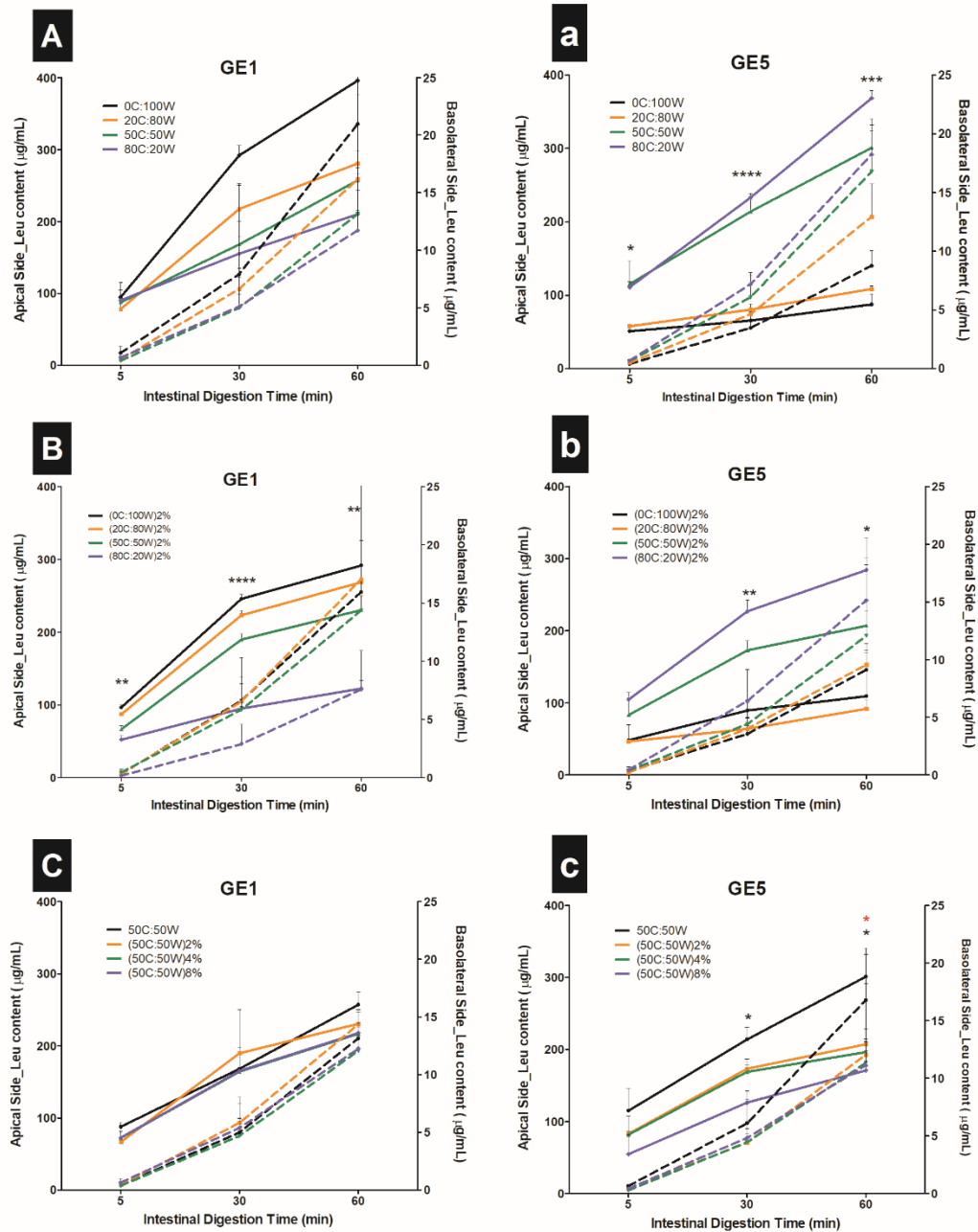
Figure 4.16 Concentration of Leu (μg/mL) of the (A, a) protein solution samples, (B, b) emulsions with 2% lipid and (C, c) comparison of the different lipid inclusion (0, 2, 4 and 8%) in the same protein composition matrix, C:W ratio of 1 during the small intestinal digestion of the digesta related to GE1 (upper case) and GE5 (lower case), both apical and basolateral sides in solid and broken line, respectively, using Ussing chamber. Values are presented as means ± SD of two independent determinations. Significance difference in Leu content between samples in each GE point was determined by one-way ANOVA, $p ≤ 0.05$ (*), $p ≤ 0.01$ (**), $p ≤ 0.001$ (***) and $p ≤ 0.0001$ (*****), black relates to the apical side axe and red relates to the basolateral side axe.

The emulsion samples with the inclusion of 2% lipid are represented in Figure 4.16 B and b. In GE1, Figure 4.16 B, these samples showed more different Leu concentration in the apical side at 5 min of intestinal digestion compared to that in the samples without lipid. The rate of increase in the concentration of accessible Leu was

165

similar in the samples (0C:100W)2%, (20C:80W)2%, (50C:50W)2% but the sample (0C:100W)2% presented the highest extent, reaching 291.74 µg/mL at the end of the small intestinal digestion. In contrast, the sample (80C:20W)2% presented the slowest rate, obtaining 122.21 µg/mL after 60 min of intestinal digestion. These patterns were reflected in the content of absorbed Leu, the samples (0C:100W)2%, (20C:80W)2%, (50C:50W)2% followed a similar trend accounting for 15.94, 17.04 and 14.37 µg/mL respectively after 60 min of intestinal digestion whereas a lower rate and extent of Leu was obtained in the sample (80C:20W)2% (7.59 µg/mL after 60 min of intestinal digestion).The behaviour of the samples in GE1 contrasted to that obtained in GE5 (Figure 4.16 b), in which there was a rapid and higher pattern in the sample (80C:20W)2% accounting for 284.44 µg/mL at the end of the digestion, following by (50C:50W)2% (207.23 µg/mL) and, (0C:100W)2% and (20C:80W)2% showing similar trends. The Leu absorption was higher and more rapid in the case of (80C:20W)2%, in particular after 60 min, in which the Leu concentration was 15.14 µg/mL, in contrast to those obtained for (0C:100W)2% and (20C:80W)2% representing 9.13 and 9.55 µg/mL respectively.

The samples with different inclusions of lipid using the sample protein C:W ratio of 1 i.e. 50C:50W, (50C:50W)2%, (50C:50W)4% and (50C:50W)8% were compared in Figure 4.16 C for GE1 and Figure 4.16 c for GE5. The samples presented similar rates and extent of Leu concentration in GE1 both apical and basolateral sides. Conversely, in GE5, the sample without lipid (50C:50W) showed more rapid rate and higher concentration of Leu that was accessible, which led to a higher absorbed Leu concentration, in particular after 60 min of intestinal digestion accounting for 301.24 µg/mL. In contrast, the sample (50C:50W)8% presented the lowest rate and extent of Leu concentration in the apical side but the absorbed Leu concentration was similar than that obtained for the rest of the samples where lipid was included.

4.4 Discussion

4.4.1 Influence of Protein Formulation on Gastric Behaviour

The different protein formulations exhibited a wide range of behaviours during gastric digestion using the semi-dynamic model. The formulations containing at least 50% of casein showed the formation of insoluble aggregates that led to the formation of mozzarella-like coagula that remained in the gastric compartment until the end of digestion and this behaviour was more remarkable as the concentration of casein increased (Figure 4.3). This behaviour was also observed in the micrographs showing the persistence of a compact protein network at the end of the gastric digestion in

both 50C:50W and 80C:20W samples (Figure 4.10). In contrast, the sample containing only whey proteins (0C:100W) presented the formation of aggregates that dissipated over time resulting in a clear solution by the end of the digestion and this pattern was not significantly affected by the addition of lower amounts of casein, i.e. 20%. This behaviour was confirmed following the microstructure development over time, showing almost no protein aggregates at the end of the gastric digestion. The distinct behaviour of the milk proteins observed in the present study is in agreement with the suggestions presented in the literature (Boirie *et al.*, 1997; Hall *et al.*, 2003; Mahé *et al.*, 1996). However, there is no direct evidence of the gastric behaviour in humans and the *in vitro* evidence is limited. Similar to our results, Wang *et al.* (2018) showed, using the Human Gastric Simulator (HGS), that MPC presented a firm coagulation whereas WPI did not present any aggregation after 220 min of gastric digestion. Moreover, the authors reported that the coagulation of the MPC sample was visible in the first 10 min of digestion corresponding to a pH of approximately 6, in agreement to the present study.

The difference of the gastric behaviour between the main milk proteins can be attributed to their native molecular structure and physico-chemical properties. Caseins form supramolecular colloidal particles, called casein micelles, having an average diameter of 120 nm (Fox *et al.*, 1998). In a micelle, caseins are linked by colloidal calcium phosphate by hydrophobic and electrostatic interactions. Electrostatic interactions provides structural stability to the casein micelles and steric effects of the protruding "hair" from the C-terminal regions of κ-casein causing steric repulsion between micelles thus preventing aggregation. In contrast, whey proteins are globular proteins with high levels of secondary, tertiary and, in most cases, quaternary structures. Caseins are insoluble at pH 4.6 (isoelectric point) whereas whey proteins remain soluble at that pH. In the present study, the protein aggregation started after 10 min of gastric digestion at pH values of about 6 for both 50C:50W and 80C:20W, which was much higher pH than the isolectric point of caseins. This suggests that the initial coagulation was driven by the action of pepsin that has been reported to favour the hydrolysis of κ-caseins among the other caseins at pH 6.0 (Tam *et al.*, 1972), which will reduce the steric repulsion between micelles. Then, the coagulation might be caused by the destabilisation of casein micelles since pepsin cleaves the Phe-105-Met-106 bond in κ-casein liberating caseinomacropeptide.

With regards to the strength of the coagula within the digesta at GE2, the effect of protein formulation seemed to have a more important role than the lipid inclusion as shown in Figure 4.6 B, where the influence of lipid was greater in the C:W ratio of 4 in contrast to the C:W ratio of 1. Similarly, Lambers *et al.* (2013) showed that the

viscosity, measured by an in-line rheometer during the gastric digestion, of caseins was higher than the whey proteins in solution. However, the casein source was from sodium caseinate, which might affect the formation of the solid coagula and differ from the observed coagula using MPC. Indeed, Wang *et al.* (2018) reported that the coagulation formed in sodium caseinate was loose and fragmented compared to the dense coagula obtained in the MPC sample, which can be attributed to differences in the casein association.

The inclusion of 2% lipid in the same protein formulations did not show substantial differences in the behaviour during the gastric digestion, showing solid coagulation in the (50C:50W)2% and (80C:20W)2% samples in which the lipid droplets remained embedded in the protein network, since there was no evidence of creaming during gastric digestion (Figure 4.4). However, it seemed that the addition of lipid weakened the protein structure formed, which was particularly observed in the particulate coagula obtained at the end of the digestion, in particular for (80C:20W)2%. This fragmented coagulation was enhanced as more lipid was added, showing a great number of protein particles of different sizes with some free droplets, particularly in (50C:50W)8% (Figure 4.5). It seems that lipids hamper the casein interactions, which leads to the formation of a less cohesive protein network. Therefore, it was shown that lipid inclusion impacted the consistency of the coagula but it was only significant in the hardest protein network of C:W ratio of 4 (Figure 4.6 A).

Little information is available on the effect of food structure on gastric behaviour. However, there is extensive research on the properties of rennet coagulation for cheese making and since chymosin displays a similar mechanism of hydrolysis to pepsin it seems possible to draw parallels to the processes occurring in the stomach. The rheological properties of the rennet coagulum depend on a number of factors including pre-treatment and composition of milk (Guinee *et al.*, 1997). Mateo *et al.* (2009) showed that an increase in fat content impaired the syneresis, showing a reduced amount of serum produced and the impairment of the casein gel firmness. Therefore, in a similar way, the presence of lipid in the initial samples of the present study might weaken the structure of the coagula formed in the simulated stomach altering the kinetics of digestion.

To better simulate the *in vivo* gastric digestion, a semi-dynamic model was used in this study. This model reproduces some of the main dynamic processes in the human stomach, including the gradual pH decrease (Figure 4.2). The pH is a crucial factor affecting the structure of proteins and enzyme activity and therefore affecting the kinetics of protein degradation. A predetermined curve was used to simulate the

acidification curve seen in the human stomach for a standard meal, in which the pH decreases gradually during time reaching a pH of about 3.5 halfway and pH 2 at the end of gastric digestion (Malagelada *et al.*, 1976). Also, the pH curve obtained was similar to that obtained using milk proteins in calf (Yvon *et al.*, 1992). However, there were some differences among the samples, which can be attributed to the different structures formed during the gastric phase. The sample 0C:100W presented the lowest pH values at the first stage of the gastric digestion, which can be related to the lower buffering capacity of the soluble aggregates, and the pH gradually decreased during digestion (Figure 4.2 A). In contrast, the sample 80C:20W presented irregular pH values during the gastric time, showing a sharp reduction of pH in the middle of the digestion due to the formation of a dense coagula which hampered the emptying of protein, and there was an increase at the end of the digestion due to the increased buffering capacity resulting from the emptying of more protein that had accumulated in the simulated stomach. The pH curve in 50C:50W was more regular despite its coagulation due to the weaker coagulation obtained, which made the protein delivery and, thus the buffering capacity of the emptied digesta, more constant between GE points.

GE is the other main essential parameter in the gastric phase. In the semi-dynamic model, the rate of GE was based on the caloric content of the sample for an easier methodology and the emptying was performed by means of a syringe with plastic tubing. This GE approach implied that the emptying time of the samples was the same regardless the behaviour of the proteins in the simulated stomach. However, this may not be totally accurate since casein might present longer times of gastric digestion due to the formation of the solid coagula that remains longer in the stomach to be broken down and emptied, which might influence the extent of the protein hydrolysis. In humans, Boutrou *et al.* (2013) found that, after casein ingestion, the delivery of dietary protein in the jejunum was progressive for 6 hours and in the form of medium size-peptides (750-1,050 Da) whereas the ingestion of whey protein induced the release of larger-size peptides (1,050-1,800 Da) and was completed after 3 hours.

The regulation of GE is a complex process which depends on factors including gut hormones and properties of food, e.g. viscosity, consistency, volume, particle size and caloric density. However a simple *in vitro* model cannot take into account all of these factors so this model considered the caloric density as the main factor in regulating the rate of GE, a high caloric density inducing a slower/longer emptying. The caloric content delivered to the duodenum *in vivo* is regulated so the nutrient delivery is continuously maintained by a negative feedback through the release of

hormones in response to the nutrient content of the duodenum. Some studies have reported an average constant caloric delivery rate of about 2 kcal/min (Brener *et al.*, 1983; Costill *et al.*, 1974; Sauter *et al.*, 2011). Despite this simplification, the results showed a distinct digestion kinetics of the milk proteins showing the concept of 'slow' and 'fast' proteins observed *in vivo* as described below.

4.4.2 Effect of Gastric Behaviour on Nutrient Delivery and Protein Digestion in the Small Intestine

The gastric behaviour of the protein formulations impacted the *in vitro* kinetics of protein emptying simulating the delivery from the stomach to the small intestine. The solid coagulation, in particular in the 80C:20W sample, led to the delayed protein delivery by the retention of caseins at GE5 as seen by SDS-PAGE (Figure 4.13 A). The solid coagulum that formed, physically resisted being emptied from the stomach through the tubing, in a manner similar to the way the pylorus prevents the emptying of solids or large particulates, but allowing the liquid phase to be emptied. In contrast, the formation of small, soluble aggregates in the formulations with higher whey proteins concentration allowed the liquid phase containing the aggregates to be emptied, enabling a higher protein delivery at the earlier stage of digestion that was gradually decreasing. This was related to the emptying of intact β-Lg and was controlled mainly by the dilution of the gastric contents by the continuous secretions. Similarly, Wang *et al.* (2018) showed that, in the gastric digestion of WPI, β-Lg remained intact over the gastric digestion due to the well-known property of the native β-Lg to resist hydrolysis by pepsin because its globular structure. Moreover, in the same study, the authors detected strong bands of intact caseins from the coagulum particles after 220 min of digestion for MPC, similarly to the present results. Interestingly, the sample 50C:50W presented an intermediate pattern of protein delivery, which can be attributed to the softer coagula formed in the gastric digestion that was more easily emptied. Moreover, the latter sample presented a more constant emptying of both caseins and whey proteins as observed in the electrophoresis gel (Figure 4.13 A), which may be related to a reduced syneresis in that sample.

The protein matrix also affected the kinetics of lipid emptying. As seen in Figure 4.8, the lipid delivery during gastric digestion was driven by the structure formed in the simulated stomach by the protein. This showed low and high lipid delivery in GE2 and GE5, respectively, for the formulations in which solid coagulation was obtained. However, the addition of lipid did not show significant differences in protein delivery with the exception of the C:W ratio of 1 in GE5 (Figure 4.8) but it seemed that caseins were more gradually delivered through the gastric phase, showing less intensity at

the end of the digestion, which can be related to the softer coagula measured (Figure 4.6). This shows that lipid droplets were incorporated in the protein network formed in the gastric digestion and that protein structure was the main driver for the nutrient delivery. The addition of higher amounts of lipid in the C:W ratio of 1, in particular 8%, resulted in a lower release of protein and lower intensity of casein bands at the end of the digestion, which is related to the softer and more fragmented coagula obtained (Figure 4.5 H). As seen in the present study, the incorporation of other nutrients might affect the protein network structure and modify their digestion and behaviour within the GI tract. Guo *et al.* (2015) studied, in whey protein emulsion gels (hard versus soft), the effect of gastric disintegration using HGS on lipid bioaccessibility during a simulated intestinal digestion. The size of the gel particles was reduced after 60 min of gastric digestion in both samples but the initial rate of lipolysis of the soft gel was significantly higher than the hard gel, even though the solid content of that digesta was lower. At 240 min, the digesta from the soft gel consisted of individual oil droplets as well as smaller particles, compared to the hard gel in which most of the oil droplets remained within the protein network. The latter study represents an example of the enginnering of gels, however the same principle can be applied for protein structures formed within the gastric conditions. Therefore, this shows that protein networks can modulate the release of lipid to the intestine and impact on the subsequent digestion rates.

The formation of the solid coagula within the simulated stomach of the protein formulations of 50C:50W and 80C:20W affected the protein hydrolysis in the early stages of the gastric digestion (G1 and G3) resulting in the release of fewer free amino groups (Figure 4.14) despite the fact that caseins have been reported to be more easily digested than whey proteins in solution during the gastric phase. This was illustrated by Macierzanka *et al.* (2009) who showed that β-Lg was resistant to pepsinolysis due to the complact globular structure compared to the loose, disordered structure of β-casein. These conflicting results could be explained on the basis that the solid coagulum formed by the caseins could reduce accessibility of pepsin and, thus, hamper the hydrolysis of caseins within the protein network. Indeed, some work presented in Chapter 6 showed that pepsin activity was mainly found in the surface of the compact coagula formed during the gastric digestion of milk whereas pepsin was absent inside of the coagula. However, that solid coagulation did not seem to impact the protein hydrolysis in the small intestinal phase, showing a more effective hydrolysis of milk protein in that phase, regardless the structure of the digesta. During the intestinal digestion of the last emptied aliquot for both 30 and 120 min, i.e. G5I and G5I120, there was higher hydrolysis in the samples that presented solid gastric

coagulation, which was also reflected in the higher total AAs content (Figure 4.15), this pattern was obtained regardless the inclusion of 2% lipid. These results differ from the study by Macierzanka *et al.* (2009) where the degree of proteolysis in β-Lg was increased when emulsified with oil, which was due to the partial unfolding of the β-Lg secondary structure improving accessibility to pepsin. In the present study we did not find significant differences in the presence of an emulsion, which may be due to the high concentration of protein present in the sample where most of the protein was in solution instead of being absorbed on the interface of the lipid droplet. In the samples containing higher proportion of whey proteins, in contrast, there was more constant hydrolysis and presence of total AAs during the intestinal phase with a higher hydrolysis at the G1I, which can be attributed to the more regular and gradual protein delivery of the soluble aggregates.

The results showed that there was rapid protein hydrolysis for all the samples after 30 min of small intestinal digestion. This finding is in agreement with the study of Macierzanka *et al.* (2009) showing that milk proteins were partially hydrolysed, after just 1 min, into lower molecular weight peptides under intestinal conditions. The intestinal proteolysis is highly efficient resulting in a mixture of free AAs and oligopeptides (2-6 AAs) that account for approximately 40% and 60%, respectively, of the total α-amino nitrogen (Erickson *et al.*, 1990) and some peptides are further hydrolysed by aminopeptidases located on the brush border membranes. Therefore, the joint action of the gastric, intestinal and brush border proteolysis provides the availability of free AAs, di- and tri-peptides allowing their transport across the brush border membrane.

4.4.3 Effect of Gastric Behaviour on AA Bioaccessibility and Absorption

The behaviour of the protein matrix in the gastric phase was shown to alter the extent and rate of nutrients that was released over time from the *in vitro* stomach. This, in turn, controlled the further protein digestion in the small intestine, affecting the bioaccessibility and absorption of AAs.

The Leu level was selected to follow the kinetics of absorption since it plays a key role in the body protein deposition (Garlick, 2005), and the digesta emptied in the early (i.e. GE1) and late (i.e. GE5) stages of the gastric digestion were selected to assess the behaviour of the samples. The Ussing chamber experiment was performed using an *in situ* intestinal digestion in order to simulate the simultaneous processes of protein/peptide hydrolysis and AA absorption, in contrast to the use of

pre-digested samples in most of the studies previously presented in the literature (Awati *et al.*, 2009). This *ex vivo* model using intact intestinal tissue segments from an animal provides a better representation of the *in vivo* situation since it provides the morphological and physiological features of the intestinal wall, including the multicellular conglomeration and presence of the mucus layer allowing the simulation of the possible further hydrolysis of some peptides by aminopeptidases located on the brush border membranes. It is important to note that a lower concentration of Leu in the basolateral side was obtained comparing to the apical side, which could be attributed to the reduce area of the mouse tissue in the Ussing chamber experiment resulting in possible saturation in the tissue hampering the AA transport. There are a few studies investigating the absorption of AAs by Ussing chamber but the results are difficult to compare since the experimental set ups are different, including the source of the animal tissue (Grøndahl *et al.*, 1997).

In general, it was shown quite clearly that the different rates of delivery of Leu from the different samples at different stages of digestion, explained how whey proteins and caseins are responsible for most of the early and late AA delivery, respectively (Figure 4.16). For protein solutions, the sample 0C:100W presented the highest rate and extent of both Leu accessibility and absorption in the first GE aliquot when compared with the samples 50C:50W and 80C:20W. In contrast, the latter samples presented a higher level of digestion and absorption in GE5, which might be attributed to the delayed protein delivery to the intestinal phase due to the coagula that remained at the end of the gastric digestion. These results could be related to the plasma Leu concentrations after protein ingestion obtained by Boirie *et al.* (1997), in which they described whey proteins and casein as 'fast' and 'slow' proteins respectively, a concept previously adopted for dietary carbohydrates due to the evidence of the link between their rate of digestion and absorption, and metabolic response. Boirie *et al.* (1997) showed that there was a rapid increase in plasma Leu levels after the ingestion of a whey protein drink when compared to that of caseins, which showed a more attenuated pattern over time. Similarly, in the present study, the rate and extent of Leu absorption at early stages of digestion was higher in the sample 0C:100W whereas the sample with higher content of casein presented low levels of Leu absorption at the beginning but a substantial increase in the later stage of the digestion, that could have been prolonged if the gastric digestion had lasted longer.

The structure of the milk protein networks formed within gastric conditions, in which whey proteins showed a more open structure and the high casein samples showed denser aggregation (Figure 4.10), could have somehow an impact on the

absorption but this was less probable since the hydrolysis levels of the samples were not different in that point, G1I (Figure 4.14). Also, the protein content at this stage of gastric digestion presented no significant differences between the protein solution samples (Figure 4.7), which might be related to the incomplete formation of the solid coagula by that time. Therefore the distinct absorption pattern could be attributed to a higher level of Leu present in whey proteins compared to caseins (Gorissen *et al.*, 2018). In the current study the protein content was matched but they differed in the Leu content due to the nature of the proteins. Nevertheless, this did not affect the distinct absorption pattern of the milk proteins as studied by Boirie *et al.* (1997), in which both casein and whey proteins drinks were matched in Leu content as well, showing that that Leu content was not the limiting factor for the protein synthesis. Moreover, the patterns for the other measured BCAAs reflected that of Leu pattern (Appendix C) showing the relevance of the kinetics of digestion. Indeed, the independence of the protein digestion rate on modulating postprandial deposition of protein was also confirmed by Dangin *et al.* (2001).

With the inclusion of 2% lipid, the pattern of Leu absorption for (50C:50W)2% in GE1 was similar to those of the samples with higher whey protein content whereas it presented an intermediate behaviour between the two extremes in the last point of the gastric digestion. The inclusion of higher levels of lipid did not affect the Leu absorption pattern at the early stage but it lowered the Leu absorption in the latest stage, which could be attributed to the lower protein delivery at the end of gastric digestion due to the softer coagula formed. These findings are in contrast with that of Gaudichon *et al.* (1999), showing no difference in postprandial protein utilization was seen when milk protein was supplemented by milk fat compared to the milk protein alone. This contrasts with Elliot *et al.* (2006), in which the ingestion of whole milk was suggested to increase the utilization of AAs for protein synthesis when compared to fat-free isocolaric milk. There is little information about the influence of other macronutrients in the postprandial nitrogen utilization to draw any conclusion hence more research is needed.

The results presented showed that the rate of absorption of AAs by the gut depended on the physico-chemical properties of the ingested protein. AAs have several roles in the body, including the synthesis, breakdown and oxidation of protein. Therefore, different patterns in postprandial protein digestion might result in different metabolic responses.

4.4.4 Physiological Relevance

The different kinetics of protein digestion have been reported to modulate the postprandial metabolic and hormonal responses, similarly to carbohydrate metabolism. Boirie *et al.* (1997) reported that the rapid appearance of levels of Leu in plasma for whey proteins enhanced the protein synthesis to a greater extent than for caseins, however, the latter resulted in an inhibition of body protein breakdown due to the low and slow plasma appearance of Leu. In the current study, we presented two extremes of behaviour in Leu absorption from the samples of pure whey proteins (0C:100W) versus milk (80C:20W), which might exert the mentioned postprandial effects of the 'fast' and 'slow' proteins, respectively. Interestingly, the sample 50C:50W, showing a solid coagulation with weaker coagula consistency, could present an intermediate metabolic effect since the kinetics of protein delivery and Leu absorption were overall showing middle levels. It is important to note that the sample containing 100% casein was not included in this study however a similar behaviour to the sample containing 80% can be expected. Lacroix *et al.* (2006a) showed that a milk protein drink containing 20:80 whey protein:casein ratio presented no significant difference in the dietary nitrogen utilization when compared to 100% casein drink, which might be due to the profound effect of solid coagulation in the stomach from a casein content level higher than 80%.

There is evidence showing that a slower pattern of protein digestion leads to a better postprandial utilization of dietary nitrogen, improving AA retention (Boirie *et al.*, 1997; Bos *et al.*, 2003). Lacroix *et al.* (2006a) showed that the rapid appearance of high plasma AA concentrations from the 'fast' protein such as whey proteins induced greater deamination rates by the liver, which decreases the AA concentration in plasma. However, the effect of the protein digestion rates on the protein metabolism seemed to be age-dependent (Dangin *et al.*, 2003; Pennings *et al.*, 2011). Pennings *et al.* (2011) showed that whey proteins resulted in a more effective enhancement in protein retention than casein in the elderly.

In general, the understanding of the gastric phase and how it modulates the gastric behaviour for instance of protein formulation needs further investigation since it offers great potential to design foods that can exert several physiological effects such as satiety (Hall *et al.*, 2003), glycaemic control (Gannon *et al.*, 2010), lipemia control (Mariotti *et al.*, 2015) and improve GI complications such as reflux and aspiration pneumonia (van den Braak *et al.*, 2013).

4.5 Conclusions

This study has proposed underlying mechanisms behind the denoted 'fast' and 'slow' digested protein for whey proteins and caseins, respectively. The main milk proteins presented different digestibilities and AA availabilities, which are key for defining protein quality, and the gastric phase of digestion was shown to be the rate limiting step. The solid coagulation of the casein-rich samples contributed to the delay in nutrient delivery and thus overall digestion and AAs absorption kinetics. In contrast, whey proteins formed soluble aggregates during gastric digestion that led to a gradual decrease of nutrient delivery and a higher Leu absorption in early stages of GI digestion. The modulation of the solid coagula could be obtained by addition of whey proteins and lipid, which modulated the kinetics of digestion. The differences in AA absorption kinetics, as modulated through gastric behaviour, can be associated to different physiological effects. Therefore, this methodological approach is a powerful tool to understand the mechanisms underlying the physiological impact of foods, in order to design foods with different rates of nutrient digestion addressed to the nutritional and health needs of different populations.

Chapter 5

Effect of Process-induced Changes in Whole Milk on *in Vitro* Gastric Restructuring and Nutrient Digestion Kinetics[‡]

[‡]This chapter is based on the published peer-reviewed article, Mulet-Cabero, A.-I., Mackie, A. R., Wilde, P. J., Fenelon, M. A., & Brodkorb, A. (2019). Structural mechanism and kinetics of in vitro gastric digestion are affected by process-induced changes in bovine milk. Food Hydrocolloids, 86, 172-183.

5.1 Introduction

Bovine milk is conventionally heat treated and homogenised to improve consumer acceptance, ensure microbial stability and extend shelf life. These dairy processes cause changes in the physical structure, which have been widely characterised. Homogenisation results in size reduction of the native fat globule, initially surrounded by the milk fat globule membrane (MFGM), from an average size of 3-5 µm to below 1 µm (Michalski *et al.*, 2006). Moreover, homogenisation disrupts the MFGM, drastically changing the interfacial composition, to mainly consist of adsorbed milk protein (Lopez, 2005; Sharma *et al.*, 1993) and reduces the average casein micelle size when high pressure homogenisation (100-300 MPa) is applied (Lodaite *et al.*, 2009) The most common heat treatments applied to milk are pasteurisation that consists of heating at 70-90°C for ≥ 15 s and ultra-high temperature (UHT) sterilization involving heating at 135-150°C for a few seconds. These thermal processes cause the denaturation of whey proteins, in particular β-lactoglobulin (β-Lg) (Singh, 2004), which can then become bound to κ-casein via hydrophobic interaction and disulphide bonding on both the new formed droplet surface and serum (Anema *et al.*, 2003; Guyomarc'h *et al.*, 2003; Sharma *et al.*, 1993).

The structure of food at different length scales has been shown to impact nutrient digestion and absorption. However, there has been little research performed on the impact of these process-induced changes on milk digestion. In some cases, conflicting results have been obtained mainly due to the different digestion models applied. The gastric compartment is a key site to regulate nutrient digestion and control the rate of delivery to the small intestine. Differences in intestinal absorption kinetics of dairy structures have been associated with changes in gastric emptying (GE) rates (Gaudichon *et al.*, 1994). The first steps of breakdown of food are in the gastric compartment mainly due to the presence of pepsin, gastric lipase and acid. Digested products are progressively emptied through the pylorus and released into the small intestine, which has important implications for postprandial responses.

Studies of the *in vivo* digestion of processed milk are very rare. Lacroix *et al.* (2008) found, in healthy humans, that UHT-treated milk consumption induced a significantly higher and faster transfer of dietary nitrogen into serum amino acids and proteins but also to body urea compared to pasteurised and microfiltrated milk. It was suggested, but not investigated, that this modulation of the digestive kinetics was due to the possible formation of a softer coagulum in the stomach and a higher enzyme accessibility in the case of UHT-treated milk. These results were consistent with the findings of Bach *et al.* (2017), in which urinary nitrogen secretion was greater for UHT-

milk compared to raw and pasteurised milk using young dairy calves as a model. In addition, Miranda *et al.* (1987) found that heat treated milk (UHT and autoclaving) increased GE rate and casein hydrolysis in rats. This contrasts to other work, in which a higher mean retention time in the stomach of heated skim milk (90°C, 10 min) was observed compared to a non-heated system observed in mini-pigs (Barbé *et al.*, 2013). It is broadly reported that heat treatment, using temperatures above 90°C, facilitates protein digestion, which has been observed for β-Lg (Wada *et al.*, 2014). This is linked with the thermal denaturation of β-Lg being between 70°C and 90°C, depending on heating time (Fang *et al.*, 1997), which provokes the exposure of the hydrophobic region. However, opposing observations have been made for caseins. Heating skim milk (90°C, 10 min) promoted hydrolysis resistance of the casein fraction compared to unheated skim milk during gastric digestion using an *in vitro* adult dynamic model (Sánchez-Rivera *et al.*, 2015) and *in vitro* infant static model (Dupont *et al.*, 2010), which could affect the kinetics of protein digestion in a mini-pig model (Barbé *et al.*, 2013). This was reportedly related to chemical modifications of the protein during heating, i.e. lactosylation, glycosylation as well as casein-whey interactions, resulting in different peptides generated during digestion. In contrast, using a static digestion model, Tunick *et al.* (2016) found a rapid digestion of caseins in the gastric phase of both processed (heated at pasteurisation and UHT conditions and homogenised) and non-processed samples. Moreover, homogenisation was observed to increase β-Lg hydrolysis compared to pasteurised milk (Islam *et al.*, 2017). Despite the differences in enzymatic digestion of the major milk proteins, Wada *et al.* (2014) reported no significant differences in the overall *in vitro* digestion kinetics among the heat treatments (pasteurisation, UHT and in-can sterilisation). A sophisticated *in vitro* model, the Human Gastric Simulator (HGS), was used to investigate the effect of milk treatment on the gastric behaviour (Ye *et al.*, 2017) . They showed the formation of coagula of different structures led to different protein digestion behaviour. The homogenisation and heat treatment resulted in the formation of a crumbly structure compared to the tight clot obtained in raw milk. This was similar to what was proposed to occur *in vivo* and highlights the limitations of the static *in vitro* digestion models. However, the heating conditions used, 90°C for 20 min, are less representative of the typical conditions used in industrial milk processing.

In addition, the gastric conditions may induce different gastric colloidal behaviours, which could affect postprandial responses through different rates of nutrient delivery. Mackie *et al.* (2013) showed that homogenised droplets stabilised by milk proteins caused creaming in the human stomach, as monitored by magnetic resonance imaging, and decreased fullness due to the delayed lipid emptying, in

contrast to the early delivery of nutrients from a mixture of cheese and yogurt, which sustained fullness.

In this study, we aimed to investigate how processing affected milk microstructure during gastric digestion and nutrient digestion kinetics. The most commonly used milk processes, homogenisation and the heat treatments of pasteurisation and UHT, were used and compared to raw milk in order to assess the influence on gastric behaviour, protein coagulation, nutrient delivery and protein digestion. For that, the developed semi-dynamic model described in Chapter 3 was used, which simulates the main dynamics of the stomach including gradual acidification, gastric fluid and enzyme secretion and emptying.

5.2 Materials and Methods

5.2.1 Materials

Fresh whole bovine milk was collected from a bulk tank of the Moorepark Dairy Unit, Teagasc Animal and Grassland Research and Innovation Center, Moorepark, Fermoy, Co. Cork, Ireland. The milk was from Friesian cows that were fed a total mixed ration diet consisted of grass silage, maize silage and concentrates. Bulk milk samples were collected post-morning milking. The sampling was conducted between November 2016 and February 2017.

Pepsin from porcine gastric mucosa had an enzymatic activity of 3,875 units/mg protein, calculated by measuring the TCA-soluble products using haemoglobin as substrate as described by Minekus *et al.* (2014).

5.2.2 Methods

Figure 5.1 illustrates the experimental procedure followed in the study related to this chapter.
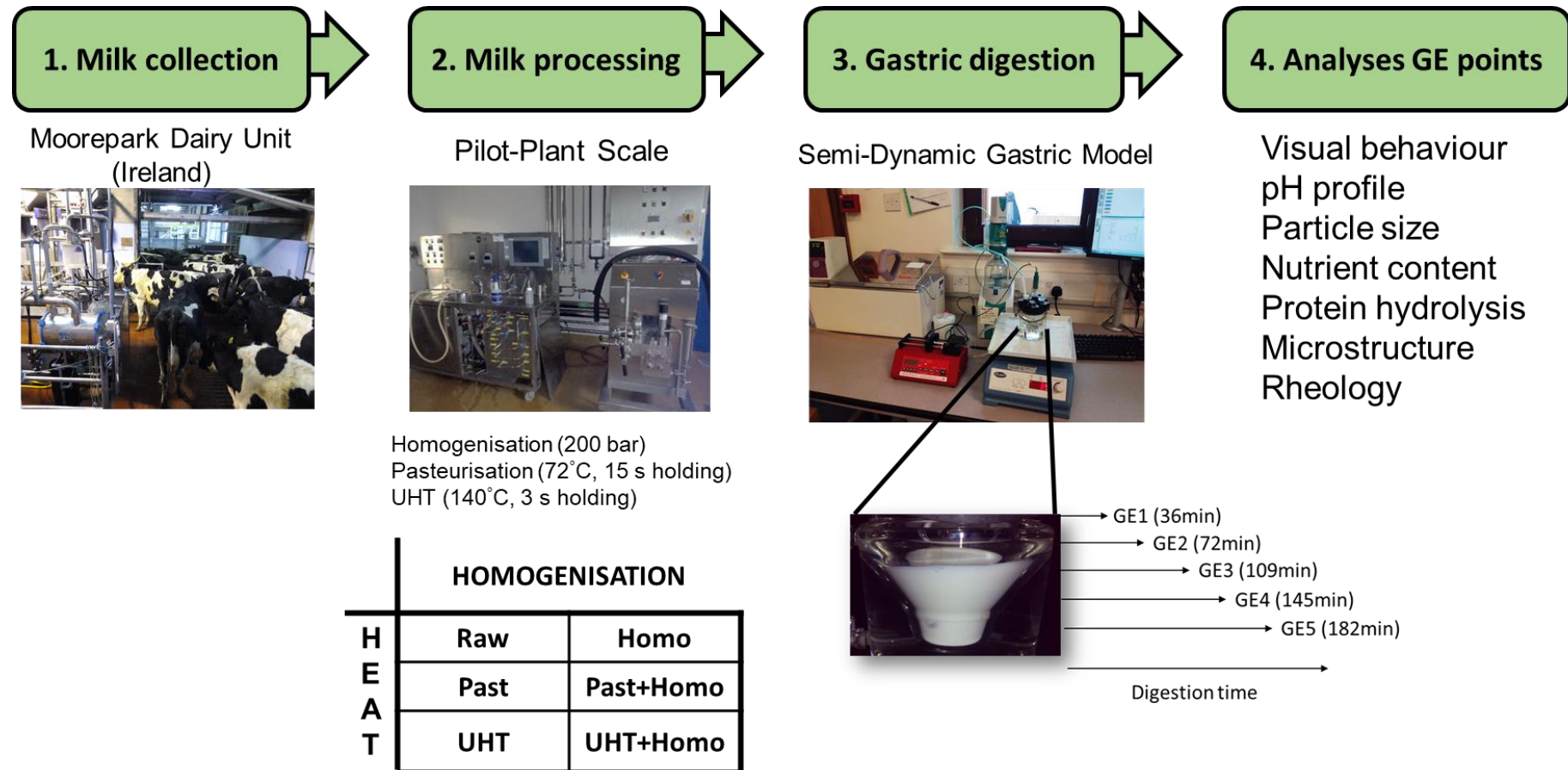
Figure 5.1 Flow diagram of the four main steps of the experimental procedure of the study in relation to Chapter 5. Each step has been described in the corresponding Methods section.

5.2.2.1 Milk Processing at Pilot-Plant Scale

The raw milk was collected on different days for each process performed. The processes were conducted at pilot-plant scale using industrially relevant conditions. Homogenisation was applied at 40°C, to disperse the lipid phase, using a two-stage valve-type homogeniser (Gaulin Labor, type Lab 60; APV Gaulin GmbH, Lubeck, Germany). The pressures used were 15 and 5 MPa for first and second stage, respectively. The sample is referred as Homo in the chapter. Pasteurisation and UHT treatments were carried out using a MicroThermics® tubular heat exchanger (MicroThermics®, NC, USA). The conditions were a final heat temperature at 72°C with a holding time of 15 s for pasteurisation and 140°C with a holding time of 3 s for UHT treatment (pre-heating temperature of 91°C). The samples are referred as Past and UHT respectively in the chapter. These heat treatments were also carried out with a subsequent homogenisation step using an in-line two-stage valve homogeniser, Model NS 2006H (Niro Soavi, Parma, Italy) employing a first-stage pressure of 15 MPa and a second-stage pressure of 5 MPa. The samples are referred as Past+Homo and UHT+Homo respectively in the chapter. The samples were stored at 4°C after preparation. The Raw, Homo, Past and UHT were studied within 1 day and Past/UHT+Homo were used within 2 days. Figure 5.2 illustrates the six studied samples with the schematic representation of the main structural and molecular changes expected to occur.
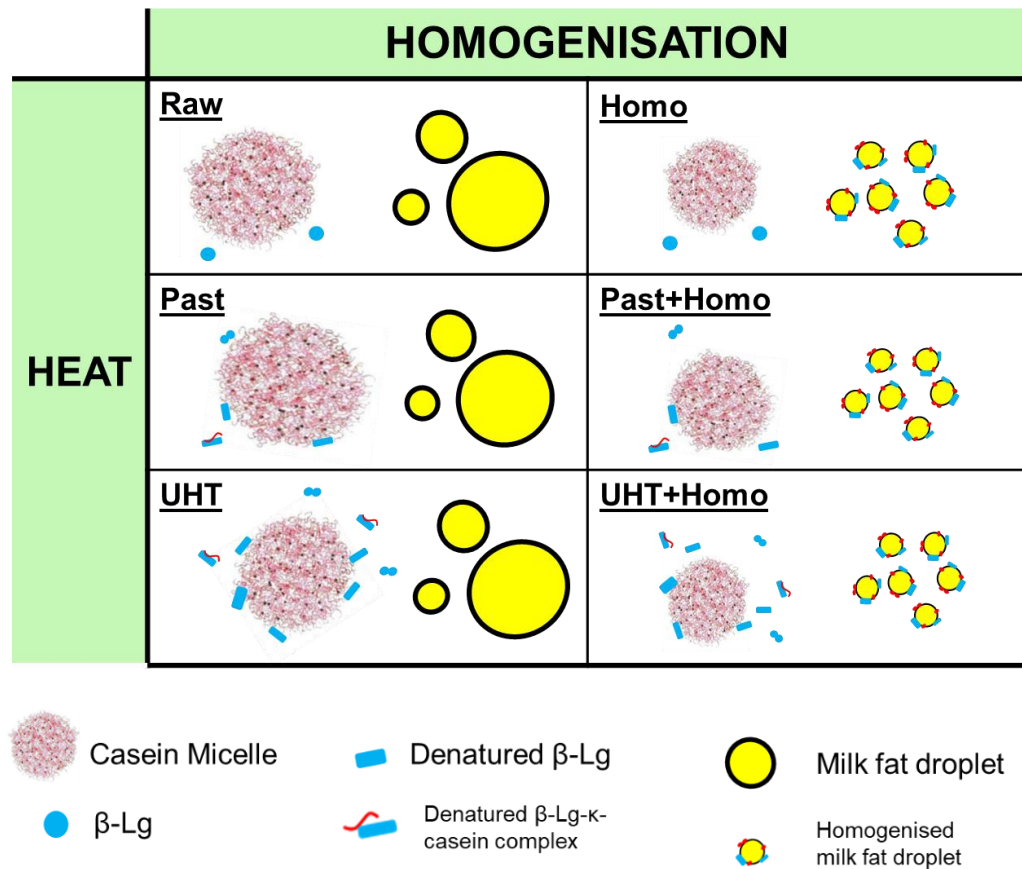
Figure 5.2 Schematic representation of the molecular structure of the samples of studied after the different processing combining homogenisation and heat processes.

The nutritional content of raw milk was measured before each experiment in order to calculate the parameters for the simulated gastric digestion. Milk fat, protein, lactose and total solids values were obtained using a Milkoscan FT 6000 (FOSS, Denmark) with a tolerance of ± 0.06%. This analysis was performed by Jim Flynn (laboratory technician at Moorepark Teagasc Food Research Centre). The nutrient composition of milk was measured before each sample (see Table 5.1), showing no significant effect of the different treatments, and the caloric content was calculated using the Atwater factors. This ranged from 0.78 to 0.68 kcal/mL during the period of the study.

Table 5.1 Nutritional composition of the studied milk samples. Values are the mean and standard deviation of two independent replicates

	% Lipid	% Protein	% Lactose	% Total solids
Raw	4.67±0.26	3.44±0.41	4.72±0.09	13.53±0.67
Past	4.55±0.43	3.32±0.25	4.71±0.10	13.24±0.59
UHT	4.49±0.53	3.43±0.42	4.71±0.05	13.35±1.03
Homo	4.74±0.28	3.76±0.09	4.66±0.02	13.82±0.25
Past+Homo	4.55±0.43	3.32±0.25	4.71±0.10	13.24±0.59
UHT+Homo	4.49±0.53	3.43±0.42	4.71±0.05	13.35±1.03

5.2.2.2 Semi-Dynamic Gastric Digestion Model

After collection of the raw milk and the respective processing, the samples went through a simulated, semi-dynamic gastric digestion. This was performed using two independent samples on different days. Therefore, the simulated digestion experiments were conducted independently, and subsequent analyses were performed from these independent samples.

The simulation of the oral and gastric phase was performed using the semi-dynamic adult digestion model previously detailed in the Chapter 3 and the protocol used with some modifications is described in the section 2.2.2.1.

The oral phase was simulated before the gastric digestion. 20 g of sample was mixed with a volume of the oral mixture containing 79.9% SSF (1.25x),19.6% MilliQ® water and 0.5% $CaCl_2(H_2O)_2$ (0.3 mol/L). The volume of the oral mixture corresponded to the total solids content of the sample (Table 5.1). The volume added of oral mixture varied slightly between samples, ranging from 2.52 to 2.82 mL due to the difference of the total solid concentration in the analysed milk samples during the period of study. The mixing was performed using a rotator (SB3 Model, Stuart, Bibby Scientific, UK) at 30 rpm for 2 min. The temperature was kept at 37°C using an incubator (BF56, Binder GmbH, Germany).

The resulting mixture was then put through the gastric digestion using a reaction vessel, which was a v-form glass vessel (5-70 mL titration vessel, Metrohm, Switzerland) with thermostat jacket (37°C). The sample from the oral phase was

placed in the reaction vessel after the addition of the basal volume, which consisted of the 10% of the constituents SGF (1.25x), MilliQ® water, HCl (1.5 mol/L) and $CaCl_2(H_2O)_2$ (0.3 mol/L) from the total volume of the gastric mixture. The total gastric mixture contained 80% SGF (1.25x), 7.78% MilliQ® water, 8.7% HCl (1.5 mol/L) and 3.48% pepsin and 0.04% $CaCl_2(H_2O)_2$ (0.3 mol/L). Two solutions were added at a constant rate, which depended on the corresponding gastric time: (1) the simulated gastric electrolyte mixture containing the 90% of the constituents SGF (1.25x), MilliQ® water, HCl (1.5 mol/L) and $CaCl_2(H_2O)_2$ (0.3 mol/L) from the total volume of the gastric mixture and (2) 0.8 mL pepsin solution (made with MilliQ® water). The simulated gastric electrolyte mixture of SGF (1.25x), HCl, water and $CaCl_2(H_2O)_2$ was delivered by a dosing device (800 Dosino, Metrohm, Switzerland) of an automatic titrator (842 Titrando, Metrohm, Switzerland) and the enzyme solution was delivered by a syringe pump (New Era Pump Systems, Inc., NY, USA). A 3D action shaker (Mini-gyro rocker, SSM3 Model, Stuart, Barloworld Scientific limited, UK) at 35 rpm was used for agitating the vessel.

After 25 min of gastric digestion, the sample was mixed using a 50 mL plastic syringe (BD Plastipak, Ireland), the aperture of which had an inner diameter of 6.80 mm with a plastic tube attached (6 mm inner diameter). This mixing was required to make the sampling more accurate. Nevertheless, the colloidal behaviour during digestion seemed not to be impaired by the initial mixing. Gastric emptying (GE) was simulated by taking 5 aliquots, referred to as GE1-5 in the text. The average time of those were 36 min (GE1), 73 min (GE2), 109 min (GE3), 145 min (GE4) and 182 min (GE5). GE aliquots were taken from the bottom of the vessel using a serological pipette with a tip internal diameter of 2 mm because it approximates the upper limit of particle size that has been seen to pass through the pyloric opening into the duodenum (Thomas, 2006). It is important to note that there was some residue left in the last GE point that could not be taken using a pipette; this was taken using a spatula and included in the last point. An aliquot of these GE aliquots was used for microscopic and particle size analysis. Otherwise, the sample was mixed using a homogeniser (T10 basic Ultra-Turrax®, IKA®, Germany) at approximately 30,000 rpm for 30 s to obtain a homogenous sample for the remaining analysis. The pH of each GE aliquot was measured using a pH meter and a sufficient volume of NaOH (2 mol/L) was added to the samples to increase the pH above 7, inhibiting pepsin activity. Finally, GE aliquots were snap-frozen in liquid nitrogen and stored at -80°C until subsequent analysis.

The simulation of the emptying was based on caloric density, using a linear GE rate of 2 kcal/min as explained in Chapter 3. This implied that the volume and time of

each emptying point (Table 5.2) differed due to the slight variations in the caloric content of the milk samples during the period of the study.

Table 5.2 Calculated time (min) at which gastric emptying (GE) was applied in the milk samples. Five emptying points were used. Values are the mean of two independent replicates.

	Gastric Emptying Time (min)					
	Raw	Past	UHT	Homo	Past+Homo	UHT+Homo
Initial	0.0 ± 0.0	0.0 ± 0.0	0.0 ± 0.0	0.0 ± 0.0	0.0 ± 0.0	0.0 ± 0.0
GE1	36.2 ± 0.2	36.2 ± 2.7	36.4 ± 3.2	36.7 ± 0.6	36.2 ± 2.7	36.4 ± 3.2
GE2	72.4 ± 0.5	72.4 ± 5.3	72.9 ± 6.3	73.3 ± 1.4	72.4 ± 5.3	72.9 ± 6.3
GE3	108.6 ± 0.7	108.6 ± 8.0	109.4 ± 9.5	110.0 ± 2.1	108.6 ± 8.0	109.4 ± 9.5
GE4	144.8 ± 0.9	144.8 ± 10.6	145.8 ± 12.6	146.6 ± 2.8	144.8 ± 10.6	145.8 ± 12.6
GE5	180.9 ± 1.2	181.0 ± 13.3	182.3 ± 15.8	183.3 ± 3.5	181.0 ± 13.3	182.3 ± 15.8

5.2.2.3 Confocal Laser Scanning Microscopy

The microstructure of the initial and digested samples was observed using a confocal laser scanning microscope, Leica TCS SP5 (Leica Microsystems, Baden-Württemberg, Germany) as described in the section 2.2.3.3. A mixture of 0.1% Fast green FCF solution and 0.1% Nile red solution at 1:1 proportion was used. 500 μL of initial/digested sample was gently mixed with 50 μL of mixed dye.

5.2.2.4 Particle Size Distribution

The particle size was measured using a laser-light diffraction unit (Mastersizer, Malvern Instruments Ltd, Worcestershire, UK) as described in the section 2.2.3.1. The optical parameters chosen were a particle and dispersant (water) refractive index of 1.456 and 1.330, respectively. The absorbance value of the fat globules was 0.001. A volume of initial and digested samples was added in order to reach a laser obscuration range of 5-10 %. A volume of the initial and GE5 samples (0.2 mL) was dispersed in 10 mL of 0.02 M sodium dodecyl sulphate (SDS) to dissociate clusters of proteins (as described in van Aken *et al.* (2011)). The measurement of each independent sample was carried out in triplicate.

5.2.2.5 Total Protein and Lipid Content Analysis in Emptied Aliquots

The total protein and lipid contents of the initial sample and emptied digesta were determined using a LECO FP628 nitrogen analyser and CEM SMART Trac™ fat analyser, respectively. Details of these techniques have been described in the sections 2.2.4.1 and 2.2.5.1. The measurement of each independent sample was carried out in duplicate.

5.2.2.6 OPA Assay for Quantification of Protein Hydrolysis

The concentration of the free amino groups was analysed by OPA assay, which has been described in the section 2.2.4.3. The absorbance was measured at 340 nm using a multi-mode microplate reader, Synergy™ HT (BioTek® Instruments, Inc., Winooski, VT). The measurement of each independent sample was carried out in duplicate.

5.2.2.7 SDS-PAGE for Identification of Proteins during Digestion

The composition of the main proteins in the gastric emptied aliquots was determined by SDS-PAGE, which has been described in the section 2.2.4.2. SDS-PAGE was performed on the initial and digested samples normalised to 0.1% of total protein concentration.

5.2.2.8 Rheological Analysis

The consistency of the coagulum that persisted at the end of digestion, after about 182 min (GE5 point) was analysed by small deformation rheology (see section 2.2.3.2). The coagulum was separated from the serum using a 70 µm Nylon cell strainer, BD Falcon™ (BD Biosciences, Oxford, UK). The mass of the sample and, the separated coagulum and serum was recorded. The coagulum was gently placed in a rheometer, AR 2000 (TA Instruments, Crawley, UK). The rheometer geometry consisted of a 40 mm diameter parallel steel plate using a shear strain of 0.5 and an oscillation frequency of 1 Hz for 30 min at 37°C. The complex modulus (G*) was calculated as follows G*=stress*/strain.

5.2.2.9 *In Vivo* Gastric Imaging

Intragastric *in vivo* imaging of the stomach was performed as a part of an educational TV programme (no ethical permission was required). The study was conducted at the Mercy University Hospital (Cork, Ireland) with the supervision of medically qualified clinical staff. The imaging was performed using MiroCam® technology capsule endoscope. The camera wirelessly transmitted images at approximately three images per second to the receptors/electrodes that were attached to the torso of the subject and was equipped with a light emitting diode, which transmitted light to allow correct imaging of solution. A young healthy man swallowed the camera and then, drank about 500 mL of whole raw milk, equivalent to the Raw sample described earlier.

5.2.2.10 Statistical Analysis

The results were expressed as means ± standard deviation of two replicates. For each replicate, raw milk was collected, analysed (composition) and processed independently, i.e. one milk per day. To identify differences in normally distributed results within groups during gastric digestion, one-way ANOVA was applied. Where overall significant interaction was observed ($P < 0.05$), the means of individual milk treatments were compared using Tukey's post hoc test. Statistical analyses were performed using GraphPad Prism software (Prism 5 for Windows, Version 5.04).

5.3 Results

5.3.1 Gastric pH Profile

The simulation of the gastric phase was performed using the developed semi-dynamic model described in Chapter 3 that can simulate the main biochemical dynamics of the human stomach. These are gradual enzyme and acid secretion and progressive GE. The changes in pH of the gastric emptied aliquots taken during digestion are shown in Figure 5.3. The gastric model had a low initial pH of about 1 simulating the basal conditions and the pH increased rapidly, up to values of about 6, after the addition of a sample from the oral phase. Subsequently, there was a progressive decrease reaching pH values below 1.4 after 3 hours due to the continuous gastric fluid secretion containing acid as well as the reduction of buffering capacity of the digested food by GE. All samples showed a similar pH behaviour to the predefined profile observed in *in vivo* studies (Malagelada *et al.*, 1976). The mean pH of the samples did not show any statistically significant differences except in the initial (p = 0.034) and GE1 (p = 0.041) points. The mean pH between Raw and UHT+Homo in GE1 were significantly different using the Tukey's multiple comparison post-hoc test.
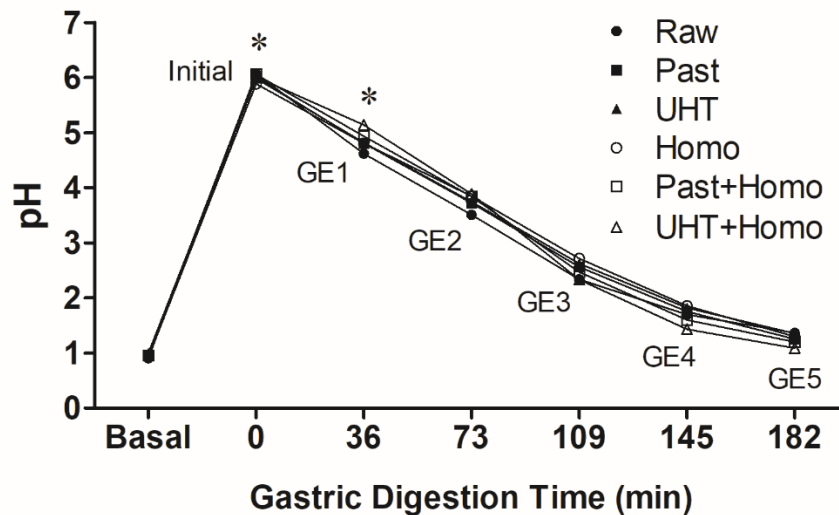
Figure 5.3 Change in pH of milk aliquots emptied from the gastric digestion in the semi-dynamic model corresponding to each gastric emptying (GE) point. The time represents an approximation of the actual values displayed in Table 5.2. The pH values are referred to the basal stage (before gastric digestion), initial (milk sample including oral phase and basal volumes) and the different GE samples (GE1-GE5). Each data point is the mean of 2 independent determinations. Significance difference in pH between milk samples in each GE point was determined by one-way ANOVA, $p < 0.05$ (*).

In addition, the influence of removing the pepsin on the pH behaviour was investigated. The pH profile of non-heated milk was affected by the presence of pepsin (see Appendix D). In the case of Raw, the pH of the sample containing pepsin decreased more promptly during the first hour than that of the sample without pepsin. In contrast, the pH profile of the heat-treated samples without using pepsin did not differ much to that with pepsin, in particular in the case of the UHT-treated samples.

5.3.2 Gastric Behaviour

Using the semi-dynamic model, a range of different structures and behaviours during gastric digestion were observed to form within the gastric compartment (Figure 5.4 and Figure 5.5). Protein coagulation was visible for all the samples within the first 10 min of digestion and the formation of larger aggregates was observed a few minutes later, at which time the pH ranged from 5.5 to 6. Subsequently, there was the formation of a more compact coagulum with clear serum within the following 15 min.

Differences in coagulum consistency were observed throughout the gastric phase as illustrated in Figure 5.4. There were remarkable differences, in particular, between the firm coagulum of Raw (Figure 5.4 A) and the fragmented structure of UHT+Homo (Figure 5.4 I). In the absence of pepsin, we observed delayed aggregation and formation of coagula. Protein coagulation was visually observed after 75 min at which

time the pH was around 5, with the exception of the UHT-treated samples in which the aggregation was first seen at 35 min. Appendix E illustrates the behaviour of the six samples in the stomach model in all the GE points when pepsin was not added, compared to the gastric behaviour including pepsin.
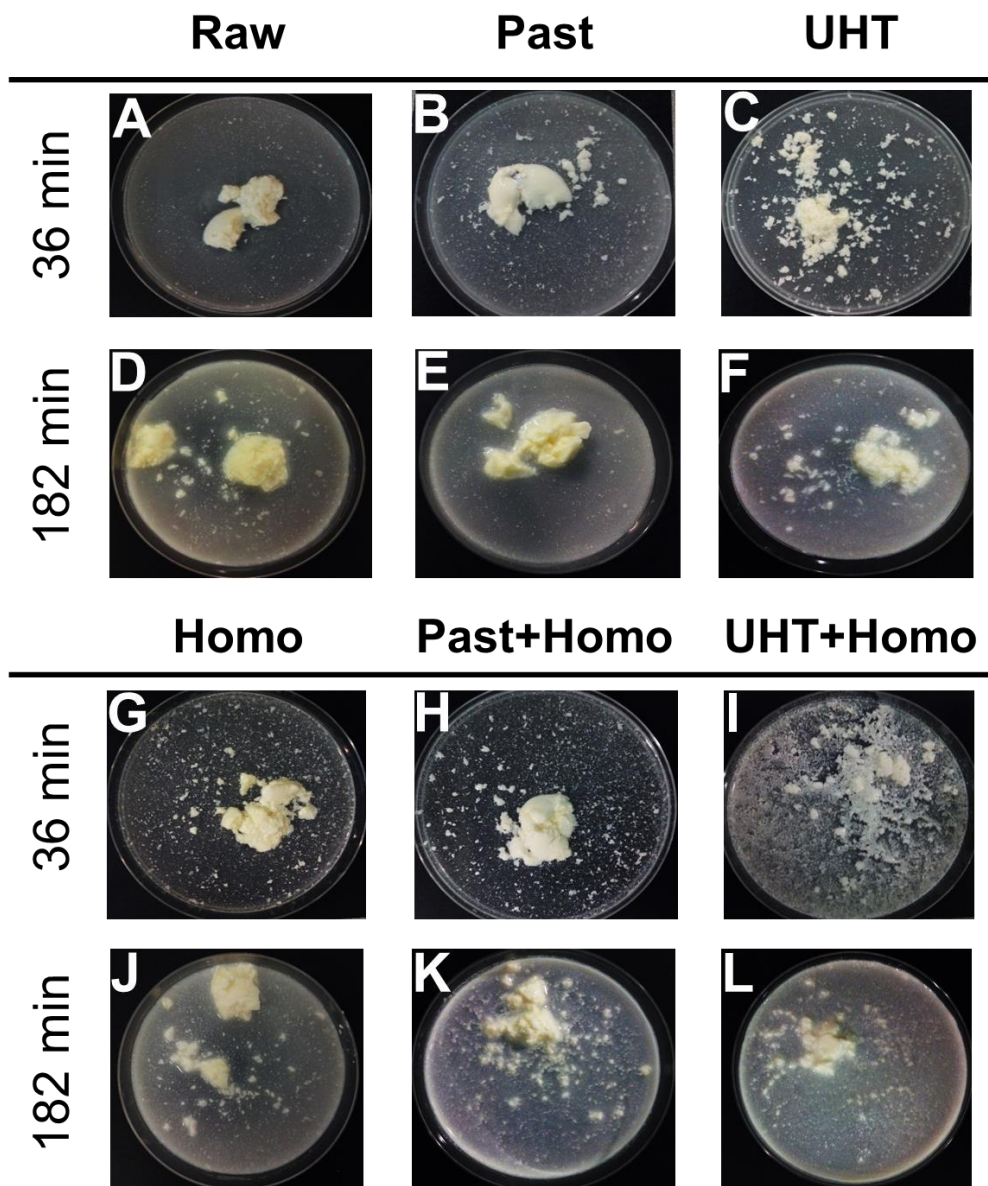
Figure 5.4 Images of the milk samples at approximately 36 and 182 min of gastric digestion (displayed in a petri dish), corresponding to the behaviour right before the first and last gastric emptying points. Raw milk (A, D), pasteurised milk (B, E), UHT milk (C, F), homogenised milk (G, J), pasteurised+homogenised milk (H, K) and UHT+homogenised milk (I, L). Note: the diameter of the petri dish in the samples at 36 min and 182 min was 13.5 cm and 8.5 cm, respectively.

Figure 5.5 shows the gastric behaviour of the milk samples in the model stomach *in situ* at about 36 min (Figure 5.5 A, B, C, G, H, I) and 182 min (Figure 5.5 D, E, F, J, K, L) of gastric digestion. The homogenised samples showed evidence of creaming at 182 min, having an opaque layer on the top, (Figure 5.5 J, K, L) whereas

the non-homogenised samples displayed sedimentation throughout the digestion (Figure 5.5 D, E, F). In the homogenised samples, phase separation was initially observed when aggregates could form a layer at the top, with a cloudy layer in the middle part and clearer layer in the bottom at about 109 min. The behaviour of the samples was different in the absence of pepsin since there was no phase separation and the coagulum of all the samples remained on the bottom of the vessel (see Appendix E 2, 5 and 6).
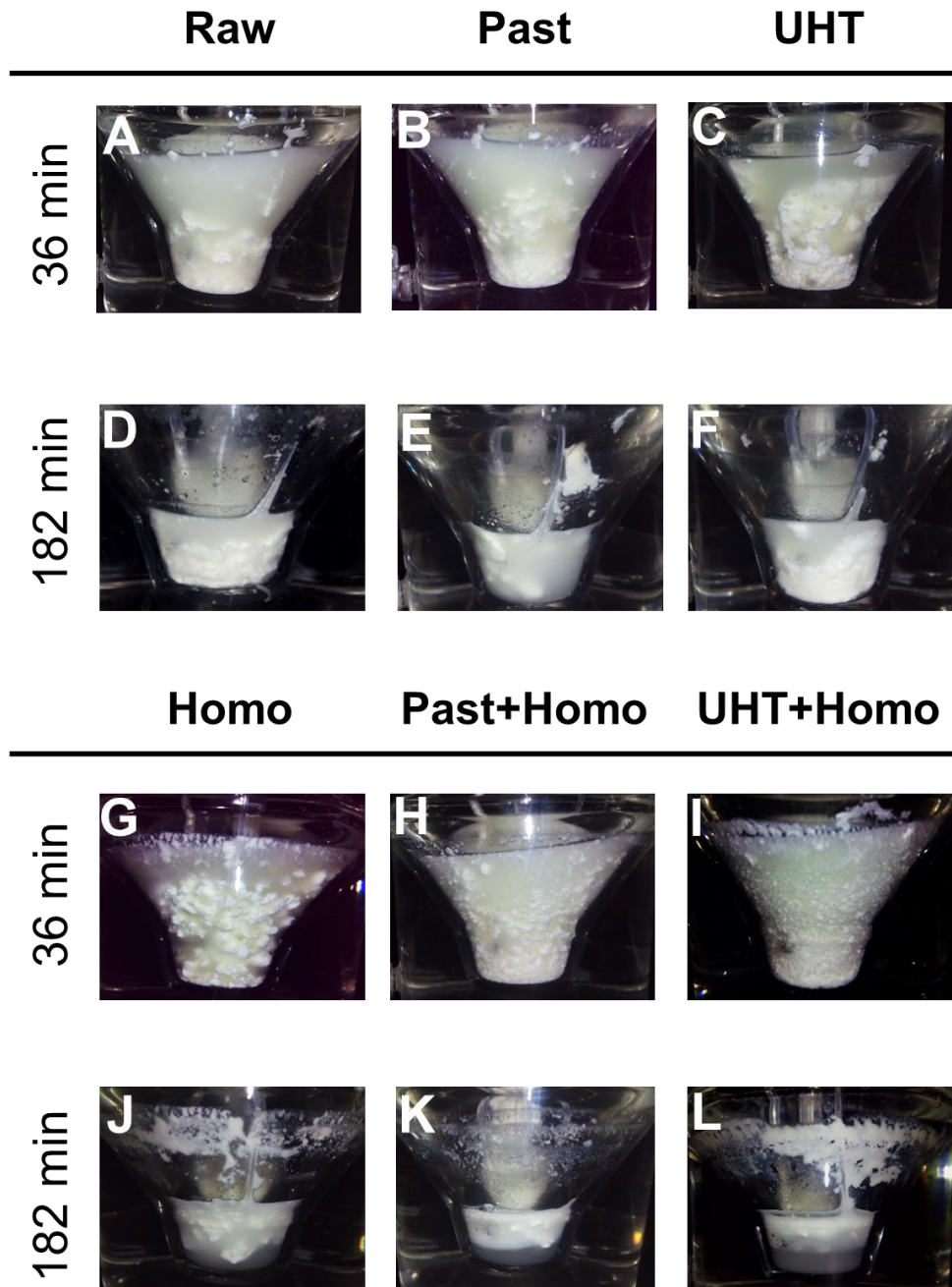
Figure 5.5 Images of the milk samples at approximately 36 and 182 min displayed in the reaction vessel of the gastric model. Raw milk (A, D), pasteurised milk (B, E), UHT milk (C, F), homogenised milk (G, J), pasteurised+homogenised milk (H, K) and UHT+homogenised milk

(I, L). The images correspond to the behaviour right before the emptying corresponding to that time, i.e. GE1 at 36 min and GE5 at 182 min.

The consistency of the milk coagulum was further studied by small deformation rheology analysing the coagulum remaining in the last point of digestion, at 180 min. Table 5.3 shows the values of the complex modulus (G*) obtained after 15 min of measurement. The non-heated samples, Raw and Homo, generated the highest value of G*. The pasteurised samples (Past and Past+Homo) presented intermediate values. The lowest G* values were found in UHT and UHT+Homo, which were an order of magnitude lower than the Raw and Homo samples. The same behaviour was observed during the rheological analysis, which was performed for 30 min. It is important to note that some alteration of the structure could have been induced while transferring the sample to the rheometer in order to perform the analysis.

Table 5.3 Mean diameter ($d_{4,3}$) of the initial samples (before digestion), with and without SDS addition, and the last gastric emptying (GE) point, i.e. GE5, including SDS. The values represent the mean and standard deviation of two independent replicates. Values of the complex module, G*, at 15 min of shear of the milk coagulum collected at GE5 time (after about 182 min). Means within the same column and having the same superscript lowercase letter and means within the same superscript uppercase letter are not significantly different by Tukey's t-test at $p < 0.05$.

	$d_{4,3}$ (µm)			
	Initial	**Initial+SDS**	**GE5+SDS**	**G* (Pa)**
Raw	2.48 ± 0.48^{aA}	2.96 ± 0.08^{aA}	8.26 ± 5.44^{aA}	$4{,}555\pm236^{a}$
Past	2.49 ± 0.61^{aA}	3.62 ± 0.65^{aA}	6.92 ± 2.26^{aA}	$2{,}934\pm1426^{a}$
UHT	2.49 ± 0.15^{aA}	$3.82\pm0.02^{aA,B}$	4.28 ± 0.57^{aB}	501 ± 186^{b}
Homo	0.42 ± 0.02^{bA}	0.37 ± 0.01^{bA}	0.42 ± 0.03^{aA}	$4{,}113\pm501^{a}$
Past+Homo	0.34 ± 0.01^{bA}	0.87 ± 0.77^{bA}	2.99 ± 2.23^{aA}	$1{,}569\pm730^{b}$
UHT+Homo	0.35 ± 0.06^{bA}	0.41 ± 0.08^{bA}	0.97 ± 0.70^{aA}	206 ± 45^{b}

5.3.3 Microstructure of the Gastric Emptied Aliquots

The coagulation, observed within the first 15 min of digestion, was reflected in the microstructures of the emptied samples determined using confocal microscopy (Figure 5.6). There were differences in the structure of the protein matrix in the first stages of gastric digestion. The non-heated samples, in particular Raw, seemed to form a more compact and dense network (Figure 5.6 D) in accordance with the visual observation. This differed from the heated samples, in particular UHT (Figure 5.6 F), in which the structure of the protein coagulum was open with more pores. This can be linked with the particulate and soft macrostructure observed. Moreover, in the GE1 point of the non-homogenised samples (Figure 5.6 D, E, F), there appeared to be more native fat droplets in the aqueous phase compared to non-homogenised samples, and also showing some coalescence. In contrast, the fat droplets seemed

to be easily entrapped in protein network of the homogenised samples (Figure 5.6 M, N, O), in which fine particles could be seen distributed within the coagulum particles, in particular UHT+Homo (Figure 5.6 O). The effect of homogenisation on the structure at the end of gastric digestion (182 min) was significant. All the homogenised samples presented a great number of small aggregates (Figure 5.6 P, Q, R) compared to the large particles of non-homogenised samples (Figure 5.6 G, H, I).
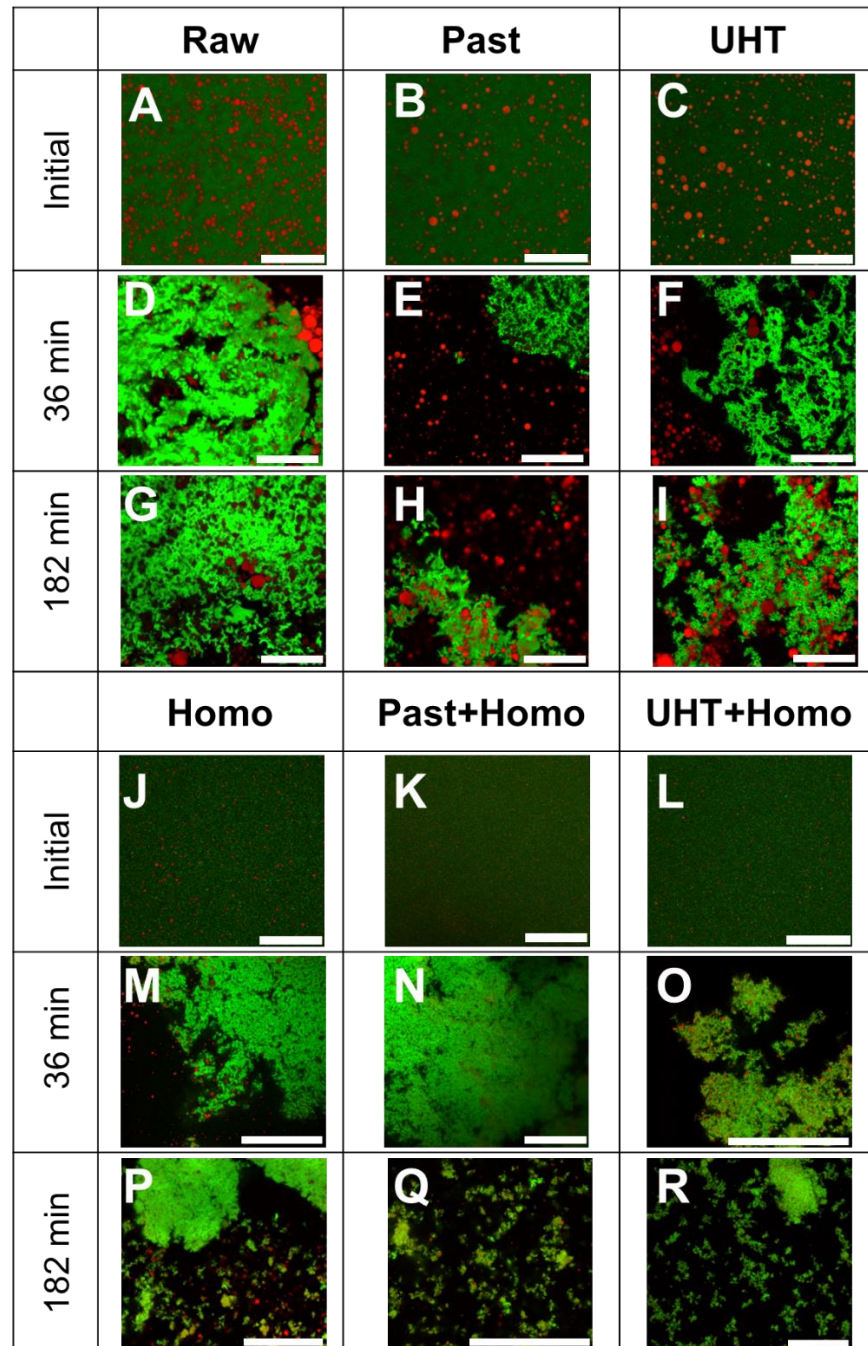
Figure 5.6 Examples of confocal microscopy images of the milk samples before digestion (Initial) and, at about 36 min (GE1) and 182 min (GE5) of gastric digestion. Raw milk (A, D, G), pasteurised milk (B, E, H), UHT milk (C, F, I), homogenised milk (J, M, P), pasteurised+homogenised milk (K, N, Q), UHT+homogenised milk (L, O, R). Red shows the lipid and green shows the protein. The scale bar corresponds to 75 μm.

Pepsin had a significant effect on the microstructure of the protein network as illustrated in the confocal micrographs of the emptied aliquots (Appendix E). The microstructure obtained at 36 min when pepsin was not added showed a high proportion of protein still in solution (i.e. non-aggregated), confirming the visual observation of the delayed coagulation. In contrast, UHT-samples presented similar microstructure at 36 min, regardless addition of pepsin. Once the coagulum was formed, the microstructure remained without major changes when pepsin was not added. This contrasts to the disintegration of the matrix observed during digestion of the samples when pepsin was added, in which phase separation could be observed.

The changes in the droplet size were followed during digestion (Table 5.3). Initially, the mean particle diameter, $d_{4,3}$, of non-homogenised samples was about 2.5 µm whereas that of homogenised samples was about 0.4 µm, showing the significant size reduction due to homogenisation treatment. The particle size of the milk samples, with the addition of SDS, increased to a different extent at the end of digestion. The digestion of the raw milk resulted in an increase from the initial size of 2.96 µm to 8.26 µm after 182 min of digestion but the particle size of UHT+Homo increased from 0.41 to 0.97 µm.

5.3.4 Nutrient Delivery of the Gastric Emptied Aliquots

The nutrient content measured, both protein and lipid, was intended to simulate the delivery of the digesta from the stomach to the duodenum. The protein (Figure 5.7 A) and lipid (Figure 5.7 B) content was low in the first GE points and then there was an increase in the last point, GE5. The latter GE point included the remaining coagulum so the nutrient content was expected to be higher in samples with more extensive coagulation. The content in GE5 ranged from 3.42 to 9.45% and from 7.21 to 16.14% for protein and lipid, respectively. The means of protein and lipid content were significantly different in both GE1 and GE5 due to differences between Raw and UHT+Homo. The profile of the protein content showed a more constant and higher levels in the first GE points in comparison to those in lipid profile. In the case of lipid content profile, in GE5, the homogenised samples seemed to have higher levels with exception of UHT+Homo.
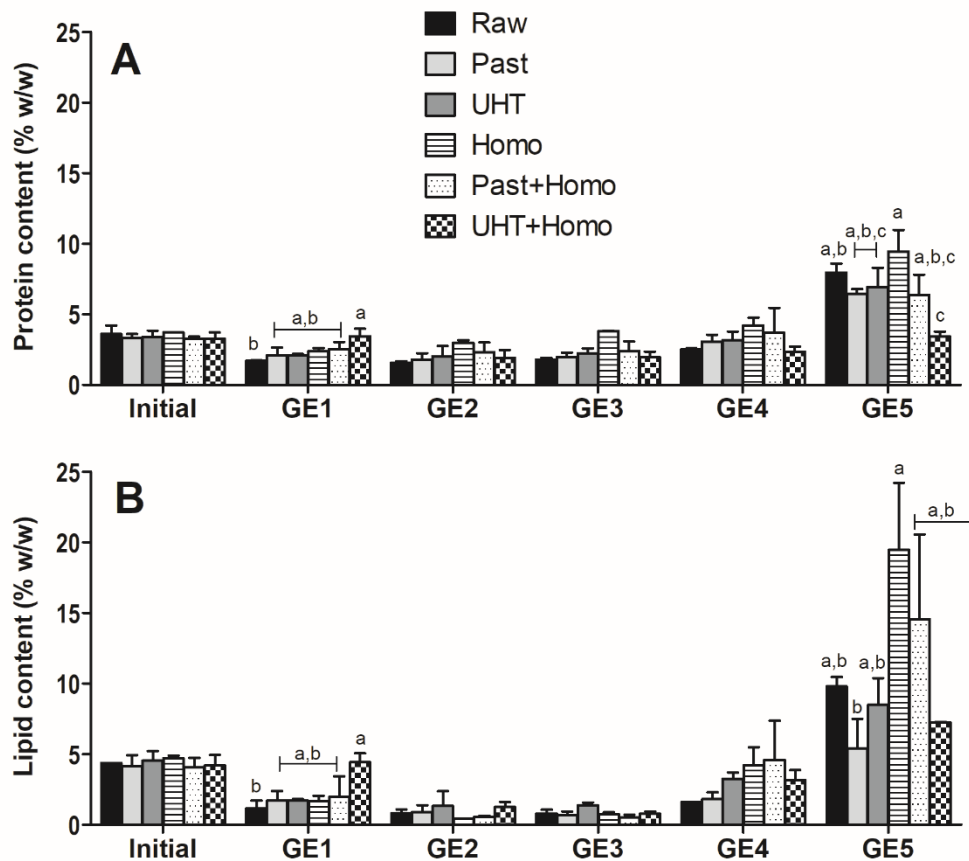
Figure 5.7 The nutrient content (%, w/w) in terms of (A) protein and (B) lipid of initial (before digestion) and the gastric emptying point (GE1-GE5). Each data point is the mean and error bars represent standard deviation of two independent replicates. The values were corrected by the different gastric dilution in each point. Mean values within a column with different superscript letters (a, b, c) were significantly different ($p < 0.05$).

Appendix F1 and Appendix F2 show the implications of pepsin addition on lipid and protein delivery, respectively. In the absence of pepsin, the nutrient delivery both lipid and protein tended to lower at the end of the gastric digestion, probably due to an easier emptying of the sample in the early points.

5.3.5 Protein Digestion of the Gastric Emptied Aliquots

Figure 5.8 shows the levels of free amino groups (R-NH_2) of the milk samples before digestion and in the different GE aliquots. The means of the initial samples were significantly different ($p=0.0008$) due to the samples in which UHT treatment was applied. The low values obtained in these samples may be due to the Maillard reaction products, which might be favoured by the high heating of UHT treatment (Morgan *et al.*, 1999). The proteolysis showed a similar profile in all samples. There was an increase in the three first GE points, after which it levelled off showing no

increase in the GE4 point. After that, the level of proteolysis decreased in GE5. Levels of proteolysis among samples differed greatly in GE1 and GE5. In GE1, Raw and UHT+Homo were statistically different accounting for 921.07 and 354.31 mmol/L R-NH_2/g, respectively. Conversely, in GE5, UHT+Homo showed the highest level of proteolysis (1,736 mmol/L R-NH_2/g) being statistically different from Raw and Homo (897 and 1,065 mmol/L R-NH_2/g, respectively).
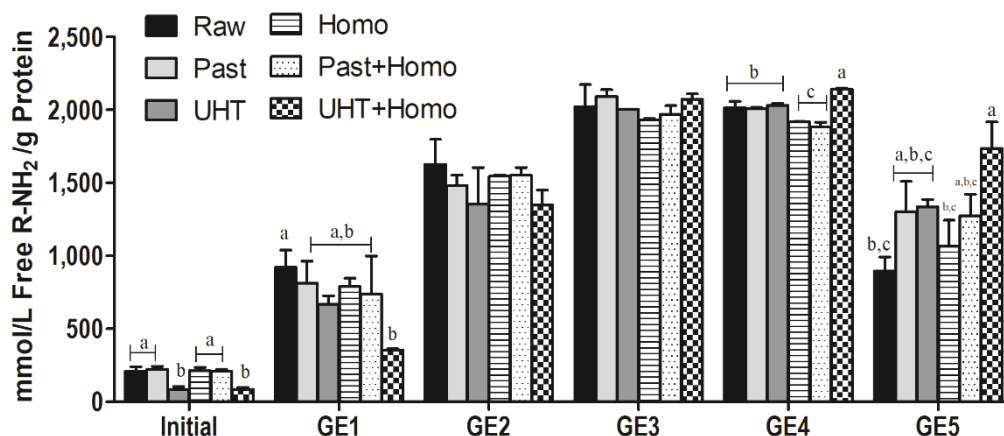
Figure 5.8 Concentration of free amino groups per mass of total protein in sample; initial (before digestion) and gastric emptying points (GE1-GE5). Each data point is the mean and error bars represent standard deviation of two independent replicates. The values were corrected by the different gastric dilution in each point. Mean values within a column with different superscript letters (a, b, c) were significantly different ($p < 0.05$).

The protein composition during the gastric phase was also studied by SDS-PAGE and shown in Figure 5.9. The bands corresponding to the samples before digestion (referred to I) did not differ due to processing. Moreover, there were no differences between homogenised and non-homogenised samples. The non-heated samples, Raw and Homo, had similar patterns than those of pasteurised samples (Past and Past+Homo). The caseins were detectable in the first emptying points, in particular GE1 and GE2 points, but they were almost not observed in GE3 and GE4 points. In the last emptying point (GE5) intact caseins could again be observed together with a wide range of peptides. β-Lg, in contrast, was present during gastric digestion even though the band weakened in the last GE points. Also, α-La was present in the three first GE points, after which it was not detected anymore. Many small molecular weight peptides were present during digestion and could be seen from GE1 onwards. This behaviour differed from that observed in the UHT-treated samples (i.e. UHT and UHT+Homo). In those samples, both caseins and whey proteins could only be observed in the two first GE points.
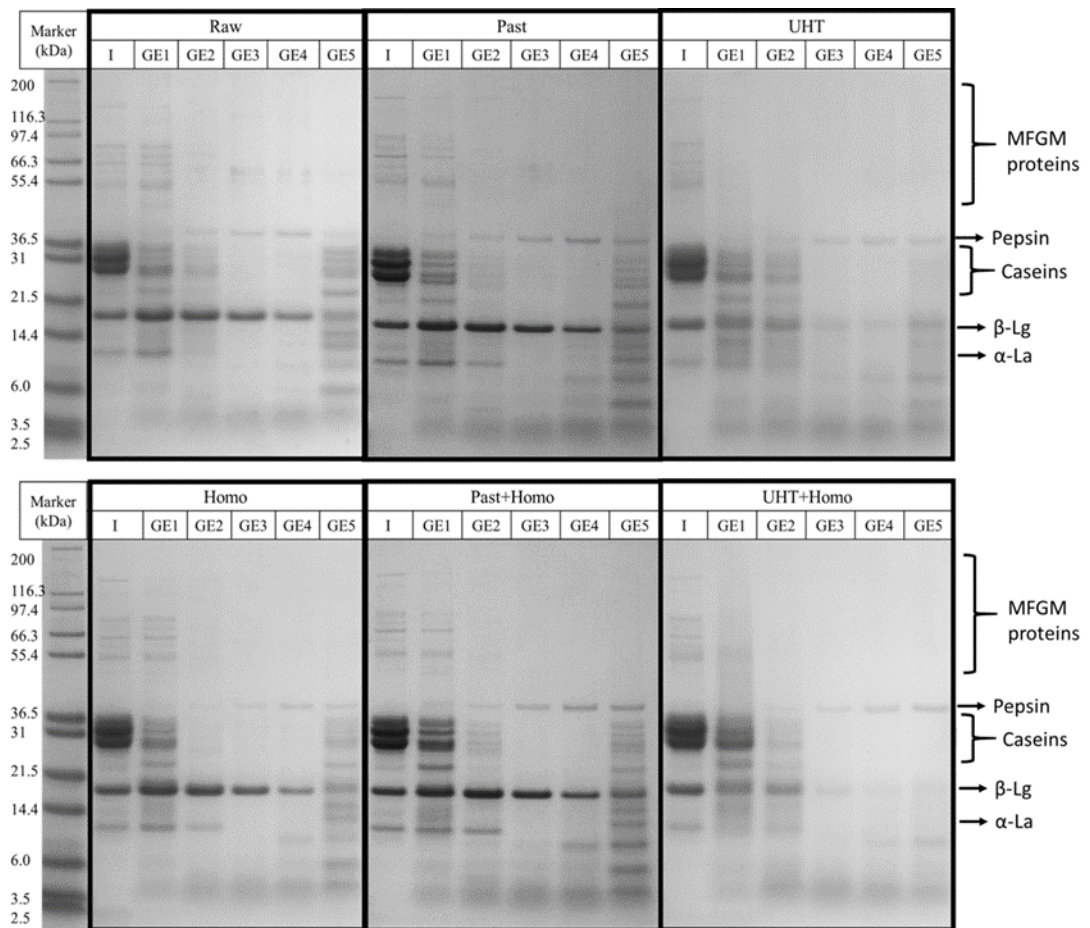
Figure 5.9 SDS-PAGE (under reducing conditions) of the milk samples, initial (I) referred to before digestion and the gastric emptying points (GE1-GE5), and a molecular weight marker. The samples are labelled in the figure accordingly. The protein content in each sample was 0.1%.

Appendix G1 to Appendix G6 show the protein composition in the emptied points when pepsin was not added, in comparison to the samples in which pepsin was added. The patterns in all the GE points in absence of pepsin were the same showing no effect of protein degradation due to acidification.

5.3.6 *In Vivo* Intragastric Imaging

In vivo intragastric imaging using capsule endoscopy was performed in one subject and some of the resulting images are shown in Figure 5.10. Following consumption of raw whole milk, the formation of solid chunks of different sizes was clearly observed after 160 min as seen in Figure 5.10 B, even though there was evidence of this aggregation earlier on in the gastric digestion.
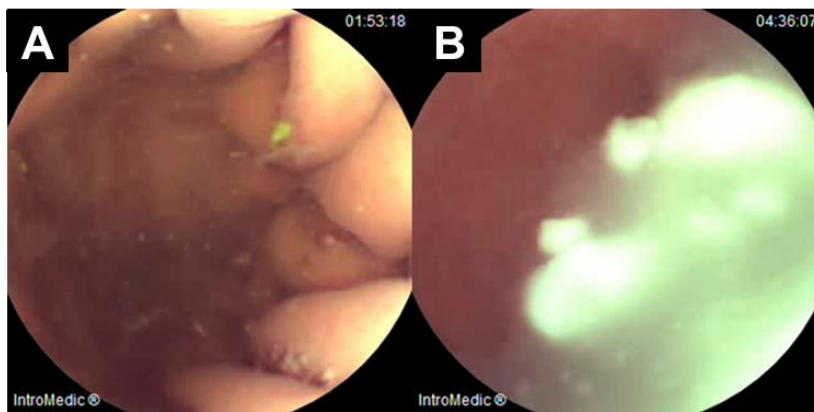
Figure 5.10 . *In vivo* images taken by MiroCam® of (A) emptied human stomach and (B) after 160 min gastric digestion of raw whole milk.

5.4 Discussion

5.4.1 Influence of Process-Induced Changes of milk on Gastric Behaviour

By using a physiologically relevant gastric model described in Chapter 3, we have been able to show that homogenised samples showed significantly more creaming compared to non-homogenised samples where sedimentation was observed, regardless of the heat treatment (Figure 5.5). Homogenisation caused the disruption of the native MFGM, reduced the droplet size and promoted adsorption of milk proteins, in particular caseins, onto the droplet surface (Lopez, 2005; Sharma *et al.*, 1993). This change of the droplet interfacial composition might be one of the main reasons for the distinct gastric behaviour. The milk proteins on the droplet surface, especially the denatured and aggregated proteins in the heated UHT+Homo sample, were more susceptible to be hydrolysed by pepsin leading to the destabilisation of the droplets by flocculation and some coalescence, and ultimately leading to the phase separation observed. The non-homogenised samples, in contrast, still possessed the native MFGM, which could provide more stability during gastric digestion. These structural changes were certainly due to the proteolytic action of pepsin since there was less phase separation and no creaming in the homogenised samples when pepsin was absent (Appendix E 2, 5 & 6). Further investigation was undertaken in order to gain insight into the mechanism of the different gastric behaviour observed. The lipid/protein ratio in both coagulum and serum in the first GE point was determined (Figure 5.11) and the separate amount of protein and lipid is shown in Appendix H. The non-homogenised samples had significantly higher lipid/protein ratio in the serum compared to the homogenised samples. Moreover, the microstructure

imaging showed that most of the droplets in the non-homogenised samples tended to be in the serum (Figure 5.6 D-F) compared to those of the homogenised samples (Figure 5.6 M-O). This might be due to easier incorporation of the smaller droplets into the coagulum and also the possible interactions of the milk proteins adsorbed onto the droplet surface following homogenisation, with the protein network that was formed within the gastric compartment. Therefore, a higher inclusion of droplets into the protein matrix could lead to a lower density of the coagulum resulting in the creaming whereas the higher lipid content in the serum seen in the non-homogenised samples could lead to a dense coagulum that sedimented. Hence, the different colloidal behaviour of the samples was driven by both droplet destabilisation and aggregate density. These possible underlying mechanisms of this gastric behaviour are illustrated in Figure 5.12.
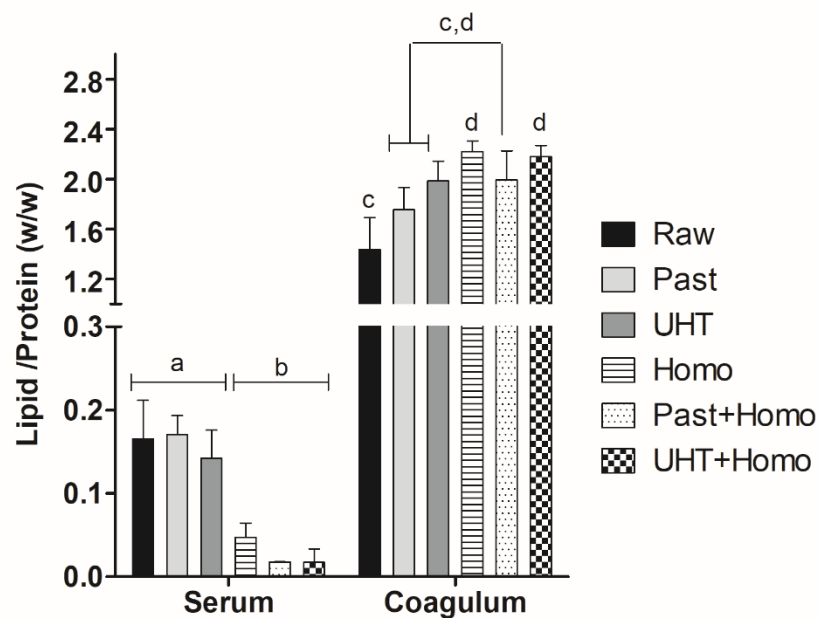
Figure 5.11 Lipid/protein ratio (w/w) of both serum and coagulum in the digesta at approximately 36 min of digestion (time referred to GE1 point). Mean values within a column with different superscript letters (a, b, c, d) were significantly different ($p < 0.05$).
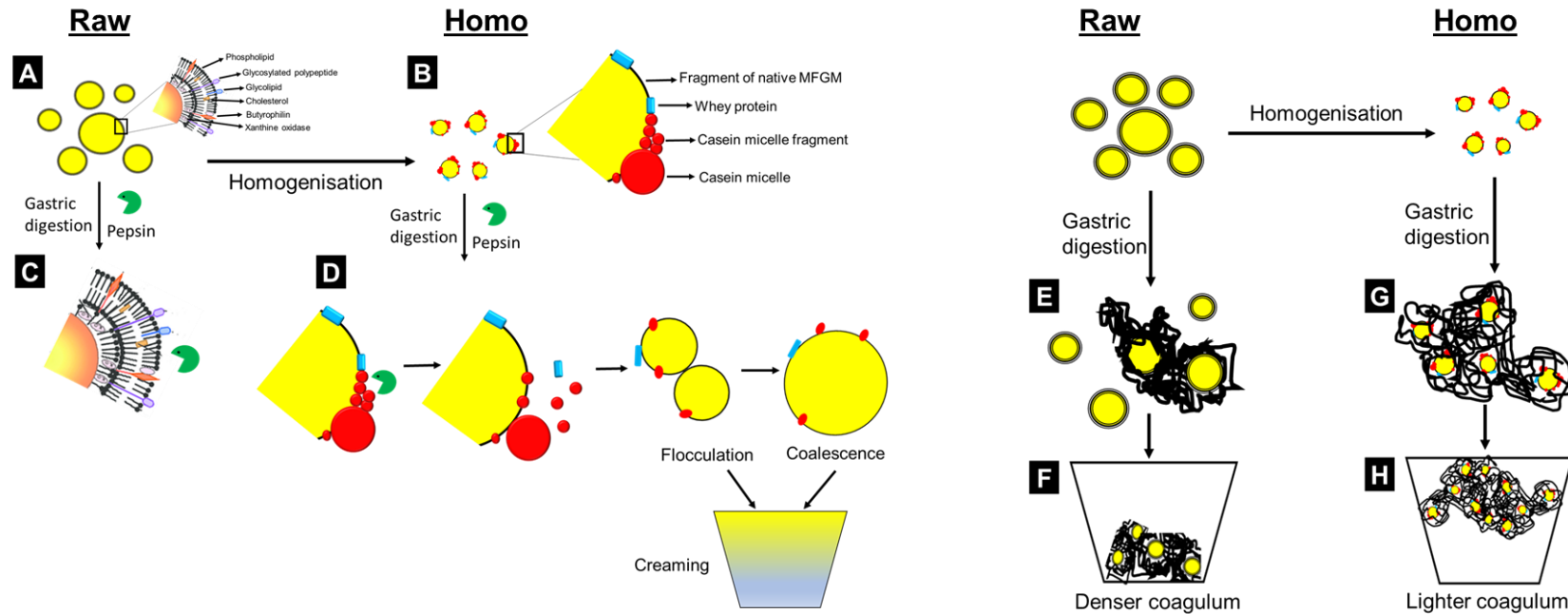
Figure 5.12 Schematic representation of the possible mechanisms for the creaming observed in homogenised milks. These two mechanisms may occur simultaneously. (A) Fat globules in raw milk are surrounded by the complex milk fat globule membrane (MFGM). (B) Homogenisation forms smaller droplets with new interface consisting mainly of absorbed milk proteins (adapted from Michalski *et al.* (2006)) (C) the fat droplet membrane could provide some protection against protein hydrolysis. In contrast, (D) the absorbed milk proteins at the droplet interface could be more susceptible to be hydrolysed by pepsin. This could lead to destabilisation of the fat droplets (flocculation and coalescence), resulting in creaming. The second possible mechanism involves the entrapment of the fat droplets. During gastric digestion, casein micelles coagulate forming a coagulum of different consistency. (E) the larger droplets of the non-homogenised milks might be less prone to be entrapped in the protein network, providing denser coagulum that sediments (F). In contrast, (G) the incorporation of the smaller, homogenised droplets into the protein matrix might be easier, which could also imply a higher extent of interaction. This could lead to the formation of a lighter coagulum that could cream within the stomach model (H).

Heat treatment was shown to be the main driver for the differences in coagulum consistency. The possible mechanism is illustrated in Figure 5.13. Both pasteurisation (72°C for 15 s) and UHT (140°C for 3 s) treatments were used and compared to the non-heated raw milk. It is well established that heating above 70°C induces the denaturation of whey proteins, in particular β-Lg. The extent of whey protein denaturation in UHT milk is much higher than that in pasteurised milk (Douglas *et al.*, 1981). The denatured whey proteins have been reported to interact with κ-casein, forming complexes both at casein micelle surface and in serum phase, the prevalence of which depends on the pH of the heated milk (Anema *et al.*, 2011). Therefore, the level of protein association is higher in UHT-treated compared to that of pasteurised milk. This could have impaired casein coagulation and led to the more fragmented structures obtained in heated milk samples, in particular UHT (Figure 5.4). This different consistency persisted throughout digestion and the rheological analysis (Table 5.3) confirmed that the heat treatment was the main cause of the change in consistency of the coagulum.
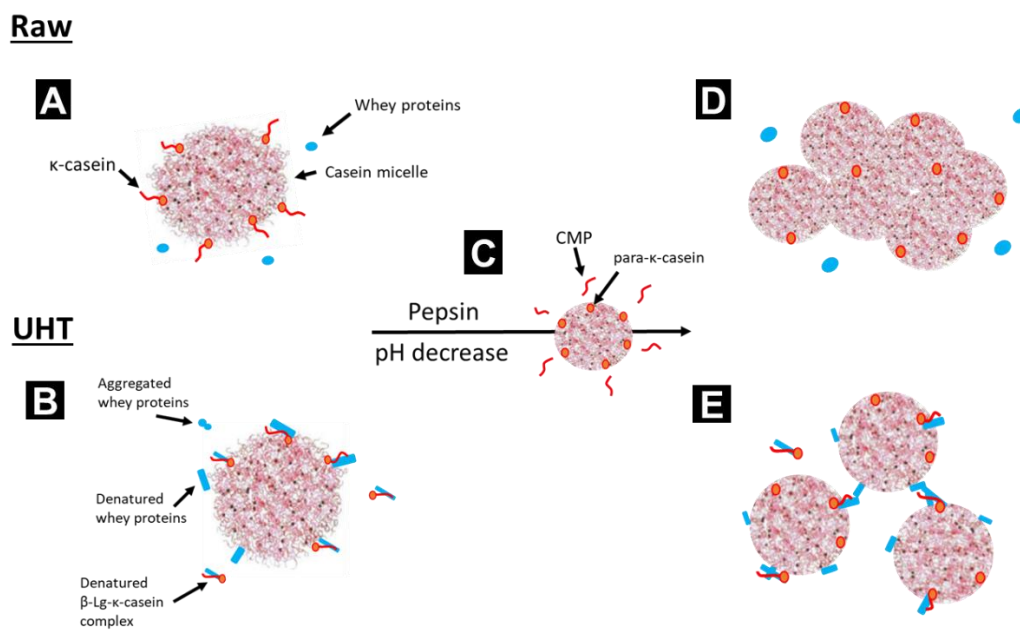
Figure 5.13 Schematic representation of the possible mechanism for the different consistency of the coagulum observed in heat-treated milks. (A) In raw milk, caseins are ensembled in micelles, with κ-casein on the surface providing steric stability, and whey proteins are in the native state. (B) When heat treatment above 70°C are applied, whey proteins are denatured, which can interact with κ-casein both at the surface of the micelle and forming complexes in the serum. (C) During gastric digestion, pepsin cleaves the Phe[105]-Met[106] bond, which separates para-κ-casein from caseinomacropeptide (CMP). This destabilises the casein micelles leading to aggregation. (D) In the case of raw milk, this coagulation is compact. In contrast, (E) the coagulation of casein micelles in the UHT-treated samples is impaired due to the steric effect of the modified micelle surface and the complexes in the serum. The different ionic calcium availability could also have an effect.

The initial protein aggregation to form the coagulum and the gastric behaviour was induced by pepsin action. The protein aggregation was visually observed within the first 10 min, at which time the pH was above 5.5. In contrast, when pepsin was not included, the protein aggregation was observed after 75 min at which the pH was around 5. It has been reported that the pH for coagulation of unheated and heated milk is about 5 and 5.3 respectively (Donato *et al.*, 2007). In accordance to Ye *et al.* (2016a) there was an abrupt decrease of pH when pepsin was absent in raw milk digestion linked to the late formation of the solid coagulum. In contrast, the pH profile of the UHT-treated samples was similar in the absence of pepsin due to the similar gastric behaviour (Appendix D). Pepsin has been reported to favour the hydrolysis of κ-caseins among the other caseins at pH 6.0 (Tam *et al.*, 1972). The coagulation is caused by the destabilisation of casein micelles since pepsin cleaves the Phe-105-Met-106 bond in κ-casein liberating caseinomacropeptide, which is the same mechanism than that for chymosin (Drøhse *et al.*, 1989) that is used for cheese making. Hence, it seems possible to draw parallels to the effects of heat-induced

changes on the functional properties, which has been widely reported for rennet coagulation. Kethireddipalli *et al.* (2010) showed that the poor rennet clotting of heat-treated milk resulting in weak curds was due to the interactive effect of the following: (i) modification of the surface of casein micelles with bound denatured whey proteins; (ii) formation of soluble complexes between denatured whey proteins and κ-casein; (iii) reduction of calcium concentration in the serum. In the present study, milk was heated at its natural pH (6.67). It was shown that about 30% of whey proteins can bind to the micelle surface when milk, at the mentioned pH, was heated at 90°C (Kethireddipalli *et al.*, 2010). This impairs the micelle aggregation by steric effects, which in combination with the protein complexation and alteration of the ionic equilibrium in the serum may explain the different consistency of the coagulum obtained in the present study. For cheese, it was also reported that smaller fat droplets can reduce curd contraction, resulting in higher cheese moisture (Giroux *et al.*, 2014; Thomann *et al.*, 2008), which is in line with the more compact coagulum obtained in the non-homogenised milks.

It is important to note that in this study the heat treatment was followed by homogenisation. Lee *et al.* (2002) reported that the content of milk protein on the droplet surface was not significantly different whether homogenisation was performed before and after heat treatment. However, the impact of the order of these processes is still subject of past and current research projects.

The comparison of the obtained gastric behaviour with other studies is difficult because the *in vivo* studies using similar samples did not show the structural changes in the stomach even though they suggested similar behaviours in terms of the consistency of coagulum (Lacroix *et al.*, 2008). Moreover, most *in vitro* studies use a static model, which does not allow full assessment of the structural changes. Nevertheless, the results in terms of coagulation behaviour, timing and consistency, were in agreement with the findings reported by Ye *et al.* (2017) using a dynamic model, the Human Gastric Simulator. Moreover, the *in vivo* images showed the formation of these solid coagula (Figure 5.10 B) in accordance to our findings.

5.4.2 Effect of Gastric Behaviour on Nutrient Delivery and Protein Digestion

The gastric behaviour caused by the milk processing affected the nutrients emptied and protein digestion kinetics. The sampling method simulating the GE, by sampling from the bottom of the vessel, was influenced by the consistency of the coagulum. Mostly serum liquid was emptied in the first GE points for the samples

having a firmer coagulum, in particular Raw (Figure 5.4 A) accounting for the lowest content of nutrients delivered in the GE1 (Figure 5.7). In contrast, the very soft coagulum obtained from UHT+Homo (Figure 5.4 F) allowed more of the coagulum to be emptied. Hence, the delivery of both lipid and protein in GE1 was the highest for UHT+Homo (Figure 5.7). It was found that the release of lipid (Figure 5.7 A) was influenced by the phase separation obtained in the homogenised samples. The lipid content in GE5 point was generally higher in the homogenised samples, as the cream layer remained at the top of the *in vitro* stomach until the last GE point. One exception for that was UHT+Homo due to the high nutrient content at early stage. Similar results could be seen in the protein profile (Figure 5.7 B) even though the differences were more subtle. This might be due to the more constant delivery of protein throughout digestion, which might be attributed to the emptying of serum containing mainly whey proteins.

The proteolysis levels might be linked to the consistency of the coagulum, which was mainly affected by heat treatment. The softness of the coagulum (Table 5.3) and the greater number of smaller particles (Figure 5.4) from the heat-treated samples, in particular in the UHT+Homo could provide a greater particle surface area for pepsin activity and allow pepsin diffusion within the structure leading to the higher proteolysis obtained at the end of digestion (Figure 5.8). In contrast the lowest level of proteolysis was found in raw milk, in which the hardness of the coagulum and larger particles hampered the pepsin accessibility. The UHT treatment resulted in an enhancement of both caseins and whey protein digestion (Figure 5.9). For the UHT samples, almost no detectable intact caseins or whey proteins were found after 73 min, corresponding to the GE2 point. This finding is in agreement with the protein composition of the heated homogenised milk shown in Ye *et al.* (2017). UHT treatment has been reported to greatly denature β-Lg, which exposes the peptide bonds to pepsin. The temperature of the pasteurisation process was not sufficient to induce any important changes in the protein digestion; the SDS-PAGE profile did not differ from that obtained of the non-heated samples similarly to the observations of Wada *et al.* (2014) during *in vitro* gastric digestion. β-lg remained largely intact during gastric digestion, which was already reported in humans with the ingestion of purified caseins and β-Lg (Mahé *et al.*, 1996). The degradation of α-La was observed after about 109 min (GE3) at which the pH was under 4, which is in agreement with its pepsin hydrolysis susceptibility by the change of protein conformation at that pH.

5.4.3 Physiological Relevance

This study has shown that the processing of milk can result in different coagulation and colloidal behaviour during gastric digestion influencing the nutrient digestion kinetics *in vitro*, and the restructuring of milk in the human stomach was clearly illustrated. This may influence nutrient bioavailability and rates of absorption in the intestine, and the subsequent metabolic responses.

The gastric behaviour of dairy systems observed in the stomach have been shown to influence satiety responses, which are linked partly to the release of gut hormones such as cholecystokinin (CCK). The clinical study performed by Mackie *et al.* (2013) showed that the sedimentation of a semi-solid matrix (cheese and yogurt) caused a lower GE rate and prolonged fullness response, in contrast to the isocaloric comparison in a liquid matrix, which creamed and resulted in increased hunger. In the present study, we observed creaming and sedimentation processes in the homogenised and non-homogenised samples respectively. Therefore, one might expect that non-homogenised samples may induce more fullness compared to the homogenised samples. However, according to the nutrient delivery results obtained in this study, UHT+Homo showed early release of both protein and lipid, which may promote the release of CCK and thus increase satiety. This information could be used to design products which behave in the gastric phase in a way to control rate and profiles of nutrient release and to optimise the satiety response.

The heat treatment of milk has been reported to affect protein postprandial kinetics *in vivo*. Lacroix *et al.* (2008) showed that the UHT treatment enhanced the rate of digestion of milk protein causing a higher transfer of dietary nitrogen into serum amino acids and protein, but pasteurisation treatment did not alter the outcome. In the present study, in agreement with the *in vivo* data, the UHT treated samples had a higher protein release in the early stages of digestion, in particular UHT+Homo. Also, these samples showed higher digestion of both caseins and whey proteins, which may lead to a different postprandial release of peptides (Boutrou *et al.*, 2013). This different digestion may favour certain population groups, for instance the elderly and athletes may benefit from a higher postprandial nitrogen absorption rate.

The metabolic responses relate to the nutrients delivered as a result of GE, which is linked with the different structural changes occurring in the stomach. In the present study, we used a linear GE rate of 2 kcal/min, which is considered to be the average caloric content that is emptied in a regulated manner by the antrum (Hunt *et al.*, 1985). However, this is a simplistic approach since the GE rate may differ over time in response to the dynamic nutrient release profile caused by the

physicochemical behaviour developed during gastric conditions, as was shown by Mackie *et al.* (2013). Therefore, depending on the structural changes observed during gastric digestion in the differently processed milk presented in this study, we expect that the GE rate in humans would strongly depend on the sample processing conditions.

5.5 Conclusion

In this study, it was shown that different forms of dairy processing induced changes in the physicochemical properties of milk which affect their behaviour during gastric digestion *in vitro*. This behaviour may impact nutrient metabolism *in vivo*. This study showed for the first time, clear evidence of different milk behaviours, sedimentation versus creaming *in vitro*, and the restructuring and coagulation of milk in the human stomach. Homogenisation was the main driver for the gastric phase separation (creaming), which was caused by the different droplet surface, droplet-coagulum interactions and the overall effect on coagulum density. The different consistencies of the coagula were as a consequence mainly of the heat treatment. The non-heated samples, especially Raw, formed a firm coagulum whereas the heated samples had a fragmented coagulum particularly observed in UHT+Homo. This stems from the formation of complexes between whey proteins and caseins, which weakens the protein network. These structural changes occurring during the gastric phase resulted in different nutrient emptying profiles, with significant differences between Raw and UHT+Homo, and quicker digestion of milk proteins in the UHT-treated samples due to the drastic heat treatment. This study provides valuable information for understanding the mechanisms controlling the GE of milk in relation to its processing. This knowledge can be applied to manipulate the nutrient release rate from dairy matrices addressed to specific population groups such as increasing protein uptake in the elderly and athletes and prolonging satiety for those at risk of obesity.

Chapter 6

Pepsin Diffusion and Proteolysis in Commercial Milks during Gastric Digestion

6.1 Introduction

In Chapter 5, it was showed that raw milk formed a very tight coagulum compared to the loose coagula obtained in the most processed milk (UHT treatment and homogenisation). This resulted in faster protein digestion kinetics in the latter sample and it was hypothesised that the main limiting factor was the diffusion of pepsin in the coagula. Therefore, the present study aims to determine how the diffusion of pepsin is affected by the gastric restructuring of commercial milks. The activity of pepsin in different parts of the digesta at early and late stages of gastric digestion was measured together with the hydrolysis and composition of protein in order to follow the presence and action of pepsin. To investigate the microstructural implications, scanning electron microscopy (SEM) was performed. Also, fluorescence recovery after photobleaching (FRAP) technique was tested as a potential tool to quantify the diffusion coefficient of pepsin during gastric digestion. This study provides fundamental knowledge of gastric digestion in relation to pepsin diffusion, showing for the first time the effect of pepsin during gastric digestion in commercial milks.

The structure of food has been reported to control nutrient digestion kinetics, which is influenced by the interactions with the gastrointestinal (GI) tract. The disintegration of food in the stomach has been seen to play a key role, as the site at which enzymatic, chemical and physical processing occurs. The physiological processes of the stomach are well understood although their influence in food structures are not fully clear. The diffusion of enzymes is greatly influenced by the structural characteristics and properties of the matrix, affecting the bioaccessibility of nutrients (Singh *et al.*, 2015).

The digestion of proteins begins in the stomach where pepsin breaks down proteins into peptides. Pepsinogen is the precursor of pepsin, which is released by chief cells in the stomach walls and is activated by acid hydrolysis to form pepsin. The acidic pH is provided by the hydrochloric acid of the gastric juice. Pepsin is an aspartic protease with two Asp-Thr-Gly sequences separated by 170-190 amino acids (AAs) conferring its unique catalytic site (Dunn, 2001), in which the catalysis based on the general acid-base mechanism occurs. The molecular weight from porcine pepsin is 34,620 Da and exhibits the maximum activity at pH 2 but it is inactive at pH 8 (Piper *et al.*, 1965). The preferential cleavage side of pepsin is in the aromatic AAs groups of Phe, Tyr or Trp (Inouye *et al.*, 1967).

Protein hydrolysis is affected by processing of milk protein gels differing in the coagulation mode, concentration and heat treatment conditions, which confer different structures. Macierzanka *et al.* (2012) studied the effect of gel structure, induced by

different thermal conditions and pH values, of whey proteins during *in vitro* static digestion. The authors showed that fine stranded gels providing large surface area led to fast proteolysis compared to those with particulate structure. Also, pepsin was suggested to be able to act only at the surface of the aggregates based on observations from SDS-PAGE and electron microscopy imaging. Soft and hard gels of whey protein emulsion gels were used by Guo *et al.* (2015) to investigate the effect of protein disintegration kinetics using the Human Gastric Simulator (HGS). They showed that soft gel disintegrated faster than that in the harder gel, which was accelerated by the presence of pepsin. The faster disruption of the soft particles led to greater emptying of these particles. The dairy gel structuring might consequently impact the bioavailability of peptides and AAs. Barbé *et al.* (2014a), using mini pigs, compared the rates of protein digestion between rennet and acid gels from milk proteins. The rennet gel presented lower levels of both caseins and whey proteins in the duodenum and much lower levels of AAs in the plasma, compared to those of acid gel. This was partly attributed to lower accessibility of pepsin in the rennet gel structure, which could be induced by the syneresis of this gel under the acidic conditions of the stomach.

Therefore, the limited accessibility of pepsin to the substrates of food matrices in relation to the nutrient hydrolysis has been repeatedly suggested to explain the patterns of protein digestion however its study has been overlooked.

Some microscopy techniques can be used to investigate the diffusion of molecules in protein networks, e.g. scanning electron microscopy, atomic force microscopy, transmission electron microscopy or confocal laser scanning microscopy (Einhorn-Stoll *et al.*, 2015). There are only a few studies looking at the diffusion of pepsin in dairy systems and they have used confocal microscopy to performed techniques such as fluorescence correlation spectroscopy (FCS) and FRAP. In both techniques any molecule can be measured if it is fluorescent or fluorescently labelled. In FCS, the movement of the particles of interest is associated with fluctuations in fluorescence and it uses statistical autocorrelation analysis of the time-dependent fluctuations in order to measure different characteristic kinetic rates (Krichevsky *et al.*, 2002). This technique was used by Luo *et al.* (2017) to investigate pepsin diffusivity in whey protein gels with different concentrations (15% wt and 20% wt) after heat treatment (90°C, 30 min). The diffusion of pepsin labelled with the dye Alexa 633 in the gel matrices was slower than that in water, possibly due to the temporary binding to the protein network. However, there was no difference in diffusion between the two gel matrices. They also reported that pepsin hydrolysis was constrained to a 2 mm

layer at the surface of the gel, suggesting that pepsin has a limited depth of penetration even after 6 hours of *in vitro* static digestion.

In the FRAP technique, fluorescent molecules in a defined region are bleached by laser pulses; unbleached molecules from the outside area start to diffuse into the bleached area while bleached molecules diffuse out the fluorescence recovery in the bleached area is measured as a function of time and correlated to the rate of diffusion (Lorén *et al.*, 2009). Thevenot *et al.* (2017) studied pepsin diffusion in rennet casein gels with different casein concentration (0-130 g casein/kg) using the FRAP technique. The authors found the diffusion coefficient of pepsin of 51.4 μm^2/s in the 32.5 g/kg gel compared to the 21.2 μm^2/s in the 130 g/kg gel. The microstructural parameters including physico-chemical properties of the gel network such as volume fraction and particle size of the gels were suggested as the main factors in pepsin diffusion.

The breakdown of dairy protein gels was also investigated in a recent study using time-lapse synchrotron deep-UV fluorescence microscopy (Floury *et al.*, 2018), in which acid and rennet-induced milk gels, having identical composition but different coagulation mode, were studied. The authors showed that rennet gel underwent significant changes in the microstructure under acidic conditions due to a rapid syneresis, whereas acid-formed gel had no significant changes. They also found spatial variations that reflected the pH gradients within the particle. When both gels were exposed to both acid and pepsin, the particles of the rennet-formed gel were digested slower compared to those of acid-formed gel, which was associated with the compact aggregates obtained. The consistent shape of the particles and the fitting of data to exponential model showed that surface erosion was the predominant mechanism of breakdown, which was also suggested in the study by Luo *et al.* (2017).

However, these advanced techniques require special facilities and equipment, sample preparation and well-trained staff, what makes their application difficult. Physico-chemical analysis can be performed to give an indication of the diffusion of pepsin and its action. Measurement of the pepsin activity and the proteolysis in different parts of the matrix gives an option to track the presence of pepsin. This approach combined with electron microscopy imaging was used to relate the diffusion behaviour of pepsin in the digesta formed during gastric digestion.

6.2 Materials and Methods

6.2.1 Materials

Pasteurised standardised homogenised whole milk (Past+H) and long-life UHT standardised homogenised whole milk (UHT+H) were bought from a local supermarket (Tesco, Norwich, UK). The nutritional composition of both milks is indicated in Table 6.1, as indicated in the corresponding labels.

Table 6.1 Nutrient composition of Past+H and UHT+H.

	Content (%)	
Component	**Past+H**	**UHT+H**
Protein	3.2	3.4
Fat	3.6	3.6
Lactose	4.6	4.6
Salt	0.1	0.2
Total solids	11.6	11.8

Oregon Green™ 488-X dye (Succinimidyl ester, 6-isomer) was purchased from Fisher Scientific, Eugene, OR, USA. PD-10 desalting Column, Sephadex™ G-25M, was from GE Healthcare Life Sciences, Little Chalfont, UK. Pepsin from porcine gastric mucosa (Sigma Chemical Co., USA) had an enzymatic activity of 4,530 units/mg protein, calculated by measuring the TCA-soluble products using haemoglobin as substrate as described by Minekus *et al.* (2014).

6.2.2 Methods

6.2.2.1 Semi-Dynamic Gastric Digestion

The simulation of the oral and gastric phase was done using the semi-dynamic adult digestion model previously described in the section 5.2.2.2.

Gastric emptying (GE) was simulated in the same manner than described in Chapter 5 by taking 5 aliquots (GE points). The average time of those were 32 min (GE1), 64 min (GE2), 97 min (GE3), 129 min (GE4) and 161 min (GE5).

The focus of study was the characterisation of the coagulum at GE1 and GE5 points. For that, gastric digestion was stopped at GE1/ GE5 time and the digesta was collected, and different parts were separated and analysed. The procedure followed

for the collection of each part is illustrated in Figure 6.1. The digesta obtained at GE1 time, i.e. 32 min of Past+H sample was clearly separated into a tight coagulum and serum, which contained small aggregates. A piece of the surface and inner parts from the coagulum was taken using a blade and a volume of the serum was collected. Then, the serum was filtered using a Buchner funnel with a Whatman paper filter no. 1 (Whatman®, Maidstone, UK) under vacuum, and a volume of the filtrated (called Liquid) was collected. After 161 min (GE5 time), only a small piece of coagulum was remaining, which had a soft consistency. The Figure 6.1 B shows the whiter serum obtained, suggesting that part of the coagulum was dissolved into the serum. This digesta was filtered in the same manner than previously described and a piece of the surface and inner of the remaining coagulum was taken, as well as a volume of the filtrated. The gastric behaviour of the UHT+H sample in gastric conditions was totally different, which influenced the possibilities of the sampling. At 32 min of gastric digestion the coagulum was very particulate and loose, which impaired the sampling of the same parts than in Past+H sample. A volume of digesta was collected and separated into solid and liquid fraction by filtration, collecting a portion of both fractions. After 161 min of gastric digestion, the loose aggregates became even softer, which was difficult to collect after filtration. Therefore a sample of the digesta was only collected for analysis.

0.2 g of each mentioned parts was taken to measure the pepsin activity. Also, about 0.3 g of the described parts of the sample was taken and mixed with 2.5 mL of water. The sample was then mixed using a homogeniser (T25 Ultra-Turrax®, Ika-Labortechnik, Germany) at approximately 9,500 rpm for 1 min to obtain a homogenous sample for the remaining analysis. Then, the pH was increased above pH 7 using NaOH (2 mol/L) in order to stop pepsin activity. Finally, samples were snap-frozen in liquid nitrogen and stored at -20°C until subsequent treatment of SDS-PAGE and OPA analyses.
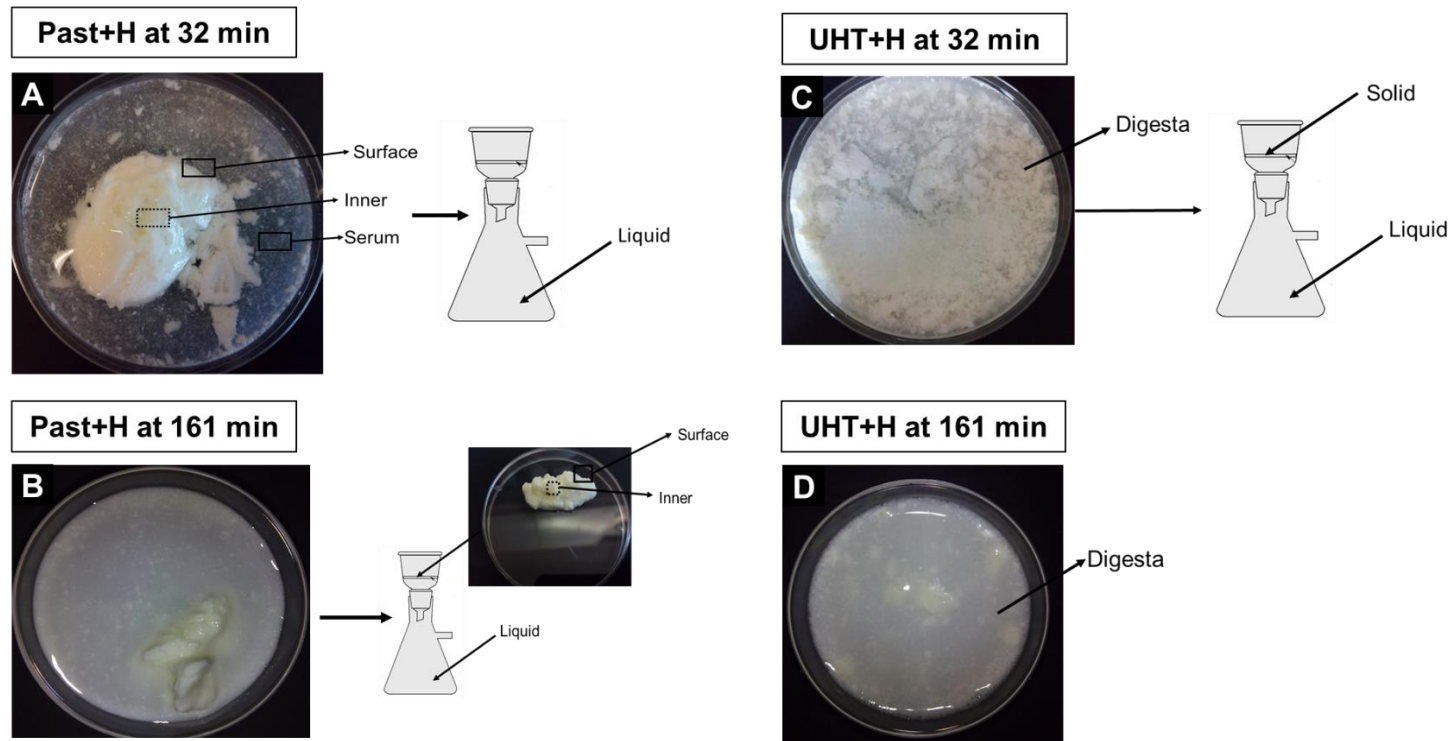
Figure 6.1 Schematic representation of the parts of the samples collected for subsequent analysis. Appearance of Past+H sample during gastric digestion at (A) 32 min and (B) 161 min. Appearance of UHT+H sample during gastric digestion at (A) 32 min and (B) 161 min.

6.2.2.2 Pepsin Activity Analysis

Pepsin activity was measured in the different parts of the coagulum following the protocol of Meisel *et al.* (1984) with some modifications. The collected sample (0.2 g) was mixed with 1 mL HCl (0.01 mol/L) and the pH was adjusted to pH 2. Then, high mixing by Ultra-Turrax® (9,500 rpm for 1 min) was used to break the structure of, in particular, the solid particles of the Past+H at GE1 time. Then, 5 mL of haemoglobin from bovine blood (25 g/L in 0.01 mol/L HCl) was added and the samples were incubated at 37°C for 10 min. After incubation, the samples were treated with 10 mL of 10% TCA and centrifuge at 5,000 rpm for 15 min at room temperature. The filtrated was measure at 280 nm using a spectrophotometer (Libra S50, Biochrom US, Holliston, MA). The blank sample received the same treatment as the sample, except the addition of the sample was performed after the mixing of TCA and haemoglobin. The equation for the calculation of the activity was as follows:

Equation 6.1 Equation used for the calculation of pepsin activity, calculated in units.

$$\text{Activity (U)} = \frac{(A_{280} - A_{\text{Blank}}) \text{ x dilution}}{\text{incubation time (min)x } 0.001}$$

6.2.2.3 OPA Assay for Quantification of Protein Hydrolysis

The concentration of free amino groups was determined using OPA assay, which has been described in the section 2.2.4.3. The absorbance was measured at 340 nm using a multi-mode microplate spectrophotometer (Benchmark Plus™, Bio-Rad, CA, USA).

6.2.2.4 SDS-PAGE for Identification of Proteins during Digestion

The protein composition in the samples was analysed by SDS-PAGE, described in the section 2.2.4.2. The samples were further diluted 1:1 with water previous to the treatment for the electrophoresis protocol.

6.2.2.5 Scanning Electron Microscopy

A separate gastric digestion was performed to obtain the coagulum of Past+H and UHT+H, both GE1 and GE5 times, for imaging by scanning electron mycroscopy (SEM). The coagulum obtained at 32 and 161 min of gastric digestion was cut into cubes, measuring approximately 2x2x2 mm using a razor blade and fixed overnight in 2.5% glutaraldehyde in 0.1 mol/L piperazine-N,N′-bis(2-ethanesulfonic acid) (PIPES) buffer (pH 7.4). After washing with 0.1 mol/L PIPES buffer, the pieces were

post-fixed in 1% osmium tetroxide for 2 hours. The osmium tetroxide was then removed and the pieces were washed three times in distilled water. Four pieces of each sample were each put into a microporous specimen capsule (EMS, Hatfield, USA) for critical point drying purposes. The sample pieces were dehydrated in a series of ethanol solutions (30, 50, 70, 80, 90, 3x 100%). Samples were dried in a Leica EM CPD300 critical point dryer using liquid carbon dioxide as the transition fluid. Then, the sample pieces were mounted onto SEM stubs using agar silver paint and left at room temperature to dry overnight. The pieces were then gently knocked with the tip of fine-tipped tweezers to expose a fresh surface. The samples were coated with gold in an agar high resolution sputter-coater apparatus. Electron microscopy was carried out using a Zeiss Supra 55 VP FEG SEM, operating at 3 kV. This analysis was performed by Kathryn Cross at Quadram Institute Bioscience.

6.2.2.6 Pepsin Labelling

Pepsin was labelled with Oregon Green™ 488-X dye according the manufacturer instructions with some modifications. Five mg of pepsin was dissolved in 0.5 mL sodium bicarbonate buffer (0.1 mol/L, pH 8.3). The fluorescence dye Oregon Green 488 was dissolved in dimethyl sulfoxide at 10 mg/mL. A total amount of 5 µL Oregon Green 488 was slowly added to the pepsin solution while mixing with a magnetic stirrer. The mixture was incubated for 1 hour at room temperature with continuous mixing protected from light. After incubation, the conjugate was purified using PD-10 desalting column, Sephadex™ G-25M, which was previously equilibrated with phosphate buffer saline (pH 7.4) and repeated twice in a different column. The calculated degree of labelling was 1.56 and the activity of the labelled pepsin was 13.1 U/mg, which was negligible compared to the activity of unlabelled pepsin.

6.2.2.7 FRAP Experiments

The diffusion of pepsin was tested with FRAP technique using a laser scanning confocal microscope, Zeiss LSM 780 confocal (Carl Zeiss, Inc.). Samples were observed using a 40/1.2 water immersion objective lens. The pepsin conjugated with Green Oregon was excited at wavelength of 488 nm and fluorescence was filtered using a 500-600 nm spectral filter. The scan area was 283.4 µm x 70.8 µm. The procedure used for FRAP measurement started with the acquisition of 20 scans, following by the bleach in 10x10 square and using 100% power laser of 405 and 488 nm.

A small piece of the part of digesta at GE1 (Inner, Surface and Serum from Past+H, and digesta from UHT+H) was placed in a concave slide and 1 µL of the pepsin-Oregon Green conjugate was added for the analysis under the microscope. It is important to mention that in previous experiments the gradual addition of pepsin-Oregon conjugate during digestion was tested but the low fluorescence intensity observed under the microscope required its direct addition to the digesta piece of interest.

6.3 Results

6.3.1 Pepsin Activity

Figure 6.2 shows the pepsin activity obtained in different parts of the digesta in an early and late stages of gastric digestion using the semi-dynamic model. It is worth noting that the same parts of the digesta could not be analysed for both samples since the consistency of the coagulum was different between the two stages of gastric digestion studied, i.e. at 32 and 161 min. The parts of the tight coagulum obtained in Past+H at 32 min (Figure 6.1 A) had a significant different pepsin activity; Inner part presented no activity (-8.03 ± 2.00) whereas Surface part had 985.5 ± 417.9 U. The maximum activity found among the analysed parts was in Serum, accounting for 2,927 ± 227 U. After 161 min of gastric digestion, the digestion of the coagulum was noticeable by not only the small size but the softness of the coagulum that remained (Figure 6.1 B). The Inner part presented some activity accounting for 2,832 ± 459 and there was an increase of activity in the Surface part. In UHT+H sample, in contrast, pepsin was incorporated in the Solid of the digesta at the early time of digestion, i.e. 32 min, accounting for 3,920 ± 494 U. The activity in the Digesta considerably increased during digestion, accounting for 10,174 ± 1,087 U at 181 min compared to 2,516 ± 606 obtained at 32 min of gastric digestion.
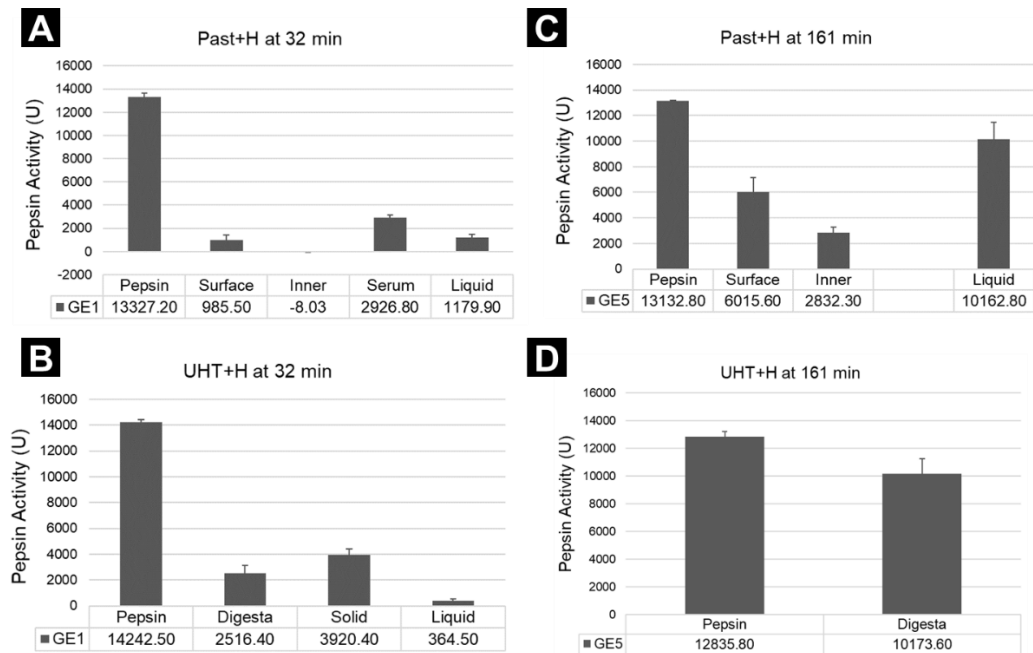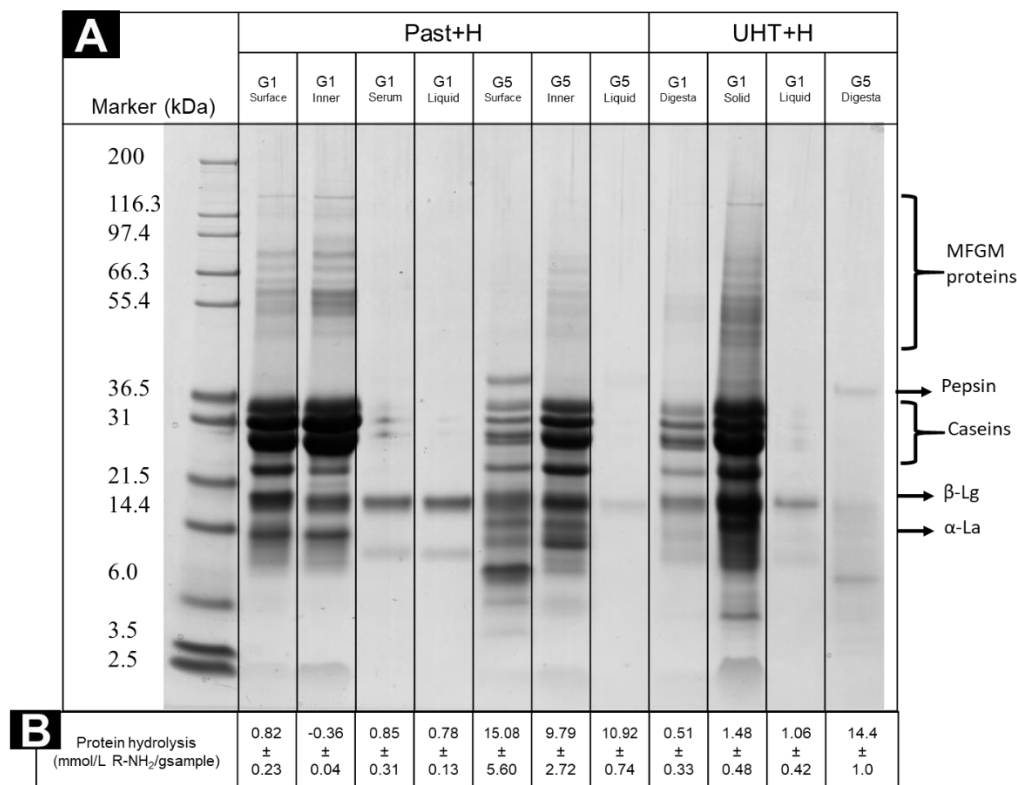
Figure 6.2 Pepsin activity (U) in the different parts of the digesta (as indicated in Figure 6.1) for Past+H milk at (A) 32 min and (B) 161 min of gastric digestion and for UHT+H at (C) 32 min and (D) 161 min. Pepsin solution was used as a control. The activity was calculated according to the Equation 6.1. Values are presented as means ± SD (n=3).

6.3.2 Protein Hydrolysis

The hydrolysis pattern of the milk proteins in the studied parts of the digesta is illustrated in Figure 6.3 A. The pattern of Past+H in both inner and surface parts at 32 min of gastric digestion was very similar, with both caseins and whey proteins present mainly in their native form. This was substantially different at the end of digestion, in particular in the case of the Surface part, in which the degradation of milk proteins into peptides could be observed, which was similar in the Inner part but in lower extent. The Liquid part at 32 min consisted mainly of whey proteins, showing the complete coagulation of the caseins that formed the coagulum whereas the band of whey proteins could not be observed at the end of the digestion. The degradation of milk proteins was observed in UHT+H at 32 min of gastric digestion and almost no bands were observed at the end of digestion at that protein concentration, showing the high extent of hydrolysis in milk proteins.

The quantitative analysis of the protein hydrolysis was performed by OPA assay, which is shown in Figure 6.3 B. There was no evidence of hydrolysis in the Inner part of the Past+H coagulum at 32 min of gastric digestion (-0.36 ± 0.04 mM amino group/g sample) whereas the Surface part accounted for 0.82 ± 0.23 mM amino group/g sample. After 161 min of gastric digestion there was an increase of free amino groups at the Surface accounting for 15.08 ± 5.60 mM/g sample and the presence of

hydrolysis in the Inner part (9.79 ± 2.72 mM amino group/g sample). The protein hydrolysis levels increased in the Liquid part from 0.78 to 10.92 mmol/g sample during digestion. In contrast, some hydrolysis was already obtained in early stage of gastric digestion for UHT+H in the Digesta accounting for 0.51 ± 0.33 mM/g sample, which substantially increased to 14.4 ± 1.0 mM/g sample at the end of the digestion.

	Past+H							UHT+H			
Marker (kDa)	G1 Surface	G1 Inner	G1 Serum	G1 Liquid	G5 Surface	G5 Inner	G5 Liquid	G1 Digesta	G1 Solid	G1 Liquid	G5 Digesta
B Protein hydrolysis (mmol/L R-NH₂/gsample)	0.82 ± 0.23	-0.36 ± 0.04	0.85 ± 0.31	0.78 ± 0.13	15.08 ± 5.60	9.79 ± 2.72	10.92 ± 0.74	0.51 ± 0.33	1.48 ± 0.48	1.06 ± 0.42	14.4 ± 1.0

Figure 6.3 (A) SDS-PAGE (under reducing conditions) of the studied parts of the digesta of Past+H and UHT+H samples, and a molecular weight marker. The samples are labelled in the figure accordingly. (B) Free amino group concentration (mM/g sample) of the different parts of the digesta of Past+H and UHT+H samples. Values are presented as means ± SD (n=3).

6.3.3 Microstructure of Gastric Digesta

Figure 6.4 shows examples of SEM micrographs of the coagula obtained in both Past+H and UHT+H at 32 and 161 min of gastric digestion. The degradation caused by digestion time can be clearly observed in the micrographs referring to 161 min. This is particularly noticeable in Past+H Figure 6.4 E-H, in which the structure was more open having more porous surface, compared to the smoother surface of the micrographs after 31 min of gastric digestion. At this early time, it seemed that the units that formed the structure of both samples were the same but they were more interconnected in the case of Past+H compared to UHT+H. However, these differences seemed to be very subtle to draw any definitive conclusion.
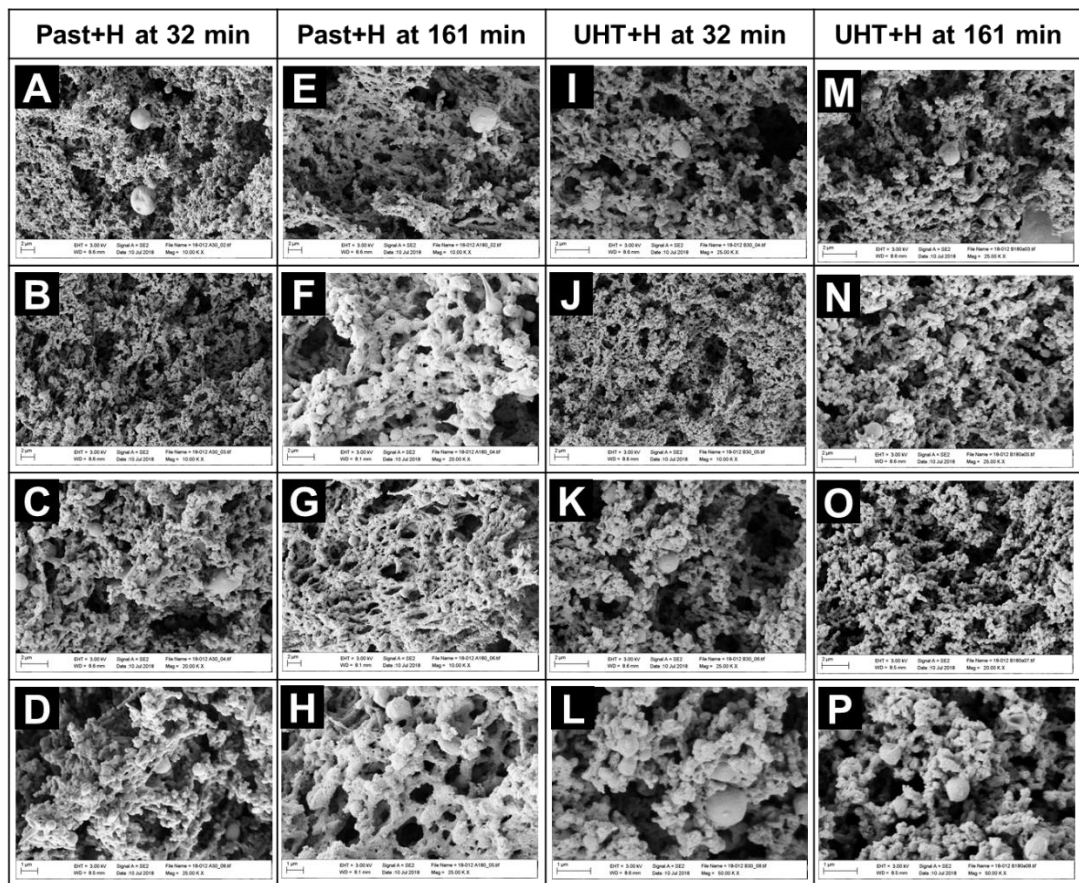
Figure 6.4 Examples of SEM micrographs of the coagula of Past+H sample at (A-D) 32 min of gastric digestion and (E-H)161 min, and UHT+H at (I-L) 32 min and (M-P) 161 min. Scale bars are indicated below each micrograph.

6.3.4 FRAP Experiment

Figure 6.5 A shows the recovery profile of fluorescence intensity of the Past+H sample at 32 min of three different parts of the digesta, i.e. Serum and, Inner and Surface of the coagulum. The Inner part of the coagulum did not show any recovery which contrasts to the recovery observed in the Serum and Surface part of the coagulum. However, the precise differentiation between these two samples is difficult to assess from that graph. An intermediate behaviour between those latter sample was observed in the profile of recovery in the Digesta at 32 min of UHT+H (Figure 6.5 B).
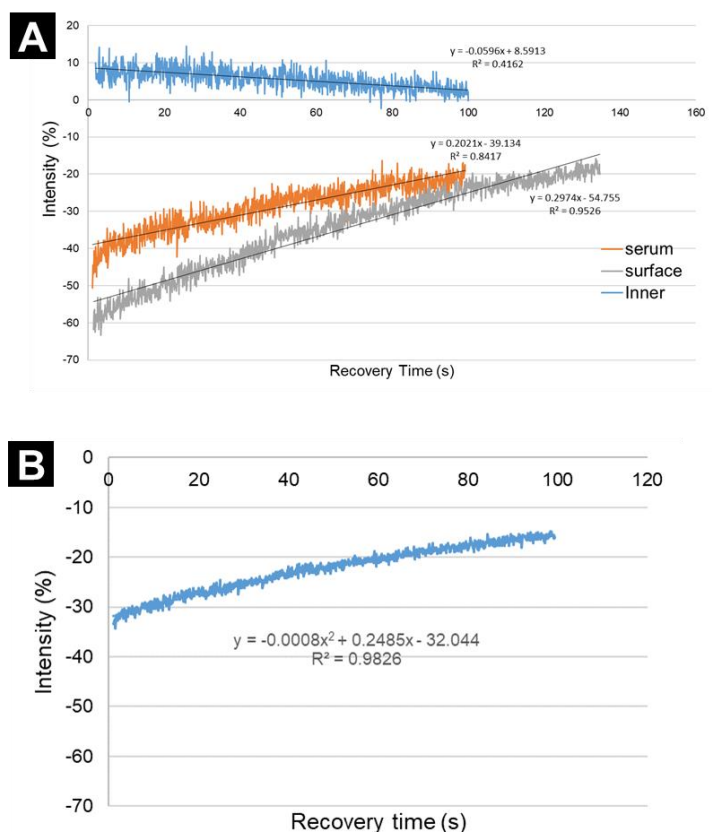
Figure 6.5 Fluorescence intensity of the recovery period after bleaching in FRAP experiment for (A) Past+H and (B) UHT+H after 32 min of gastric digestion at different part of the digesta.

6.4 Discussion

The study of pepsin diffusion within the food matrix is relevant to understand the mechanisms of protein digestion. In this study, the aim was the investigation of the implications of the main milk heat treatments of pasteurisation and UHT, on the disintegration of the coagulum formed in gastric conditions.

6.4.1 Pepsin Action is Influenced by the Coagulum Structure

By following the activity of pepsin in the different parts of the digesta we could understand its proteolysis behaviour. The results of pepsin activity (Figure 6.2) and the analysis of protein hydrolysis (Figure 6.3) are very much linked. In Past+H sample, pepsin seemed unable to diffuse into the inner part of the coagulum at the early stages of gastric digestion, and was mostly present in the serum. There was no activity in the Inner part of the dense coagulum obtained after 32 min of gastric behaviour (Figure 6.1 A), which was supported by the lack of protein hydrolysis, and the intact milk proteins observed by SDS-PAGE (Figure 6.3). The rapid formation of a dense coagulum (Figure 6.1 A) could lead the exclusion of pepsin from the serum. It is

important to highlight that the pepsin concentration at early stages of digestion is low due to the nature of the semi-dynamic model, therefore there will be less pepsin incorporated into the structure considering that the sample tended to form more firm coagula. Indeed, the surface part of the coagulum presented some pepsin activity (Figure 6.2) and there was some free amino group concentration, suggesting the action of pepsin at the surface. Ye *et al.* (2016a) studied the effect of unheated and heated (90°C, 20 min) of commercial skimmed milk during gastric digestion using the HGS. Similarly, they suggested that the diffusion of pepsin to the inner part of the coagulum was reduced as suggested by the limited hydrolysis of caseins observed from the inner part by SDS-PAGE, whereas protein degradation was observed at the surface part of the coagulum in line with the present study. At the end of the gastric digestion, i.e. at 161 min, there was some pepsin activity (Figure 6.2) and increased hydrolysis level (Figure 6.3 B) indicating that pepsin seemed to be able to penetrate to the inner part of the coagulum. This could be attributed to the degradation of the structure during the gastric phase as observed in the SEM micrographs (Figure 6.4), which could facilitate the diffusion of pepsin. The gradual acidification might degrade the protein network by opening the structure, with the aid of the continuous emptying. This behaviour was not observed by Ye *et al.* (2016b) since the intensity of the casein bands in the electrophoresis gel of unheated milk, more similar to Past+H structurally, did not appear to change with the digestion time, showing then no activity in the Inner part of the coagulum.

In contrast, the coagulum obtained in the simulated stomach for UHT+H was fragmented with a crumbly structure (Figure 6.1 D), which influenced the action of pepsin. It seems that pepsin was already integrated in the Solid part of the digesta since early gastric time, which was supported by a higher pepsin activity (Figure 6.2) and hydrolysis (Figure 6.3) at 32 min of gastric digestion. The higher surface area of the crumbly coagula could facilitate the dispersion of pepsin in the digesta thereby increasing its action. The activity of pepsin increased during digestion as observed by the higher degree of hydrolysis and no distinct bands of caseins and whey proteins could be observed after 161 min of gastric digestion in gel electrophoresis (Figure 6.3 A), suggesting the complete hydrolysis of milk proteins. Similarly, Ye *et al.* (2016a) did not obtain any bands of intact caseins after digestion for 160 min in heated milk sample (90°C, 20 min). Meisel *et al.* (1984), similarly to our findings, showed that pepsin activity was approximately 1,000 U/g protein in raw milk in contrast to the approximate value of 33,000 U/g protein measured in UHT+homogenised milk, when chyme was analysed at 360 min in mini-pigs.

With regards to whey proteins, the band of β-Lg in the Solid part of the coagula at 32 min appeared to be more intense in the case of UHT+H than Past+H. This could suggest greater involvement in the formation of the coagula due to the interactions between whey proteins and caseins, which was higher in the case of UHT compared to pasteurisation treatment. Miranda *et al.* (1987) reported that whey proteins did not form part of the coagulum in non-heated milk and then preferentially evacuated from the stomach. It has been reported that the heat treatment of milk proteins above 70°C causes the denaturation of β-Lg in particular, and these denatured proteins can interact with κ-casein at interface, which could subsequently form part of the coagulum. Also, the band of β-Lg was very faint after 161 min of gastric digestion, indicating the susceptibility of whey proteins to be hydrolysed by pepsin after drastic heat treatment. It is known that native β-Lg is resistant to pepsin action, but heating increases its susceptibility to hydrolysis by pepsin (Macierzanka *et al.*, 2012). Moreover, as evident in the gel electrophoresis (Figure 6.3), β-Lg was mostly present in the Serum/Liquid part of the digesta in Past+H sample suggesting that was readily available to be emptied, when compared to the solid part formed mainly by caseins. The predominance of whey protein in the emptied fraction was also observed in human studies (Barbé *et al.*, 2014b).

Overall, the results suggest that the structure in the gastric digestion, i.e. crumbly versus dense, had a significant impact on the protein hydrolysis, in particular on the rate of casein hydrolysis. The digestion of whey proteins was influence by both the structure and prior heat treatment that increased the exposure of the cleave bonds in the protein structures. The changes of the molecular structure of the proteins affected the gastric behaviour, which in turn have been shown to impact the activity of pepsin and its subsequent action of hydrolysis. This effect not only impacts bioaccessibility of proteolytic products but absorption of amino acids. Lacroix *et al.* (2008) showed that UHT treatment induced a higher postprandial nitrogen utilization in humans, when compared with pasteurisation.

6.4.2 Pepsin Diffusion by FRAP

The different diffusion coefficient of molecules can be assessed by confocal microscopy using advanced techniques such as FRAP. The diffusion of pepsin has been rarely study; the studies of Luo *et al.* (2017) using FCS and Thevenot *et al.* (2017) using FRAP are the only reports available so far. In the present study, we attempted to study the diffusivity of pepsin by the addition of pepsin-Oregon Green conjugate during gastric digestion together with the gradual addition of unlabelled pepsin. However, the low intensity obtained in these experiments led to the use of

conjugate directly onto the sample of interest. The increase of the conjugate concentration added and the adjustment of the microscope parameters did not improve the noise as seen in the Figure 6.5. Nevertheless, it is apparently clear that there was no recovery in the Inner part of the coagulum in Past+H, which is in accordance with the results based on pepsin activity and protein hydrolysis; there was very little, if any, diffusion of pepsin in the inside of the coagulum, further slowing down the digestion of the proteins within the coagulum. However, in general, the data obtained using FRAP did not provide any clear outcomes and further work should be undertaken in relation to sample preparation to obtain a conclusive diffusion coefficient that can provide more insight about protein degradation in the stomach.

6.5 Conclusion

The effect of pepsin on the structure formed in the gastric environment was investigated. Pepsin has been seen as key factor influencing the formation of the coagulum and the behaviour in the course of digestion. The restructuring of milk was initially driven by pepsin as shown in Chapter 5. Past+H milk formed a firm coagulum similar to the one obtained in raw milk, compared to the crumbly coagula obtained in UHT+H sample. These different structures caused different patterns of protein hydrolysis, which was attributed to the different activity of pepsin in the different parts of the digesta, affecting the bioaccessibility of proteins in the small intestine. There are different aspects working together at the same time that might influence these outcomes. Firstly, the amount of pepsin being incorporated inside the coagulum was lower in the Past+H sample as the coagula were forming more quickly, that could inhibit diffusion into the coagulum. Secondly, the viscosity of the Past+H coagulum suggests a stronger and tighter structure, which could further slow down diffusion. Thirdly, the nature of the semi-dynamic gastric model of the experiment, in which pepsin and acid were added gradually resulting in low amount of pepsin and relatively high pH in the initial stage of digestion, should be taken into account. This all contributes the knowledge to the mechanisms underpinning the slower digestion of the less processed samples.

Therefore, this study provides more insight into the behaviour of pepsin in complex structures during gastric digestion, which is of high interest since it affects the subsequent bioaccessibility and absorption of nutrients in the small intestine.

Chapter 7

Effect of Dairy Macrostructure on *in Vitro* Gastric Restructuring and Nutrient Digestion Kinetics, and *in Vivo* Correlation[‡]

7.1 Introduction

The worldwide prevalence of diet-related diseases such as obesity is one of the main health concerns. The cost of the National Health Service in the UK related to obesity was in 2007 estimated at £2.3 billion, with a projection to rise to £7.1 billion by 2050 (Butland *et al.*, 2007). Several strategies have been developed to address this problem, mainly by reducing the caloric content of the diet focussing on lipid and/or sugar (Fiszman *et al.*, 2013). However, this strategy does not seem to be working, given the ongoing increase of obesity and this is, at least in part, due to the decrease in palatability of foods. Therefore, approaches looking beyond caloric content have to be investigated. Enhancing satiation and satiety could provide a method to control energy intake helping weight management, which does not imply the increase of food intake but the enhancement of the potential benefit from specific foods (Wilde, 2009). Food companies have developed products with claims related to satiety with the aim to induce feelings of fullness for a longer time (Hetherington *et al.*, 2013).

The satiety cascade is a complex phenomenon involving different pathways (Benelam, 2009). The main factors affecting food intake are mechanical stimulation, such as gastric distension, and release of peptides secreted in response to ingested food (Cummings *et al.*, 2007). Some of the most studied satiety-related peptides released from the intestine are glucagon-like peptide 1 (GLP-1), peptide YY (PYY) and cholecystokinin (CCK) (Frost *et al.*, 2006). The release of CCK occurs in the upper small intestine as response to nutrients, in particular lipid and protein (Frost *et al.*, 2006). Moreover, the release of CCK has important consequences for gastrointestinal (GI) flow including the delay of gastric emptying (GE) (Wren *et al.*, 2007). Rapid emptying leads to a reduction of negative feedback satiety signals and then promotes overconsumption of calories (Delzenne *et al.*, 2010). Therefore, GE can be modulated by controlling the rate of nutrient digestion and then leading to specific postprandial physiological responses. However, the delivery of nutrients in the small intestine is affected by their behaviour in the stomach. In this context, the design of the structure in which nutrients are presented in food to exert specific biophysical behaviour in the stomach comprised the core of this piece of work.

The physical state of food influences satiety perception through different physico-chemical changes in the GI tract, affecting the nutrient flow in *in vivo*. For example Marciani *et al.* (2012) studied two meals with different consistency, solid/liquid and homogenised soup. The authors showed that the homogenised meal delayed GE and enhanced satiation compared to the same meal consumed in solid

state. This was attributed to the steady release of nutrients into the duodenum of the soup meal, which maintained a homogenous appearance throughout gastric digestion. In contrast, using similar food structures but dairy-based systems, Mackie *et al.* (2013) found that a semi-solid meal increased the feeling of fullness by a slower rate of GE compared to the same isocaloric meal in a liquid form. However, in this case, different gastric behaviours of sedimentation and creaming were observed, using magnetic resonance imaging (MRI), for semi-solid and liquid sample, respectively. The authors suggested a link between the satiety responses observed and differences in composition of the chyme being emptied from the stomach.

Gastric conditions such as pH and ionic strength can affect the physico-chemical properties of proteins. Caseins lose their micellar structure in the stomach at around pH 4.6, their iso-electric point, and precipitate forming aggregates whereas whey proteins remain soluble which has led to differences in digestion. This has been reported to result in more rapid GE of whey proteins and a delayed GE of caseins based on the collected digesta from the jejunum (Mahé *et al.*, 1996). Moreover, a higher satiating effect after consumption of whey protein drink was shown and was associated with higher secretion of CCK, GLP-1 and GIP in plasma and elevated levels of branched amino acids, compared with casein drink (Hall *et al.*, 2003).

Lipid is another important nutrient playing a key role in satiety and there are several *in vivo* studies looking at the impact of emulsion structure on lipid digestion rate (Marciani *et al.*, 2008). They have shown that lipid droplets can be designed to exert specific behaviours in the stomach taking into account different colloidal processes (i.e. flocculation, coalescence and creaming) that they might undergo under the gastric conditions due to changes in the interfacial properties (Dickinson, 1997). Marciani *et al.* (2008) compared two emulsions with different acid stabilities showing that the acid-stable emulsion, homogenous in the stomach, provided a slower and more consistent GE, which caused the increase of CCK secretion (Marciani *et al.*, 2007) and fullness perception compared to the acid-unstable emulsion that broke into two phases upon gastric acidification.

These studies have highlighted the implications of GE and postprandial responses. However, the underlying mechanisms in terms of nutrient digestion rates are not well understood. Most of these studies have been performed *in vivo,* nevertheless, the influence of food structure on digestion can be studied using *in vitro* systems providing ease of access to samples and minimal variation. Dynamic gastric *in vitro* models such as the Human Gastric Simulator (HGS) developed at the Riddet Institute or the Dynamic Gastric Model (DGM) set up in the Institute of Food Research are sophisticated models that can closely mimic human gastric behaviour but they are

not a routine tool due to their complexity. On the other hand, static *in vitro* digestion has been designed to be easy to use on a daily basis (Minekus *et al.*, 2014), although it does not mimic many relevant factors of gastric physiology such as a progressive acidification and emptying, which might significantly affect the bioaccessibility of nutrients. The importance of the pH dynamics in the protein gastric digestion has been highlighted in previous *in vitro* studies where a pH gradient was considered (Shani-Levi *et al.*, 2013; van Aken *et al.*, 2011). The semi-dynamic gastric model described in Chapter 3 is simple to handle and more physiologically relevant than a static model as it simulates the gradual pH decrease, and it has the novelty to include emptying, and the sequential addition of digestives enzymes and gastric fluid.

Previous clinical data showed that specific dairy systems with different macrostructure could cause different satiety responses (Mackie *et al.*, 2013) but the underlying mechanisms were not elucidated. The aim of the present study was to investigate the link between these dairy structures and GI flow by analysing nutrient content of the chyme. In particular it was investigated whether the physical state and spatial distribution of nutrients within the simulated stomach could be a critical factor for the rate of digestion in the small intestine. To this end the same two meals that were isocaloric in terms of fat, protein and carbohydrates but with different structure, liquid versus semi-solid, were used. The structural changes in the gastric compartment using the semi-dynamic gastric model were studied and the digestion was finally assessed by the amount of absorbable (lipid and protein) species available as a function of time. Lastly, we correlated the absorbable nutrients with the responses observed in the previously mentioned human study (Mackie *et al.*, 2013) and compared the nutrient digestion kinetics obtained with those using the fully dynamic model, the HGS.

7.2 Materials and Methods

7.2.1 Materials

Gouda cheese (Waitrose Essential Dutch Gouda), yogurt (Waitrose Essential low-fat yogurt), icing sugar (Tate & Lyle Fairtrade cane sugar) and sunflower oil (Tesco) were purchased from local supermarkets in the UK. Sodium caseinate was kindly given by VTT (Finland) and whey protein isolate (WPI) was purchased from Davisco Foods International, USA. Lyophilized rabbit gastric extract was purchased from Germe S.A., France, (lipase had an activity of 58 U/mg solid, measured using tributyrin as substrate, and pepsin 1,113 U/mg solid, using haemoglobin as substrate).

Pepsin from porcine gastric mucosa (Sigma Chemical Co., USA) had an activity of 3,883 U/mg solid, using haemoglobin as substrate. Pancreatin from porcine pancreas (8x USP specifications) had a trypsin activity of 7.18 U/mg and lipase activity of 26.5 U/mg. Orlistat ≥ 98% and phenylmethylsulfonyl fluoride (PMSF) approx. 0.1 mol/L in ethanol were purchased from Sigma-Aldrich. D-leucine (puriss ≥ 99.0%) was obtained from Fluka analytical, USA. The standards glyceryl triheptadecanoate and heptadecanoic acid were purchased from Sigma-Aldrich, dipentadecanoin and monononadecanoin were from Nu-Check Prep, In. USA. The solvents hexane, chloroform, acetic acid, methanol, ethyl acetate and toluene were purchased from Fisher Scientific, UK.

7.2.2 Methods

A schematic diagram of the experimental planning is illustrated in Figure 7.1.
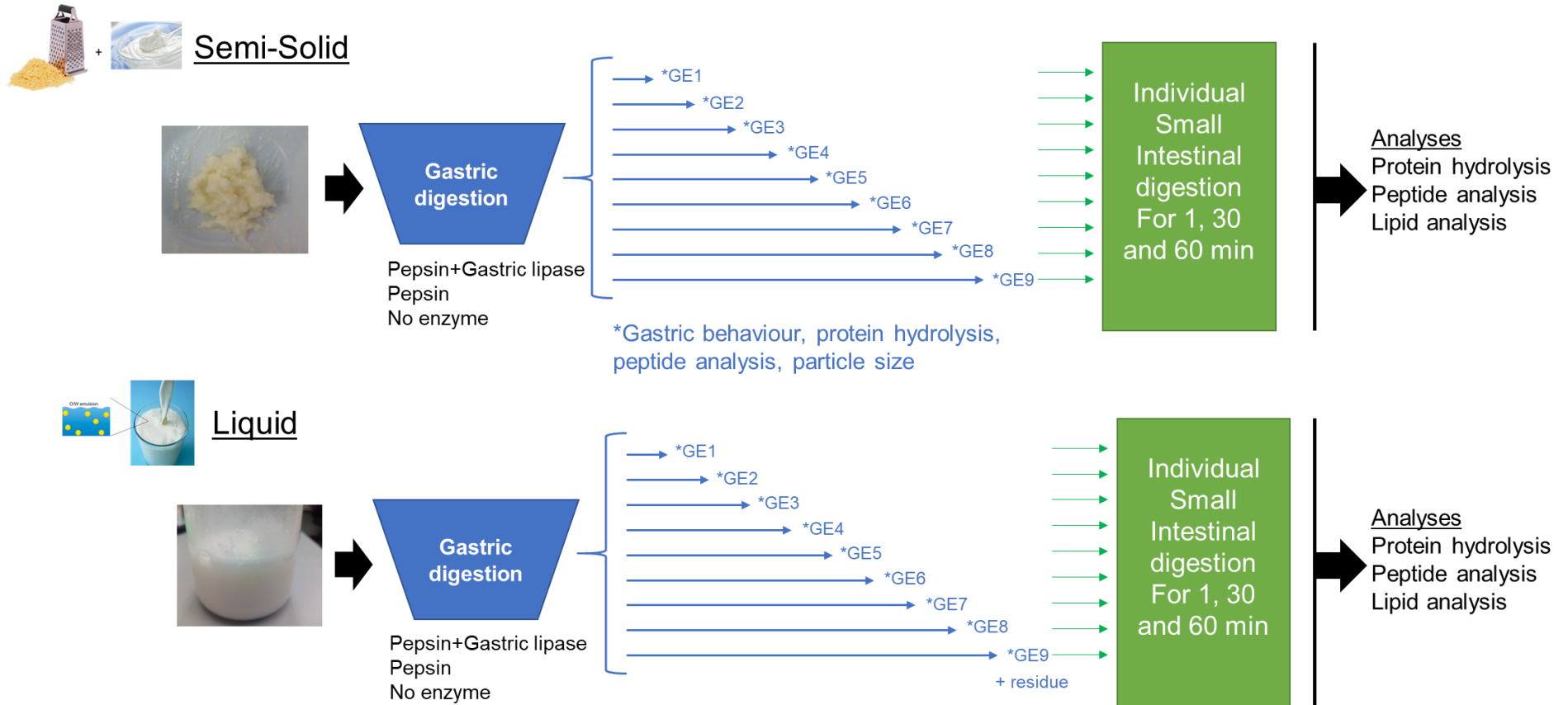
Figure 7.1 Schematic diagram flow of the experimental procedure for Chapter 7.

7.2.2.1 Preparation of Samples

The protocol followed for the preparation of the samples was as described previously by Mackie *et al.* (2013). The Liquid sample was an oil in water emulsion. A sodium caseinate solution containing 1.33 g sodium caseinate was dissolved in 110.5 g boiled tap water, the solution was stirred overnight at room temperature. 6.88 g of sunflower oil was mixed with 60.63 g of that sodium caseinate solution in a blender (BL450 series, Kenwood). The shear cycle comprised 30 s at the low shear setting, 30 s of rest, 30 s at the high shear setting, 30 s of rest and 30 s at high shear setting. Then, the emulsion was mixed with the remaining sodium caseinate solution and 5 g WPI was added a little at a time. Finally, 1.53 g of icing sugar was also added. The Semi-Solid sample was prepared by mixing 23.17 g of finely grated gouda cheese and 19.41 g yogurt. The sample also comprised 82.66 g water which was added at the start of the gastric digestion to mimic the protocol of the *in vivo* study. It is important to note that the samples were isocaloric in terms of protein, lipid and carbohydrate content to ensure that the food structure was the main factor influencing the outcome.

7.2.2.2 Gastrointestinal *in Vitro* Digestion

The following protocol was used for the set of experiments using both gastric lipase and pepsin. Two more sets were performed, in which just pepsin or no enzyme was added, and the volume of enzyme was replaced by MilliQ® water.

7.2.2.2.1 Semi-Dynamic *in Vitro* Gastric Digestion

A 20 g of freshly prepared sample was placed into a glass v-form vessel thermostated at 37°C after the addition of 3.6 mL of simulated gastric electrolyte mixture simulating the gastric fluid residue in the stomach (basal state). The simulated gastric electrolyte mixture contained SGF (1.25x), MilliQ® water, HCl (2 mol/L) and $CaCl_2(H_2O)_2$ (0.3 mol/L). Three solutions were added at a constant rate: (1) 15.4 mL of simulated gastric electrolyte mixture was added using a pH-stat (836 Titrando-Metrohm, Switzerland) dosing device at 0.09 mL/min, (2) 0.5 mL rabbit gastric extract solution (13.8 mg in 0.5 mL MilliQ® water) at 0.003 mL/min and (3) 0.5 mL pepsin solution (37.1 mg in 0.5 mL MilliQ® water) at 0.003 mL/min was also added because the addition of pepsin from rabbit gastric extract did not fulfil the protease activity required in the stomach which was 2,000 U/mL final digestion mixture (Minekus *et al.*, 2014). Enzyme solutions were added using a dual channel syringe pump (Harvard apparatus, PHD Ultra, USA). An orbital shaker (Mini-gyro rocker-SSM3-Stuart, Barloworld Scientific limited, UK) at 35 rpm was used for agitation of the vessel.

The proportions of solutions used were according to the standardized static digestion INFOGEST protocol (Minekus *et al.*, 2014). The oral phase was not simulated because when extrapolating the *in vivo* data (Mackie *et al.*, 2013) of gastric volume to this study we did not observe any significant initial dilution apart from the volume of food and residual gastric fluid.

7.2.2.2.2 Gastric Emptying Simulation

Gastric emptying (GE) was simulated by taking 9 different aliquots, referred to as GE aliquots in the text, according to a pre-set curve based on *in vivo* study data using the same dairy systems (Mackie *et al.*, 2013). Figure 7.2 shows the volume contained in the gastric vessel at each time point and, the volumes and corresponding times of each GE aliquot are indicated in Table 7.1. Samples were taken from the bottom of the vessel using a pipette with a tip that had an internal diameter of 2 mm because it approximates the upper limit of particle size that has been seen to pass through the pyloric opening into the duodenum (Thomas, 2006). It is important to note that another extra volume of the Liquid sample was also collected and analysed (referred as GE10). This was the remaining volume of the gastric digestion which mainly contained the lipid layer formed as shown below in the results section.

Sufficient NaOH (5 mol/L) was added to the aliquots to increase the pH above 7, inhibiting pepsin activity. Then, samples were snap-frozen with liquid nitrogen and stored at -80°C until subsequent treatment.

Gastric Digestion		Small Intestinal Digestion			
Sample		Time (min)			
		0	1	30	60
GE1	→	GE1/0	GE1/1	GE1/30	GE1/60
GE2	→	GE2/0	GE2/1	GE2/30	GE2/60
GE3	→	GE3/0	GE3/1	GE3/30	GE3/60
GE4	→	GE4/0	GE4/1	GE4/30	GE4/60
GE5	→	GE5/0	GE5/1	GE5/30	GE5/60
GE6	→	GE6/0	GE6/1	GE6/30	GE6/60
GE7	→	GE7/0	GE7/1	GE7/30	GE7/60
GE8	→	GE8/0	GE8/1	GE8/30	GE8/60
GE9	→	GE9/0	GE9/1	GE9/30	GE9/60
Residual gastric content (GE10)	→	GE10/0	GE10/1	GE10/30	GE10/60
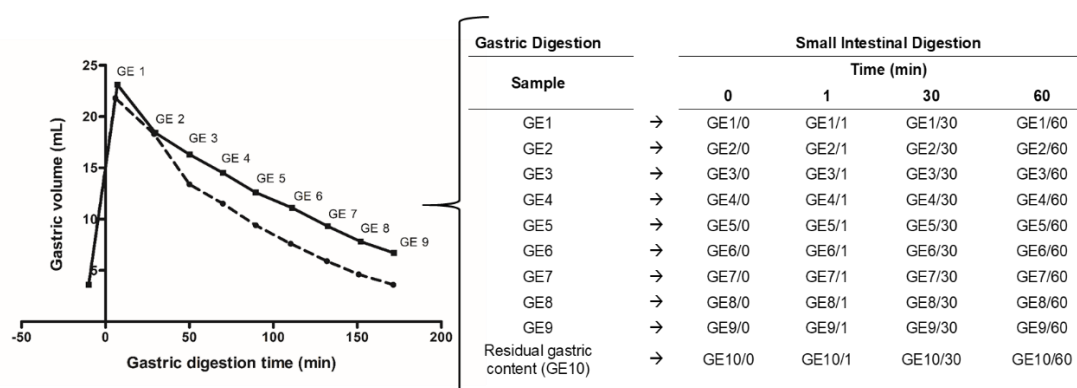
Figure 7.2 Volume (mL) contained in the stomach model as a function of time (min) of the Semi-Solid (solid line) and Liquid (broken line) samples. The data was obtained by downscaling the *in vivo* data of the referred study (Mackie *et al.*, 2013). Each gastric emptying (GE) aliquot is indicated in the graph. The table (right hand side) presents the sample names and their corresponding GE aliquots in each time point.

Table 7.1 Time (min) and target volume (mL) corresponded in each gastric emptying aliquot. These values were based on a pre-set curve obtained in the *in vivo* study data using the same dairy systems (Mackie *et al.*, 2013).

Gastric Emptying Aliquot	Semi-solid Sample		Liquid Sample	
	Time (min)	Emptied Volume (mL)	Time (min)	Emptied Volume (mL)
GE1	7.1	1.1	5.9	2.4
GE2	29.7	6.9	29.0	5.7
GE3	50.1	4.0	50.0	6.8
GE4	70.0	3.7	69.9	3.8
GE5	89.4	3.8	89.5	4.0
GE6	111.1	3.5	110.3	3.9
GE7	132.4	3.8	131.9	3.7
GE8	152.0	3.4	150.8	3.1
GE9	171.8	3.0	171.4	3.0
GE10	residual gastric content			

7.2.2.2.3 Small Intestinal *in Vitro* Digestion

Small intestinal digestion was simulated for each GE aliquot according to a standardised protocol (Minekus *et al.*, 2014). The pancreatin solution was prepared with 3 x concentrated simulated intestinal fluid in order to keep the system as constant as possible to pH 7 during digestion. The amounts of pancreatin solution, bovine bile (190 mmol/L with water), $CaCl_2(H_2O)_2$ (0.3 mol/L) and MilliQ® water were adjusted in each case depending on the gastric aliquot volume to reach the pancreatin trypsin activity required of 100 TAME units per mL, 10 mmol/L of bile and 0.6 mmol/L of $CaCl_2(H_2O)_2$ in the final digestion mixture (Minekus *et al.*, 2014). The digestion was performed for 60 min in a shaking incubator (Excella E24, New Brunswick Scientific, USA) at 37°C, 190 rpm. Samples (0.5 mL) were taken at 0, 1, 30 and 60 min (as shown in table of Figure 7.2) and 10 µl of enzyme inhibitor mix (1:1 0.1 mol/L PMSF: 10 mmol/L Orlistat in Ethanol) was added. The samples were snap-frozen using liquid nitrogen and stored at -80°C until further analysis.

7.2.2.3 Confocal Laser Scanning Microscopy

The microstructure of selected samples was observed using a confocal laser scanning microscope, Leica TCS-SP1 (Leica Microsystems, Baden-Württemberg, Germany). A mixture of 0.1% Fast green FCF solution and 0.1% Nile red solution at 1:1 proportion was used. See the section 2.2.3.3 for details.

7.2.2.4 Particle Size Distribution

The particle size was measured using a laser-light diffraction unit (Beckman Coulter LS13320®, Beckman Coulter Ltd., High Wycombe, UK) as described in the section 2.2.3.1. The optical parameters chosen were a particle and dispersant (water) refractive index of 1.456 and 1.330, respectively. A volume of sample (0.5 mL) was mixed with 5 mL of 2% SDS to dissociate clusters of proteins.

7.2.2.5 OPA Assay for Quantification of Protein Hydrolysis

The concentration of the free amino groups was determined using OPA assay, which has been described in the section 2.2.4.3. The absorbance was measured at 340 nm using a multi-mode microplate reader (Benchmark Plus, BioRad, UK).

7.2.2.6 Size-Exclusion Liquid Chromatography Analysis

In an attempt to obtain more information about the protein digestion products, we analysed the samples from the different GE aliquots after the intestinal digestion using size exclusion chromatography. The analysis was performed on a BioSep SEC S3000 column (300×7.8 mm with a 75×7.6 mm guard column; Phenomenex, Cheshire, UK) connected to a Dionex SUMMIT high pressure liquid chromatography using Chromeleon software (Dionex Ltd., Surrey, UK) and equipped with a photo diode array detector. Samples were previously treated with 5% TCA, centrifuged at 10,000 rpm for 30 min at room temperature and filtrated using a syringe filter (0.45 μm PVDF membrane, GE Healthcare Life Sciences, UK). A volume of 10 μL was eluted at 1 mL/min with buffer (50 mmol/L NaH_2PO_4, 150 mmol/L NaCl, 0.01% NaN_3, pH 7), and monitored at 210 nm for 20 min. The following standards were used: vitamin B12, aprotinin, myoglobin from horse, ovalbulmin from chicken, γ-globulin from cow and thyroglobulin from cow (Biorad). Their molecular weight and retention time (RT) were as follows in Table 7.2.

Table 7.2 Molecular weight and retention time of the standard proteins used in size-exclusion liquid chromatography analysis.

Compound	Molecular Weight (Da)	Retention Time (min)
thyroglobulin	670,000	5.982
γ-globulin	158,000	6.772
ovalbulmin	44,000	7.788
myoglobin	17,000	8.794
aprotinin	6,511	10.105
Vitamin B12	1,350	11.327

However, although the peaks of the standards eluted separately, the general pattern of the samples in this analysis did not provide clear peaks of peptides with different molecular weights. An example of the typical chromatogram obtained is shown in Figure 7.3. Therefore, this analysis could provide information about the quantification of protein hydrolysis, which was compared with data obtained by OPA assay in some examples.
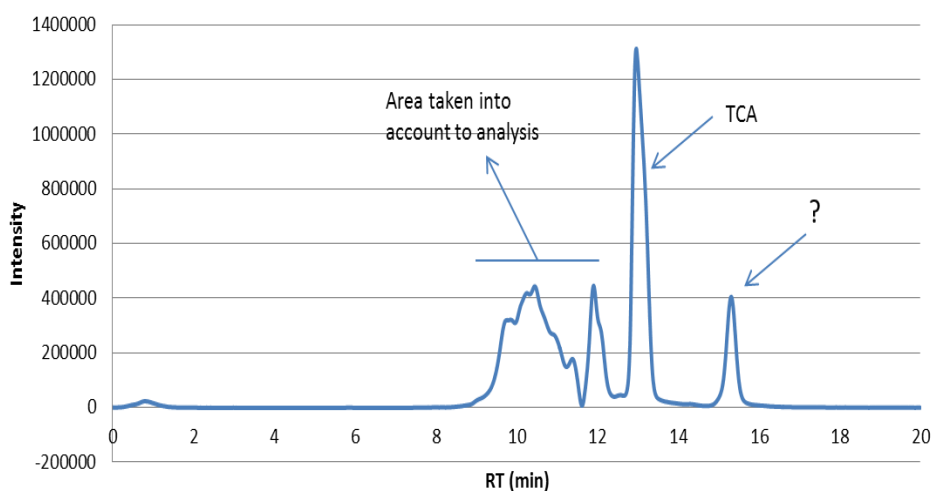
Figure 7.3 Example of a common chromatogram obtained in samples by size-exclusion chromatography analysis.

7.2.2.7 Lipid Analysis

7.2.2.7.1 Total Lipid Extraction

Lipid extraction of samples was carried out using the protocol of Bligh *et al.* (1959). The internal standard (IS) method was used, which consisted of 1.6 mg/mL of each lipid standard, i.e. glyceryl triheptadecanoate, heptadecanoic acid, glyceride

dipentadecanoin and glyceride monononadecanoin, in chloroform. For each 0.5 mL of sample, 0.625 mL IS solution and 1.25 mL methanol were added. Then, 0.625 mL chloroform and 0.625 mL water with 0.9% NaCl were included obtaining two phases. Thereafter, samples were centrifuged at 3,000 g for 10 min. The lower organic part was taken for lipid extraction.

7.2.2.7.2 Extraction of Different Lipid Classes

Fractionation of lipid samples was performed using solid phase extraction allowing the isolation of individual lipid classes: polar lipids namely free fatty acids (FFA) and neutral lipids, namely, triacylglycerol (TAG), diacylglycerol (DAG) and monoacylglycerol (MAG).

Figure 7.4 shows a schematic diagram of the experimental steps for lipid class separation. The separation was performed using a 20-port vacuum manifold (VacMaster, Biotage, UK) coupled to a vacuum pump and disposable primary aminopropyl bonded phase cartridges (Agilent HF Bond Elut LRC-NH2, Agilent Technologies UK Ltd., Wokingham, UK). The cartridge column was equilibrated by rinsing with 4 mL of hexane and allowing it to flow through the cartridge under gravity.

The volume collected in the lipid extraction step was loaded onto the cartridge. Thereafter the column was eluted with chloroform, 4 mL (fraction I, TAG and DAG) followed by 5 mL of acetone (fraction II, MAG) which were eluted under gravity. Methanol (5mL) eluted phospholipids and 5 mL of chloroform/methanol/acetic acid (100:2:2 v/v) eluted FFA (fraction IV). Next, the tubes containing fractions I and II were evaporated to dryness in a vortex evaporator (Haakebuchler, Büchi Labortechnik AG, Switzerland) applying vacuum at 40°C and speed level 4 followed by drying in a vacuum oven (Gallenkamp, England) connected to a high vacuum pump (Edwards E2M2) for 30 min at room temperature.

A second cartridge was equilibrated in the same manner as above. The fraction I was reconstituted in 0.5 mL of hexane and loaded onto the cartridge. A further 3.5 mL of hexane was applied to the column under gravity (fraction V, TAG). Then, a fraction (4 mL) of hexane:ethyl acetate (85:15 v/v) was eluted under gravity (fraction of cholesterol and other sterols). Next, 4 mL of hexane:ethyl acetate (80:20 v/v) was eluted under gravity (fraction VII, DAG). Finally, 4 mL of chloroform:methanol (2:1 v/v) was eluted under gravity collecting the total MAG in the fraction II tube. The solvent of fractions II b, V and VII were evaporated as previously described.
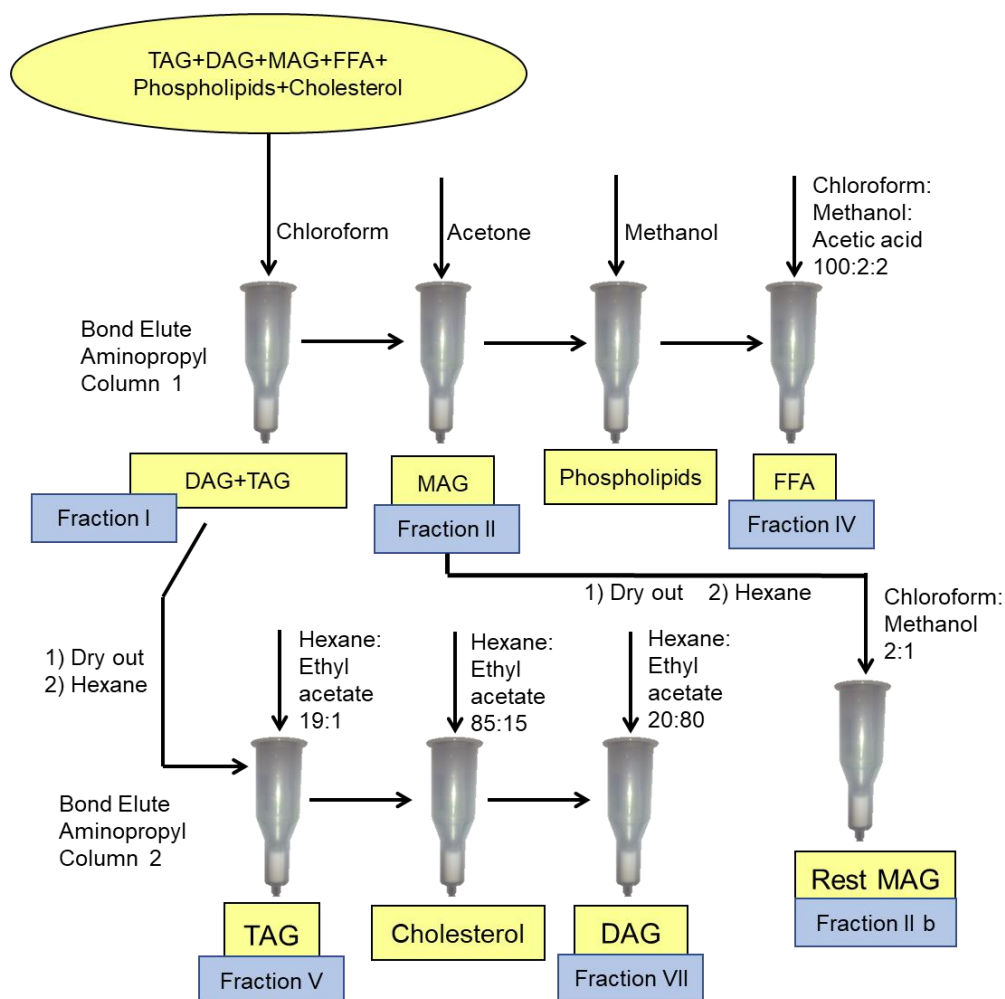
Figure 7.4 Schematic diagram of the separation of lipid classes using solid phase extraction with aminopropyl columns.

7.2.2.7.3 Derivatization of Lipid Extraction Fractions

Lipids were converted to fatty acid methyl ester (FAME) through methylation to allow subsequent analysis by gas chromatography (GC). 0.5 mL of toluene (containing 0.02% butylated hydroxytoluene as an antioxidant) and 1 mL of methylation reagent consisted of methanol containing 2% H_2SO_4 (v/v) was added to the samples, which was mixed and placed in an oven at 50°C overnight. Thereafter, tubes were removed from the oven to allow them to cool and 1 mL of neutralising solution (12.5 g $KHCO_3$ and 34.55 g K_2HCO_3 dissolved in 500 mL HPLC grade water) was added. Hexane (1 mL) was added and following vigorous mixing samples were centrifuged at 100 g for 5 min. The supernatant (organic phase) was transferred to a vial for analysing by GC.

7.2.2.7.4 Analysis of Fatty Acid Methyl Esters

Methylated samples were analysed using 7890B GC System (Agilent Technologies, USA), equipped with a model 7694 autosampler, and dual flame ionisation and 5977A mass spectrometry detector (Agilent Technologies, USA) connected by a 1:1 active splitter after the analytical column. The analytical column was a SGE BPX70 capillary column (30 m x 0.25 mm ID x 0.25 μm film thickness) operated in constant flow mode at 30 cm sec^{-1} using helium as carrier gas. Samples (1 μL) were injected with the injector in split mode (10:1 split ratio). The oven temperature program consisted of a hold programmed at 115°C for 1 min, followed by a ramp at 1.5°C min^{-1} to 240°C and, thereafter, a ramp at 30°C min^{-1} to 250°C with a 10 min hold prior to cooling ready for the next sample.

FAME mix (Supelco 37 Food FAMES) was used to confirm the retention times of FAMEs and calculate the relative response factor for the flame ionisation detector which was used to quantify the separated lipid classes. The ion source was held with the electron multiplier voltage at 70 V and scans from 50 to 550 Da were run.

7.2.2.8 Dynamic Gastric Digestion

The HGS at Massey Institute (New Zealand) was used to compare with the outcomes from the semi-dynamic model. This work was performed by Janiene Gilliland (Food Technician at Massey Institute of Food Science and Technology) in collaboration with Maria Ferrua and Alan Mackie. The Liquid and Semi-Solid samples were prepared similarly to the *in vivo* study (Mackie *et al.*, 2013). The HGS was set up as described in Kong *et al.* (2010) and samples were taken at 20, 40, 60, 80, 100, 120, 140 and 160 min of gastric digestion using pepsin and the emptied chyme was analysed in terms of droplet size, total solids, total nitrogen and lipid, and degree of hydrolysis.

7.2.2.9 Statistics

All the results are presented as mean ± standard deviation (SD) of three independent replicates. Statistical significance between the meals was tested by a two-tailed paired *t*-test using GraphPad Prism software (Prism 5 for Windows, Version 5.04). Differences were stated significant at p-value < 0.05.

7.3 Results

7.3.1 Gastric pH Profile using the Semi-Dynamic Model

The change in pH of both samples during gastric digestion using pepsin and gastric lipase is illustrated in Figure 7.5. The profiles obtained were similar, with an initial low pH about 1.0 simulating the residual acid in the stomach related to fasting conditions. After meal addition, the pH increased rapidly reaching values of 4.55 ± 0.08 and 5.37 ± 0.25 for the Semi-Solid and Liquid samples, respectively. This increase was different between samples due to differences in their buffering capacity even though they had the same protein content; the homogenous initial distribution of the protein in the Liquid sample compared to the Semi-Solid sample caused the higher pH observed. The pH then decreased in both samples reaching a value below 2.0 due to the constant addition of gastric fluid containing acid and the continuous emptying. The pH profile during the digestions using just pepsin and no enzyme was compared in Figure 7.6. There were no significant differences among these three sets of experiments in the case of the Semi-Solid sample whereas the absence of enzyme decreased the pH values between 50 and 130 min in the Liquid sample.
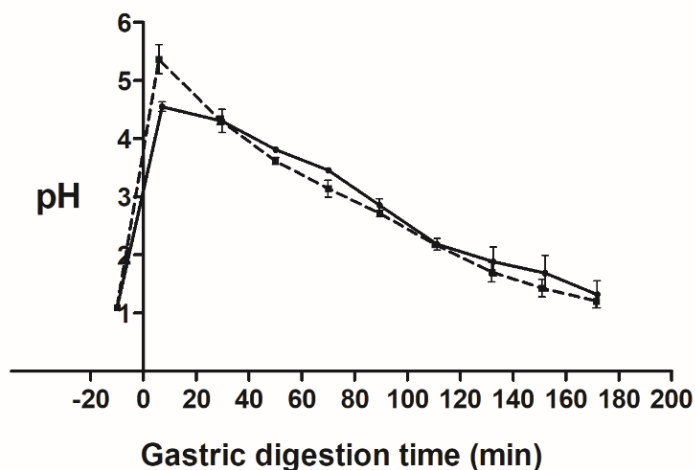
Figure 7.5 pH profile during gastric digestion in the semi-dynamic model, using pepsin and gastric lipase, of the Semi-Solid (solid line) and Liquid (broken line) samples. pH was measured in the digesta inside of the reaction vessel. Values are presented as means ± SD (n=3).
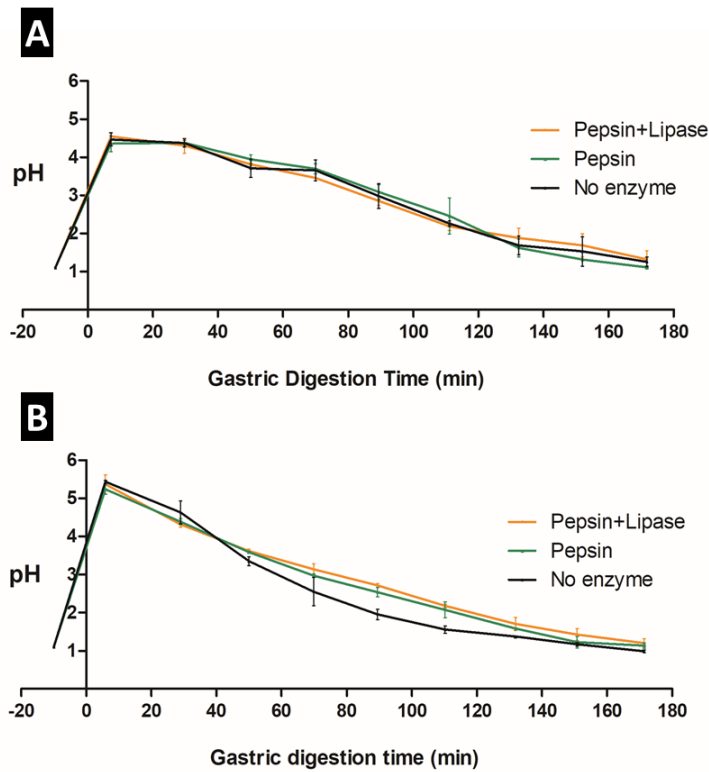
Figure 7.6 pH profile during gastric digestion in the semi-dynamic model of (A) the Semi-Solid and (B) Liquid samples with pepsin and lipase (orange line), pepsin (green line) and no enzyme (black line). pH was measured in the digesta inside of the reaction vessel. Values are presented as means ± SD (n=3).

7.3.2 Behaviour in the Gastric Compartment

Figure 7.7 shows the appearance of the samples both initially and after 110 min of simulated gastric digestion using both pepsin and gastric lipase. The Semi-Solid sample was initially a paste (Figure 7.7 A) that sedimented to the bottom part of the vessel. The particles formed by the disintegration of the initial bolus during digestion remained in the lower part as seen in Figure 7.7 B. Free oil droplets could be seen floating on the top of the gastric content at the end of digestion. In contrast, the Liquid sample was initially a homogenous milky liquid (Figure 7.7 C). Although some precipitation was observed even in the very early stage of digestion lasting for about 70 min, the solid particles tended to cream to the top and form a boundary layer. An upper cream layer could be clearly seen after approximately 110 min of gastric digestion (Figure 7.7 D). This appearance remained throughout the latter stages of digestion.
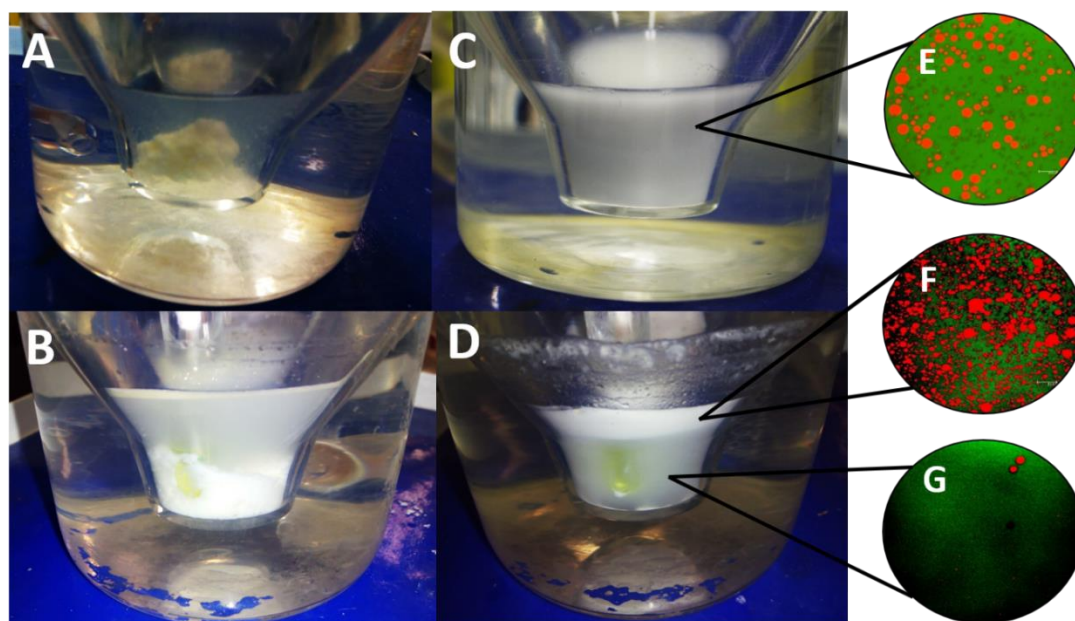
Figure 7.7 Images of Semi-Solid (A-B) and Liquid (C-D) samples in the initial state (A and C) and after 111.1 min (B) and after 110.3 min (D) of gastric digestion in the semi-dynamic gastric model using pepsin and gastric lipase. Representation of microstructure in the liquid sample before gastric digestion (E) and, the upper cream layer (F) and the bottom aqueous layer (G) after gastric digestion. Proteins and lipids are present in green and red, respectively. To note that the yellow block seen in images B and D corresponds to the pH probe.

The behaviour during the digestions using only pepsin and no enzyme was also compared in Appendix I1 and Appendix I2 for Semi-Solid and Liquid samples, respectively. In the Semi-Solid sample, the particles of the meal remained mainly in the bottom of the vessel and there was a layer of oil droplets in all the sets although it was more substantial in the case of gastric digestion including pepsin and gastric lipase. In the Liquid sample, there was precipitation in all three sets, but the formation of the cream layer was only observed in the digestion using enzymes, which was more pronounced when gastric lipase was included.

7.3.3 Protein Hydrolysis Analysis

The extent of protein hydrolysis, using OPA assay, of both samples at each GE point is displayed in the Figure 7.8. The samples were analysed during small intestinal digestion at 0 (corresponding to the end of gastric digestion), 1, 30 and 60 min. The gastric hydrolysis obtained in both meals GE1-9/0 ranged from 4.2 ± 3.4 to 36.9 ± 2.2 mmol/L and from 32.5 ± 10.2 to 12.5 ± 3.8 mmol/L for the Liquid and Semi-Solid samples, respectively. This was substantially lower than the subsequent time samples produced by small intestinal digestion, GE1-9/1, GE1-9/30 and GE1-9/60, demonstrating the rapid action of small intestinal proteases. The samples showed different proteolysis behaviour during small intestinal digestion. The Semi-Solid

sample exhibited a U-shape profile indicating a higher rate of proteolysis in the GE1 and GE9 aliquots and lower levels at intermediate time points. The highest level of proteolysis was achieved in the GE1/60 point, delivering 250.4 ± 35.9 mmol/L of free amino groups. The increase in proteolysis in the last aliquots might be due to the release of protein associated with particles that were only emptied later on. The Liquid sample, in contrast, had lower levels of proteolysis in the early GE aliquots which were more constant throughout compared to Semi-Solid sample. The highest amount of proteolysis was found in the GE10/60 point resulting in 246.7 ± 7.2 mmol/L of free amino groups.
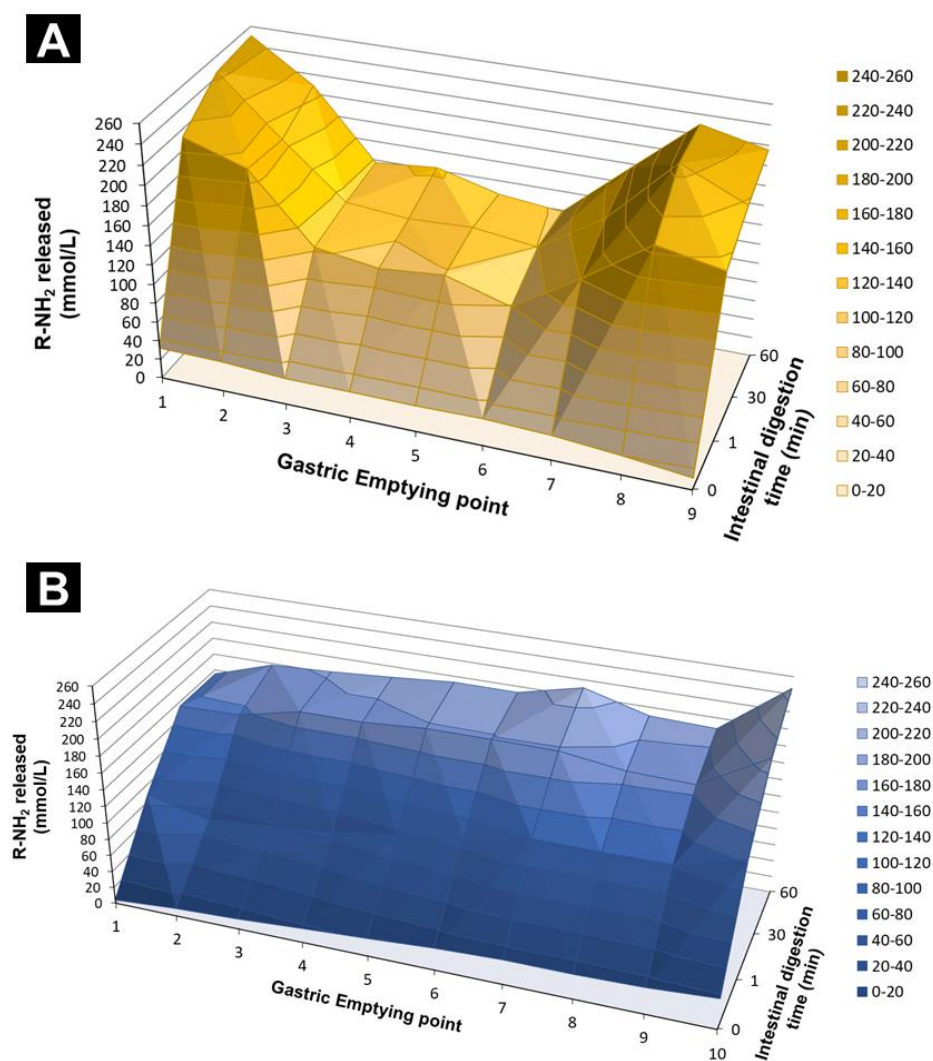
Figure 7.8 Surface plot representation of concentration of free amino groups (mmol/L) for each gastric emptying aliquot (GE) at 0 (referred to end point of gastric digestion), 1, 30 and 60 min after small intestinal digestion for both (A) Semi-Solid and (B) Liquid samples. The values were corrected by the different gastric and intestinal dilution in each point. The data represents the mean of three independent replicates.

Figure 7.9 shows the peak area obtained by size exclusion chromatography, in both samples at the different GE aliquot. The patterns were fairly similar to those obtained by OPA assay; the Semi-Solid sample presented U-shape (Figure 7.9 A) and the release of peptides in the Liquid sample was constant with some increase at the end of the digestion (Figure 7.9 B). This pattern was not altered when the values of the enzyme blank, i.e. the pancreatin solution without the addition of sample, were subtracted from those when sample was added (Figure 7.10) showing that there was no effect from the protein of the enzyme.
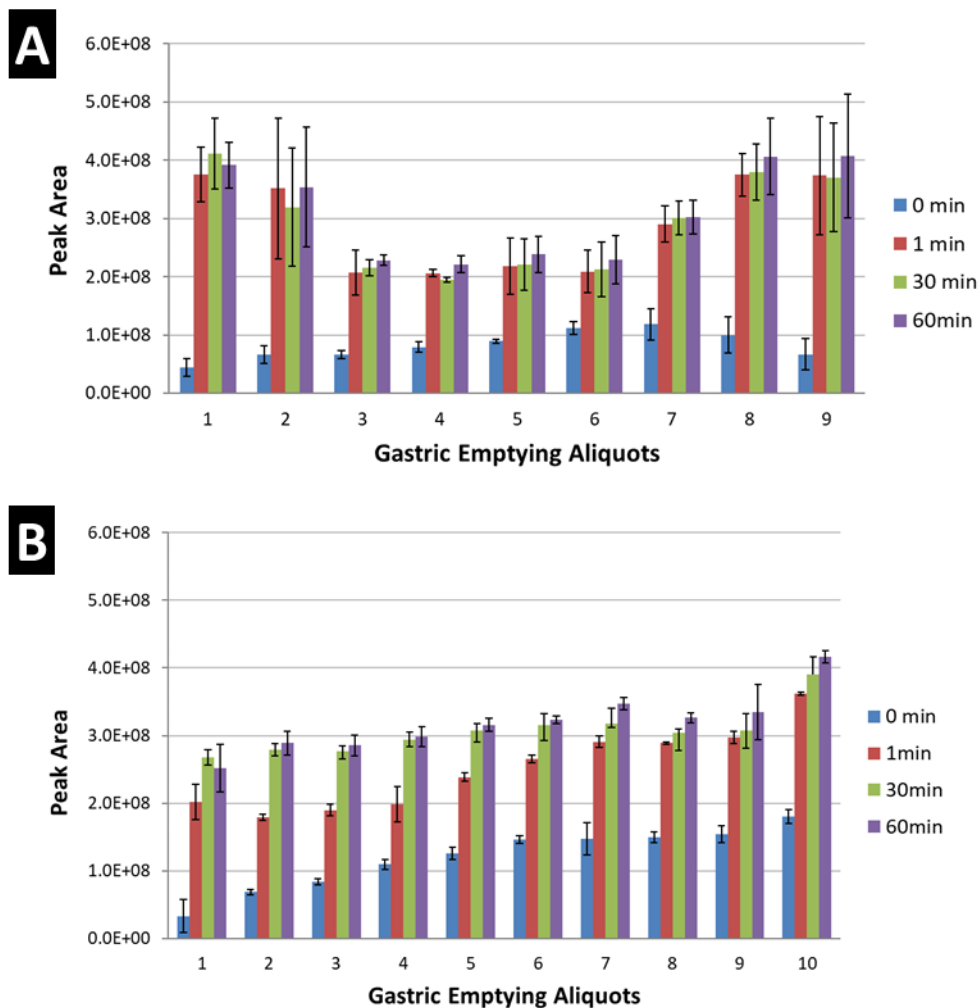
Figure 7.9 Peptide analysis of (A) Semi-Solid and (B) Liquid samples at the different GE aliquots after 0 (referred to end point of gastric digestion), 1, 30 and 60 min small intestinal digestion. This is referred to the aliquots from the gastric digestion in the semi-dynamic model using both gastric lipase and pepsin. The values were corrected by the different gastric and intestinal dilution in each point. Values are presented as means ± SD (n=3).
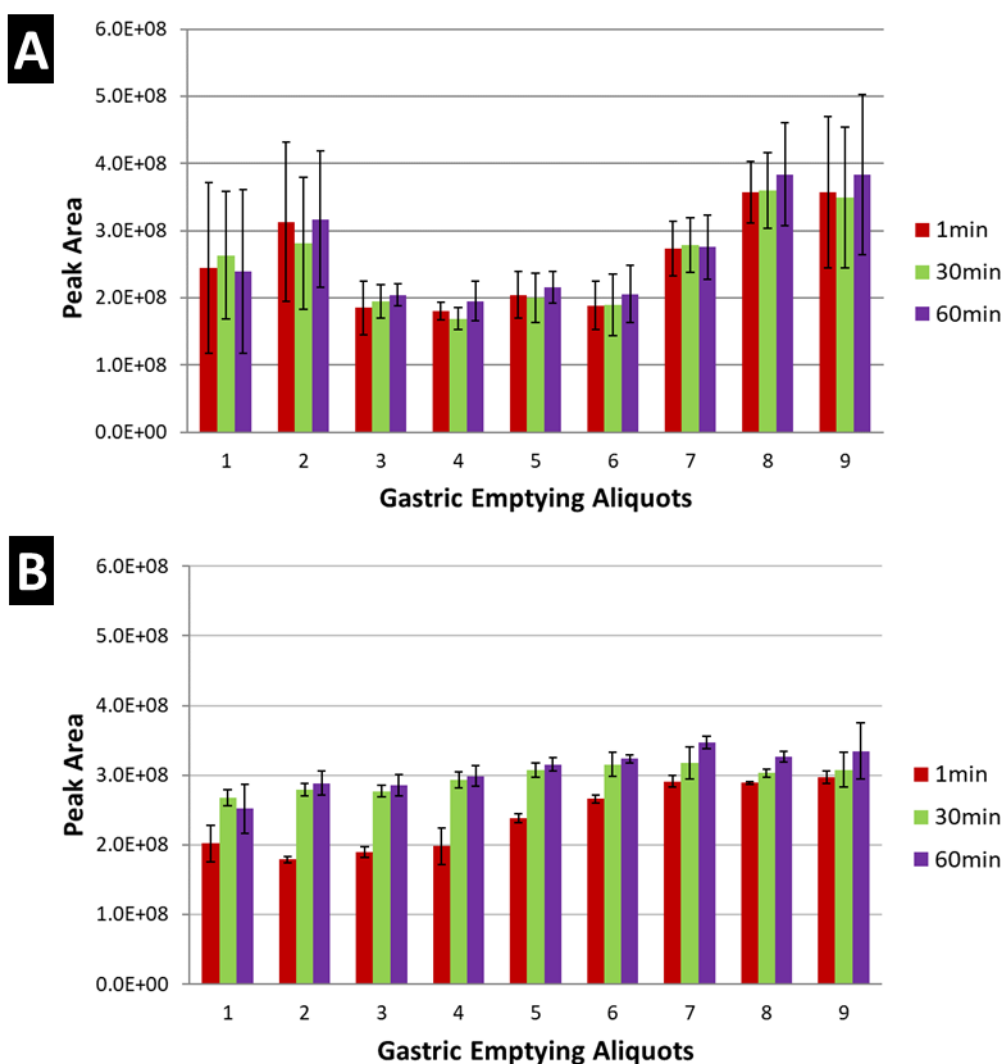
Figure 7.10 Peptide analysis of (A) Semi-Solid and (B) Liquid samples at the different GE aliquots at 1, 30 and 60 min after small intestinal digestion. The values are referred to the intestinal digestion after gastric digestion using both gastric lipase and pepsin with subtraction of the blank, i.e. only enzyme included. The values were corrected by the different gastric and intestinal dilution in each point. Values are presented as means ± SD (n=3).

7.3.4 Lipid Analysis

Figure 7.11 shows the levels (% w/w) of TAG and lipolytic products (FFA, MAG and DAG) in relation to the total lipid in each aliquot emptied at the different GE times. GE aliquots were quantified during the small intestinal digestion at 1, 30 and 60 min. In general, both samples followed the logical trends of lipolysis during intestinal digestion showing a decrease of TAG, an increase of FFA and MAG, and about constant levels of the intermediate product DAG. However, the rate of lipolysis was different between the samples. The Semi-Solid sample presented the highest levels of TAG in GE1/1, GE2/1 and GE3/1 points, accounting for 58.16 ± 11.67%, 59.05 ± 6.22% and 60.31 ± 4.91%, respectively. By contrast, the Liquid sample presented

56.90 ± 8.61% in the GE1/1 and the highest amount of TAG (75.15 ± 16.25%) was found in the GE10 aliquot corresponding to the residual top cream layer. With regards to FFA, the highest amounts were obtained in points GE4/60, GE5/60 and GE6/60 of the Semi-Solid sample which contained about 75%, in contrast to the Liquid sample, where the highest levels were found in GE7/60 and GE8/60 points which contained 72.11 ± 12.93% and 71.58 ± 19.57%, respectively. The GE10 showed the lowest levels of FFA in the Liquid sample representing the 33.07 ± 5.99%.
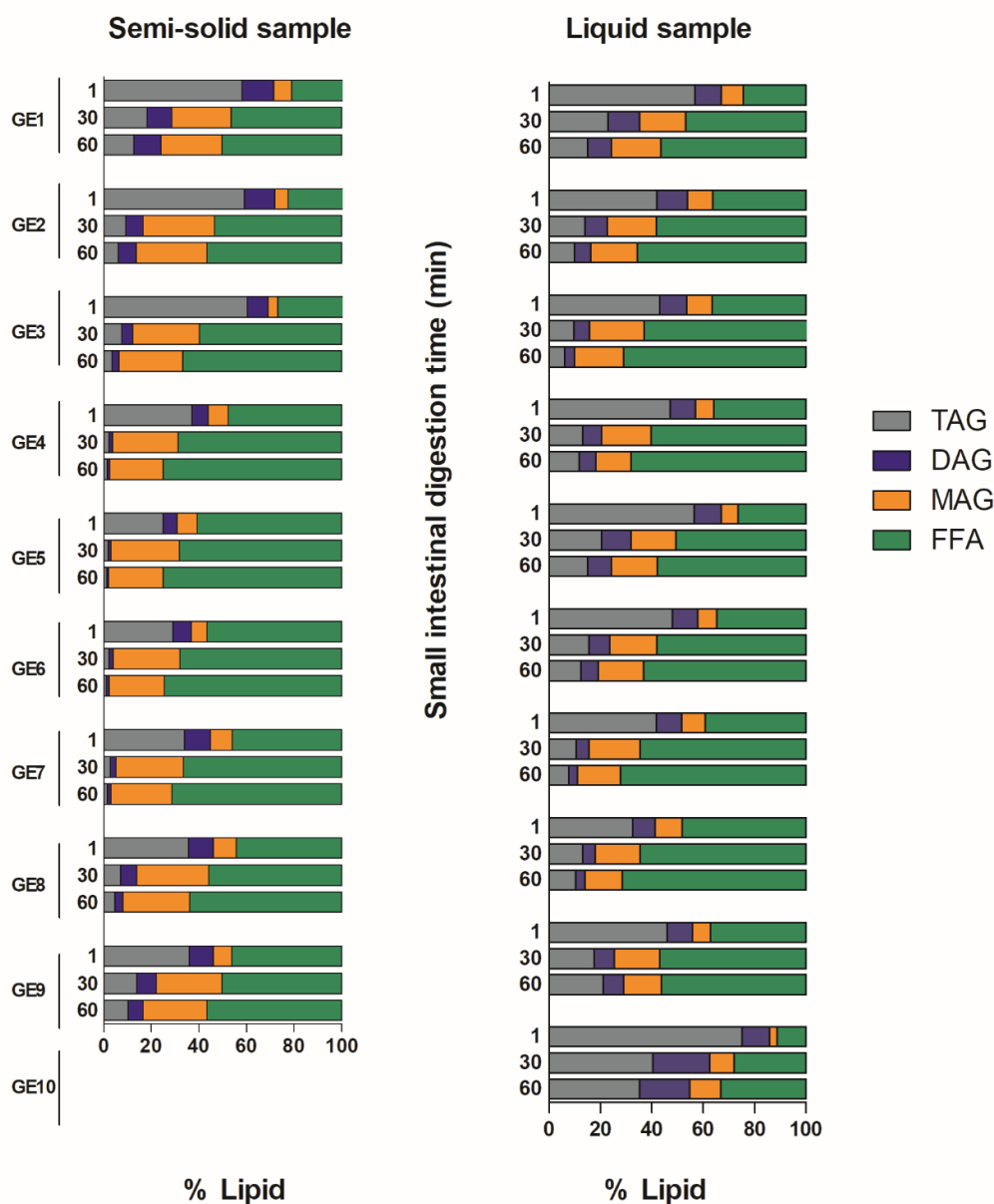
Figure 7.11 Levels (expressed as mass percentage) of lipid classes (TAG, DAG, MAG and FFA) in each gastric emptying (GE) aliquot at 1, 30 and 60 min after small intestinal digestion for both Semi-Solid and Liquid samples (mean of 3 replicates). The values were corrected by the different gastric and intestinal dilution in each point. The SD averages for Semi-Solid sample are 2.5, 5.3, 4.5 and 1.6% for MAG, FFA, TAG and DAG respectively. The SD averages for liquid sample are 1.7, 7.6, 7.3 and 2.4% for MAG, FFA, TAG and DAG respectively

In addition, we analysed the individual FFA classes in each GE point for each time of small intestinal digestion (Appendix J). The data showed a different FFA profile between samples. The Semi-Solid sample showed a greater variety of FFA types although the most abundant FFAs, i.e. 18:1, 18:0 and 16:0, were present in both samples. No particular trend in their rates of digestion was found.

7.4 Discussion

7.4.1 Simulation of Human Gastric Behaviour

The semi-dynamic model of gastric digestion used in the present study could closely simulate the structural changes reported in the human stomach with the same two meals (Mackie *et al.*, 2013). This was a result of the inclusion of relevant dynamic aspects of gastric physiology, i.e. gradual acidification, emptying and enzyme secretion.

The pH profile obtained with the samples (Figure 7.5) was similar to that seen previously in other *in vivo* studies (Malagelada *et al.*, 1976), although some differences can be found depending on the type of the meal digested. Unfortunately, the pH profile for the food matrices studied was not measured *in vivo* by Mackie *et al.* (2013). The effect of pH on gastric digestion is important to consider because it affects the protein structure and interactions with other components of the matrix as well as enzyme activity (Dekkers *et al.*, 2016). As a result, gastric pH has important consequences for the rest of digestion and subsequent nutrient bioavailability. The pH profile in the Liquid sample when it was compared among the three sets (i.e. using pepsin and gastric lipase, pepsin and no enzyme) was different, showing lower pH values in absence of enzymes. This might be related to a more homogenous digesta during the gastric phase, in which there was not the formation of a cream layer (Appendix I2).

GE plays an important role in the pH profile because it lowers the overall buffering capacity of the gastric contents through the progressive emptying of food and acid contained in the gastric chyme. The importance of GE on pH was observed in some additional experiments using the same samples. The pH of the Semi-Solid sample was lower than the Liquid meal for longer when GE was excluded because of the lower buffering capacity of the Semi-Solid sample caused by the lower exposure of the protein (Figure 7.12). However, introducing GE significantly reduced the difference, as seen in Figure 7.5. The GE displayed in Figure 7.2 was obtained by downscaling the clinical data on gastric volume reported by Mackie *et al.* (2013) in

which the Liquid sample emptied more quickly than the Semi-Solid sample; the emptying rate of the Liquid meal was double that of the Semi-Solid meal after 25 min of digestion. This differs from other studies (Marciani *et al.*, 2012; Santangelo *et al.*, 1998) in which a combination of solid and liquid food emptied faster than the same meal homogenised into a liquid form. It is important to note that in these studies the liquid meal remained homogenous throughout gastric digestion in contrast to the phase separation that occurred in the study by Mackie *et al.* (2013). This highlights the importance of gastric behaviour in controlling the emptying rate. Other studies (Marciani *et al.*, 2007) reporting phase separation of emulsions in the stomach showed a faster emptying rate compared to a homogenous system.
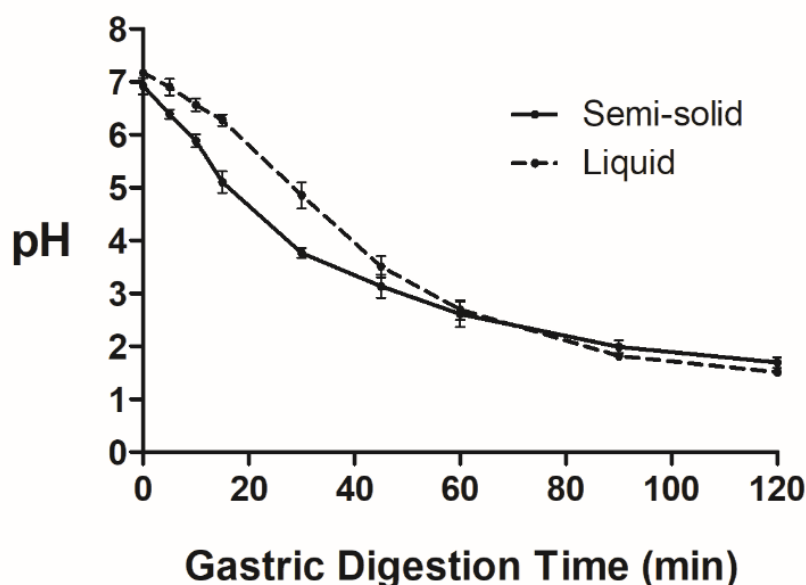
Figure 7.12 pH profile of both Semi-Solid (solid line) and Liquid (broken line) samples where gastric emptying was not included. pH was measured in the digesta inside of the reaction vessel. The gastric digestion was carried out for 2 hours using the semi-dynamic gastric model (gastric basal volume was not considered). Values are presented as means ± SD (n=5).

7.4.2 Influence of Gastric Digestion Conditions on Food Restructuring

The Semi-Solid and Liquid samples underwent sedimentation and creaming, respectively (Figure 7.7). The Liquid sample, an emulsion stabilised by milk proteins, presented some precipitation in the early stages of gastric digestion (about pH 5), which remained for about 70 min. This precipitation of the emulsion occurred as a result of the pH approaching the iso-electric point of the caseins (pH 4.6) at which point the net charge at the surface becomes zero. This change of charge on the protein led to the loss of electrostatic repulsion and consequently stability as has been

shown previously (Day *et al.*, 2014). Other aspects of the gastric environment including ionic strength and proteolysis could also have affected the stability of lipid droplets (Helbig *et al.*, 2012). The salts contained in the simulated gastric fluid could induce flocculation by screening the repulsive forces. In addition, the protective layer of protein absorbed at the interface might be compromised by the proteolytic action of pepsin resulting in the reduction of steric stability. Furthermore, the products of lipolysis, i.e. FFA, MAG and DAG, are surface active and could displace the protein from the emulsion interface leading to further destabilization. Indeed, these compounds at GE1/1 point accounted for 41.84 and 43.1% of the total lipid in the Semi-Solid and Liquid samples, respectively. All these factors could potentially contribute to the destabilisation of the emulsion causing flocculation and some coalescence of lipid droplets which progressively creamed to the top part during digestion due to their lower density. The action of the enzymes, both pepsin and gastric lipase, had an important role in the formation of this layer since the digestion performed in the absence of enzymes did not show phase separation (Appendix I2).

A clear phase separation was observed after 110 min of gastric digestion (Figure 7.7 D) but this trend already started to be observed after 30 min of digestion. Figure 7.7 F confirms the presence of lipid droplets in the top layer leaving an aqueous part in the bottom (Figure 7.7 G) and the extent of flocculation and coalescence in that cream layer compared to the stabilised droplets presented in the initial sample (Figure 7.7 E). The behaviour of phase separation showing the formation of a cream layer at the top of the stomach was also shown in *in vivo* using MRI (Mackie *et al.*, 2013) as a result of destabilisation in gastric conditions. The comparison of the gastric behaviour between these two digestion systems is illustrated in Figure 7.13. The phase separation of the liquid sample was clearly obtained in an earlier stage in the *in vivo* study, i.e. after 25 min. This might be due to the complex peristaltic movements that were less well simulated in the gastric *in vitro* model used, where the shear rates may have been lower than *in vivo* with regards to the gastric antrum.
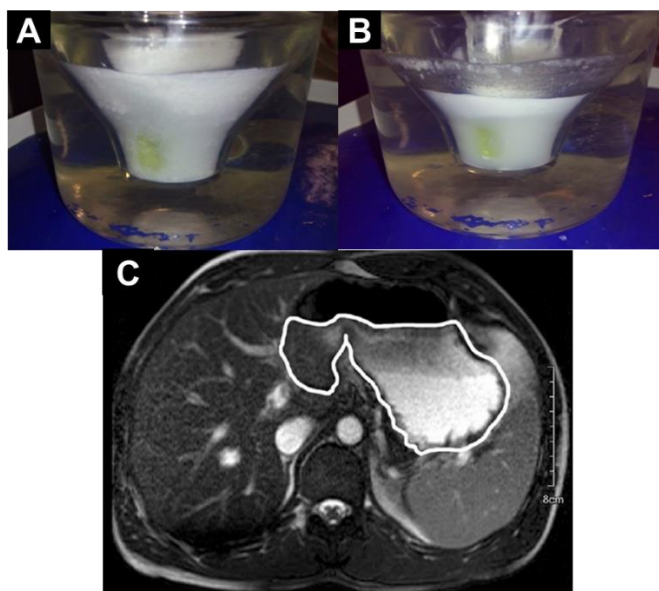
Figure 7.13 Comparison of the gastric behaviour in the Liquid sample obtained using the semi-dynamic model at (A) 29.7 min and (B) 111.1 min of gastric digestion and (C) MRI image reported in Mackie *et al.* (2013) showing the gastric digestion of liquid sample at 25 min of gastric digestion (human stomach was highlighted). This illustrates the colloidal behaviour of phase separation in both digestion systems.

Conversely, in the Semi-Solid sample, the density of the cheese-yogurt matrix resulted in the sedimentation of particles to the bottom of the simulated stomach model leaving the top part a more aqueous system. This behaviour was consistent throughout the digestion. Lipid from the cheese and yogurt was trapped in the food matrix that generated the sediment. However, the combination of gastric conditions including low pH and proteolysis led to the release of some oil droplets seen floating on the top at the end of digestion, although phase separation overall was very limited. Similar structural behaviour of both samples was observed in the MRI of the comparative in vivo study using the same dairy systems (Mackie *et al.*, 2013). Figure 7.14 illustrates the comparison of the gastric behaviour between these two digestion systems.
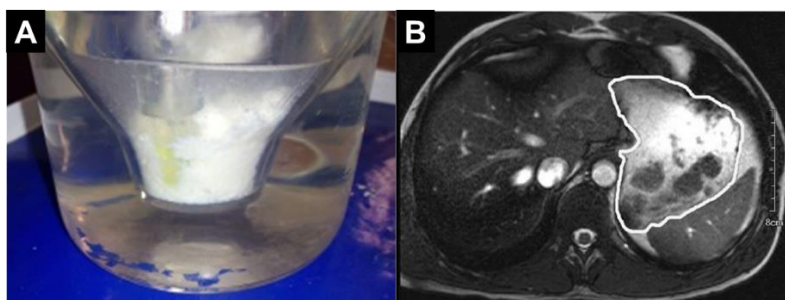
Figure 7.14 Comparison of the gastric behaviour in the Semi-Solid sample obtained using (A) the semi-dynamic model at 5.9 min of gastric digestion and (B) MRI image reported in Mackie *et al.* (2013) showing the gastric digestion of liquid sample at 5 min of gastric digestion (human stomach was highlighted). This illustrated the colloidal behaviour of sedimentation in both digestion systems.

A schematic representation of the possible molecular mechanisms occurring in the stomach leading to the observed behaviours is illustrated in Figure 7.15 and Figure 7.16. for the Semi-Solid and Liquid samples, respectively.
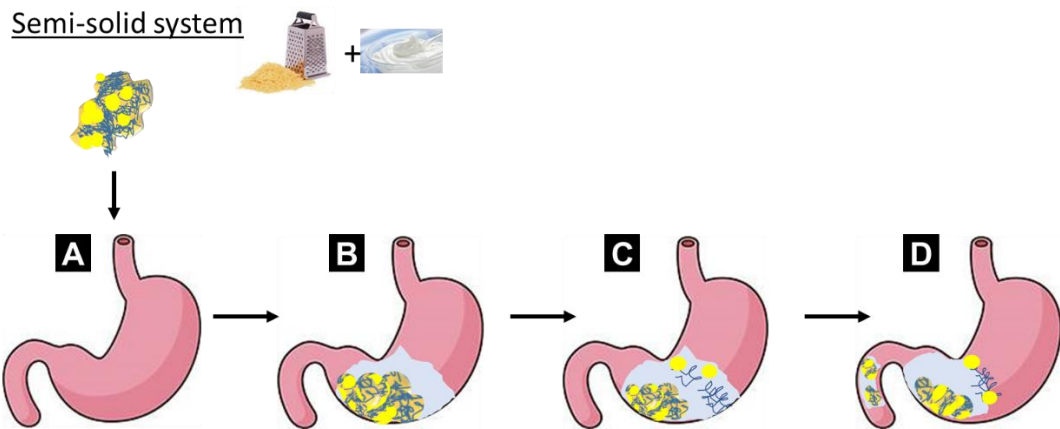
Figure 7.15 Schematic representation of the molecular mechanisms causing the outcomes obtained in Semi-Solid sample. (A) Semi-Solid sample is a complex protein matrix in which lipid droplets are entrapped. (B)This sample enters in the stomach, and is located in the bottom part within liquid phase of water and gastric fluids. (C) There is very limited phase separation and prolonged nutrient entrapment. (D) There is an early nutrient emptying together with the liquid phase of water and secretions, leading to fast lipid and protein hydrolysis.
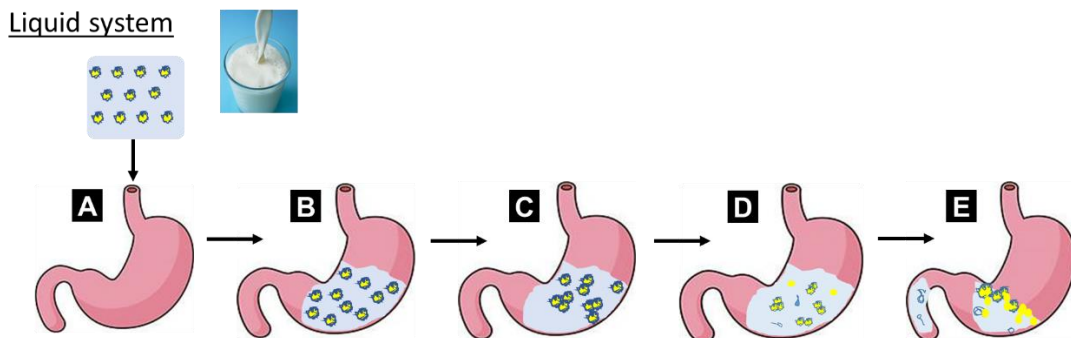
Figure 7.16 Schematic representation of the molecular mechanisms causing the outcomes obtained in Liquid sample. (A) Liquid sample is an oil in water emulsion. (B)This sample enters in the stomach and is mixed with gastric secretions. (C) There are changes in interfacial composition of the droplet due to the gastric environment, causing protein destabilisation and precipitation. (D) There is some coalescence (E) There is phase separation, in which the cream layer is located in the top, leading to the delay of lipid emptying and lipolysis in the small intestine.

7.4.3 Influence of Gastric Behaviour on Small Intestinal Protein Digestion

Figure 7.8 shows the different protein digestion rates that were observed between the samples. In the Semi-Solid sample there was a higher level of proteolysis in the GE1 and GE2 aliquots compared to the Liquid sample, which might be related to the early emptying of high density particles containing a greater amount of protein

which was subsequently digested throughout the small intestinal phase. The contribution of the proteolysis due to the proteolytic activity of the bacterial culture during fermentation and storage in cheese and yogurt should also be considered but the GE1/0 data in Figure 7.9 shows similar peptide values for both samples. In addition, the Semi-Solid sample showed high levels of proteolysis in the GE7, GE8 and GE9 aliquots which might be due to the emptying of soluble protein released gradually from the matrix. In contrast, the Liquid sample showed a more consistent extent of hydrolysis at all GE points because the proteins were more homogeneously distributed within the sample. The highest level of proteolysis in the liquid sample was obtained in the last volume collected, which might again be attributed to the protein associated with the lipid that creamed to the top. However, these results differ from those of van Aken *et al.* (2011), using a dynamic pH profile, in which the protein distribution in the bottom layer was higher than in the cream layer obtained after the gastric digestion of emulsions stabilised by milk proteins. These differences are likely to be due to the gradual emptying that we carried out throughout the gastric digestion, which was not included in the previous study. Indeed, the intestinal delivery from the stomach has been found to be one of the major factors controlling intestinal absorption kinetics, showing the high correlation between the rate of GE and absorption of nitrogen in milk and yogurt (Gaudichon *et al.*, 1994). The GE of the semi-solid structure of yogurt was more regular compared to the liquid matrix of milk, which is in accordance with the present study.

The results showed that there was rapid protein hydrolysis after 1 min of small intestinal digestion. This finding is in agreement with the study of Macierzanka *et al.* (2009), using β-lactoglobulin and β-casein- stabilized emulsions, showing that proteins were partially hydrolysed, in particular β-casein, after 1 min into low molecular weight peptides under intestinal conditions. The distinction between the different milk proteins was not assessed in the present study because of differences in the nature of the two starting materials; the two samples contained the same amount of protein, although the dairy products used (yogurt and cheese) usually contain less whey proteins due to the processing, which makes comparison problematic. Nevertheless, it is important to note that the behaviour during the GI tract of casein and whey proteins was different, resulting in that concept of 'fast' and 'slow' protein digestion observed in Chapter 4.

Protein digestion has been less well studied than lipid digestion in relation to the impact on colloidal behaviour under GI conditions. However, the understanding of the behaviour of protein networks and how protein is emptied from the stomach is relevant

to the study of the nutritional impact of foods related to satiety responses (Mackie *et al.*, 2010), affecting lipid digestion kinetics as well.

7.4.4 Influence of Gastric Behaviour on Small Intestinal Lipid Digestion

The rate of lipid hydrolysis was controlled by the nutrient composition of the aliquot emptied into the small intestine which varied because of the different colloidal behaviour within the stomach model. In the case of the Semi-Solid sample, the lipid availability was much higher in the early stages of digestion as a consequence of the high nutrient content of the sedimented particles. A substantial part of the initial TAG was emptied early on i.e. the GE1/1, GE2/1 and GE3/1 time points compared to the following digestion aliquots (Figure 7.11). In contrast, the lipid delivery of the Liquid sample was quite steady at all the GE aliquots but was substantially higher in the last residual volume analysed (GE10) that consisted almost entirely of the cream layer, which resulted in a delay of lipid delivery into the small intestine. The coalescence and phase separation observed in the Liquid sample led to reduction of the interfacial area available for lipolysis as seen in the limited decrease of TAG in GE10 (Figure 7.11). The TAG percentage in GE10/30 and GE10/60 was 40 and 35% respectively compared to 75% of TAG found in GE10/1. This could also be attributed to the saturation of substrate compared to the availability of the enzyme. Similarly, van Aken *et al.* (2011) reported a higher lipid distribution in the top layer when creaming was observed after the gastric digestion of triolein emulsions stabilised by milk proteins. They also observed that the FFA concentration in the bottom layer was much lower than in the cream layer, probably because FFA were protonated in the low gastric pH therefore they were oil-soluble and remained in the cream layer. In the present study there was also a higher absolute amount of FFA present in the cream layer compared to the lower aqueous layer, even though the relative values in Figure 7.11 do not reflect it. The levels of FFA in GE1/0 accounted for 17 mg whereas the point GE10/0 contained 54.6 mg, which could be also due to the gastric lipase activity given the time difference. The creaming process led to the concentration of the lipid droplets on the top promoting coalescence and decreasing the rate of lipolysis. Another study looking at the lipid digestion of protein stabilised emulsions using a dynamic GI system at TNO, (Helbig *et al.*, 2012) also showed the delay of lipid delivery into the small intestine due to creaming of lipid in the stomach. They showed a higher amount of lipid compounds, especially FFA and TAG, in the cream layer compared to the bottom part. The authors pointed out that even though different gastric behaviour of the samples was observed (homogeneous versus creaming), the total amount of FFA

released at the end of digestion remained similar, in line with our study. However, the importance of the kinetics of lipid accessibility in postprandial lipaemia was shown by Sanggaard *et al.* (2004) when comparing milk and yogurt. There was a faster increase and higher peak concentration of TAG in blood after yogurt consumption when compared to milk, suggesting that the homogenous and consistent fluid in the gastric compartment emptied more quickly than the more heterogenous gastric behaviour that could be obtained in milk.

Lipid digestion occurs mainly in the small intestine but we considered the addition of gastric lipase relevant because there is evidence suggesting that it accounts for the 5-40% of total TAG lipolysis (Armand *et al.*, 1997). The gastric lipase used in the present study was from rabbit gastric extract. This has been reported to be similar to human gastric lipase (HGL) having similar specificity for sn-3 position and optimum pH ranged between 5 and 3.5 (Carriere *et al.*, 1991). Moreover, the lipolytic products from gastric digestion may facilitate subsequent pancreatic lipolysis (Armand, 2007). The digestion of lipid by the action of pancreatic lipase accounts typically for 40-75%. The levels of lipolysis found in this study were in line with these ranges. The extent of lipolysis obtained after an additional 60 min in the simulated small intestine was determined and the Liquid sample showed 63% whereas the Semi-Solid sample reached 82%. These values were calculated taking into account the sum of the total FFA and MAG in relation to the sum of the total lipid obtained on a weight basis. The Semi-Solid sample showed higher lipolysis than liquid sample along GI tract, which could be attributed to the presence of a larger surface area of the particles in the Semi-Solid sample whereas the reduced area available in the phase separated and coalesced Liquid sample decreased the available surface area for lipase action. It is important to state that the performance of the GE in this study was quite complex due to the heterogeneity of the matrixes, which led to some losses during the experimental procedure. This could lead to some variability of the total initial and final lipid content and therefore the underestimation of lipid concentrations.

7.4.5 Possible Link to Physiological Responses

Since satiety related physiological responses such as CCK secretion and GE are linked to the rate and extent of lipid and protein sensing by intestinal endocrine cells, we can expect different satiety responses between the two samples. To provide a better understanding of the physiological trends in our study, the previous data for protein and lipid was replotted in a form representing the absorbable nutrient as a function of linear time. We assumed the protein hydrolysates quantified were absorbable since the protein digestion by intestinal proteases have been seen to be

efficient to further protein breakdown into amino acids and small peptides (2-3 amino acids) which are absorbable. The absorbable lipid referred to the FFA and MAG fractions that can be absorbed by enterocytes (Armand, 2007). Figure 7.17 A shows a similar absorbable protein profile for both samples. The Semi-Solid sample presented statistically higher levels of absorbable protein (p = 0.0341, paired, two-sided t-test) in the first time point (i.e. 10 min). The samples were also statistically different (p = 0.0356, paired, two-sided t-test) in the last time point (i.e. > 170 min) with the Liquid sample having a higher concentration of absorbable protein. On the other hand, the samples differed statistically in all the time points with regards to absorbable lipid (i.e. FFA+MAG), which is illustrated in Figure 7.17 B. The Semi-Solid sample presented higher levels of absorbable lipid than the Liquid sample in all the time points except in the last one (i.e. > 170 min). These patterns can be linked with the different gastric behaviour of the samples. Sedimentation of the Semi-Solid sample led to the early detection of higher concentrations of both protein and lipid seen in Figure 7.17 A and Figure 7.17 B in the first time points. The early delivery of a higher amount of nutrients to the small intestine might trigger an increase of negative hormonal feedback and thus slower GE, which could promote the feeling of fullness. It could also result in increasing the period of time that food remained in the stomach leading to a greater gastric distension and enhancing sensations of fullness (Delzenne *et al.*, 2010). Conversely, the effect of creaming observed in the Liquid sample caused a delay of the nutrient release in the small intestine, seen in the last time point (i.e. > 170 min) of Figure 7.17 A and Figure 7.17 B. Since the amount of nutrient delivered during digestion was lower, especially in the case of lipid, we can assume that this would cause the release of low levels of CCK. Conversely, Mackie *et al.* (2013) found the CCK levels of the liquid emulsion were higher than those in the structured sample for the first 40 min. The authors suggested that the lower viscosity of liquid sample induced the rapid emptying and delay of CCK regulation. Nevertheless, Marciani *et al.* (2007) showed a decrease of fullness and less CCK released from an emulsion that layered in the stomach compared to another emulsion which remained homogenous. The faster GE rate of the Liquid sample observed in the parallel clinical study can now be explained with the lower nutrient concentration in the aqueous layer that emptied first from the stomach. Mackie *et al.* (2013) also showed differences in fullness and hunger between the samples. The Semi-Solid sample induced substantially more fullness than the Liquid sample after just 15 min of digestion. This could potentially be due to the higher levels of protein and lipid released in the small intestine after the first 10 min from the Semi-Solid sample compared to Liquid sample as shown in Figure 7.17. The *in vivo* study also found that these differences in fullness were prolonged after two hours suggesting that the

impact of the high caloric chyme initially emptied was not only on satiation but satiety could also be affected. However, we could not correlate the high levels of nutrients in the last point of digestion from Liquid sample with the satiety responses seen in *in vivo* (Mackie *et al.*, 2013) because the clinical measurements were not taken for long enough to detect any distinct peak related to this high caloric-content fraction. In accordance with the present study, Golding *et al.* (2011) showed a delay in blood TAG presenting a distinct peak after 180 min of ingestion when using sodium stearyl lactylate-stabilised emulsion which phase separated in gastric conditions.
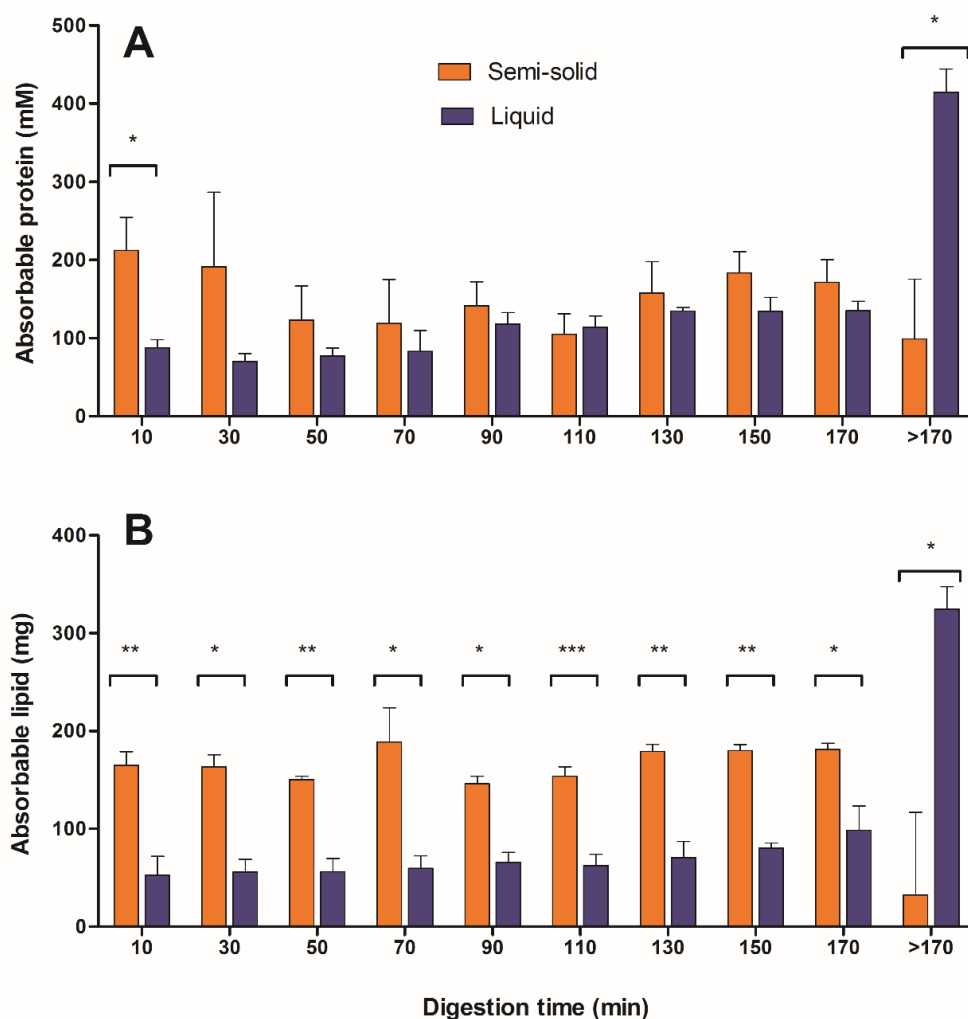
Figure 7.17 Representation of potentially absorbable nutrients, (A) protein and (B) lipid, during the digestion time. Absorbable protein refers to the free amino group levels obtained, and absorbable lipid refers to the sum of the amount of FFA and MAG obtained. This representation is based on the data in Figure 7.8 and Figure 7.11 but expressed in linear time (values are presented as means ± SD of three replicates). $p < 0.001$ (***); $p < 0.01$ (**); $p < 0.05$ (*).

7.4.6 Comparison between *in Vitro* Dynamic and Semi-Dynamic Gastric Models

The HGS is one of the dynamic gastric models that have been developed to more accurately simulate the conditions of the human stomach. This model was used to test the two studied dairy meals (work carried out by Janiene Gilliland, Maria Ferrua and Alan Mackie) and compare the results with those obtained using the semi-dynamic model.

Regarding the pH profile, Figure 7.18 shows the comparison between both digestive systems. In the HGS, the initial pH of the Liquid sample (6.7 ± 0.1) was higher than that in Semi-Solid sample (4.4 ± 0.1) whereas in the last point measured the pH of Liquid sample (1.2) was lower than in the Semi-Solid sample (2.0), which was similar to the results from the semi-dynamic model. The different mixing applied could have led to some differences in the results; the HGS reproduces the motor activity of the antral contraction waves using rubber conveyor belts along the simulated stomach compared to the more simplistic approach of the semi-dynamic model. Nevertheless, similar gastric behaviour was obtained using HGS as assessed visually, in which a cream layer in the Liquid sample was observed. In fact, the particle size distribution obtained in both digestion systems was similar (Figure 7.19); there were no differences in the emptied aliquots along the gastric digestion of the Liquid sample whereas variable droplet size distribution was obtained in the case of Semi-Solid sample.
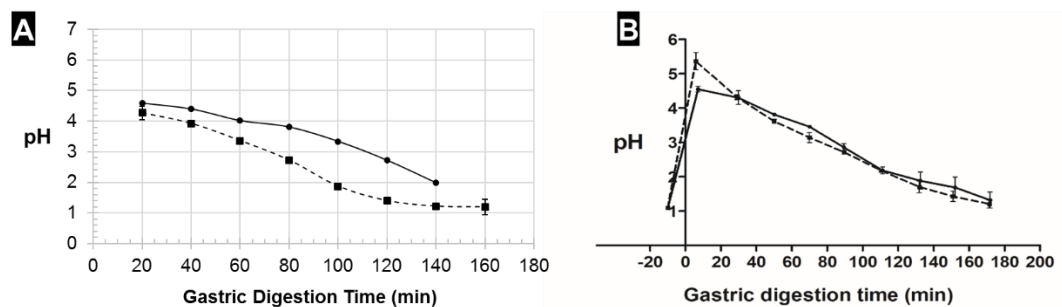
Figure 7.18 pH profile obtained in (A) HGS and (B) semi-dynamic model, solid line for Semi-Solid sample and broken line for Liquid sample.
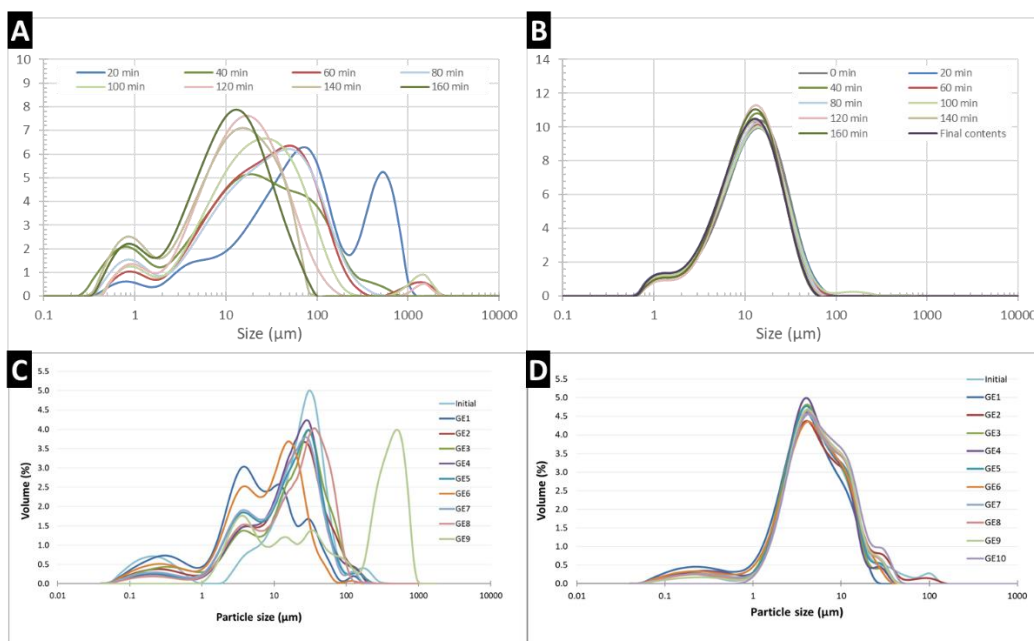
Figure 7.19 Particle size obtained in the HGS (A,B) and semi-dynamic model (C,D) for both Semi-Solid (A,C) and Liquid samples (B,D).

The solid composition of the emptied digesta from the HGS was also analysed (Figure 7.20). During the first hour of gastric digestion, the solid content emptied in the Semi-Solid sample was higher than that in the Liquid sample, which might be associated with the different distribution of the meal inside the HGS. A higher concentration of the Semi-Solid sample was more readily located at the bottom of the system to be emptied, in contrast to the more homogenous system in the Liquid sample leading to a constant delivery of solid content. The analysis of total protein and lipid that remained in the HGS model (see Figure 7.21) showed that the both nutrients were intimately associated to the Semi-Solid matrix, which were delivered at the same rate during the first hour of gastric digestion. Thereafter, there was a delay in lipid released probably due to the release of fat droplets from the cheese. This is in accordance with the higher values of protein and lipid observed at early stages of the gastric digestion and the oil-droplet layer that was observed at the end using the semi-dynamic model. The Liquid sample, in contrast, presented a delay of lipid and rapid protein delivery from the start of digestion. This might be linked with a higher impact of proteolysis due to the more homogenous sample leading to the flocculation of the droplets and the formation of the cream layer that was also observed in the semi-dynamic model. However, there was no clear comparison between the two digestion systems in terms of the degree of hydrolysis measured by OPA assay (Figure 7.22). In the HGS, the rate of protein digestion in both meals was quite constant during the gastric digestion time.
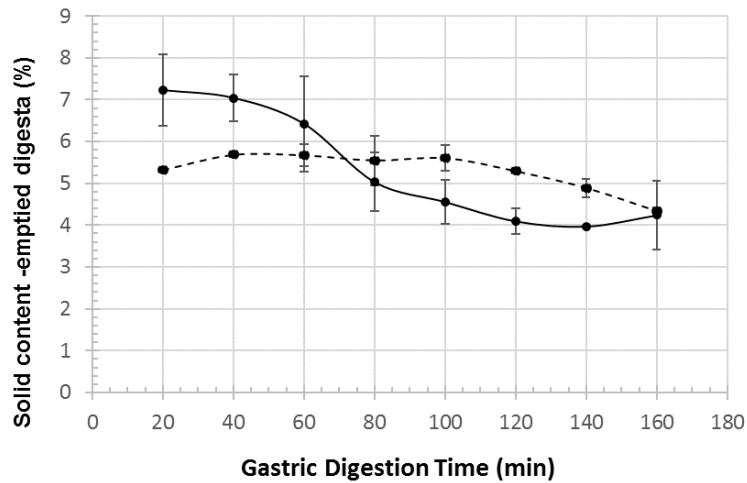
Figure 7.20 Solid content (%) of the emptied digesta during gastric digestion in HGS, solid line for Semi-Solid sample and broken line for Liquid sample.
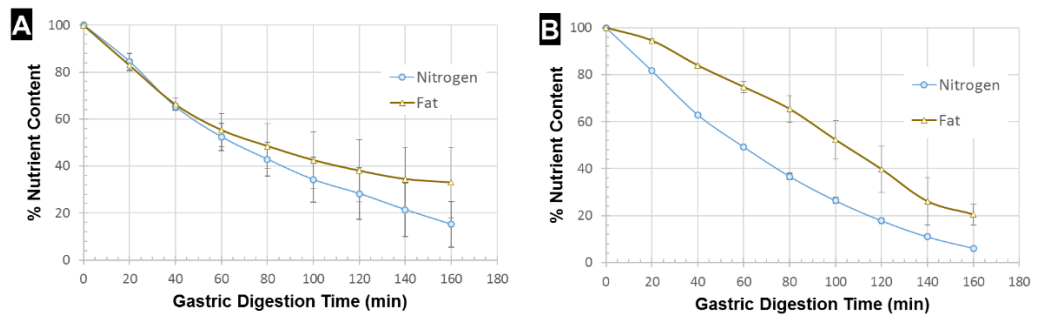
Figure 7.21 Nitrogen and lipid content (%), as compared to the original sample, of the digesta retained in the HGS during gastric digestion for (A) Semi-Solid and (B) Liquid samples.
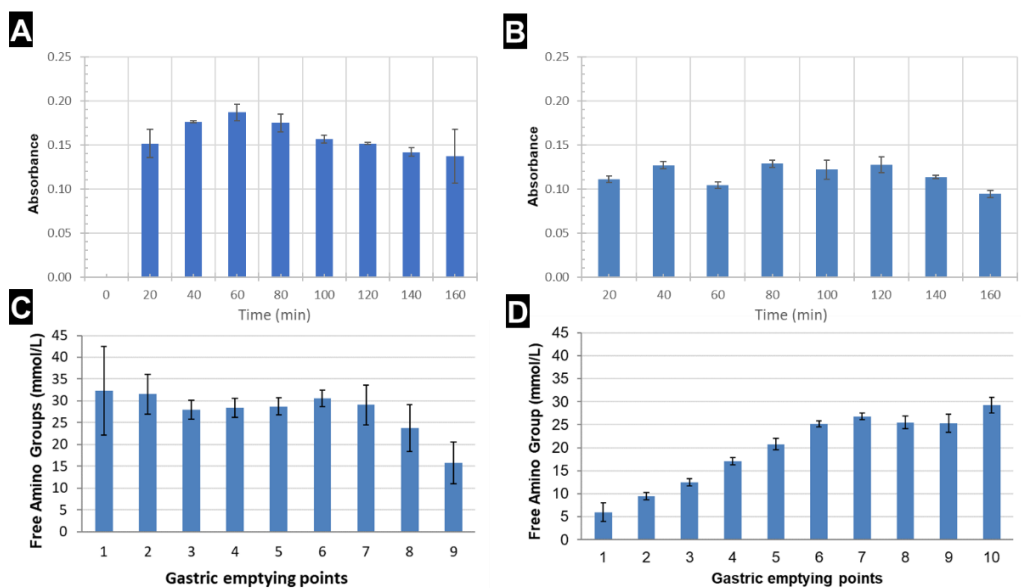
Figure 7.22 Degree of hydrolysis obtained in the HGS values express in absorbance(A,B) and the semi-dynamic model values expressed in mmol/L of amino groups (C,D), for both Semi-Solid (A,C) and Liquid (B,D) samples.

In general, the more simplistic approach of the semi-dynamic gastric model provided similar results to the more sophisticated dynamic model of the HGS for these specific dairy structures. Moreover, the comparison with the *in vivo* results illustrated that this model can be an effective approach to simplify the complex dynamic models and provide more physiological relevant data.

7.5 Conclusion

The present study shows that the *in vitro* gastric digestion of two dairy meals with the same macronutrient composition was influenced by their macrostructure and physico-chemical behaviour during gastric digestion. Their behaviour in the semi-dynamic model was very similar to that observed in the human stomach and that in a more advanced fully dynamic *in vitro* model. The colloidal behaviour of creaming and sedimentation obtained in the Liquid and Semi-Solid samples, respectively, controlled the composition of chyme delivered into the small intestinal phase. In the Liquid system, the change of interfacial composition during gastric digestion was the main driver for destabilisation of lipid droplets and formation of cream layer which led to the delay in nutrient release. In contrast, the sedimented particles of the Semi-Solid sample in the gastric phase caused the early emptying of high nutrient concentrations. The results showed differences in protein and lipid digestion between the two meals. The patterns of digestion observed in the *in vitro* system provided a plausible explanation for the satiety responses seen *in vivo* showing a decrease in appetite for the more structured meal.

Chapter 8

Conclusions and Future Perspectives

8.1 General conclusions

Milk and dairy products are associated with benefitial health and nutritional effects, but the mechanistic understanding of this association remains unresolved, which may be related to how the wide array of dairy structured matrices behave in the gastrointestinal tract. The present thesis investigated the digestive behaviour of different dairy matrices, from macrostructures to microstructures at the molecular level of the milk proteins. The general conclusion was that the structure and physical properties of the dairy sample in the gastric phase determined the kinetics of nutrient digestion, and those properties were modulated by formulation and processing. This thesis provided more detail in the growing subject area of food structure and digestion, highlighting the importance of the structures formed by the dairy products in the gastrointestinal tract, in which the stomach was shown to play a key role. This study provided for the first time, a mechanist insight regarding the factors controlling the physical and chemical properties of the digesta, which ultimately can control the rate of nutrient uptake and metabolic responses.

As shown in the literature review of Chapter 1, some studies have suggested the gastric digestion as one of the possible limiting factors for the metabolic effects observed *in vivo*. In order to investigate this hypothesis, a more accurate simulation of the gastric phase was essential, thus, the semi-dynamic model was developed in Chapter 3, which simulated the gradual pH decrease, secretion of fluids and gastric emptying. This model could closely mimic the intragastric behaviour seen in the human stomach by magnetic resonance imaging using the same dairy matrices. Thus, it provides a better simulation of the main dynamics of the human stomach compared to static models and, it is an easier and more cost-effective tool than fully dynamic models. The semi-dynamic model has provided a useful tool to investigate the role of structure upon nutrient digestion and has contributed to the international scientific community with a new system to investigate food digestion.

There is an increased interest in protein consumption and supplementation adressed to specific population needs, for instance, athletes and the elderly, and also high protein diets are quite popular in the general population for weight reduction. However, the digestive behaviour of proteins are not the same, which will impact the metabolic responses. The main milk proteins, whey proteins and caseins, have been generaly accepted as 'fast' and 'slow' proteins respectively, according to the rate of amino acid appearance in plasma. However, the controlling factor has not been fully explored yet. The objective of the research presented in the Chapter 4 was to determine the gastric behaviour of the main milk proteins with different blends and

lipid inclusion, and the possible impact on intestinal digestion and absorption of nutrients in order to understand the key limiting factors controlling the rate of absorption of milk proteins. The results showed that different milk proteins presented different nutrient digestion rates and amino acid absorption, and the gastric digestion was found to be the main rate limiting step. The solid coagulation of the casein component resulted in the delay of nutrients emptied from the gastric phase and thus slowed the overall digestion and amino acid absorption kinetics. In contrast, whey proteins presented soluble aggregates during gastric digestion that led to a more rapid emptying of protein from the stomach followed by a gradual decrease of nutrient delivery and subsequent absorption. Therefore, these findings support the generalised hypothesis that proposes the gastric phase as the main driver of the different digestion rates of milk proteins. Moreover, a second important finding was the modulation of the solid coagula by addition of whey proteins and lipid, a higher lipid content resulted in a reduction of the firmness of the coagula. Moreover, the protein matrix provided a kind of carrier for lipid and modulated lipid emptying behaviour. This behaviour further controlled nutrient digestion and might be associated with different physiological effects such as satiety and hyperlipidaemia. This research shows the great potential for food formulation in modulating nutrient digestion rate, through gastric restructuring, which could be potentially used by the food and drink industry.

The design of foods should also consider how they are processed, by which the structure of food matrices could be highly affected due to different ingredient/nutrient interactions leading to different structures and physico-chemical properties. Processing is widely used in order to provide consumers safe and convenient products, and milk is a clear example. The main processing used in dairy industry is homogenisation and heat treatment, and those treatments can change the native microstructure of the milk matrix, and thus impact the kinetics of nutrient digestion. In Chapter 5, we investigated the impact of process-induced changes of milk in the gastric digestion. The results showed that processing induced different gastric restructuring and coagulation in the simulated stomach. Homogenisation was the main driver for the gastric creaming whereas the different consistencies of the coagula were a consequence mainly of the heat treatment. The non-heated samples, especially Raw, formed a firm coagulum whereas the heated samples developed a weaker, fragmented coagulum particularly observed in UHT+Homo. These structural changes occurring during the gastric phase resulted in different nutrient emptying profiles, with significant differences between Raw and UHT+Homo, and quicker digestion of milk proteins in the UHT-treated samples due to the drastic heat treatment reducing the strength of the coagulum. This research showed a dramatic effect on the

interactions and subsequent matrix formation within the gastrointestinal tract although the processing did not have an obvious effect on the initial properties of the matrix.

Chapters 4 and 5 illustrated that the formation of the dense coagula in the stomach from caseins can be modulated by formulation and processing. The inclusion of lipid in the milk matrix as well as the processes of homogenisation and heat treatment change the nutrient arrangement and interactions of the initial sample, which impacts the syneresis and casein gel firmness in the stomach, illustrated in Figure 8.1. The presence of lipid droplets can imply a physical obstacle for casein micelles aggregation, which can also be affected by the size of the droplet by homogenisation. Moreover, the process of homogenisation results in a new droplet interface covered with absorbed milk proteins, which can induce to new casein interactions. Heat treatment, at temperatures higher than 70°C, induced the denaturation of whey proteins which interact with κ-casein at the surface of the casein micelles and it might hamper the micelle aggregation by steric effects. Therefore, these processes disrupt the formation of that compact micellar framework in the gastric conditions, forming structures with different consistencies and colloidal behaviours which affects the extent and composition of gastric emptying and, then, the intestinal digestion and absorption.
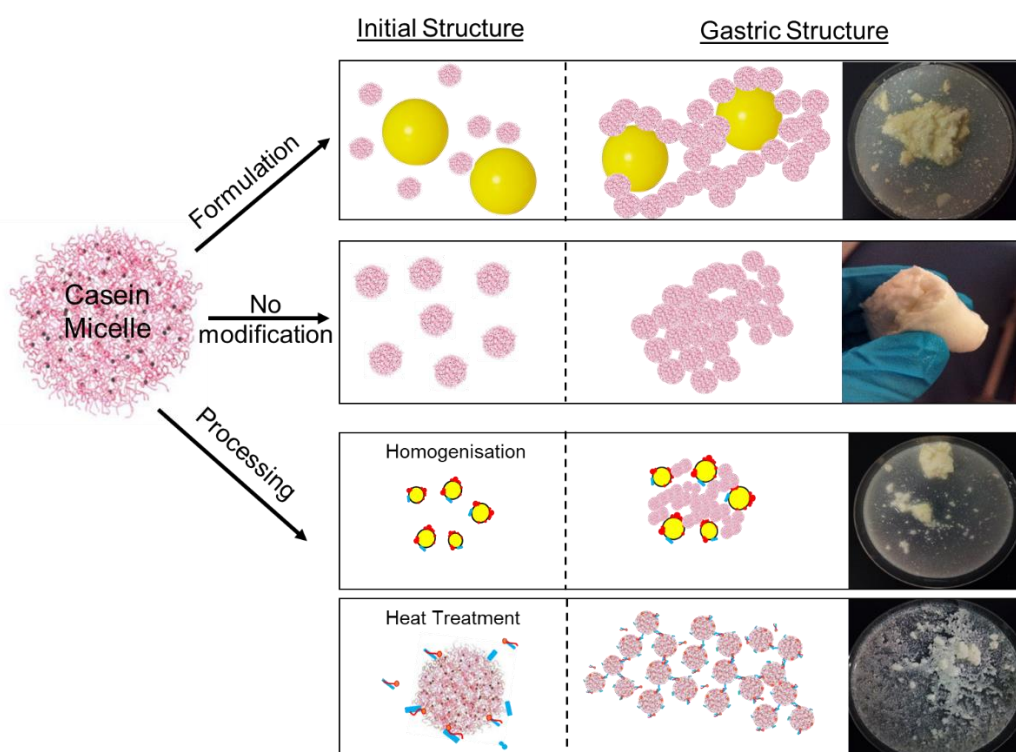
Figure 8.1 Schematic representation of how the initial structure of casein micelle can be modified by formulation (inclusion of lipid) and processing (homogenisation and heat treatment), comparing to their native state and how these changes affect the structure that is formed in the stomach. The latter is shown by schematic representation and images of digesta obtained in the different studies.

As illustrated, food formulation and processing can affect the arrangement and interactions of nutrients within the matrix, which might influence the interaction with the gastrointestinal factors, such as enzymes. Pepsin plays an important role in the restructuring formed in the gastric compartment since the results of Chapter 5 showed that it induced the formation of the coagulum earlier in the digestion, at pH values higher than the isoelectric point of caseins (pH 4.6). Moreover, the activity of pepsin depended on the structural changes in the stomach obtained in processed milk, which was illustrated in Chapter 6. In general, the formation of the dense coagula obtained in less processed milks prevented subsequent pepsin from penetrating the coagula. However, further work needs to be performed using sophisticated techniques such as confocal microscopy in order to obtain quantitative data. The study in Chapter 6 provided more insight into the behaviour of pepsin in complex structures during gastric digestion, which is of high interest since it affects the subsequent bioaccessibility and bioavailability of nutrients in the small intestine.

The bioaccessibility and bioavailability of nutrients might differ in dairy products with different consistency due to the different processing of milk, such as cheese and yogurt, when compared with milk. A comparison between two dairy meals with the same caloric content but different macrostructure, semi-solid versus liquid, was assessed in Chapter 7. The results showed that the colloidal behaviour of creaming and sedimentation obtained in the Liquid and Semi-Solid samples, respectively, controlled the composition of chyme delivery into the small intestinal phase. The nutrient digestion and bioaccessibility was delayed in the Liquid sample due to the late emptying of the dense-nutrient content of the cream layer formed, whereas the sedimented particles in the Semi-Solid sample were emptied earlier, leading to a rapid bioaccessibility of nutrients.

The correlation of *in vivo* and *in vitro* outcomes, as performed in Chapter 7, provided a valuable approach to correlate the physico-chemical mechanisms with the physiological effects and provide insight into the role of food digestion on health. In that study comparing the Liquid and Semi-Solid samples, the different patterns of protein and lipid digestion obtained in the simulated small intestine provided a plausible explanation for the satiety responses observed in the corresponding human study.

In conclusion, this thesis provides valuable insights addressing the relationship between food structure and nutrient digestion. The dramatic effect of matrix structure and its processing has been shown on the digestion kinetics of milk and dairy products. This can be translated to other foods, showing that the nutritional/health value of foods should therefore be considered as the functionality of the arrangement

and interactions of the nutrients within the matrix instead of just individual nutrients. Research should focus on mechanistic studies to understand how food matrices are digested through the gastrointestinal tract, then, providing insights into their nutritional and health effects, and the food restructuring in the stomach can be exploited to develop food structures addressed to different physiological functionalities.

8.2 Future perspectives

The semi-dynamic model provided a suitable tool for the studies presented in this thesis, however, as with any model, it is not able to completely simulate the processes of the gastrointestinal tract. Therefore, human studies would be helpful to correlate with the present results and would provide important insights into the interactions of food within the gut. For instance, the use of techniques such as magnetic resonance imaging would enable greater understanding of the restructuring of dairy products in the stomach and their pattern of gastric emptying.

As mentioned above, there is an increased demand for protein-based products. In this regard, there is an emergent area of research that involves proteins from plant sources, due to the growing consumer market interest and the standpoint of global environmental sustainability, which translates into plant-protein-based diets including non-dairy milks and convenience foods such as bars and yogurts. Some examples of sources of plant proteins are soy, quinoa, pea and rice.

There is currently little evidence of the metabolic effects of plant-based proteins, mainly soy protein, but it has been generalised that these proteins result in lower stimulation of muscle protein synthesis, compared to animal sources due to their generally lower digestibility (based on conventional nutritional evaluation methods), lower Leu content and deficiencies in certain essential amino acids (Gorissen *et al.*, 2018). There are some studies showing the increase of postprandial muscle protein synthesis after the ingestion of isolated soy protein in young men (Tang *et al.*, 2009; Wilkinson *et al.*, 2007). When compared with the response to milk proteins, the ingestion of soy protein induced a greater effect when compared with casein but lower response compared to whey protein and milk. The authors attributed this different muscle protein synthesis to differences in protein digestion kinetics, suggesting an intermediate behaviour between the fast whey protein and the slow casein protein. Bos, 2003 showed that soy protein resulted in earlier and higher kinetics of dietary amino acids in plasma, showing a peak at 2.5 hours compared to milk protein (3.9 hours). The faster amino acid absorption kinetics led to faster transfer of N into urea

and, thus, lower N retention, which reduced the support required for muscle protein synthesis.

Research has shown that the protein digestion rate determines the rate and extent of amino acid absorption and the overall metabolic responses (Dangin *et al.*, 2001), and this thesis has shown that gastric digestion can play a key role. There is no evidence explaining the possible intermediate behaviour of soy protein or other plant-based protein. Also, soy protein has mostly been studied in its isolate form, however, there are other processes applied to soy bean that might change its functionality, also some plant-based proteins are usually associated with the cell wall, which may affect bioaccessibility, and which should be considered. The more widely investigated animal proteins (e.g. milk, egg and meat) present different behaviour, which is affected by formulation and processing. This raises several questions, each of which would lead to potential avenues of further research in food structure and digestion. Do all plant proteins exhibit the same properties in the gastrointestinal conditions? Processing might induce changes in their molecular structure and interaction/aggregation behaviour, therefore, to what extent does processing of proteins impact digestion? Do they have different gastric behaviour? And, does their functionality differ from their source, taking into account the other components of the matrix? Therefore, there is the need for more research on proteins from plants in relation to digestion that will provide insights in the role of plant proteins in not only skeletal muscle mass but other physiological responses such as satiety.

However, plant-based proteins are, in general, not complete proteins, in that they are missing one or more essential amino acids, in contrast to milk proteins. Therefore, there is the need to improve the quality in terms of nutrition and functionality of plant proteins that could be achieved by some approaches such as breeding and genetic selection, improve protein functionality, improve digestibility and bioavailability of proteins during digestion. In that sense, proteins could be modified by processes (enzymatic, chemical or physical) to improve or create new functionalities, which could be beneficial for modulating nutrient digestion, for instance inducing a different gastric behaviour that, consequently could modulate nutrient bioavailability. The consumption of blends of different plant proteins or with other protein sources that would satisfy all the essential amino acid requirements could be an option to improve digestion and better muscle protein synthesis response, which has not been investigated yet. Investigating different approaches may drive future research towards novel formulations to achieve unique digestive properties, which will allow an optimal nutrient profile absorption and subsequent metabolic response. For instance, Reidy *et al.* (2013) showed that the blend of soy protein with milk proteins

showed more benefits in muscle protein synthesis than a single protein, and illustrated the relevance of the protein blends that have been incorporated in commercial sports nutrition products. Therefore, the design of food formulation should be performed taking into account the digestive behaviour in order to induce specific rate of nutrient digestion and, tailor and optimise nutritional and health effects.

Industrial processes such as homogenisation are widely used in the food and drink industry to provide long-shelf life products. However, this process affects the size of the droplets and the interactions with other nutrients, which can affect the functionality within the gastrointestinal tract. Following the observations in Chapter 5, two milk protein stabilised emulsions differing in droplet size (approximately 1.3 versus 0.1 μm) were investigated (results not shown). Preliminary results showed that some creaming was obtained in both samples during the gastric digestion using the semi-dynamic model, however, the extent and rate of that creaming was higher in the emulsion with smaller droplet size. This could potentially result in a different nutrient digestion and absorption kinetics. Therefore, relatively small changes in the production of food matrix could have significant impact on the metabolic effects. Indeed, there are a few studies showing the effect of droplet size of emulsions on physiological responses such as satiety (Armand *et al.*, 1999; Lett *et al.*, 2016a). Therefore, food processing offers possibilities to modulate nutrient digestion, hence, it is a potent tool to tailor metabolic effects.

When considering dairy products it is not only important to consider the macronutrients but minerals; calcium is highly important for both textural and nutritional roles. Calcium also plays an important role in lipid digestion since it has been reported that calcium can form complexes with free fatty acids, which are insoluble at the intestinal pH, called calcium soaps. This process can enhance the rate of hydrolysis by preventing free fatty acids from accumulating at the droplet surface, however, at the same time, hamper the accessibility and subsequent absorption of free fatty acids. The formation of these calcium soaps has been indicated to be one possible explanation for the reduction of cholesterol reported in the consumption of dairy products by the reduction of bile acid reabsorption. However, this might be affected by the type of matrix. Indeed, Lamothe *et al.* (2017) showed that, in a simulated digestion, for the equivalent calcium content, a solid matrix resulted in higher content of calcium soaps compared to liquid or semi-solid matrices but the underlying mechanisms were not understood. A detailed understanding of the influence of the matrix of the formation of calcium soaps is crucial to understand its contribution in lipid digestion and provide new insights into cardiovascular effects. This is an interesting area of research that needs further work. Moreover, in relation

to the emergent area of the gut microbiota, would different structures of fermented dairy products modify gut health?

References

Acheson, K. J., Blondel-Lubrano, A., Oguey-Araymon, S., Beaumont, M., Emady-Azar, S., Ammon-Zufferey, C., Monnard, I., Pinaud, S., Nielsen-Moennoz, C., & Bovetto, L. (2011). Protein choices targeting thermogenesis and metabolism1–3. *The American journal of clinical nutrition, 93*(3), 525-534.

Alfenas, R. d. C. G., Bressan, J., & Paiva, A. C. d. (2010). Effects of protein quality on appetite and energy metabolism in normal weight subjects. *Arquivos Brasileiros de Endocrinologia & Metabologia, 54*(1), 45-51.

Almiron-Roig, E., Chen, Y., & Drewnowski, A. (2003). Liquid calories and the failure of satiety: how good is the evidence? *Obesity reviews, 4*(4), 201-212.

Anderson, G. H., & Moore, S. E. (2004). Dietary proteins in the regulation of food intake and body weight in humans. *The Journal of nutrition, 134*(4), 974S-979S.

Anema, S. G., & Li, Y. (2003). Association of denatured whey proteins with casein micelles in heated reconstituted skim milk and its effect on casein micelle size. *Journal of Dairy Research, 70*(1), 73-83.

Anema, S. G., Lee, S. K., & Klostermeyer, H. (2011). Rennet-Induced Aggregation of Heated pH-Adjusted Skim Milk. *Journal of Agricultural and Food Chemistry, 59*(15), 8413-8422.

Armand, M., Hamosh, M., DiPalma, J. S., Gallagher, J., Benjamin, S. B., Philpott, J. R., Lairon, D., & Hamosh, P. (1995). Dietary fat modulates gastric lipase activity in healthy humans. *The American journal of clinical nutrition, 62*(1), 74-80.

Armand, M., Pasquier, B., Borel, P., Andre, M., Senft, M., Peyrot, J., Salducci, J., & Lairon, D. (1997). Emulsion and absorption of lipids: the importance of physicochemical properties. *Oleagineux Corps Gras Lipides (France)*.

Armand, M., Pasquier, B., André, M., Borel, P., Senft, M., Peyrot, J., Salducci, J., Portugal, H., Jaussan, V., & Lairon, D. (1999). Digestion and absorption of 2 fat emulsions with different droplet sizes in the human digestive tract. *The American journal of clinical nutrition, 70*(6), 1096-1106.

Armand, M. (2007). Lipases and lipolysis in the human digestive tract: where do we stand? *Current Opinion in Clinical Nutrition & Metabolic Care, 10*(2), 156-164.

Awati, A., Rutherfurd, S. M., Plugge, W., Reynolds, G. W., Marrant, H., Kies, A. K., & Moughan, P. J. (2009). Ussing chamber results for amino acid absorption of protein hydrolysates in porcine jejunum must be corrected for endogenous protein. *Journal of the Science of Food and Agriculture, 89*(11), 1857-1861.

Bach, A., Aris, A., Vidal, M., Fàbregas, F., & Terré, M. (2017). Influence of milk processing temperature on growth performance, nitrogen retention, and hindgut's inflammatory status and bacterial populations in a calf model. *Journal of Dairy Research, 84*(3), 355-359.

Barbé, F., Ménard, O., Le Gouar, Y., Buffière, C., Famelart, M.-H., Laroche, B., Le Feunteun, S., Dupont, D., & Rémond, D. (2013). The heat treatment and the gelation are strong determinants of the kinetics of milk proteins digestion and of the peripheral availability of amino acids. *Food Chemistry, 136*(3), 1203-1212.

Barbé, F., Ménard, O., Gouar, Y. L., Buffière, C., Famelart, M.-H., Laroche, B., Feunteun, S. L., Rémond, D., & Dupont, D. (2014a). Acid and rennet gels exhibit strong differences in the kinetics of milk protein digestion and amino acid bioavailability. *Food Chemistry, 143*, 1-8.

Barbé, F., Le Feunteun, S., Rémond, D., Ménard, O., Jardin, J., Henry, G., Laroche, B., & Dupont, D. (2014b). Tracking the in vivo release of bioactive peptides in

the gut during digestion: Mass spectrometry peptidomic characterization of effluents collected in the gut of dairy matrix fed mini-pigs. *Food Research International, 63*, 147-156.

Barroso, E., Cueva, C., Peláez, C., Martínez-Cuesta, M. C., & Requena, T. (2015). The computer-controlled multicompartmental dynamic model of the gastrointestinal system SIMGI. In *The Impact of Food Bioactives on Health*, (pp. 319-327): Springer.

Bendtsen, L. Q., Lorenzen, J. K., Bendsen, N. T., Rasmussen, C., & Astrup, A. (2013). Effect of Dairy Proteins on Appetite, Energy Expenditure, Body Weight, and Composition: a Review of the Evidence from Controlled Clinical Trials. *Advances in Nutrition, 4*(4), 418-438.

Benelam, B. (2009). Satiation, satiety and their effects on eating behaviour. *Nutrition Bulletin, 34*(2), 126-173.

Bhattacharya, A., Banu, J., Rahman, M., Causey, J., & Fernandes, G. (2006). Biological effects of conjugated linoleic acids in health and disease. *The Journal of Nutritional Biochemistry, 17*(12), 789-810.

Bligh, E. G., & Dyer, W. J. (1959). A rapid method of total lipid extraction and putification. *Canadian Journal of Biochemistry and Physiology, 37*(8), 911-917.

Bluemel, S., Menne, D., Fried, M., Schwizer, W., & Steingoetter, A. (2015). On the validity of the 13C-acetate breath test for comparing gastric emptying of different liquid test meals: a validation study using magnetic resonance imaging. *Neurogastroenterology & Motility, 27*(10), 1487-1494.

Bohn, T., Carriere, F., Day, L., Deglaire, A., Egger, L., Freitas, D., Golding, M., Le Feunteun, S., Macierzanka, A., Menard, O., Miralles, B., Moscovici, A., Portmann, R., Recio, I., Rémond, D., Santé-Lhoutelier, V., Wooster, T. J., Lesmes, U., Mackie, A. R., & Dupont, D. (2017). Correlation between in vitro and in vivo data on food digestion. What can we predict with static in vitro digestion models? *Critical Reviews in Food Science and Nutrition, 58*(13), 2239-2261.

Boirie, Y., Dangin, M., Gachon, P., Vasson, M.-P., Maubois, J.-L., & Beaufrère, B. (1997). Slow and fast dietary proteins differently modulate postprandial protein accretion. *Proceedings of the National Academy of Sciences, 94*(26), 14930-14935.

Bos, C., Mahé, S., Gaudichon, C., Benamouzig, R., Gausserès, N., Luengo, C., Ferrière, F., Rautureau, J., & Tomé, D. (1999). Assessment of net postprandial protein utilization of 15 N-labelled milk nitrogen in human subjects. *British Journal of Nutrition, 81*(3), 221-226.

Bos, C., Metges, C. C., Gaudichon, C., Petzke, K. J., Pueyo, M. E., Morens, C., Everwand, J., Benamouzig, R., & Tomé, D. (2003). Postprandial Kinetics of Dietary Amino Acids Are the Main Determinant of Their Metabolism after Soy or Milk Protein Ingestion in Humans. *The Journal of nutrition, 133*(5), 1308-1315.

Bourlieu, C., Ménard, O., De La Chevasnerie, A., Sams, L., Rousseau, F., Madec, M.-N., Robert, B., Deglaire, A., Pezennec, S., Bouhallab, S., Carrière, F., & Dupont, D. (2015). The structure of infant formulas impacts their lipolysis, proteolysis and disintegration during in vitro gastric digestion. *Food Chemistry, 182*, 224-235.

Boutrou, R., Gaudichon, C., Dupont, D., Jardin, J., Airinei, G., Marsset-Baglieri, A., Benamouzig, R., Tomé, D., & Leonil, J. (2013). Sequential release of milk

protein–derived bioactive peptides in the jejunum in healthy humans. *The American journal of clinical nutrition, 97*(6), 1314-1323.

Brener, W., Hendrix, T. R., & McHugh, P. R. (1983). Regulation of the gastric emptying of glucose. *Gastroenterology, 85*(1), 76-82.

Brighton, C. A., Rievaj, J., Kuhre, R. E., Glass, L. L., Schoonjans, K., Holst, J. J., Gribble, F. M., & Reimann, F. (2015). Bile acids trigger GLP-1 release predominantly by accessing basolaterally located G protein–coupled bile acid receptors. *Endocrinology, 156*(11), 3961-3970.

Burd, N. A., Yang, Y., Moore, D. R., Tang, J. E., Tarnopolsky, M. A., & Phillips, S. M. (2012). Greater stimulation of myofibrillar protein synthesis with ingestion of whey protein isolate v. micellar casein at rest and after resistance exercise in elderly men. *British Journal of Nutrition, 108*(6), 958-962.

Butland, B., Jebb, S., Kopelman, P., McPherson, K., Thomas, S., Mardell, J., & Parry, V. (2007). Foresight. Tackling obesities: future choices. Project report. *Foresight. Tackling obesities: future choices. Project report.*

Calbet, J., & MacLean, D. (1997). Role of caloric content on gastric emptying in humans. *The Journal of physiology, 498*(2), 553-559.

Calbet, J. A. L., & Holst, J. J. (2004). Gastric emptying, gastric secretion and enterogastrone response after administration of milk proteins or their peptide hydrolysates in humans. *European journal of nutrition, 43*(3), 127-139.

Camilleri, M., Malagelada, J., Brown, M., Becker, G., & Zinsmeister, A. R. (1985). Relation between antral motility and gastric emptying of solids and liquids in humans. *American Journal of Physiology-Gastrointestinal and Liver Physiology, 249*(5), G580-G585.

Carriere, F., Moreau, H., Raphel, V., Laugier, R., Benicourt, C., Junien, J. L., & Verger, R. (1991). Purification and biochemical characterization of dog gastric lipase. *European Journal of Biochemistry, 202*(1), 75-83.

Carriere, F., Barrowman, J. A., Verger, R., & Laugier, R. (1993). Secretion and contribution to lipolysis of gastric and pancreatic lipases during a test meal in humans. *Gastroenterology, 105*(3), 876-888.

Cartwright, G., McManus, B. H., Leffler, T. P., & Moser, C. R. (2005). Rapid determination ofmoisture/solids and fat in dairy products by microwave and nuclear magnetic resonance analysis: PVM 1: 2004. *Journal of AOAC International, 88*(1), 107-120.

Chen, J. (2009). Food oral processing—A review. *Food Hydrocolloids, 23*(1), 1-25.

Church, F. C., Swaisgood, H. E., Porter, D. H., & Catignani, G. L. (1983). Spectrophotometric assay using o-phthaldialdehyde for determination of proteolysis in milk and isolated milk proteins1. *Journal of Dairy Science, 66*(6), 1219-1227.

Churchward-Venne, T. A., Snijders, T., Linkens, A. M., Hamer, H. M., van Kranenburg, J., & van Loon, L. J. (2015). Ingestion of Casein in a Milk Matrix Modulates Dietary Protein Digestion and Absorption Kinetics but Does Not Modulate Postprandial Muscle Protein Synthesis in Older Men–3. *The Journal of nutrition, 145*(7), 1438-1445.

Clemente, G., Mancini, M., Nazzaro, F., Lasorella, G., Rivieccio, A., Palumbo, A. M., Rivellese, A. A., Ferrara, L., & Giacco, R. (2003). Effects of different dairy products on postprandial lipemia. *Nutrition, Metabolism and Cardiovascular Diseases, 13*(6), 377-383.

Costill, D., & Saltin, B. (1974). Factors limiting gastric emptying during rest and exercise. *Journal of Applied Physiology, 37*(5), 679-683.

Cummings, D. E., & Overduin, J. (2007). Gastrointestinal regulation of food intake. *The Journal of clinical investigation, 117*(1), 13-23.

Dalgleish, D. G., Spagnuolo, P. A., & Goff, H. D. (2004). A possible structure of the casein micelle based on high-resolution field-emission scanning electron microscopy. *International Dairy Journal, 14*(12), 1025-1031.

Dalgleish, D. G., & Corredig, M. (2012). The structure of the casein micelle of milk and its changes during processing. *Annual review of food science and technology, 3*, 449-467.

Dangin, M., Boirie, Y., Garcia-Rodenas, C., Gachon, P., Fauquant, J., Callier, P., Ballèvre, O., & Beaufrère, B. (2001). The digestion rate of protein is an independent regulating factor of postprandial protein retention. *American Journal of Physiology-Endocrinology And Metabolism, 280*(2), E340-E348.

Dangin, M., Guillet, C., Garcia-Rodenas, C., Gachon, P., Bouteloup-Demange, C., Reiffers-Magnani, K., Fauquant, J., Ballèvre, O., & Beaufrère, B. (2003). The rate of protein digestion affects protein gain differently during aging in humans. *The Journal of physiology, 549*(2), 635-644.

Day, L., Golding, M., Xu, M., Keogh, J., Clifton, P., & Wooster, T. J. (2014). Tailoring the digestion of structured emulsions using mixed monoglyceride–caseinate interfaces. *Food Hydrocolloids, 36*, 151-161.

De Kruif, C. G., Huppertz, T., Urban, V. S., & Petukhov, A. V. (2012). Casein micelles and their internal structure. *Advances in Colloid and Interface Science, 171*, 36-52.

de la Fuente, M. A., Singh, H., & Hemar, Y. (2002). Recent advances in the characterisation of heat-induced aggregates and intermediates of whey proteins. *Trends in Food Science & Technology, 13*(8), 262-274.

Dehghan, M., Mente, A., Rangarajan, S., Sheridan, P., Mohan, V., Iqbal, R., Gupta, R., Lear, S., Wentzel-Viljoen, E., & Avezum, A. (2018). Association of dairy intake with cardiovascular disease and mortality in 21 countries from five continents (PURE): a prospective cohort study. *The Lancet, 392*(10161), 2288-2297.

Dekkers, B., Kolodziejczyk, E., Acquistapace, S., Engmann, J., & Wooster, T. (2016). Impact of gastric pH profiles on the proteolytic digestion of mixed βlg-Xanthan biopolymer gels. *Food & function, 7*(1), 58-68.

Delzenne, N., Blundell, J., Brouns, F., Cunningham, K., De Graaf, K., Erkner, A., Lluch, A., Mars, M., Peters, H., & Westerterp-Plantenga, M. (2010). Gastrointestinal targets of appetite regulation in humans. *Obesity reviews, 11*(3), 234-250.

Dickinson, E. (1992). *Introduction to food colloids*: Oxford University Press.

Dickinson, E. (1997). Properties of Emulsions Stabilized with Milk Proteins: Overview of Some Recent Developments. *Journal of Dairy Science, 80*(10), 2607-2619.

Dickinson, E. (2013). Stabilising emulsion-based colloidal structures with mixed food ingredients. *Journal of the Science of Food and Agriculture, 93*(4), 710-721.

Dideriksen, K., Reitelseder, S., Petersen, S., Hjort, M., Helmark, I., Kjær, M., & Holm, L. (2011). Stimulation of muscle protein synthesis by whey and caseinate ingestion after resistance exercise in elderly individuals. *Scandinavian Journal of Medicine & Science in Sports, 21*(6).

Diepvens, K., Häberer, D., & Westerterp-Plantenga, M. (2008). Different proteins and biopeptides differently affect satiety and anorexigenic/orexigenic hormones in healthy humans. *International Journal of Obesity, 32*(3), 510.

Dinning, P. G., Arkwright, J. W., Gregersen, H., O'grady, G., & Scott, S. M. (2010). Technical advances in monitoring human motility patterns. *Neurogastroenterology & Motility, 22*(4), 366-380.

Donato, L., Alexander, M., & Dalgleish, D. G. (2007). Acid Gelation in Heated and Unheated Milks: Interactions between Serum Protein Complexes and the Surfaces of Casein Micelles. *Journal of Agricultural and Food Chemistry, 55*(10), 4160-4168.

Dougkas, A., Minihane, A. M., Givens, D. I., Reynolds, C. K., & Yaqoob, P. (2012). Differential effects of dairy snacks on appetite, but not overall energy intake. *British Journal of Nutrition, 108*(12), 2274-2285.

Douglas, F., Greenberg, R., Farrell, H., & Edmondson, L. (1981). Effects of ultra-high-temperature pasteurization on milk proteins. *Journal of Agricultural and Food Chemistry, 29*(1), 11-15.

Dove, E. R., Hodgson, J. M., Puddey, I. B., Beilin, L. J., Lee, Y. P., & Mori, T. A. (2009). Skim milk compared with a fruit drink acutely reduces appetite and energy intake in overweight men and women–. *The American journal of clinical nutrition, 90*(1), 70-75.

Dressman, J. B., Berardi, R. R., Dermentzoglou, L. C., Russell, T. L., Schmaltz, S. P., Barnett, J. L., & Jarvenpaa, K. M. (1990). Upper gastrointestinal (GI) pH in young, healthy men and women. *Pharmaceutical research, 7*(7), 756-761.

Drøhse, H. B., & Foltmann, B. (1989). Specificity of milk-clotting enzymes towards bovine κ-casein. *Biochimica et Biophysica Acta (BBA)-Protein Structure and Molecular Enzymology, 995*(3), 221-224.

Drouin-Chartier, J.-P., Tremblay, A. J., Maltais-Giguère, J., Charest, A., Guinot, L., Rioux, L.-E., Labrie, S., Britten, M., Lamarche, B., & Turgeon, S. L. (2017). Differential impact of the cheese matrix on the postprandial lipid response: a randomized, crossover, controlled trial. *The American journal of clinical nutrition, 106*(6), 1358-1365.

Drummond, M. J., & Rasmussen, B. B. (2008). Leucine-enriched nutrients and the regulation of mTOR signalling and human skeletal muscle protein synthesis. *Current opinion in clinical nutrition and metabolic care, 11*(3), 222.

Dunn, B. M. (2001). Overview of pepsin-like aspartic peptidases. *Current protocols in protein science, 25*(1), 21.23. .

Dupont, D., Mandalari, G., Mollé, D., Jardin, J., Rolet-Répécaud, O., Duboz, G., Léonil, J., Mills, C. E., & Mackie, A. R. (2010). Food processing increases casein resistance to simulated infant digestion. *Molecular Nutrition & Food Research, 54*(11), 1677-1689.

Dupont, D., Le Feunteun, S., Marze, S., & Souchon, I. (2017). Structuring food to control its disintegration in the gastrointestinal tract and optimize nutrient bioavailability. *Innovative Food Science & Emerging Technologies, 46*, 83-90.

Dupont, D., Alric, M., Blanquet-Diot, S., Bornhorst, G., Cueva, C., Deglaire, A., Denis, S., Ferrua, M., Havenaar, R., & Lelieveld, J. (2018). Can dynamic in vitro digestion systems mimic the physiological reality? *Critical Reviews in Food Science and Nutrition*, 1-17.

Efigênia, M., Povoa, B., & Moraes-Santos, T. (1997). Effect of heat treatment on the nutritional quality of milk proteins. *International Dairy Journal, 7*(8-9), 609-612.

Egger, L., Ménard, O., Delgado-Andrade, C., Alvito, P., Assunção, R., Balance, S., Barberá, R., Brodkorb, A., Cattenoz, T., & Clemente, A. (2016). The harmonized INFOGEST in vitro digestion method: From knowledge to action. *Food Research International, 88*, 217-225.

Egger, L., Schlegel, P., Baumann, C., Stoffers, H., Guggisberg, D., Brügger, C., Dürr, D., Stoll, P., Vergères, G., & Portmann, R. (2017). Physiological comparability of the harmonized INFOGEST in vitro digestion method to in vivo pig digestion. *Food Research International*.

Einhorn-Stoll, U., & Drusch, S. (2015). Methods for investigation of diffusion processes and biopolymer physics in food gels. *Current Opinion in Food Science, 3*, 118-124.

Elashoff, J. D., Reedy, T. J., & Meyer, J. H. (1982). Analysis of Gastric Emptying Data. *Gastroenterology, 83*(6), 1306-1312.

Elliot, T. A., Cree, M. G., Sanford, A. P., Wolfe, R. R., & Tipton, K. D. (2006). Milk ingestion stimulates net muscle protein synthesis following resistance exercise. *Medicine & Science in Sports & Exercise, 38*(4), 667-674.

Erickson, R. H., & Kim, Y. S. (1990). Digestion and absorption of dietary protein. *Annual Review of Medicine, 41*(1), 133-139.

Fang, X., Rioux, L.-E., Labrie, S., & Turgeon, S. L. (2016). Commercial cheeses with different texture have different disintegration and protein/peptide release rates during simulated in vitro digestion. *International Dairy Journal, 56*, 169-178.

Fang, Y., & Dalgleish, D. G. (1997). Conformation of β-Lactoglobulin Studied by FTIR: Effect of pH, Temperature, and Adsorption to the Oil–Water Interface. *Journal of Colloid and Interface Science, 196*(2), 292-298.

FAO. (2003). Food energy—methods of analysis and conversion factors. *FAO Food and Nutrition Paper. Food and Agriculture Organization of the United Nations, 77*(Rome).

Feeney, E. L., Barron, R., Dible, V., Hamilton, Z., Power, Y., Tanner, L., Flynn, C., Bouchier, P., Beresford, T., & Noronha, N. (2018). Dairy matrix effects: response to consumption of dairy fat differs when eaten within the cheese matrix—a randomized controlled trial. *The American journal of clinical nutrition, 108*(4), 667-674.

Feinle, C., Kunz, P., Boesiger, P., Fried, M., & Schwizer, W. (1999). Scintigraphic validation of a magnetic resonance imaging method to study gastric emptying of a solid meal in humans. *Gut, 44*(1), 106-111.

Fekete, Á., Givens, D., & Lovegrove, J. (2015). Casein-derived lactotripeptides reduce systolic and diastolic blood pressure in a meta-analysis of randomised clinical trials. *Nutrients, 7*(1), 659-681.

Fekete, Á. A., Givens, D. I., & Lovegrove, J. A. (2016). Can milk proteins be a useful tool in the management of cardiometabolic health? An updated review of human intervention trials. *Proceedings of the Nutrition Society, 75*(3), 328-341.

Ferreira-Lazarte, A., Montilla, A., Mulet-Cabero, A.-I., Rigby, N., Olano, A., Mackie, A., & Villamiel, M. (2017). Study on the digestion of milk with prebiotic carbohydrates in a simulated gastrointestinal model. *Journal of Functional Foods, 33*, 149-154.

Ferrua, M. J., & Singh, R. P. (2010). Modeling the Fluid Dynamics in a Human Stomach to Gain Insight of Food Digestion. *Journal of Food Science, 75*(7), R151-R162.

Ferrua, M. J., & Singh, R. P. (2015). Computational modelling of gastric digestion: current challenges and future directions. *Current Opinion in Food Science, 4*, 116-123.

Fidler, J., Bharucha, A. E., Camilleri, M., Camp, J., Burton, D., Grimm, R., Riederer, S. J., Robb, R. A., & Zinsmeister, A. R. (2009). Application of magnetic

resonance imaging to measure fasting and postprandial volumes in humans. *Neurogastroenterology & Motility, 21*(1), 42-51.

Fiszman, S., & Varela, P. (2013). The satiating mechanisms of major food constituents – An aid to rational food design. *Trends in Food Science & Technology, 32*(1), 43-50.

Flanagan, J., & FitzGerald, R. J. (2003). Characterisation and quantification of the reaction(s) catalysed by transglutaminase using the o-phthaldialdehyde reagent. *Nahrung, 47*(3), 207-212.

Flourie, B., Vidon, N., Chayvialle, J., Palma, R., Franchisseur, C., & Bernier, J. (1985). Effect of increased amounts of pectin on a solid-liquid meal digestion in healthy man. *The American journal of clinical nutrition, 42*(3), 495-503.

Floury, J., Bianchi, T., Thévenot, J., Dupont, D., Jamme, F., Lutton, E., Panouillé, M., Boué, F., & Le Feunteun, S. (2018). Exploring the breakdown of dairy protein gels during in vitro gastric digestion using time-lapse synchrotron deep-UV fluorescence microscopy. *Food Chemistry, 239*, 898-910.

Fox, P., & Brodkorb, A. (2008). The casein micelle: historical aspects, current concepts and significance. *International Dairy Journal, 18*(7), 677-684.

Fox, P. F., McSweeney, P. L., & Paul, L. (1998). *Dairy chemistry and biochemistry*: London: Blackie Academic & Professional.

Frost, G., Brynes, A. E., Ellis, S., Milton, J. E., Nematy, M., & Philippou, E. (2006). Nutritional influences on gut hormone release. *Current Opinion in Endocrinology, Diabetes and Obesity, 13*(1), 42-48.

Gannon, M. C., & Nuttall, F. Q. (2010). Amino acid ingestion and glucose metabolism—a review. *IUBMB life, 62*(9), 660-668.

Garcia, C., Antona, C., Robert, B., Lopez, C., & Armand, M. (2014). The size and interfacial composition of milk fat globules are key factors controlling triglycerides bioavailability in simulated human gastro-duodenal digestion. *Food Hydrocolloids, 35*, 494-504.

Garlick, P. J. (2005). The role of leucine in the regulation of protein metabolism. *The Journal of nutrition, 135*(6), 1553S-1556S.

Gass, J., Vora, H., Hofmann, A. F., Gray, G. M., & Khosla, C. (2007). Enhancement of dietary protein digestion by conjugated bile acids. *Gastroenterology, 133*(1), 16-23.

Gaudichon, C., Roos, N., Mahé, S., Sick, H., Bouley, C., & Tomé, D. (1994). Gastric emptying regulates the kinetics of nitrogen absorption from 15N-labeled milk and 15N-labeled yogurt in miniature pigs. *The Journal of nutrition, 124*(10), 1970-1977.

Gaudichon, C., Mahé, S., Roos, N., Benamouzig, R., Luengo, C., Huneau, J.-F., Sick, H., Bouley, C., Rautureau, J., & Tome, D. (1995). Exogenous and endogenous nitrogen flow rates and level of protein hydrolysis in the human jejunum after [15 N] milk and [15 N] yoghurt ingestion. *British Journal of Nutrition, 74*(2), 251-260.

Gaudichon, C., Mahé, S., Benamouzig, R., Luengo, C., Fouillet, H., Daré, S., Van Oycke, M., Ferrière, F., Rautureau, J., & Tomé, D. (1999). Net postprandial utilization of [15N]-labeled milk protein nitrogen is influenced by diet composition in humans. *The Journal of nutrition, 129*(4), 890-895.

Gebauer, S. K., Novotny, J. A., Bornhorst, G. M., & Baer, D. J. (2016). Food processing and structure impact the metabolizable energy of almonds. *Food & function, 7*(10), 4231-4238.

Geraedts, M. C., Troost, F. J., De Ridder, R. J., Bodelier, A. G., Masclee, A. A., & Saris, W. H. (2012). Validation of Ussing chamber technology to study satiety hormone release from human duodenal specimens. *Obesity, 20*(3), 678-682.

Gilani, G. S., Xiao, C., & Lee, N. (2008). Need for accurate and standardized determination of amino acids and bioactive peptides for evaluating protein quality and potential health effects of foods and dietary supplements. *Journal of AOAC International, 91*(4), 894-900.

Giroux, H. J., Bouchard, C., & Britten, M. (2014). Combined effect of renneting pH, cooking temperature, and dry salting on the contraction kinetics of rennet-induced milk gels. *International Dairy Journal, 35*(1), 70-74.

Givens, D. I. (2017). Saturated fats, dairy foods and health: A curious paradox? *Nutrition Bulletin, 42*(3), 274-282.

Goetze, O., Steingoetter, A., Menne, D., van der Voort, I. R., Kwiatek, M. A., Boesiger, P., Weishaupt, D., Thumshirn, M., Fried, M., & Schwizer, W. (2007). The effect of macronutrients on gastric volume responses and gastric emptying in humans: a magnetic resonance imaging study. *American Journal of Physiology-Gastrointestinal and Liver Physiology, 292*(1), G11-G17.

Goetze, O., Treier, R., Fox, M., Steingoetter, A., Fried, M., Boesiger, P., & Schwizer, W. (2009). The effect of gastric secretion on gastric physiology and emptying in the fasted and fed state assessed by magnetic resonance imaging. *Neurogastroenterology & Motility, 21*(7), 725-e742.

Golding, M., Wooster, T. J., Day, L., Xu, M., Lundin, L., Keogh, J., & Clifton, P. (2011). Impact of gastric structuring on the lipolysis of emulsified lipids. *Soft Matter, 7*(7), 3513-3523.

Goodman, B. E. (2010). Insights into digestion and absorption of major nutrients in humans. *Advances in physiology education, 34*(2), 44-53.

Gorissen, S. H., Burd, N. A., Hamer, H. M., Gijsen, A. P., Groen, B. B., & van Loon, L. J. (2014). Carbohydrate coingestion delays dietary protein digestion and absorption but does not modulate postprandial muscle protein accretion. *The Journal of Clinical Endocrinology & Metabolism, 99*(6), 2250-2258.

Gorissen, S. H., Rémond, D., & Van Loon, L. J. (2015). The muscle protein synthetic response to food ingestion. *Meat science, 109*, 96-100.

Gorissen, S. H., & Witard, O. C. (2018). Characterising the muscle anabolic potential of dairy, meat and plant-based protein sources in older adults. *Proceedings of the Nutrition Society, 77*(1), 20-31.

Griffin, B. (2017). Serum low-density lipoprotein as a dietary responsive biomarker of cardiovascular disease risk: Consensus and confusion. *Nutrition Bulletin, 42*(3), 266-273.

Grøndahl, M. L., & Skadhauge, E. (1997). Effect of mucosal amino acids on SCC and Na and Cl fluxes in the porcine small intestine. *Comparative Biochemistry and Physiology Part A: Physiology, 118*(2), 233-237.

Guerra, A., Etienne-Mesmin, L., Livrelli, V., Denis, S., Blanquet-Diot, S., & Alric, M. (2012). Relevance and challenges in modeling human gastric and small intestinal digestion. *Trends in Biotechnology, 30*(11), 591-600.

Guinee, T. P., Gorry, C. B., O'Callaghan, D. J., O'Kennedy, B. T., O'Brie, N., & Fenelon, M. A. (1997). The effects of composition and some processing treatments on the rennet coagulation properties of milk. *International Journal of Dairy Technology, 50*(3), 99-106.

Guo, M., Fox, P., Flynn, A., & Kindstedt, P. (1995). Susceptibility of β-lactoglobulin and sodium caseinate to proteolysis by pepsin and trypsin. *Journal of Dairy Science, 78*(11), 2336-2344.

Guo, Q., Ye, A., Lad, M., Dalgleish, D., & Singh, H. (2013). The breakdown properties of heat-set whey protein emulsion gels in the human mouth. *Food Hydrocolloids, 33*(2), 215-224.

Guo, Q., Ye, A., Lad, M., Dalgleish, D., & Singh, H. (2014). Behaviour of whey protein emulsion gel during oral and gastric digestion: effect of droplet size. *Soft Matter, 10*(23), 4173-4183.

Guo, Q., Ye, A., Lad, M., Ferrua, M., Dalgleish, D., & Singh, H. (2015). Disintegration kinetics of food gels during gastric digestion and its role on gastric emptying: an in vitro analysis. *Food & function, 6*(3), 756-764.

Guyomarc'h, F., Law, A. J. R., & Dalgleish, D. G. (2003). Formation of Soluble and Micelle-Bound Protein Aggregates in Heated Milk. *Journal of Agricultural and Food Chemistry, 51*(16), 4652-4660.

Hall, W., Millward, D., Long, S., & Morgan, L. (2003). Casein and whey exert different effects on plasma amino acid profiles, gastrointestinal hormone secretion and appetite. *British Journal of Nutrition, 89*(02), 239-248.

Helbig, A., Silletti, E., Aken, G. A., Oosterveld, A., Minekus, M., Hamer, R. J., & Gruppen, H. (2012). Lipid Digestion of Protein Stabilized Emulsions Investigated in a Dynamic In Vitro Gastro-Intestinal Model System. *Food Digestion, 4*(2), 58-68.

Hellström, P. M., Grybäck, P., & Jacobsson, H. (2006). The physiology of gastric emptying. *Best Practice & Research Clinical Anaesthesiology, 20*(3), 397-407.

Hetherington, M., Cunningham, K., Dye, L., Gibson, E., Gregersen, N., Halford, J., Lawton, C., Lluch, A., Mela, D., & Van Trijp, H. (2013). Potential benefits of satiety to the consumer: scientific considerations. *Nutrition research reviews, 26*(1), 22-38.

Hila, A., Bouali, H., Xue, S., Knuff, D., & Castell, D. O. (2006). Postprandial stomach contents have multiple acid layers. *Journal of clinical gastroenterology, 40*(7), 612-617.

Hinsberger, A., & Sandhu, B. (2004). Digestion and absorption. *Current Paediatrics, 14*(7), 605-611.

Hjerpsted, J., Leedo, E., & Tholstrup, T. (2011). Cheese intake in large amounts lowers LDL-cholesterol concentrations compared with butter intake of equal fat content–. *The American journal of clinical nutrition, 94*(6), 1479-1484.

Holt, S., Reid, J., Taylor, T., Tothill, P., & Heading, R. (1982). Gastric emptying of solids in man. *Gut, 23*(4), 292-296.

Hug, M. J. (2001). Transepithelial measurements using the Ussing chamber. *Provided through: The European working group on CFTR Expression*, 1-10.

Hunt, J., & Stubbs, D. (1975). The volume and energy content of meals as determinants of gastric emptying. *The Journal of physiology, 245*(1), 209-225.

Hunt, J., Smith, J., & Jiang, C. (1985). Effect of meal volume and energy density on the gastric emptying of carbohydrates. *Gastroenterology, 89*(6), 1326-1330.

Hussein, M. O., Hoad, C. L., Wright, J., Singh, G., Stephenson, M. C., Cox, E. F., Placidi, E., Pritchard, S. E., Costigan, C., & Ribeiro, H. (2015). Fat emulsion intragastric stability and droplet size modulate gastrointestinal responses and subsequent food intake in young adults. *The Journal of nutrition, 145*(6), 1170-1177.

References

Iddan, G., Meron, G., Glukhovsky, A., & Swain, P. (2000). Wireless capsule endoscopy. *Nature, 405*(6785), 417.

Inouye, K., & Fruton, J. S. (1967). Studies on the specificity of pepsin. *Biochemistry, 6*(6), 1765-1777.

Islam, M. A., Devle, H., Comi, I., Ulleberg, E. K., Rukke, E.-O., Vegarud, G. E., & Ekeberg, D. (2017). Ex vivo digestion of raw, pasteurised and homogenised milk - Effects on lipolysis and proteolysis. *International Dairy Journal, 65*, 14-19.

Janssen, P., Vanden Berghe, P., Verschueren, S., Lehmann, A., Depoortere, I., & Tack, J. (2011). Review article: the role of gastric motility in the control of food intake. *Alimentary pharmacology & therapeutics, 33*(8), 880-894.

Jauhiainen, T., & Korpela, R. (2007). Milk peptides and blood pressure. *Journal of Nutrition, 137*.

Kalantzi, L., Goumas, K., Kalioras, V., Abrahamsson, B., Dressman, J. B., & Reppas, C. (2006). Characterization of the human upper gastrointestinal contents under conditions simulating bioavailability/bioequivalence studies. *Pharmaceutical research, 23*(1), 165-176.

Karhunen, L. J., Juvonen, K. R., Huotari, A., Purhonen, A. K., & Herzig, K. H. (2008). Effect of protein, fat, carbohydrate and fibre on gastrointestinal peptide release in humans. *Regul Pept, 149*(1-3), 70-78.

Kaspar, H., Dettmer, K., Gronwald, W., & Oefner, P. J. (2008). Automated GC–MS analysis of free amino acids in biological fluids. *Journal of Chromatography B, 870*(2), 222-232.

Kaufmann, W. (1984). Influences of different technological treatments of milk on the digestion in the stomach. VI. Estimation of amino acid and urea concentrations in the blood: conclusions regarding the nutritional evaluation. *Milchwissenschaft (Germany, FR)*.

Kethireddipalli, P., Hill, A. R., & Dalgleish, D. G. (2010). Protein interactions in heat-treated milk and effect on rennet coagulation. *International Dairy Journal, 20*(12), 838-843.

Kloetzer, L., Chey, W., McCallum, R., Koch, K., Wo, J., Sitrin, M., Katz, L., Lackner, J., Parkman, H., & Wilding, G. (2010). Motility of the antroduodenum in healthy and gastroparetics characterized by wireless motility capsule. *Neurogastroenterology & Motility, 22*(5), 527.

Kong, F., & Singh, R. (2008). Disintegration of solid foods in human stomach. *Journal of Food Science, 73*(5), R67-R80.

Kong, F., & Singh, R. P. (2010). A Human Gastric Simulator (HGS) to Study Food Digestion in Human Stomach. *Journal of Food Science, 75*(9), E627-E635.

Koziolek, M., Garbacz, G., Neumann, M., & Weitschies, W. (2013). Simulating the postprandial stomach: physiological considerations for dissolution and release testing. *Molecular Pharmaceutics, 10*(5), 1610-1622.

Krichevsky, O., & Bonnet, G. (2002). Fluorescence correlation spectroscopy: the technique and its applications. *Reports on Progress in Physics, 65*(2), 251.

Kwiatek, M. A., Menne, D., Steingoetter, A., Goetze, O., Forras-Kaufman, Z., Kaufman, E., Fruehauf, H., Boesiger, P., Fried, M., & Schwizer, W. (2009). Effect of meal volume and calorie load on postprandial gastric function and emptying: studies under physiological conditions by combined fiber-optic pressure measurement and MRI. *American Journal of Physiology-Gastrointestinal and Liver Physiology, 297*(5), G894-G901.

Lacroix, M., Bos, C., Léonil, J., Airinei, G., Luengo, C., Daré, S., Benamouzig, R., Fouillet, H., Fauquant, J., Tomé, D., & Gaudichon, C. (2006a). Compared with casein or total milk protein, digestion of milk soluble proteins is too rapid to sustain the anabolic postprandial amino acid requirement. *The American journal of clinical nutrition, 84*(5), 1070-1079.

Lacroix, M., Léonil, J., Bos, C., Henry, G., Airinei, G., Fauquant, J., Tomé, D., & Gaudichon, C. (2006b). Heat markers and quality indexes of industrially heat-treated [15N] milk protein measured in rats. *Journal of Agricultural and Food Chemistry, 54*(4), 1508-1517.

Lacroix, M., Bon, C., Bos, C., Léonil, J., Benamouzig, R., Luengo, C., Fauquant, J., Tomé, D., & Gaudichon, C. (2008). Ultra High Temperature Treatment, but Not Pasteurization, Affects the Postprandial Kinetics of Milk Proteins in Humans. *The Journal of nutrition, 138*(12), 2342-2347.

Lambers, T. T., van den Bosch, W. G., & de Jong, S. (2013). Fast and Slow Proteins: Modulation of the Gastric Behavior of Whey and Casein In Vitro. *Food Digestion, 4*(1), 1-6.

Lamothe, S., Corbeil, M.-M., Turgeon, S. L., & Britten, M. (2012). Influence of cheese matrix on lipid digestion in a simulated gastro-intestinal environment. *Food & function, 3*(7), 724-731.

Lamothe, S., Rémillard, N., Tremblay, J., & Britten, M. (2017). Influence of dairy matrices on nutrient release in a simulated gastrointestinal environment. *Food Research International, 92*, 138-146.

Lang, V., Bellisle, F., Oppert, J. M., Craplet, C., Bornet, F. R., Slama, G., & Guy-Grand, B. (1998). Satiating effect of proteins in healthy subjects: a comparison of egg albumin, casein, gelatin, soy protein, pea protein, and wheat gluten. *The American journal of clinical nutrition, 67*(6), 1197-1204.

Le Feunteun, S., Barbé, F., Rémond, D., Ménard, O., Le Gouar, Y., Dupont, D., & Laroche, B. (2014). Impact of the dairy matrix structure on milk protein digestion kinetics: mechanistic modelling based on mini-pig in vivo data. *Food and bioprocess technology, 7*(4), 1099-1113.

Ledeboer, M., Masclee, A., Jansen, J., & Lamers, C. (1995). Effect of equimolar amounts of long-chain triglycerides and medium-chain triglycerides on small-bowel transit time in humans. *Journal of Parenteral and Enteral Nutrition, 19*(1), 5-8.

Lee, S. J., & Sherbon, J. W. (2002). Chemical changes in bovine milk fat globule membrane caused by heat treatment and homogenization of whole milk. *Journal of Dairy Research, 69*(4), 555-567.

Lett, A. M., Norton, J. E., & Yeomans, M. R. (2016a). Emulsion oil droplet size significantly affects satiety: A pre-ingestive approach. *Appetite, 96*, 18-24.

Lett, A. M., Yeomans, M. R., Norton, I. T., & Norton, J. E. (2016b). Enhancing expected food intake behaviour, hedonics and sensory characteristics of oil-in-water emulsion systems through microstructural properties, oil droplet size and flavour. *Food quality and preference, 47*, 148-155.

Lin, H. C., Prather, C., Fisher, R. S., Meyer, J. H., Summers, R. W., Pimentel, M., Mccallum, R. W., Akkermans, L. M., Loening-Baucke, V., & Transit, A. T. F. C. o. G. (2005). Measurement of gastrointestinal transit. *Digestive Diseases and Sciences, 50*(6), 989-1004.

Lodaite, K., Chevalier, F., Armaforte, E., & Kelly, A. L. (2009). Effect of high-pressure homogenisation on rheological properties of rennet-induced skim milk and standardised milk gels. *Journal of Dairy Research, 76*(3), 294-300.

References

Lopez, C. (2005). Focus on the supramolecular structure of milk fat in dairy products. *Reproduction Nutrition Development, 45*(4), 497-511.

Lopez, C. (2011). Milk fat globules enveloped by their biological membrane: Unique colloidal assemblies with a specific composition and structure. *Current Opinion in Colloid & Interface Science, 16*(5), 391-404.

Lorén, N., Nydén, M., & Hermansson, A.-M. (2009). Determination of local diffusion properties in heterogeneous biomaterials. *Advances in Colloid and Interface Science, 150*(1), 5-15.

Lorenzen, J., Frederiksen, R., Hoppe, C., Hvid, R., & Astrup, A. (2012). The effect of milk proteins on appetite regulation and diet-induced thermogenesis. *European journal of clinical nutrition, 66*(5), 622.

Luhovyy, B. L., Akhavan, T., & Anderson, G. H. (2007). Whey Proteins in the Regulation of Food Intake and Satiety. *Journal of the American College of Nutrition, 26*(6), 704S-712S.

Luo, J., Wang, Z. W., Wang, F., Zhang, H., Lu, J., Guo, H. Y., & Ren, F. Z. (2014). Cryo-SEM images of native milk fat globule indicate small casein micelles are constituents of the membrane. *RSC Advances, 4*(90), 48963-48966.

Luo, Q., Borst, J. W., Westphal, A. H., Boom, R. M., & Janssen, A. E. (2017). Pepsin diffusivity in whey protein gels and its effect on gastric digestion. *Food Hydrocolloids, 66*, 318-325.

Macierzanka, A., Sancho, A. I., Mills, E. C., Rigby, N. M., & Mackie, A. R. (2009). Emulsification alters simulated gastrointestinal proteolysis of β-casein and β-lactoglobulin. *Soft Matter, 5*(3), 538-550.

Macierzanka, A., Böttger, F., Lansonneur, L., Groizard, R., Jean, A.-S., Rigby, N. M., Cross, K., Wellner, N., & Mackie, A. R. (2012). The effect of gel structure on the kinetics of simulated gastrointestinal digestion of bovine β-lactoglobulin. *Food Chemistry, 134*(4), 2156-2163.

Mackie, A., Rafiee, H., Malcolm, P., Salt, L., & van Aken, G. (2013). Specific food structures supress appetite through reduced gastric emptying rate. *Am J Physiol Gastrointest Liver Physiol, 304*(11), G1038-1043.

Mackie, A. R., & Macierzanka, A. (2010). Colloidal aspects of protein digestion. *Current Opinion in Colloid & Interface Science, 15*(1), 102-108.

Mahé, S., Messing, B., Thuillier, F., & Tomé, D. (1991). Digestion of bovine milk proteins in patients with a high jejunostomy. *The American journal of clinical nutrition, 54*(3), 534-538.

Mahé, S., Marteau, P., Huneau, J.-F., Thuillier, F., & Tomé, D. (1994). Intestinal nitrogen and electrolyte movements following fermented milk ingestion in man. *British Journal of Nutrition, 71*(2), 169-180.

Mahé, S., Roos, N., Benamouzig, R., Davin, L., Luengo, C., Gagnon, L., Gausserges, N., Rautureau, J., & Tome, D. (1996). Gastrojejunal kinetics and the digestion of N-15 beta-lactoglobulin and casein in humans: The influence of the nature and quantity of the protein. *American Journal of Clinical Nutrition, 63*(4), 546-552.

Malagelada, J.-R., Longstreth, G. F., Summerskill, W. H. J., & Go, V. L. W. (1976). Measurement of Gastric Functions During Digestion of Ordinary Solid Meals in Man. *Gastroenterology, 70*(2), 203-210.

Malagelada, J.-R., Go, V. L., & Summerskill, W. (1979). Different gastric, pancreatic, and biliary responses to solid-liquid or homogenized meals. *Digestive Diseases and Sciences, 24*(2), 101-110.

Malagelada, J. R., & Azpiroz, F. (1989). Determinants of gastric emptying and transit in the small intestine. *Handbook of physiology, section, 6*, 909-937.

Maljaars, P. W., Peters, H. P., Mela, D. J., & Masclee, A. A. (2008). Ileal brake: a sensible food target for appetite control. A review. *Physiology & Behavior, 95*(3), 271-281.

Maljaars, P. W. J., van der Wal, R. J. P., Wiersma, T., Peters, H. P. F., Haddeman, E., & Masclee, A. A. M. (2012). The effect of lipid droplet size on satiety and peptide secretion is intestinal site-specific. *Clinical Nutrition, 31*(4), 535-542.

Månsson, H. L. (2008). Fatty acids in bovine milk fat. *Food & nutrition research, 52*.

Marciani, L., Gowland, P. A., Spiller, R. C., Manoj, P., Moore, R. J., Young, P., & Fillery-Travis, A. J. (2001). Effect of meal viscosity and nutrients on satiety, intragastric dilution, and emptying assessed by MRI. *American Journal of Physiology-Gastrointestinal and Liver Physiology, 280*(6), G1227-G1233.

Marciani, L., Wickham, M., Singh, G., Bush, D., Pick, B., Cox, E., Fillery-Travis, A., Faulks, R., Marsden, C., Gowland, P. A., & Spiller, R. C. (2007). Enhancement of intragastric acid stability of a fat emulsion meal delays gastric emptying and increases cholecystokinin release and gallbladder contraction. *American Journal of Physiology - Gastrointestinal and Liver Physiology, 292*(6), G1607-G1613.

Marciani, L., Faulks, R., Wickham, M. S., Bush, D., Pick, B., Wright, J., Cox, E. F., Fillery-Travis, A., Gowland, P. A., & Spiller, R. C. (2008). Effect of intragastric acid stability of fat emulsions on gastric emptying, plasma lipid profile and postprandial satiety. *British Journal of Nutrition, 101*(06), 919-928.

Marciani, L. (2011). Assessment of gastrointestinal motor functions by MRI: a comprehensive review. *Neurogastroenterology & Motility, 23*(5), 399-407.

Marciani, L., Hall, N., Pritchard, S. E., Cox, E. F., Totman, J. J., Lad, M., Hoad, C. L., Foster, T. J., Gowland, P. A., & Spiller, R. C. (2012). Preventing Gastric Sieving by Blending a Solid/Water Meal Enhances Satiation in Healthy Humans. *The Journal of nutrition, 142*(7), 1253-1258.

Mariotti, F., Mahé, S., Luengo, C., Benamouzig, R., & Tomé, D. (2000). Postprandial modulation of dietary and whole-body nitrogen utilization by carbohydrates in humans. *The American journal of clinical nutrition, 72*(4), 954-962.

Mariotti, F., Valette, M., Lopez, C., Fouillet, H., Famelart, M.-H., Mathé, V., Airinei, G., Benamouzig, R., Gaudichon, C., Tomé, D., Tsikas, D., & Huneau, J. F. (2015). Casein Compared with Whey Proteins Affects the Organization of Dietary Fat during Digestion and Attenuates the Postprandial Triglyceride Response to a Mixed High-Fat Meal in Healthy, Overweight Men. *The Journal of nutrition, 145*(12), 2657-2664.

Mateo, M., Everard, C., Fagan, C. C., O'Donnell, C., Castillo, M., Payne, F., & O'Callaghan, D. (2009). Effect of milk fat concentration and gel firmness on syneresis during curd stirring in cheese-making. *International Dairy Journal, 19*(4), 264-268.

McClements, D. J., & Li, Y. (2010). Structured emulsion-based delivery systems: Controlling the digestion and release of lipophilic food components. *Advances in Colloid and Interface Science, 159*(2), 213-228.

McHugh, P. R., & Moran, T. H. (1979). Calories and gastric emptying: a regulatory capacity with implications for feeding. *American Journal of Physiology-Regulatory, Integrative and Comparative Physiology, 236*(5), R254-R260.

References

McLauchlan, G., Fullarton, G., Crean, G., & McColl, K. (1989). Comparison of gastric body and antral pH: a 24 hour ambulatory study in healthy volunteers. *Gut, 30*(5), 573-578.

Meisel, H., & Hagemeister, H. (1984). [Influences of different technological treatments of milk on the digestion in the stomach. II. Gastric passage of different milk constituents].[German]. *Milchwissenschaft.*

Ménard, O., Picque, D., & Dupont, D. (2015). The DIDGI® System. In *The Impact of Food Bioactives on Health*, (pp. 73-81): Springer.

Ménard, O., Famelart, M.-H., Deglaire, A., Le Gouar, Y., Guérin, S., Malbert, C.-H., & Dupont, D. (2018). Gastric Emptying and Dynamic In Vitro Digestion of Drinkable Yogurts: Effect of Viscosity and Composition. *Nutrients, 10*(9), 1308.

Meyer, J. H., Elashoff, J., Porter-Fink, V., Dressman, J., & Amidon, G. L. (1988). Human postprandial gastric emptying of 1–3-millimeter spheres. *Gastroenterology, 94*(6), 1315-1325.

Michalski, M.-C., & Januel, C. (2006). Does homogenization affect the human health properties of cow's milk? *Trends in Food Science & Technology, 17*(8), 423-437.

Michalski, M.-C. (2009). Specific molecular and colloidal structures of milk fat affecting lipolysis, absorption and postprandial lipemia. *European Journal of Lipid Science and Technology, 111*(5), 413-431.

Michalski, M.-C., Genot, C., Gayet, C., Lopez, C., Fine, F., Joffre, F., Vendeuvre, J.-L., Bouvier, J., Chardigny, J.-M., & Raynal-Ljutovac, K. (2013). Multiscale structures of lipids in foods as parameters affecting fatty acid bioavailability and lipid metabolism. *Progress in Lipid Research, 52*(4), 354-373.

Mills, S., Ross, R., Hill, C., Fitzgerald, G., & Stanton, C. (2011). Milk intelligence: Mining milk for bioactive substances associated with human health. *International Dairy Journal, 21*(6), 377-401.

Minekus, M., Alminger, M., Alvito, P., Ballance, S., Bohn, T., Bourlieu, C., Carriere, F., Boutrou, R., Corredig, M., Dupont, D., Dufour, C., Egger, L., Golding, M., Karakaya, S., Kirkhus, B., Le Feunteun, S., Lesmes, U., Macierzanka, A., Mackie, A., Marze, S., McClements, D. J., Menard, O., Recio, I., Santos, C. N., Singh, R. P., Vegarud, G. E., Wickham, M. S. J., Weitschies, W., & Brodkorb, A. (2014). A standardised static in vitro digestion method suitable for food - an international consensus. *Food & function, 5*(6), 1113-1124.

Minekus, M. (2015). The TNO gastro-intestinal model (TIM). In *The impact of food bioactives on health*, (pp. 37-46): Springer.

Miranda, G., & Pelissier, J.-P. (1981). In vivo studies on the digestion of bovine caseins in the rat stomach. *Journal of Dairy Research, 48*(2), 319-326.

Miranda, G., & Pelissier, J.-P. (1987). Influence of heat treatment of bovine skim-milk on in vivo digestion in rat stomach. *Lait, 67*(3), 365-377.

Moore, J., Christian, P., & Coleman, R. (1981). Gastric emptying of varying meal weight and composition in man. *Digestive Diseases and Sciences, 26*(1), 16-22.

Moran, T. H., Wirth, J. B., Schwartz, G. J., & McHugh, P. R. (1999). Interactions between gastric volume and duodenal nutrients in the control of liquid gastric emptying. *American Journal of Physiology-Regulatory, Integrative and Comparative Physiology, 276*(4), R997-R1002.

Morgan, F., Léonil, J., Mollé, D., & Bouhallab, S. (1999). Modification of Bovine β-Lactoglobulin by Glycation in a Powdered State or in an Aqueous Solution:

Effect on Association Behavior and Protein Conformation. *Journal of Agricultural and Food Chemistry, 47*(1), 83-91.

Mortensen, L. S., Hartvigsen, M. L., Brader, L. J., Astrup, A., Schrezenmeir, J., Holst, J. J., Thomsen, C., & Hermansen, K. (2009). Differential effects of protein quality on postprandial lipemia in response to a fat-rich meal in type 2 diabetes: comparison of whey, casein, gluten, and cod protein–. *The American journal of clinical nutrition, 90*(1), 41-48.

Mu, H., & Høy, C.-E. (2004). The digestion of dietary triacylglycerols. *Progress in Lipid Research, 43*(2), 105-133.

Neirinckx, E., Vervaet, C., De Boever, S., Remon, J. P., Gommeren, K., Daminet, S., De Backer, P., & Croubels, S. (2010). Species comparison of oral bioavailability, first-pass metabolism and pharmacokinetics of acetaminophen. *Research in Veterinary Science, 89*(1), 113-119.

Nemkov, T., D'Alessandro, A., & Hansen, K. C. (2015). Three-minute method for amino acid analysis by UHPLC and high-resolution quadrupole orbitrap mass spectrometry. *Amino Acids, 47*(11), 2345-2357.

Newton, J. M. (2010). Gastric emptying of multi-particulate dosage forms. *International Journal of Pharmaceutics, 395*(1-2), 2-8.

Nielsen, P., Petersen, D., & Dambmann, C. (2001). Improved method for determining food protein degree of hydrolysis. *Journal of Food Science, 66*(5), 642-646.

Nilsson, M., Stenberg, M., Frid, A. H., Holst, J. J., & Björck, I. M. (2004). Glycemia and insulinemia in healthy subjects after lactose-equivalent meals of milk and other food proteins: the role of plasma amino acids and incretins. *The American journal of clinical nutrition, 80*(5), 1246-1253.

Norton, J. E., Wallis, G. A., Spyropoulos, F., Lillford, P. J., & Norton, I. T. (2014). Designing food structures for nutrition and health benefits. *Annual review of food science and technology, 5*, 177-195.

Pal, A., Indireshkumar, K., Schwizer, W., Abrahamsson, B., Fried, M., & Brasseur, J. G. (2004). Gastric flow and mixing studied using computer simulation. *Proceedings of the Royal Society of London B: Biological Sciences, 271*(1557), 2587-2594.

Pal, S., Ellis, V., & Dhaliwal, S. (2010). Effects of whey protein isolate on body composition, lipids, insulin and glucose in overweight and obese individuals. *British Journal of Nutrition, 104*(5), 716-723.

Panahi, S., El Khoury, D., Kubant, R., Akhavan, T., Luhovyy, B. L., Goff, H. D., & Anderson, G. H. (2014). Mechanism of action of whole milk and its components on glycemic control in healthy young men. *The Journal of Nutritional Biochemistry, 25*(11), 1124-1131.

Parada, J., & Aguilera, J. M. (2007). Food Microstructure Affects the Bioavailability of Several Nutrients. *Journal of Food Science, 72*(2), R21-R32.

Pennings, B., Boirie, Y., Senden, J. M., Gijsen, A. P., Kuipers, H., & van Loon, L. J. (2011). Whey protein stimulates postprandial muscle protein accretion more effectively than do casein and casein hydrolysate in older men–. *The American journal of clinical nutrition, 93*(5), 997-1005.

Pereira, P. C. (2014). Milk nutritional composition and its role in human health. *Nutrition, 30*(6), 619-627.

Peters, H. P. F., Bouwens, E. C. M., Schuring, E. A. H., Haddeman, E., Velikov, K. P., & Melnikov, S. M. (2014). The effect of submicron fat droplets in a drink on satiety, food intake, and cholecystokinin in healthy volunteers. *European journal of nutrition, 53*(3), 723-729.

Piper, D., & Fenton, B. H. (1965). pH stability and activity curves of pepsin with special reference to their clinical importance. *Gut, 6*(5), 506.

Rayner, C. K., Samsom, M., Jones, K. L., & Horowitz, M. (2001). Relationships of upper gastrointestinal motor and sensory function with glycemic control. *Diabetes care, 24*(2), 371-381.

Reidy, P. T., Walker, D. K., Dickinson, J. M., Gundermann, D. M., Drummond, M. J., Timmerman, K. L., Fry, C. S., Borack, M. S., Cope, M. B., & Mukherjea, R. (2013). Protein Blend Ingestion Following Resistance Exercise Promotes Human Muscle Protein Synthesis1–4. *The Journal of nutrition, 143*(4), 410-416.

Reitelseder, S., Agergaard, J., Doessing, S., Helmark, I. C., Lund, P., Kristensen, N. B., Frystyk, J., Flyvbjerg, A., Schjerling, P., Hall, G. v., Kjaer, M., & Holm, L. (2011). Whey and casein labeled with l-[1-13C]leucine and muscle protein synthesis: effect of resistance exercise and protein ingestion. *American Journal of Physiology-Endocrinology And Metabolism, 300*(1), E231-E242.

Rolls, B., & Porter, J. (1973). Some effects of processing and storage on the nutritive value of milk and milk products. *Proceedings of the Nutrition Society, 32*(1), 9-15.

Rowland, S. J. (1938). 175. The precipitation of the proteins in milk. I. Casein. II. Total proteins. III. Globulin. IV. Albumin and Proteose-peptone. *Journal of Dairy Research, 9*(1), 30-41.

Rutherfurd, S., & Moughan, P. (2005). Digestible reactive lysine in selected milk-based products. *Journal of Dairy Science, 88*(1), 40-48.

Sanaka, M., Yamamoto, T., & Kuyama, Y. (2008). Retention, fixation, and loss of the [13 C] label: A review for the understanding of gastric emptying breath tests. *Digestive Diseases and Sciences, 53*(7), 1747.

Sánchez-Rivera, L., Ménard, O., Recio, I., & Dupont, D. (2015). Peptide mapping during dynamic gastric digestion of heated and unheated skimmed milk powder. *Food Research International, 77*, 132-139.

Sanggaard, K., Holst, J., Rehfeld, J., Sandström, B., Raben, A., & Tholstrup, T. (2004). Different effects of whole milk and a fermented milk with the same fat and lactose content on gastric emptying and postprandial lipaemia, but not on glycaemic response and appetite. *British Journal of Nutrition, 92*(3), 447-459.

Santangelo, A., Peracchi, M., Conte, D., Fraquelli, M., & Porrini, M. (1998). Physical state of meal affects gastric emptying, cholecystokinin release and satiety. *British Journal of Nutrition, 80*(6), 521-527.

Sauter, M. M., Steingoetter, A., Curcic, J., Treier, R., Kuyumcu, S., Fried, M., Boesiger, P., Schwizer, W., & Goetze, O. (2011). Quantification of Meal Induced Gastric Secretion and Its Effect on Caloric Emptying by Magnetic Resonance Imaging (MRI). *Gastroenterology, 140*(5), S-297.

Scanff, P., Savalle, B., Miranda, G., Pelissier, J. P., Guilloteau, P., & Toullec, R. (1990). In vivo gastric digestion of milk proteins. Effect of technological treatments. *Journal of Agricultural and Food Chemistry, 38*(8), 1623-1629.

Schaafsma, G. (2000). The Protein Digestibility–Corrected Amino Acid Score. *The Journal of nutrition, 130*(7), 1865S-1867S.

Schreiber, R. (2001). Heat-induced modifications in casein dispersions affecting their rennetability. *International Dairy Journal, 11*(4-7), 553-558.

Schulze, K. (2006). Imaging and modelling of digestion in the stomach and the duodenum. *Neurogastroenterology & Motility, 18*(3), 172-183.

Schwizer, W., Fraser, R., Borovicka, J., Crelier, G., Boesiger, P., & Fried, M. (1994). Measurement of gastric emptying and gastric motility by magnetic resonance imaging (MRI). *Digestive Diseases and Sciences, 39*(12), 101S-103S.

Schwizer, W., Steingoetter, A., & Fox, M. (2006). Magnetic resonance imaging for the assessment of gastrointestinal function. *Scandinavian journal of gastroenterology, 41*(11), 1245-1260.

Seimon, R. V., Wooster, T., Otto, B., Golding, M., Day, L., Little, T. J., Horowitz, M., Clifton, P. M., & Feinle-Bisset, C. (2009). The droplet size of intraduodenal fat emulsions influences antropyloroduodenal motility, hormone release, and appetite in healthy males. *The American journal of clinical nutrition, 89*(6), 1729-1736.

Shani-Levi, C., Levi-Tal, S., & Lesmes, U. (2013). Comparative performance of milk proteins and their emulsions under dynamic in vitro adult and infant gastric digestion. *Food Hydrocolloids, 32*(2), 349-357.

Sharma, S. K., & Dalgleish, D. G. (1993). Interactions between milk serum proteins and synthetic fat globule membrane during heating of homogenized whole milk. *Journal of Agricultural and Food Chemistry, 41*(9), 1407-1412.

Siegel, J. A., Urbain, J. L., Adler, L. P., Charkes, N. D., Maurer, A. H., Krevsky, B., Knight, L. C., Fisher, R. S., & Malmud, L. S. (1988). Biphasic nature of gastric emptying. *Gut, 29*(1), 85-89.

Singh, H. (2004). Heat stability of milk. *International Journal of Dairy Technology, 57*(2-3), 111-119.

Singh, H., Ye, A., & Ferrua, M. J. (2015). Aspects of food structures in the digestive tract. *Current Opinion in Food Science, 3*, 85-93.

Stănciuc, N., van der PLANCKEN, I., Rotaru, G., & Hendrickx, M. (2008). Denaturation impact in susceptibility of beta-lactoglobulin to enzymatic hydrolysis: a kinetic study. *Revue roumaine de chimie, 53*(10), 921-929.

Steingoetter, A., Radovic, T., Buetikofer, S., Curcic, J., Menne, D., Fried, M., Schwizer, W., & Wooster, T. J. (2015). Imaging gastric structuring of lipid emulsions and its effect on gastrointestinal function: a randomized trial in healthy subjects. *The American journal of clinical nutrition, 101*(4), 714-724.

Szarka, L. A., & Camilleri, M. (2009). Methods for measurement of gastric motility. *American Journal of Physiology-Gastrointestinal and Liver Physiology, 296*(3), G461-G475.

Tabilo-Munizaga, G., & Barbosa-Cánovas, G. V. (2005). Rheology for the food industry. *Journal of Food Engineering, 67*(1), 147-156.

Tam, J. J., & Whitaker, J. R. (1972). Rates and Extents of Hydrolysis of Several Caseins by Pepsin, Rennin, Endothia parasitica Protease and Mucor pusillus Protease1. *Journal of Dairy Science, 55*(11), 1523-1531.

Tang, J. E., Moore, D. R., Kujbida, G. W., Tarnopolsky, M. A., & Phillips, S. M. (2009). Ingestion of whey hydrolysate, casein, or soy protein isolate: effects on mixed muscle protein synthesis at rest and following resistance exercise in young men. *Journal of Applied Physiology, 107*(3), 987-992.

Thevenot, J., Cauty, C., Legland, D., Dupont, D., & Floury, J. (2017). Pepsin diffusion in dairy gels depends on casein concentration and microstructure. *Food Chemistry, 223*, 54-61.

Tholstrup, T., Høy, C.-E., Andersen, L. N., Christensen, R. D. K., & Sandström, B. (2004). Does Fat in Milk, Butter and Cheese Affect Blood Lipids and Cholesterol Differently? *Journal of the American College of Nutrition, 23*(2), 169-176.

Thomann, S., Schenkel, P., & Hinrichs, J. (2008). Effect of homogenization, microfiltration and pH on curd firmness and syneresis of curd grains. *LWT-Food Science and Technology, 41*(5), 826-835.

Thomas, A. (2006). GastroGut motility, sphincters and reflex control. *Anaesthesia & Intensive Care Medicine, 7*(2), 57-58.

Thorning, T. K., Raben, A., Tholstrup, T., Soedamah-Muthu, S. S., Givens, I., & Astrup, A. (2016). Milk and dairy products: good or bad for human health? An assessment of the totality of scientific evidence. *Food & nutrition research, 60*(1), 32527.

Thorning, T. K., Bertram, H. C., Bonjour, J.-P., De Groot, L., Dupont, D., Feeney, E., Ipsen, R., Lecerf, J. M., Mackie, A., & McKinley, M. C. (2017). Whole dairy matrix or single nutrients in assessment of health effects: current evidence and knowledge gaps. *The American journal of clinical nutrition, 105*(5), 1033-1045.

Thuenemann, E. C., Mandalari, G., Rich, G. T., & Faulks, R. M. (2015). Dynamic Gastric Model (DGM). In K. Verhoeckx, P. Cotter, I. López-Expósito, C. Kleiveland, T. Lea, A. Mackie, T. Requena, D. Swiatecka & H. Wichers (Eds.), *The Impact of Food Bioactives on Health: in vitro and ex vivo models*, (pp. 47-59): Springer

Tipton, K. D., Ferrando, A. A., Phillips, S. M., Doyle, D., & Wolfe, R. R. (1999). Postexercise net protein synthesis in human muscle from orally administered amino acids. *American Journal of Physiology-Endocrinology And Metabolism, 276*(4), E628-E634.

Truong, T., Palmer, M., Bansal, N., & Bhandari, B. (2016). Effect of Milk Fat Globule Size on Functionalities and Sensory Qualities of Dairy Products. In *Effect of Milk Fat Globule Size on the Physical Functionality of Dairy Products*, (pp. 47-67): Springer.

Tunick, M. H. (2011). Small-Strain Dynamic Rheology of Food Protein Networks. *Journal of Agricultural and Food Chemistry, 59*(5), 1481-1486.

Tunick, M. H., Ren, D. X., Van Hekken, D. L., Bonnaillie, L., Paul, M., Kwoczak, R., & Tomasula, P. M. (2016). Effect of heat and homogenization on in vitro digestion of milk. *Journal of Dairy Science, 99*(6), 4124-4139.

Urbain, J.-L. C., Siegel, J. A., Charkes, N. D., Maurer, A. H., Malmud, L. S., & Fisher, R. S. (1989). The two-component stomach: effects of meal particle size on fundal and antral emptying. *European journal of nuclear medicine, 15*(5), 254-259.

van Aken, G. A., Bomhof, E., Zoet, F. D., Verbeek, M., & Oosterveld, A. (2011). Differences in in vitro gastric behaviour between homogenized milk and emulsions stabilised by Tween 80, whey protein, or whey protein and caseinate. *Food Hydrocolloids, 25*(4), 781-788.

van Boekel, M. (1998). Effect of heating on Maillard reactions in milk. *Food Chemistry, 62*(4), 403-414.

van den Braak, C. C. M., Klebach, M., Abrahamse, E., Minor, M., Hofman, Z., Knol, J., & Ludwig, T. (2013). A novel protein mixture containing vegetable proteins renders enteral nutrition products non-coagulating after in vitro gastric digestion. *Clinical Nutrition, 32*(5), 765-771.

Veldhorst, M., Smeets, A., Soenen, S., Hochstenbach-Waelen, A., Hursel, R., Diepvens, K., Lejeune, M., Luscombe-Marsh, N., & Westerterp-Plantenga, M. (2008). Protein-induced satiety: effects and mechanisms of different proteins. *Physiology & Behavior, 94*(2), 300-307.

Veldhorst, M. A. B., Nieuwenhuizen, A. G., Hochstenbach-Waelen, A., van Vught, A. J. A. H., Westerterp, K. R., Engelen, M. P. K. J., Brummer, R.-J. M., Deutz, N. E. P., & Westerterp-Plantenga, M. S. (2009). Dose-dependent satiating effect of whey relative to casein or soy. *Physiology & Behavior, 96*(4–5), 675-682.

Verhoeckx, K., Cotter, P., López-Expósito, I., Kleiveland, C., Lea, T., Mackie, A., Requena, T., Swiatecka, D., & Wichers, H. (2015). *The Impact of Food Bioactives on Health: in vitro and ex vivo models*: Springer.

Volpi, E., Kobayashi, H., Sheffield-Moore, M., Mittendorfer, B., & Wolfe, R. R. (2003). Essential amino acids are primarily responsible for the amino acid stimulation of muscle protein anabolism in healthy elderly adults. *The American journal of clinical nutrition, 78*(2), 250-258.

Wada, Y., & Lönnerdal, B. (2014). Effects of Different Industrial Heating Processes of Milk on Site-Specific Protein Modifications and Their Relationship to in Vitro and in Vivo Digestibility. *Journal of Agricultural and Food Chemistry, 62*(18), 4175-4185.

Walstra, P., & Jenness, R. (1984). *Dairy chemistry & physics*: John Wiley & Sons.

Walstra, P., & Smulders, I. (1997). Making emulsions and foams: an overview. *Special Publications of the Royal Society of Chemistry, 192*, 367-381.

Wang, X., Lin, Q., Ye, A., Han, J., & Singh, H. (2018). Flocculation of oil-in-water emulsions stabilised by milk protein ingredients under gastric conditions: Impact on in vitro intestinal lipid digestion. *Food Hydrocolloids, 88*, 272-282.

Watanabe, S., & Dawes, C. (1988). The effects of different foods and concentrations of citric acid on the flow rate of whole saliva in man. *Archives of oral biology, 33*(1), 1-5.

West, D. W., Burd, N. A., Coffey, V. G., Baker, S. K., Burke, L. M., Hawley, J. A., Moore, D. R., Stellingwerff, T., & Phillips, S. M. (2011). Rapid aminoacidemia enhances myofibrillar protein synthesis and anabolic intramuscular signaling responses after resistance exercise–. *The American journal of clinical nutrition, 94*(3), 795-803.

Wilde, P. J. (2009). Eating for Life: Designing Foods for Appetite Control. *Journal of Diabetes Science and Technology, 3*(2), 366-370.

Wiles, P. G., Gray, I. K., & Kissling, R. C. (1998). Routine analysis of proteins by Kjeldahl and Dumas methods: Review and interlaboratory study using dairy products. *Journal of AOAC International, 81*(3), 620-632.

Wilkinson, S. B., Tarnopolsky, M. A., MacDonald, M. J., MacDonald, J. R., Armstrong, D., & Phillips, S. M. (2007). Consumption of fluid skim milk promotes greater muscle protein accretion after resistance exercise than does consumption of an isonitrogenous and isoenergetic soy-protein beverage. *The American journal of clinical nutrition, 85*(4), 1031-1040.

Wolfe, R. R. (2002). Regulation of muscle protein by amino acids. *The Journal of nutrition, 132*(10), 3219S-3224S.

Wren, A. M., & Bloom, S. R. (2007). Gut hormones and appetite control. *Gastroenterology, 132*(6), 2116-2130.

Ye, A., Cui, J., Dalgleish, D., & Singh, H. (2016a). Formation of a structured clot during the gastric digestion of milk: Impact on the rate of protein hydrolysis. *Food Hydrocolloids, 52*, 478-486.

Ye, A., Cui, J., Dalgleish, D., & Singh, H. (2016b). The formation and breakdown of structured clots from whole milk during gastric digestion. *Food & function, 7*(10), 4259-4266.

References

Ye, A., Cui, J., Dalgleish, D., & Singh, H. (2017). Effect of homogenization and heat treatment on the behavior of protein and fat globules during gastric digestion of milk. *Journal of Dairy Science, 100*(1), 36-47.

Yvon, M., Beucher, S., Scanff, P., Thirouin, S., & Pelissier, J. P. (1992). In vitro simulation of gastric digestion of milk proteins: comparison between in vitro and in vivo data. *Journal of Agricultural and Food Chemistry, 40*(2), 239-244.

Appendices

Appendix A

Operating parameters of the method for determination of the branch chain amino acids (Leucine, Isoleucine and Valine) by triple quadrupole LC-MS/MS.

Compound Name	Precursor Ion	Product Ion	Dwell Time (ms)	Fragmentor (V)	Collision Energy	Cell Accelerator (V)	Polarity
D3-Leu	135.20	89	100	380	10	4	Positive
Leu	132.11	86	100	380	10	4	Positive
Leu	132.11	43	100	380	30	4	Positive
D10-Ile	142.24	96.1	100	380	14	4	Positive
Ile	132.11	86	100	380	10	4	Positive
Ile	132.11	56	100	380	50	4	Positive
Ile	132.11	44	100	380	26	4	Positive
D8-Val	126.21	80.1	100	380	14	4	Positive
Val	118.11	72	100	380	14	4	Positive
Val	118.11	58.1	100	380	34	4	Positive

Appendix B

Appendix B1: Concentration of the individual AAs of the 0C:100W sample in the gastric emptied aliquots of G1, G3 and G5 and the corresponding intestinal digestion for 30 min (i.e. G1I, G3I and G5I), and 120 min in G5 (i.e. G5I120).

	0C:100W						
	G1	G3	G5	G1I	G3I	G5I	G5I120
Asp (µg/mL)	0.00 ± 0.00	0.00 ± 0.00	0.00 ± 0.00	22911 ± 1185	22566 ± 1436	37051 ± 1760	47858 ± 957
Thr (µg/mL)	0.00 ± 0.00	0.00 ± 0.00	131.16 ± 21.07	100284 ± 2452	93288 ± 4748	115033 ± 16002	150769 ± 7578
Ser (µg/mL)	0.67 ± 1.15	8.85 ± 15.33	0.00 ± 0.00	30423 ± 2833	33831 ± 2181	59110 ± 1718	86670 ± 4970
Glu (µg/mL)	0.00 ± 0.00	0.00 ± 0.00	0.00 ± 0.00	67243 ± 467	61122 ± 1253	99920 ± 2279	130000 ± 1605
Gly (µg/mL)	0.32 ± 0.56	0.40 ± 0.69	0.00 ± 0.00	17060 ± 1641	17525 ± 1305	29073 ± 1464	37543 ± 1237
Ala (µg/mL)	0.29 ± 0.51	0.00 ± 0.00	2.48 ± 4.30	41823 ± 756	41373 ± 1645	61349 ± 3469	87285 ± 3739
Cys (µg/mL)	29.00 ± 8.21	45.73 ± 18.69	135.24 ± 34.41	61413 ± 4532	55138 ± 6605	74644 ± 9155	101381 ± 10793
Val (µg/mL)	0.45 ± 0.78	17.79 ± 7.57	114.86 ± 33.88	87778 ± 6509	70998 ± 2408	69338 ± 5016	102688 ± 3030
Met (µg/mL)	1.10 ± 1.90	11.77 ± 10.48	5.64 ± 9.77	46125 ± 8314	30073 ± 3496	25911 ± 5247	36322 ± 5426
Ile (µg/mL)	0.00 ± 0.00	7.23 ± 12.53	0.00 ± 0.00	63805 ± 883	51198 ± 1808	53477 ± 4381	94801 ± 3110
Leu (µg/mL)	0.31 ± 0.54	12.94 ± 11.99	22.90 ± 5.32	251444 ± 10926	200079 ± 13477	160408 ± 16589	211322 ± 17678
Tyr (µg/mL)	42.28 ± 10.92	1151.89 ± 33.39	1386.50 ± 355.48	235966 ± 14575	166520 ± 13922	121577 ± 9928	140552 ± 11156
Phe (µg/mL)	0.00 ± 0.00	0.00 ± 0.00	0.00 ± 0.00	251589 ± 26390	162236 ± 21890	81240 ± 7111	102920 ± 10531
His (µg/mL)	99.17 ± 10.33	537.34 ± 69.45	1081.03 ± 146.38	106914 ± 2444	81719 ± 1288	64638 ± 405	70649 ± 2395
Lys (µg/mL)	6.37 ± 0.29	3.54 ± 4.07	0.00 ± 0.00	366778 ± 9821	265622 ± 13312	206784 ± 6760	236963 ± 8829
Trp (µg/mL)	0.00 ± 0.00	0.00 ± 0.00	0.00 ± 0.00	163932 ± 28481	103037 ± 25355	59387 ± 22816	109051 ± 31382
Arg (µg/mL)	8.28 ± 1.32	6.46 ± 2.60	8.03 ± 7.53	148058 ± 5830	117788 ± 6249	130801 ± 4771	149331 ± 2533
Pro (µg/mL)	0.95 ± 1.64	7.62 ± 13.20	26.36 ± 38.57	3033 ± 2630	3095 ± 3492	4978 ± 7959	22081 ± 1054
Total (mg/mL)	0.19 ± 0.04	1.81 ± 0.20	2.91 ± 0.66	2067 ± 131	1577 ± 126	1455 ± 127	1918 ± 128

Appendix B2: Concentration of the individual AAs of the 20C:80W sample in the gastric emptied aliquots of G1, G3 and G5 and the corresponding intestinal digestion for 30 min (i.e. G1I, G3I and G5I), and 120 min in G5 (i.e. G5I120).

	20C:80W						
	G1	G3	G5	G1I	G3I	G5I	G5I120
Asp (µg/mL)	0.41 ± 0.71	0.00 ± 0.00	0.00 ± 0.00	21349 ± 1413	21717 ± 181	37529 ± 3374	60708 ± 17403
Thr (µg/mL)	0.77 ± 1.33	1.21 ± 2.09	34.55 ± 59.84	92894 ± 5647	86289 ± 2866	108114 ± 2206	161952 ± 7682
Ser (µg/mL)	1.42 ± 1.24	0.34 ± 0.59	0.00 ± 0.00	31201 ± 976	31719 ± 475	56773 ± 3886	87691 ± 2250
Glu (µg/mL)	84.31 ± 136.86	58.95 ± 94.72	0.00 ± 0.00	61083 ± 3509	58412 ± 2069	102017 ± 11912	139442 ± 11262
Gly (µg/mL)	4.27 ± 1.23	3.51 ± 1.18	0.00 ± 0.00	17364 ± 1344	17549 ± 739	29141 ± 2242	40686 ± 1498
Ala (µg/mL)	0.00 ± 0.00	0.62 ± 1.07	0.00 ± 0.00	38635 ± 787	39016 ± 1177	57023 ± 3658	87183 ± 4469
Cys (µg/mL)	31.53 ± 8.90	40.97 ± 16.96	146.46 ± 60.74	52754 ± 4763	52047 ± 4989	72482 ± 8423	99561 ± 10187
Val (µg/mL)	0.00 ± 0.00	77.90 ± 27.79	68.66 ± 118.92	72543 ± 3421	64343 ± 5425	63767 ± 3845	102830 ± 4846
Met (µg/mL)	0.96 ± 1.66	0.00 ± 0.00	0.00 ± 0.00	41375 ± 6075	31932 ± 8891	21891 ± 1566	33983 ± 2509
Ile (µg/mL)	0.35 ± 0.61	0.00 ± 0.00	0.00 ± 0.00	51174 ± 1382	43977 ± 1786	47454 ± 2486	90376 ± 4358
Leu (µg/mL)	0.00 ± 0.00	19.59 ± 3.79	15.69 ± 27.18	222979 ± 11130	181436 ± 15482	136573 ± 13153	198791 ± 21476
Tyr (µg/mL)	11.65 ± 12.07	545.71 ± 473.47	1260.94 ± 18.33	223799 ± 7365	166793 ± 16319	114521 ± 11500	141639 ± 9947
Phe (µg/mL)	2.25 ± 3.90	206.63 ± 357.89	0.00 ± 0.00	232138 ± 19987	154918 ± 22525	77193 ± 11264	100849 ± 8313
His (µg/mL)	66.22 ± 4.91	429.25 ± 40.76	929.26 ± 40.19	104865 ± 8943	78233 ± 5249	58650 ± 3336	71136 ± 3517
Lys (µg/mL)	5.94 ± 0.85	1.15 ± 1.99	0.00 ± 0.00	333402 ± 9310	248864 ± 11243	186782 ± 13246	231529 ± 14870
Trp (µg/mL)	0.00 ± 0.00	0.00 ± 0.00	0.00 ± 0.00	150743 ± 27518	95107 ± 24712	48042 ± 22105	85603 ± 36264
Arg (µg/mL)	5.37 ± 1.75	3.29 ± 2.96	2.76 ± 4.77	157814 ± 3172	124016 ± 7143	128954 ± 9443	159582 ± 7610
Pro (µg/mL)	2.35 ± 4.07	23.87 ± 12.07	0.00 ± 0.00	667 ± 1155	0 ± 0	5697 ± 4982	24380 ± 5352
Total (mg/mL)	0.22 ± 0.18	1.41 ± 1.04	2.46 ± 0.33	1907 ± 118	1496 ± 131	1353 ± 133	1918 ± 174

Appendix B3: Concentration of the individual AAs of the 50C:50W sample in the gastric emptied aliquots of G1, G3 and G5 and the corresponding intestinal digestion for 30 min (i.e. G1I, G3I and G5I), and 120 min in G5 (i.e. G5I120).

	50C:50W						
	G1	G3	G5	G1I	G3I	G5I	G5I120
Asp (µg/mL)	0.00 ± 0.00	0.00 ± 0.00	0.78 ± 1.35	19535 ± 1292	20840 ± 1427	32920 ± 4980	33876 ± 8184
Thr (µg/mL)	0.65 ± 1.12	9.32 ± 6.20	8.34 ± 7.97	75979 ± 8530	80867 ± 7303	145122 ± 29708	225880 ± 45105
Ser (µg/mL)	2.28 ± 2.42	0.26 ± 0.45	1.35 ± 2.33	29470 ± 2611	32443 ± 2384	53780 ± 9393	79928 ± 19406
Glu (µg/mL)	255.42 ± 410.85	130.68 ± 205.51	144.59 ± 239.47	53278 ± 2828	57544 ± 2813	83939 ± 310	118169 ± 26100
Gly (µg/mL)	8.73 ± 0.31	9.60 ± 3.79	6.16 ± 5.38	16734 ± 1605	17797 ± 1746	31683 ± 6525	37207 ± 7910
Ala (µg/mL)	1.78 ± 1.74	20.90 ± 30.13	2.38 ± 4.13	34599 ± 1778	37024 ± 1955	59145 ± 11632	88058 ± 21010
Cys (µg/mL)	33.68 ± 6.81	93.59 ± 83.97	84.65 ± 37.86	46372 ± 4864	47250 ± 2600	86123 ± 3946	114391 ± 11138
Val (µg/mL)	1.38 ± 0.51	94.37 ± 91.32	252.36 ± 89.18	52705 ± 3945	52313 ± 3849	89823 ± 15422	142687 ± 25737
Met (µg/mL)	0.00 ± 0.00	0.00 ± 0.00	1.57 ± 2.71	27253 ± 5320	24393 ± 2613	54616 ± 8166	80450 ± 16959
Ile (µg/mL)	0.00 ± 0.00	0.75 ± 1.29	2.16 ± 3.74	39225 ± 3010	35396 ± 2503	58745 ± 10168	95207 ± 18150
Leu (µg/mL)	0.00 ± 0.00	17.79 ± 6.02	34.51 ± 19.46	159785 ± 22826	151124 ± 19180	314411 ± 45005	440964 ± 76308
Tyr (µg/mL)	8.23 ± 14.25	427.67 ± 382.07	543.93 ± 47.16	163909 ± 30253	140839 ± 24666	329761 ± 50906	362507 ± 48357
Phe (µg/mL)	1.18 ± 1.03	124.69 ± 215.96	142.43 ± 46.37	147960 ± 26606	116458 ± 27901	276440 ± 40904	295367 ± 41224
His (µg/mL)	48.82 ± 13.51	305.03 ± 265.06	826.43 ± 212.64	78267 ± 13277	72584 ± 9471	170013 ± 24967	163627 ± 18157
Lys (µg/mL)	4.72 ± 0.43	0.00 ± 0.00	1.60 ± 1.42	229052 ± 19892	203696 ± 16803	414380 ± 48330	467054 ± 51969
Trp (µg/mL)	0.00 ± 0.00	0.00 ± 0.00	0.00 ± 0.00	106559 ± 30938	78237 ± 22299	190928 ± 32706	220250 ± 40552
Arg (µg/mL)	10.00 ± 1.15	6.97 ± 3.14	3.02 ± 2.91	130187 ± 18035	123392 ± 12027	283706 ± 36091	294330 ± 36470
Pro (µg/mL)	6.74 ± 9.37	2.36 ± 4.09	24.02 ± 24.63	3033 ± 3931	1133 ± 1060	3040 ± 2726	11044 ± 9620
Total (mg/mL)	0.38 ± 0.46	1.24 ± 1.30	2.08 ± 0.75	1414 ± 202	1293 ± 163	2679 ± 382	3271 ± 522

Appendix B4: Concentration of the individual AAs of the 80C:20W sample in the gastric emptied aliquots of G1, G3 and G5 and the corresponding intestinal digestion for 30 min (i.e. G1I, G3I and G5I), and 120 min in G5 (i.e. G5I120).

	80C:20W						
	G1	G3	G5	G1I	G3I	G5I	G5I120
Asp (µg/mL)	2.88 ± 2.55	1.37 ± 2.37	0.00 ± 0.00	18880 ± 388	20703 ± 2981	27537 ± 1670	27068 ± 2128
Thr (µg/mL)	1.90 ± 1.84	0.67 ± 1.15	2.65 ± 1.08	78098 ± 7956	63974 ± 8911	137392 ± 11494	212942 ± 22759
Ser (µg/mL)	1.38 ± 2.38	1.37 ± 2.37	2.08 ± 2.03	30242 ± 1141	32302 ± 5056	43457 ± 4047	64685 ± 6288
Glu (µg/mL)	300.42 ± 467.56	255.49 ± 410.25	156.34 ± 235.52	50567 ± 463	50637 ± 4732	81496 ± 8537	105962 ± 13695
Gly (µg/mL)	15.05 ± 2.80	13.44 ± 4.09	11.22 ± 4.06	17452 ± 2287	17040 ± 2586	27645 ± 1871	37291 ± 4271
Ala (µg/mL)	3.57 ± 1.94	1.71 ± 1.53	6.13 ± 10.62	30796 ± 1710	31317 ± 5019	46232 ± 2576	68686 ± 6609
Cys (µg/mL)	34.74 ± 19.58	55.38 ± 13.39	70.73 ± 34.76	46557 ± 5119	39258 ± 2740	69154 ± 9177	102141 ± 3504
Val (µg/mL)	5.17 ± 5.17	192.43 ± 13.26	248.47 ± 74.97	43094 ± 5341	35771 ± 5893	70648 ± 3388	129129 ± 10256
Met (µg/mL)	0.00 ± 0.00	0.00 ± 0.00	2.62 ± 4.54	24658 ± 4684	13991 ± 2046	52611 ± 3409	82046 ± 5317
Ile (µg/mL)	0.00 ± 0.00	0.93 ± 1.61	0.93 ± 1.61	31568 ± 3707	24253 ± 4588	48070 ± 3025	78668 ± 5705
Leu (µg/mL)	0.00 ± 0.00	17.37 ± 5.85	102.87 ± 131.47	145908 ± 27965	81133 ± 13018	301446 ± 19777	460343 ± 38101
Tyr (µg/mL)	4.80 ± 4.16	318.79 ± 173.97	435.18 ± 32.02	169179 ± 39101	75878 ± 14554	381271 ± 17437	448579 ± 29579
Phe (µg/mL)	1.35 ± 1.70	136.76 ± 165.95	359.49 ± 311.29	140437 ± 33701	56668 ± 13701	327663 ± 13679	388092 ± 44787
His (µg/mL)	39.80 ± 4.16	463.41 ± 29.47	652.17 ± 175.22	86790 ± 18909	41311 ± 5514	199306 ± 5610	202371 ± 10071
Lys (µg/mL)	4.62 ± 0.50	1.45 ± 1.30	8.57 ± 13.10	197796 ± 31000	110197 ± 14138	417640 ± 27153	513859 ± 19893
Trp (µg/mL)	0.00 ± 0.00	0.00 ± 0.00	84.27 ± 145.96	87212 ± 37836	30907 ± 14149	175739 ± 29075	244311 ± 36706
Arg (µg/mL)	12.95 ± 1.44	5.76 ± 0.37	37.43 ± 57.24	149255 ± 26923	83923 ± 10052	327814 ± 17225	361966 ± 14608
Pro (µg/mL)	15.11 ± 22.03	19.66 ± 10.23	14.18 ± 24.55	169 ± 292	5313 ± 3433	9076 ± 10116	7142 ± 3549
Total (mg/mL)	0.44 ± 0.54	1.49 ± 0.84	2.20 ± 1.26	1349 ± 249	815 ± 133	2744 ± 189	3535 ± 278

Appendix B5: Concentration of the individual AAs of the (0C:100W)2% sample in the gastric emptied aliquots of G1, G3 and G5 and the corresponding intestinal digestion for 30 min (i.e. G1I, G3I and G5I), and 120 min in G5 (i.e. G5I120).

	(0C:100W)2%						
	G1	G3	G5	G1I	G3I	G5I	G5I120
Asp (µg/mL)	0.00 ± 0.00	0.00 ± 0.00	0.00 ± 0.00	24715 ± 1283	25312 ± 1620	47083 ± 11478	53305 ± 670
Thr (µg/mL)	0.00 ± 0.00	33.61 ± 2.12	143.34 ± 36.41	102739 ± 11822	94335 ± 5780	118086 ± 5579	159727 ± 10386
Ser (µg/mL)	1.21 ± 1.06	0.00 ± 0.00	0.00 ± 0.00	33148 ± 2224	35826 ± 1722	62204 ± 281	89497 ± 1891
Glu (µg/mL)	0.72 ± 1.24	52.73 ± 88.03	177.42 ± 307.30	73709 ± 10961	77698 ± 9759	108024 ± 3055	139282 ± 6359
Gly (µg/mL)	0.16 ± 0.27	1.19 ± 1.18	2.65 ± 2.76	17937 ± 1506	18947 ± 782	31922 ± 122	40785 ± 1161
Ala (µg/mL)	0.24 ± 0.41	0.00 ± 0.00	62.24 ± 103.09	45081 ± 3828	45250 ± 2520	67492 ± 1672	92407 ± 6061
Cys (µg/mL)	35.74 ± 11.64	68.13 ± 23.69	157.06 ± 25.97	58430 ± 3501	56308 ± 4263	78941 ± 4954	105258 ± 5650
Val (µg/mL)	0.00 ± 0.00	46.35 ± 36.72	80.41 ± 72.16	90854 ± 8899	77372 ± 4007	74010 ± 4159	107727 ± 4671
Met (µg/mL)	0.00 ± 0.00	26.14 ± 3.80	8.09 ± 7.46	48412 ± 4672	34215 ± 5629	25937 ± 2043	35519 ± 2484
Ile (µg/mL)	1.39 ± 2.40	0.00 ± 0.00	0.00 ± 0.00	61803 ± 6278	53665 ± 3638	58925 ± 4524	99030 ± 4891
Leu (µg/mL)	2.01 ± 3.48	43.57 ± 12.74	29.19 ± 25.39	245033 ± 25736	199119 ± 14389	167614 ± 14875	218254 ± 20602
Tyr (µg/mL)	42.19 ± 22.79	1349.76 ± 186.92	1106.54 ± 223.56	209973 ± 23197	162411 ± 5474	125567 ± 14361	140623 ± 7811
Phe (µg/mL)	3.12 ± 3.47	14.21 ± 24.62	157.01 ± 137.58	226175 ± 26098	157872 ± 10480	90966 ± 17127	102391 ± 5369
His (µg/mL)	85.12 ± 3.65	620.91 ± 43.16	1136.78 ± 386.77	110177 ± 2840	80552 ± 9117	67677 ± 5965	72397 ± 2601
Lys (µg/mL)	7.92 ± 1.07	5.05 ± 2.97	13.48 ± 23.35	367000 ± 22948	270775 ± 8838	214448 ± 5012	248226 ± 9627
Trp (µg/mL)	2.91 ± 5.03	0.00 ± 0.00	23.38 ± 40.50	160494 ± 39772	113212 ± 9309	63108 ± 25681	83456 ± 30006
Arg (µg/mL)	8.01 ± 2.56	4.35 ± 2.33	8.38 ± 8.72	146425 ± 8712	119638 ± 3826	137310 ± 870	159510 ± 2009
Pro (µg/mL)	17.34 ± 4.51	32.09 ± 39.95	27.31 ± 47.30	1848 ± 2364	1216 ± 2106	3106 ± 3696	20957 ± 7391
Total (mg/mL)	0.21 ± 0.06	2.30 ± 0.47	3.13 ± 1.45	2024 ± 207	1624 ± 103	1542 ± 125	1968 ± 130

Appendix B6: Concentration of the individual AAs of the (20C:80W)2% sample in the gastric emptied aliquots of G1, G3 and G5 and the corresponding intestinal digestion for 30 min (i.e. G1I, G3I and G5I), and 120 min in G5 (i.e. G5I120).

	(20C:80W)2%						
	G1	G3	G5	G1I	G3I	G5I	G5I120
Asp (µg/mL)	0.76 ± 1.32	0.19 ± 0.33	3.10 ± 2.69	23820 ± 6391	23288 ± 613	46939 ± 11467	53519 ± 3085
Thr (µg/mL)	2.35 ± 4.07	1.43 ± 2.47	101.04 ± 4.64	88599 ± 19462	94476 ± 7329	118285 ± 9669	156403 ± 11059
Ser (µg/mL)	1.40 ± 1.27	0.60 ± 1.03	0.00 ± 0.00	30305 ± 924	33778 ± 1353	62720 ± 899	89682 ± 1558
Glu (µg/mL)	123.82 ± 210.53	98.52 ± 160.25	167.45 ± 285.68	56258 ± 2900	66770 ± 1835	114551 ± 7923	159744 ± 220
Gly (µg/mL)	3.93 ± 0.60	4.34 ± 0.46	9.05 ± 3.80	16211 ± 714	18070 ± 782	31836 ± 1144	41485 ± 442
Ala (µg/mL)	1.17 ± 1.04	2.05 ± 2.91	0.00 ± 0.00	37225 ± 3847	41309 ± 3177	64937 ± 2479	89344 ± 830
Cys (µg/mL)	32.80 ± 3.10	31.89 ± 12.11	218.44 ± 19.91	48017 ± 2549	52043 ± 5511	73847 ± 3634	98008 ± 8466
Val (µg/mL)	0.11 ± 0.20	53.92 ± 19.66	158.74 ± 59.73	61988 ± 12516	67271 ± 5191	71804 ± 760	106214 ± 4169
Met (µg/mL)	1.39 ± 1.22	0.58 ± 1.00	7.34 ± 12.72	33803 ± 11359	35816 ± 4082	27049 ± 3522	35963 ± 1370
Ile (µg/mL)	0.86 ± 1.49	1.34 ± 2.32	6.05 ± 10.49	43510 ± 6000	46225 ± 2713	53509 ± 2545	91698 ± 1062
Leu (µg/mL)	3.98 ± 3.08	34.08 ± 8.81	59.98 ± 14.07	173250 ± 41845	186131 ± 16141	150727 ± 9597	209993 ± 15230
Tyr (µg/mL)	3.43 ± 5.94	499.80 ± 113.50	749.82 ± 290.83	176367 ± 36181	175990 ± 34273	119985 ± 5696	144644 ± 7596
Phe (µg/mL)	7.05 ± 12.21	118.32 ± 45.07	248.17 ± 202.26	162595 ± 49504	160764 ± 33813	82338 ± 5860	103414 ± 6010
His (µg/mL)	61.26 ± 5.50	426.15 ± 101.01	1004.34 ± 258.28	85878 ± 30986	81867 ± 4196	63629 ± 4242	72344 ± 6618
Lys (µg/mL)	7.79 ± 3.76	4.76 ± 2.18	6.29 ± 5.93	269222 ± 68223	272066 ± 42544	208437 ± 15061	242177 ± 20995
Trp (µg/mL)	0.00 ± 0.00	0.00 ± 0.00	0.00 ± 0.00	106403 ± 51462	102860 ± 31419	55531 ± 20369	114238 ± 33303
Arg (µg/mL)	5.70 ± 1.57	3.50 ± 3.03	10.00 ± 8.91	128598 ± 28142	131285 ± 16912	140286 ± 6218	162855 ± 8885
Pro (µg/mL)	24.45 ± 7.79	7.12 ± 12.34	28.24 ± 24.46	1014 ± 370	3102 ± 5373	10742 ± 7715	21111 ± 11676
Total (mg/mL)	0.28 ± 0.26	1.29 ± 0.49	2.78 ± 1.20	1543 ± 373	1593 ± 217	1497 ± 119	1993 ± 143

Appendix B7: Concentration of the individual AAs of the (50C:50W)2% sample in the gastric emptied aliquots of G1, G3 and G5 and the corresponding intestinal digestion for 30 min (i.e. G1I, G3I and G5I), and 120 min in G5 (i.e. G5I120).

	(50C:50W)2%						
	G1	G3	G5	G1I	G3I	G5I	G5I120
Asp (µg/mL)	2.23 ± 0.89	0.00 ± 0.00	0.00 ± 0.00	24200 ± 6075	26350 ± 8708	38673 ± 7562	48612 ± 14341
Thr (µg/mL)	2.09 ± 1.90	0.58 ± 1.00	5.11 ± 4.74	92154 ± 10069	73914 ± 18874	142386 ± 18283	204110 ± 31751
Ser (µg/mL)	1.29 ± 1.16	1.43 ± 2.48	1.17 ± 2.03	32251 ± 733	34586 ± 1465	54998 ± 1706	90630 ± 5306
Glu (µg/mL)	233.84 ± 376.40	142.04 ± 227.76	117.95 ± 189.40	58692 ± 124	64019 ± 1473	101496 ± 724	172624 ± 15187
Gly (µg/mL)	8.91 ± 1.27	6.45 ± 1.62	14.66 ± 9.34	18050 ± 738	18288 ± 444	29726 ± 1499	38176 ± 762
Ala (µg/mL)	7.82 ± 0.90	2.60 ± 4.50	5.82 ± 10.09	37410 ± 2504	38692 ± 1743	59004 ± 1838	88072 ± 1144
Cys (µg/mL)	39.55 ± 3.97	46.02 ± 13.83	99.32 ± 93.79	49148 ± 6776	46252 ± 5054	73560 ± 4999	107202 ± 6874
Val (µg/mL)	2.73 ± 1.14	78.26 ± 10.95	307.82 ± 174.74	57947 ± 2656	52570 ± 743	82992 ± 4087	131252 ± 3629
Met (µg/mL)	0.00 ± 0.00	0.00 ± 0.00	121.38 ± 210.23	30388 ± 2046	25353 ± 1653	42946 ± 3425	65009 ± 2216
Ile (µg/mL)	0.00 ± 0.00	0.00 ± 0.00	1.50 ± 2.61	42088 ± 2412	36455 ± 623	53520 ± 3543	89579 ± 754
Leu (µg/mL)	4.45 ± 1.13	22.87 ± 13.40	51.64 ± 31.40	173442 ± 14746	145378 ± 3836	238192 ± 23175	349721 ± 15248
Tyr (µg/mL)	10.69 ± 14.07	278.62 ± 242.08	418.80 ± 334.57	184560 ± 13824	133485 ± 4873	232822 ± 35202	274592 ± 18277
Phe (µg/mL)	2.82 ± 4.88	113.42 ± 60.12	121.64 ± 75.32	161178 ± 14232	111844 ± 4841	188619 ± 25463	222105 ± 19122
His (µg/mL)	41.03 ± 2.35	399.33 ± 89.31	886.69 ± 139.95	91576 ± 7300	68184 ± 1691	123183 ± 15721	133422 ± 7384
Lys (µg/mL)	5.28 ± 1.93	4.61 ± 2.78	4.31 ± 4.46	264567 ± 12737	194633 ± 7119	314553 ± 34726	384833 ± 24052
Trp (µg/mL)	0.00 ± 0.00	0.00 ± 0.00	0.00 ± 0.00	118719 ± 28103	72183 ± 16328	125562 ± 42067	162106 ± 61648
Arg (µg/mL)	9.23 ± 3.10	2.99 ± 2.64	3.74 ± 4.04	150098 ± 7463	117583 ± 4675	207296 ± 23663	243064 ± 13547
Pro (µg/mL)	8.59 ± 11.07	13.61 ± 13.25	12.87 ± 12.19	2595 ± 3674	3463 ± 4642	10065 ± 8739	13803 ± 4049
Total (mg/mL)	0.38 ± 0.43	1.11 ± 0.69	2.17 ± 1.30	1589 ± 136	1263 ± 89	2120 ± 256	2819 ± 245

Appendix B8: Concentration of the individual AAs of the (80C:20W)2% sample in the gastric emptied aliquots of G1, G3 and G5 and the corresponding intestinal digestion for 30 min (i.e. G1I, G3I and G5I), and 120 min in G5 (i.e. G5I120).

	(80C:20W)2%						
	G1	G3	G5	G1I	G3I	G5I	G5I120
Asp (µg/mL)	2.54 ± 2.20	1.77 ± 1.80	2.47 ± 1.90	19362 ± 1481	20582 ± 1025	25183 ± 448	26852 ± 1221
Thr (µg/mL)	1.50 ± 0.90	5.52 ± 4.99	3.88 ± 3.57	74693 ± 12987	80569 ± 25226	106816 ± 5314	191526 ± 31632
Ser (µg/mL)	2.36 ± 2.07	3.80 ± 3.05	3.74 ± 3.32	31291 ± 1607	33006 ± 468	39796 ± 4286	58115 ± 3303
Glu (µg/mL)	407.92 ± 665.14	292.48 ± 474.12	239.31 ± 397.18	52431 ± 6774	56978 ± 892	75420 ± 14589	94519 ± 10150
Gly (µg/mL)	12.99 ± 0.69	9.90 ± 1.04	16.53 ± 6.03	16938 ± 1340	18001 ± 1517	22992 ± 490	30812 ± 2275
Ala (µg/mL)	6.23 ± 2.82	6.76 ± 3.82	6.16 ± 8.67	30844 ± 2952	31955 ± 2293	39923 ± 3864	57824 ± 6318
Cys (µg/mL)	33.77 ± 8.40	82.98 ± 20.41	96.58 ± 15.76	43708 ± 1731	45422 ± 3802	59281 ± 6515	93730 ± 6113
Val (µg/mL)	1.43 ± 1.36	235.93 ± 47.90	287.29 ± 13.62	40099 ± 5339	43000 ± 10287	57601 ± 4049	114118 ± 12876
Met (µg/mL)	0.00 ± 0.00	0.00 ± 0.00	0.00 ± 0.00	19179 ± 3683	22917 ± 13737	35337 ± 10386	66496 ± 9146
Ile (µg/mL)	0.57 ± 0.98	0.00 ± 0.00	0.00 ± 0.00	29971 ± 3704	28894 ± 5886	38521 ± 3826	70814 ± 4543
Leu (µg/mL)	0.71 ± 1.22	38.33 ± 17.00	46.37 ± 16.53	112186 ± 20858	129024 ± 69373	191154 ± 49562	366335 ± 44878
Tyr (µg/mL)	7.37 ± 8.42	268.32 ± 232.57	352.69 ± 27.69	117408 ± 15894	140768 ± 104342	230577 ± 99453	367461 ± 35489
Phe (µg/mL)	2.83 ± 2.86	357.80 ± 65.73	116.78 ± 10.10	86148 ± 3926	113684 ± 93937	183882 ± 93178	309689 ± 46778
His (µg/mL)	48.42 ± 1.45	482.42 ± 44.14	633.70 ± 65.61	67516 ± 11636	92652 ± 69664	113507 ± 66840	182699 ± 12001
Lys (µg/mL)	6.22 ± 3.14	3.18 ± 3.69	2.38 ± 4.12	154211 ± 20705	173895 ± 95556	283112 ± 104093	439939 ± 28689
Trp (µg/mL)	0.00 ± 0.00	0.00 ± 0.00	0.00 ± 0.00	69749 ± 28276	107852 ± 73218	95805 ± 40757	231088 ± 36346
Arg (µg/mL)	8.50 ± 1.14	6.98 ± 1.40	3.55 ± 3.37	110526 ± 18588	131017 ± 76297	212599 ± 78591	297044 ± 29537
Pro (µg/mL)	8.30 ± 11.82	30.12 ± 36.68	25.77 ± 22.44	7088 ± 4629	1599 ± 1926	6492 ± 5267	11232 ± 542
Total (mg/mL)	0.55 ± 0.71	1.83 ± 0.96	1.84 ± 0.60	1083 ± 166	1272 ± 649	1818 ± 592	3010 ± 322

Appendix C

Appendix C1: BCAAs (Leu, Ile and Val) concentration of the 0C:100W sample in the apical and basolateral side of the Ussing chamber experiment during 5, 30 and 60 min of intestinal digestion in the G1 and G5 emptied aliquot. Values are presented as means ± SD of two independent replicates.

		0C:100W			
G1		**Leu (µg/mL)**	**Ile (µg/mL)**	**Val (µg/mL)**	**BCAAs (µg/mL)**
	Intestinal digestion time				
Apical	5 min	94.62 ± 9.81	20.27 ± 2.77	26.39 ± 2.88	141.28 ± 15.45
	30 min	291.89 ± 14.01	74.47 ± 10.96	94.15 ± 2.57	460.51 ± 0.48
	60 min	396.04 ± 56.55	126.70 ± 14.50	140.10 ± 18.68	662.84 ± 89.73
	Total concentration	782.56 ± 80.36	221.44 ± 6.31	260.63 ± 18.99	1264.62 ± 105.66
Basolateral	5 min	0.64 ± 0.61	0.33 ± 0.33	0.47 ± 0.40	1.43 ± 1.35
	30 min	4.64 ± 4.62	2.06 ± 2.10	2.71 ± 2.53	9.42 ± 9.25
	60 min	12.62 ± 11.80	6.74 ± 4.81	7.73 ± 6.99	27.10 ± 23.60
	Total concentration	17.90 ± 17.04	9.13 ± 7.24	10.91 ± 9.92	37.95 ± 34.21
G5					
Apical	5 min	51.19 ± 8.27	16.33 ± 2.18	20.25 ± 3.48	87.77 ± 13.93
	30 min	65.79 ± 12.78	26.50 ± 7.39	27.57 ± 7.27	119.86 ± 27.43
	60 min	87.59 ± 13.96	43.84 ± 1.80	42.07 ± 5.33	173.51 ± 21.09
	Total concentration	204.57 ± 18.47	86.68 ± 7.01	89.89 ± 9.12	381.13 ± 34.59
Basolateral	5 min	0.41 ± 0.11	0.18 ± 0.02	0.28 ± 0.06	0.87 ± 0.19
	30 min	3.48 ± 0.60	1.90 ± 0.28	2.33 ± 0.03	7.70 ± 0.91
	60 min	8.77 ± 1.27	5.57 ± 2.66	5.67 ± 0.70	20.01 ± 4.63
	Total concentration	12.66 ± 1.98	7.64 ± 2.96	8.28 ± 0.79	28.58 ± 5.74

Appendix C2: BCAAs (Leu, Ile and Val) concentration of the 20C:80W sample in the apical and basolateral side of the Ussing chamber experiment during 5, 30 and 60 min of intestinal digestion in the G1 and G5 emptied aliquot. Values are presented as means ± SD of two independent replicates.

		20C:80W			
G1		Leu (µg/mL)	Ile (µg/mL)	Val (µg/mL)	BCAAs (µg/mL)
	Intestinal digestion time				
Apical	5 min	78.21 ± 36.49	14.79 ± 8.60	20.50 ± 11.45	113.50 ± 56.55
	30 min	217.43 ± 35.44	55.91 ± 9.45	67.81 ± 14.36	341.14 ± 59.26
	60 min	280.83 ± 95.81	82.73 ± 25.60	95.53 ± 30.08	459.09 ± 151.49
	Total concentration	576.46 ± 167.74	153.43 ± 43.66	183.84 ± 55.90	913.73 ± 267.29
Basolateral	5 min	0.49 ± 0.32	0.19 ± 0.13	0.28 ± 0.13	0.97 ± 0.59
	30 min	6.63 ± 1.79	3.34 ± 1.01	3.26 ± 0.20	13.24 ± 0.98
	60 min	16.17 ± 2.46	8.70 ± 2.79	8.80 ± 0.21	33.67 ± 0.12
	Total concentration	23.30 ± 4.58	12.24 ± 3.67	12.33 ± 0.54	47.87 ± 1.45
G5					
Apical	5 min	57.87 ± 0.90	20.17 ± 1.35	25.13 ± 2.57	103.17 ± 4.82
	30 min	80.55 ± 7.80	36.40 ± 5.50	39.84 ± 6.06	156.78 ± 19.36
	60 min	108.71 ± 3.90	53.30 ± 1.02	57.03 ± 5.88	219.04 ± 3.00
	Total concentration	247.12 ± 4.80	109.88 ± 7.86	121.99 ± 14.51	478.99 ± 27.18
Basolateral	5 min	0.52 ± 0.16	0.30 ± 0.07	0.36 ± 0.06	1.18 ± 0.30
	30 min	4.66 ± 0.19	2.11 ± 0.29	3.01 ± 0.51	9.78 ± 0.99
	60 min	12.95 ± 2.80	8.21 ± 0.94	8.50 ± 2.44	29.65 ± 4.30
	Total concentration	18.13 ± 2.83	10.61 ± 0.72	11.87 ± 2.88	40.61 ± 5.00

Appendix C3: BCAAs (Leu, Ile and Val) concentration of the 50C:50W sample in the apical and basolateral side of the Ussing chamber experiment during 5, 30 and 60 min of intestinal digestion in the G1 and G5 emptied aliquot. Values are presented as means ± SD of two independent replicates.

50C:50W

G1		Leu (µg/mL)	Ile (µg/mL)	Val (µg/mL)	BCAAs (µg/mL)
	Intestinal digestion time				
	5 min	87.58 ± 6.26	18.33 ± 2.58	24.82 ± 1.12	130.73 ± 9.96
Apical	30 min	168.28 ± 82.02	47.66 ± 17.63	57.82 ± 24.37	273.75 ± 124.02
	60 min	257.15 ± 17.46	87.38 ± 16.78	101.28 ± 19.77	445.82 ± 54.01
	Total concentration	513.01 ± 70.81	153.37 ± 3.44	183.92 ± 5.72	850.30 ± 79.97
	5 min	0.40 ± 0.09	0.18 ± 0.06	0.29 ± 0.09	0.88 ± 0.23
Basolateral	30 min	4.99 ± 1.22	2.23 ± 0.21	3.02 ± 0.14	10.24 ± 1.57
	60 min	13.15 ± 0.27	6.27 ± 0.62	8.71 ± 0.68	28.13 ± 1.03
	Total concentration	18.53 ± 1.40	8.68 ± 0.46	12.03 ± 0.62	39.25 ± 0.31
G5					
	5 min	115.10 ± 31.52	19.10 ± 6.47	25.50 ± 6.20	159.70 ± 44.20
Apical	30 min	214.06 ± 16.98	50.09 ± 15.24	68.76 ± 12.33	332.92 ± 44.55
	60 min	301.24 ± 31.02	86.83 ± 30.58	105.71 ± 29.08	493.77 ± 90.69
	Total concentration	630.40 ± 16.48	156.02 ± 39.35	199.97 ± 35.20	986.39 ± 91.04
	5 min	0.65 ± 0.03	0.26 ± 0.08	0.40 ± 0.13	1.31 ± 0.19
Basolateral	30 min	6.09 ± 2.09	2.33 ± 0.14	3.35 ± 0.16	11.77 ± 2.39
	60 min	16.78 ± 4.50	6.53 ± 0.93	9.93 ± 0.07	33.25 ± 3.64
	Total concentration	23.52 ± 6.62	9.12 ± 0.87	13.69 ± 0.10	46.33 ± 5.84

Appendix C4: BCAAs (Leu, Ile and Val) concentration of the 80C:20W sample in the apical and basolateral side of the Ussing chamber experiment during 5, 30 and 60 min of intestinal digestion in the G1 and G5 emptied aliquot. Values are presented as means ± SD of two independent replicates.

	80C:20W			
G1	Leu (µg/mL)	Ile (µg/mL)	Val (µg/mL)	BCAAs (µg/mL)
Intestinal digestion time				
Apical 5 min	90.44 ± 1.88	17.19 ± 4.44	21.04 ± 0.92	128.68 ± 3.48
30 min	155.09 ± 23.22	42.86 ± 10.29	53.63 ± 11.54	251.57 ± 45.05
60 min	210.30 ± 33.22	65.83 ± 11.35	82.58 ± 15.56	358.71 ± 60.13
Total concentration	455.83 ± 54.56	125.88 ± 26.08	157.25 ± 28.02	738.95 ± 108.67
Basolateral 5 min	0.66 ± 0.05	0.42 ± 0.18	0.48 ± 0.08	1.57 ± 0.31
30 min	5.11 ± 2.50	2.66 ± 0.03	2.93 ± 1.14	10.70 ± 3.66
60 min	11.72 ± 4.93	5.01 ± 2.28	7.48 ± 3.28	24.21 ± 10.49
Total concentration	17.49 ± 7.38	8.09 ± 2.13	10.89 ± 4.34	36.47 ± 13.84
G5				
Apical 5 min	111.09 ± 7.53	12.26 ± 0.40	18.37 ± 1.91	141.73 ± 9.05
30 min	233.24 ± 5.73	45.99 ± 6.83	63.77 ± 2.07	343.01 ± 10.49
60 min	368.72 ± 9.88	81.82 ± 3.97	114.58 ± 0.03	565.12 ± 13.88
Total concentration	713.06 ± 23.13	140.08 ± 10.41	196.72 ± 0.13	1049.86 ± 33.41
Basolateral 5 min	0.69 ± 0.08	0.32 ± 0.04	0.44 ± 0.08	1.45 ± 0.20
30 min	7.20 ± 0.73	2.97 ± 0.60	4.14 ± 0.77	14.31 ± 2.10
60 min	18.25 ± 2.01	7.42 ± 1.30	10.59 ± 2.07	36.26 ± 5.39
Total concentration	26.14 ± 2.82	10.72 ± 1.94	15.16 ± 2.91	52.01 ± 7.68

Appendix C5: BCAAs (Leu, Ile and Val) concentration of the (0C:100W)2% sample in the apical and basolateral side of the Ussing chamber experiment during 5, 30 and 60 min of intestinal digestion in the G1 and G5 emptied aliquot. Values are presented as means ± SD of two independent replicates.

(0C:100W)2%				
G1	Leu (µg/mL)	Ile (µg/mL)	Val (µg/mL)	BCAAs (µg/mL)
Intestinal digestion time				
5 min	96.49 ± 3.85	23.83 ± 2.24	28.46 ± 3.73	148.77 ± 9.82
30 min	245.65 ± 5.81	63.12 ± 1.06	81.07 ± 1.64	389.85 ± 3.10
Apical 60 min	291.74 ± 33.99	93.24 ± 19.87	104.93 ± 17.88	489.90 ± 71.74
Total concentration	633.88 ± 24.33	180.19 ± 18.70	214.45 ± 15.79	1028.52 ± 58.82
5 min	0.32 ± 0.06	0.15 ± 0.02	0.22 ± 0.02	0.69 ± 0.10
30 min	6.62 ± 2.04	4.16 ± 2.43	3.74 ± 0.90	14.53 ± 5.37
Basolateral 60 min	15.94 ± 1.18	7.18 ± 0.01	9.29 ± 1.12	32.42 ± 2.29
Total concentration	22.89 ± 3.16	11.50 ± 2.40	13.25 ± 2.00	47.64 ± 7.56
G5				
5 min	143.89 ± 156.33	32.74 ± 31.40	46.21 ± 45.46	222.84 ± 233.19
30 min	95.28 ± 22.69	38.05 ± 8.69	39.96 ± 6.70	173.29 ± 38.07
Apical 60 min	87.69 ± 42.03	37.41 ± 16.79	38.32 ± 20.14	163.42 ± 78.96
Total concentration	326.86 ± 221.05	108.20 ± 56.87	124.49 ± 72.31	559.55 ± 350.23
5 min	2.74 ± 3.45	1.17 ± 1.43	1.50 ± 1.78	5.41 ± 6.67
30 min	4.62 ± 2.19	2.94 ± 1.68	2.61 ± 0.81	10.17 ± 4.67
Basolateral 60 min	8.67 ± 1.06	6.32 ± 2.65	5.95 ± 0.64	20.94 ± 4.36
Total concentration	16.03 ± 6.70	10.43 ± 5.76	10.06 ± 3.23	36.53 ± 15.69

Appendix C6: BCAAs (Leu, Ile and Val) concentration of the (20C:80W)2% sample in the apical and basolateral side of the Ussing chamber experiment during 5, 30 and 60 min of intestinal digestion in the G1 and G5 emptied aliquot. Values are presented as means ± SD of two independent replicates.

G1	(20C:80W)2%			
	Leu (µg/mL)	Ile (µg/mL)	Val (µg/mL)	BCAAs (µg/mL)
Intestinal digestion time				
Apical				
5 min	87.16 ± 1.41	17.49 ± 2.15	22.61 ± 0.41	127.25 ± 3.96
30 min	223.22 ± 6.49	59.55 ± 4.60	76.94 ± 2.15	359.72 ± 0.26
60 min	268.57 ± 23.96	97.39 ± 2.99	111.88 ± 3.84	477.84 ± 23.11
Total concentration	578.95 ± 29.05	174.43 ± 3.76	211.43 ± 6.40	964.81 ± 18.89
Basolateral				
5 min	0.34 ± 0.14	0.16 ± 0.02	0.22 ± 0.02	0.73 ± 0.18
30 min	6.52 ± 3.78	3.96 ± 2.99	3.49 ± 1.82	13.97 ± 8.59
60 min	17.04 ± 8.41	6.86 ± 3.29	9.89 ± 5.85	33.79 ± 17.55
Total concentration	23.91 ± 12.33	10.98 ± 6.31	13.61 ± 7.69	48.50 ± 26.32
G5				
Apical				
5 min	46.61 ± 0.19	16.43 ± 2.24	14.18 ± 5.85	77.22 ± 3.80
30 min	64.01 ± 15.13	27.10 ± 4.27	28.40 ± 4.02	119.51 ± 23.41
60 min	91.94 ± 12.24	45.01 ± 3.37	43.08 ± 2.64	180.03 ± 18.25
Total concentration	202.55 ± 27.56	88.54 ± 5.40	85.66 ± 12.50	376.75 ± 45.45
Basolateral				
5 min	0.23 ± 0.01	0.13 ± 0.02	0.18 ± 0.03	0.54 ± 0.06
30 min	4.01 ± 1.00	1.64 ± 0.04	2.29 ± 0.04	7.94 ± 1.08
60 min	9.56 ± 1.08	4.56 ± 0.32	5.73 ± 0.45	19.85 ± 0.96
Total concentration	13.80 ± 2.09	6.32 ± 0.38	8.20 ± 0.37	28.32 ± 2.10

Appendix C7: BCAAs (Leu, Ile and Val) concentration of the (50C:50W)2% sample in the apical and basolateral side of the Ussing chamber experiment during 5, 30 and 60 min of intestinal digestion in the G1 and G5 emptied aliquot. Values are presented as means ± SD of two independent replicates.

G1	(50C:50W)2%			
	Leu (µg/mL)	Ile (µg/mL)	Val (µg/mL)	BCAAs (µg/mL)
Intestinal digestion time				
Apical				
5 min	66.57 ± 4.77	13.71 ± 2.76	16.58 ± 1.30	96.86 ± 8.84
30 min	189.64 ± 7.59	53.96 ± 1.51	68.90 ± 1.15	312.51 ± 10.25
60 min	230.52 ± 18.80	81.15 ± 3.37	94.27 ± 4.44	405.94 ± 26.61
Total concentration	486.73 ± 21.62	148.82 ± 2.11	179.75 ± 4.29	815.31 ± 28.02
Basolateral				
5 min	0.45 ± 0.28	0.24 ± 0.14	0.34 ± 0.20	1.03 ± 0.62
30 min	5.82 ± 2.23	2.68 ± 1.05	3.84 ± 1.64	12.34 ± 4.91
60 min	14.37 ± 1.29	7.38 ± 0.77	10.16 ± 2.44	31.91 ± 4.51
Total concentration	20.64 ± 3.80	10.29 ± 1.96	14.34 ± 4.29	45.28 ± 10.04
G5				
Apical				
5 min	83.24 ± 24.10	17.06 ± 4.89	20.92 ± 8.48	121.21 ± 37.47
30 min	173.16 ± 13.56	47.77 ± 4.53	58.89 ± 4.80	279.82 ± 22.89
60 min	207.23 ± 20.68	73.93 ± 6.36	84.93 ± 8.92	366.08 ± 35.96
Total concentration	463.62 ± 58.34	138.76 ± 15.78	164.73 ± 22.20	767.12 ± 96.31
Basolateral				
5 min	0.38 ± 0.10	0.19 ± 0.03	0.29 ± 0.04	0.86 ± 0.18
30 min	4.41 ± 1.78	2.18 ± 0.72	2.83 ± 0.76	9.43 ± 3.26
60 min	12.05 ± 6.16	7.21 ± 0.65	7.82 ± 1.88	27.07 ± 7.39
Total concentration	16.84 ± 8.05	9.58 ± 0.10	10.94 ± 2.68	37.36 ± 10.83

Appendix C8: BCAAs (Leu, Ile and Val) concentration of the (80C:20W)2% sample in the apical and basolateral side of the Ussing chamber experiment during 5, 30 and 60 min of intestinal digestion in the G1 and G5 emptied aliquot. Values are presented as means ± SD of two independent replicates.

		(80C:20W)2%			
G1		**Leu (µg/mL)**	**Ile (µg/mL)**	**Val (µg/mL)**	**BCAAs (µg/mL)**
	Intestinal digestion time				
Apical	5 min	51.96 ± 6.02	15.56 ± 0.24	16.68 ± 2.74	84.20 ± 9.00
	30 min	94.91 ± 3.02	34.43 ± 3.93	39.65 ± 2.98	168.98 ± 3.90
	60 min	122.21 ± 11.29	48.75 ± 6.58	59.22 ± 8.47	230.17 ± 26.33
	Total concentration	269.08 ± 2.25	98.74 ± 10.27	115.54 ± 8.71	483.36 ± 21.23
Basolateral	5 min	0.17 ± 0.03	0.10 ± 0.01	0.16 ± 0.01	0.43 ± 0.05
	30 min	2.88 ± 1.70	1.27 ± 0.42	1.81 ± 0.59	5.96 ± 2.72
	60 min	7.59 ± 3.33	3.50 ± 1.05	5.22 ± 1.30	16.30 ± 5.69
	Total concentration	10.64 ± 5.06	4.87 ± 1.48	7.18 ± 1.91	22.69 ± 8.46
G5					
Apical	5 min	104.77 ± 9.98	15.81 ± 2.09	22.35 ± 3.59	142.93 ± 11.48
	30 min	227.06 ± 15.36	58.45 ± 2.12	74.59 ± 1.64	360.10 ± 14.88
	60 min	284.44 ± 17.22	89.57 ± 0.15	105.69 ± 5.16	479.70 ± 12.22
	Total concentration	616.26 ± 42.56	163.82 ± 4.05	202.63 ± 0.08	982.72 ± 38.59
Basolateral	5 min	0.45 ± 0.28	0.18 ± 0.07	0.25 ± 0.07	0.87 ± 0.43
	30 min	6.42 ± 2.72	3.00 ± 0.99	3.23 ± 0.20	12.66 ± 1.93
	60 min	15.14 ± 5.43	8.58 ± 2.48	8.65 ± 0.00	32.38 ± 2.95
	Total concentration	22.01 ± 8.43	11.76 ± 3.40	12.13 ± 0.27	45.90 ± 5.30

Appendix C9: BCAAs (Leu, Ile and Val) concentration of the (50C:50W)4% sample in the apical and basolateral side of the Ussing chamber experiment during 5, 30 and 60 min of intestinal digestion in the G1 and G5 emptied aliquot. Values are presented as means ± SD of two independent replicates.

G1	(50C:50W)4%			
	Leu (µg/mL)	Ile (µg/mL)	Val (µg/mL)	BCAAs (µg/mL)
Intestinal digestion time				
Apical				
5 min	72.00 ± 9.52	16.19 ± 3.75	19.07 ± 3.34	107.27 ± 16.61
30 min	164.15 ± 3.81	46.98 ± 8.67	62.00 ± 6.21	273.14 ± 18.69
60 min	216.79 ± 8.28	75.18 ± 0.28	86.69 ± 2.00	378.66 ± 10.01
Total concentration	452.95 ± 5.04	138.36 ± 12.69	167.76 ± 7.55	759.07 ± 25.29
Basolateral				
5 min	0.37 ± 0.12	0.18 ± 0.06	0.24 ± 0.03	0.79 ± 0.22
30 min	4.69 ± 1.55	2.91 ± 1.57	2.84 ± 0.53	10.44 ± 3.65
60 min	12.06 ± 3.39	9.87 ± 0.80	7.99 ± 0.69	29.92 ± 4.88
Total concentration	17.12 ± 5.06	12.96 ± 2.44	11.08 ± 1.25	41.15 ± 8.74
G5				
Apical				
5 min	81.54 ± 4.76	15.33 ± 3.68	18.16 ± 3.65	115.03 ± 12.08
30 min	168.94 ± 9.28	43.72 ± 11.18	55.95 ± 11.44	268.61 ± 31.90
60 min	196.43 ± 17.75	60.76 ± 3.37	70.20 ± 1.92	327.38 ± 23.04
Total concentration	446.91 ± 3.71	119.81 ± 11.49	144.31 ± 13.16	711.02 ± 20.94
Basolateral				
5 min	0.27 ± 0.09	0.14 ± 0.05	0.19 ± 0.03	0.60 ± 0.17
30 min	4.45 ± 1.18	1.95 ± 0.23	2.74 ± 0.39	9.14 ± 1.80
60 min	11.33 ± 1.86	6.96 ± 2.55	7.42 ± 0.22	25.71 ± 0.46
Total concentration	16.05 ± 3.13	9.05 ± 2.27	10.35 ± 0.64	35.45 ± 1.51

Appendix C10: BCAAs (Leu, Ile and Val) concentration of the (50C:50W)8% sample in the apical and basolateral side of the Ussing chamber experiment during 5, 30 and 60 min of intestinal digestion in the G1 and G5 emptied aliquot. Values are presented as means ± SD of two independent replicates.

G1	(50C:50W)8%			
	Leu (µg/mL)	Ile (µg/mL)	Val (µg/mL)	BCAAs (µg/mL)
Intestinal digestion time				
Apical				
5 min	72.37 ± 7.46	15.07 ± 5.92	18.00 ± 3.02	105.43 ± 16.40
30 min	165.14 ± 1.19	51.46 ± 9.27	60.75 ± 11.77	277.35 ± 19.85
60 min	217.82 ± 11.68	80.73 ± 19.51	86.42 ± 15.85	384.98 ± 47.04
Total concentration	455.33 ± 17.95	147.26 ± 34.69	165.17 ± 30.65	767.76 ± 83.29
Basolateral				
5 min	0.64 ± 0.33	0.33 ± 0.16	0.43 ± 0.16	1.40 ± 0.65
30 min	5.39 ± 2.09	2.54 ± 0.81	3.31 ± 0.76	11.25 ± 3.66
60 min	12.25 ± 2.19	7.89 ± 2.48	8.27 ± 0.29	28.41 ± 0.01
Total concentration	18.28 ± 4.62	10.76 ± 1.52	12.01 ± 1.21	41.05 ± 4.31
G5				
Apical				
5 min	54.60 ± 27.90	11.20 ± 9.08	12.43 ± 8.81	78.23 ± 45.80
30 min	126.34 ± 15.82	38.29 ± 0.97	46.00 ± 0.14	210.63 ± 14.99
60 min	170.96 ± 0.16	60.55 ± 7.11	65.75 ± 12.28	297.26 ± 19.23
Total concentration	351.90 ± 11.92	110.04 ± 17.16	124.18 ± 20.95	586.12 ± 50.03
Basolateral				
5 min	0.42 ± 0.03	0.21 ± 0.01	0.26 ± 0.01	0.89 ± 0.05
30 min	4.82 ± 0.41	3.01 ± 1.58	3.05 ± 0.58	10.89 ± 2.58
60 min	11.12 ± 1.31	5.08 ± 0.83	7.58 ± 1.82	23.78 ± 3.96
Total concentration	16.37 ± 1.69	8.30 ± 2.41	10.90 ± 2.39	35.56 ± 6.49
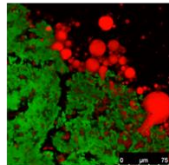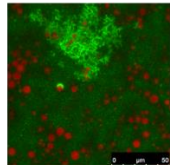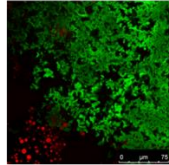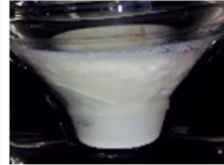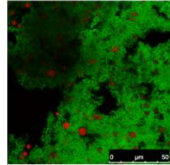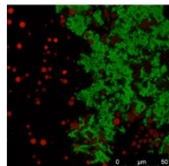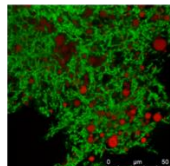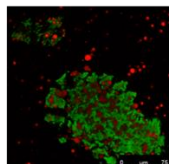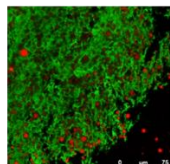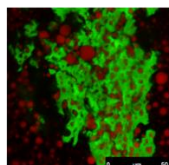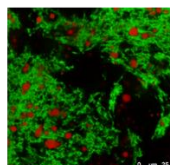
Appendix D

Change in pH of milk samples during gastric digestion in the semi-dynamic model corresponding to each gastric emptying (GE) aliquot with pepsin (closed dots) and without pepsin (open dots) addition. The time represents an approximation of the actual values displayed in Table 4.3. The pH values are referred to the basal stage (before gastric digestion), initial (t=0 min, milk sample including oral phase and basal volumes). Each data point corresponds to one determination.
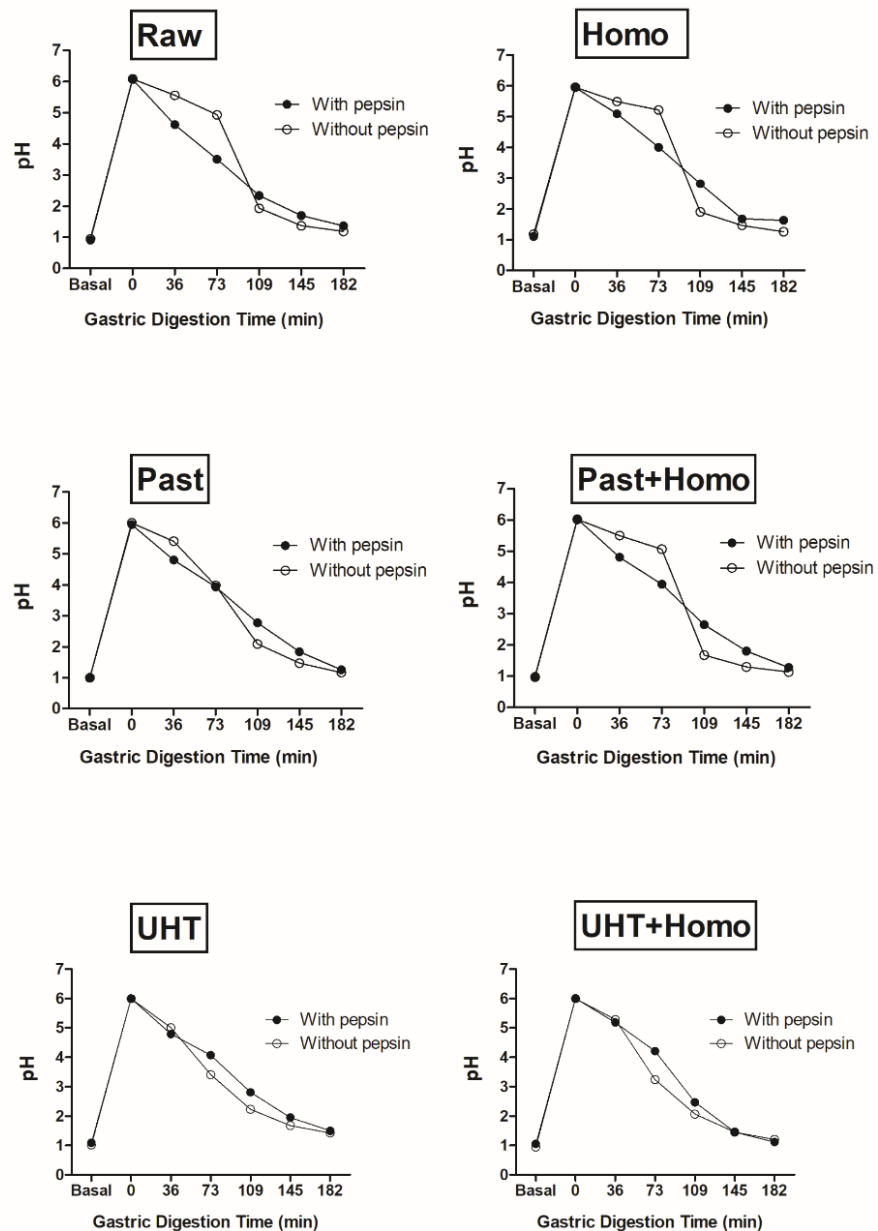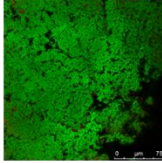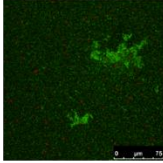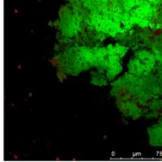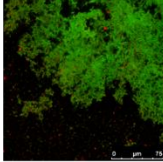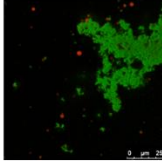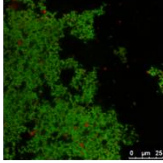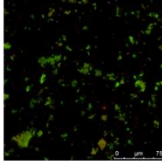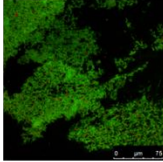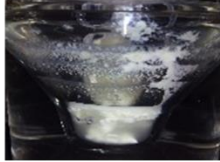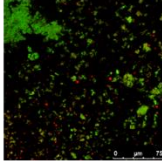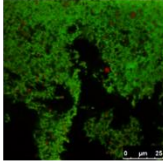
Appendix E
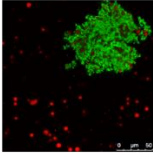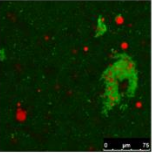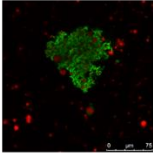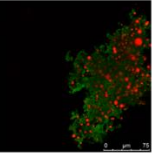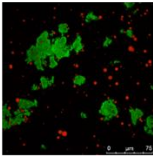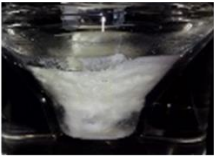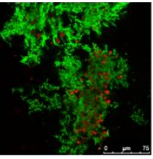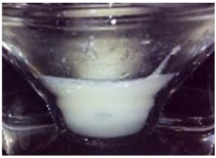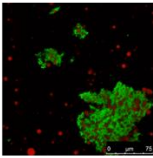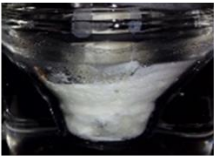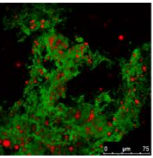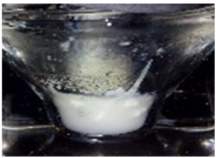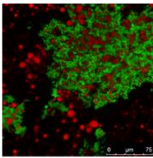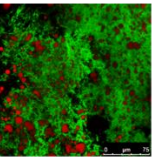
Appendix E1: Behaviour of the Raw sample with and without the addition of pepsin solution during the simulated gastric digestion. The images correspond to the behaviour in the stomach model right before the emptying, and examples of confocal microscopy images of the emptied aliquots in each gastric emptying (GE) point. The average of GE time was 36 min (GE1), 73 min (GE2), 109 min (GE3), 145 min (GE4) and 182 min (GE5). Red shows the lipid and green shows the protein.

Gastric digestion time	Raw with pepsin		Raw without pepsin	
	Gastric behaviour before emptying	Microstructure of emptied sample	Gastric behaviour before emptying	Microstructure of emptied sample
36 min				
73 min				
109 min				
145 min				
182 min				

Appendix E2: Behaviour of the Homo sample with and without the addition of pepsin solution during the simulated gastric digestion. The images correspond to the behaviour in the stomach model right before the emptying, and examples of confocal microscopy images of the emptied aliquots in each gastric emptying (GE) point. The average of GE time was 36 min (GE1), 73 min (GE2), 109 min (GE3), 145 min (GE4) and 182 min (GE5). Red shows the lipid and green shows the protein.
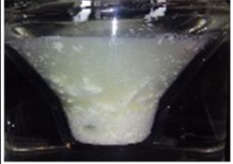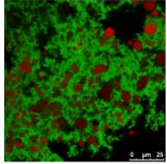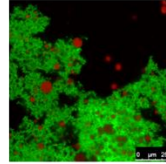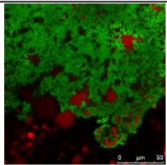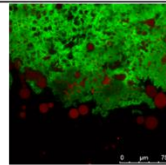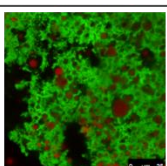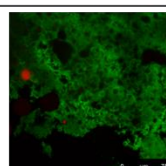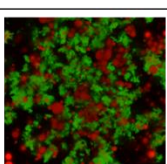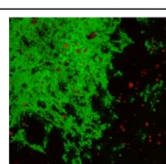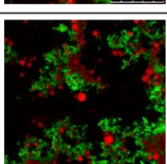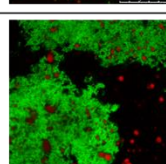
Gastric digestion time	Homo with pepsin		Homo without pepsin	
	Gastric behaviour before emptying	Microstructure of emptied sample	Gastric behaviour before emptying	Microstructure of emptied sample
36 min				
73 min				
109 min				
145 min				
182 min				

311

Appendix E3: Behaviour of the Past sample with and without the addition of pepsin solution during the simulated gastric digestion. The images correspond to the behaviour in the stomach model right before the emptying, and examples of confocal microscopy images of the emptied aliquots in each gastric emptying (GE) point. The average of GE time was 36 min (GE1), 73 min (GE2), 109 min (GE3), 145 min (GE4) and 182 min (GE5). Red shows the lipid and green shows the protein.
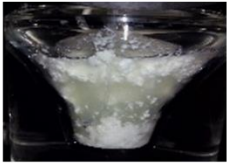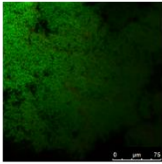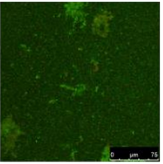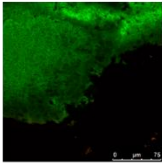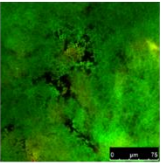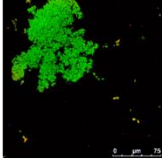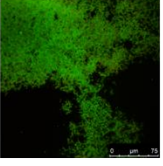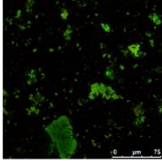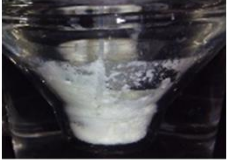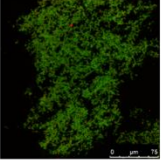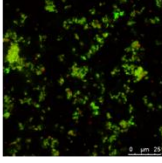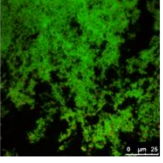
Gastric digestion time	Past with pepsin		Past without pepsin	
	Gastric behaviour before emptying	Microstructure of emptied sample	Gastric behaviour before emptying	Microstructure of emptied sample
36 min				
73 min				
109 min				
145 min				
182 min				
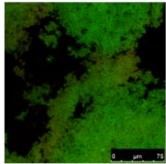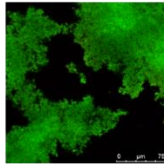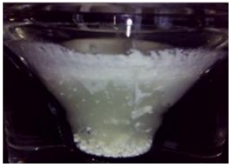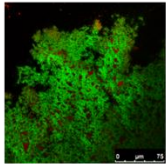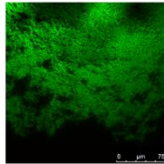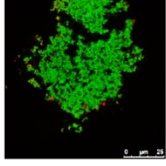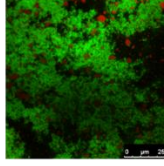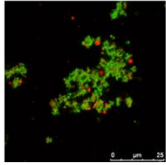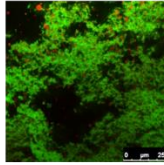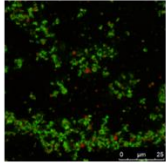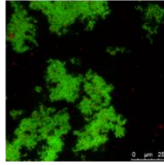
Appendix E4: Behaviour of the UHT sample with and without the addition of pepsin solution during the simulated gastric digestion. The images correspond to the behaviour in the stomach model right before the emptying, and examples of confocal microscopy images of the emptied aliquots in each gastric emptying (GE) point. The average of GE time was 36 min (GE1), 73 min (GE2), 109 min (GE3), 145 min (GE4) and 182 min (GE5). Red shows the lipid and green shows the protein.

Gastric digestion time	UHT with pepsin		UHT without pepsin	
	Gastric behaviour before emptying	Microstructure of emptied sample	Gastric behaviour before emptying	Microstructure of emptied sample
36 min				
73 min				
109 min				
145 min				
182 min				

Appendix E5: Behaviour of the Past+Homo sample with and without the addition of pepsin solution during the simulated gastric digestion. The images correspond to the behaviour in the stomach model right before the emptying, and examples of confocal microscopy images of the emptied aliquots in each gastric emptying (GE) point. The average of GE time was 36 min (GE1), 73 min (GE2), 109 min (GE3), 145 min (GE4) and 182 min (GE5). Red shows the lipid and green shows the protein.

Gastric digestion time	Past+Homo with pepsin		Past+Homo without pepsin	
	Gastric behaviour before emptying	Microstructure of emptied sample	Gastric behaviour before emptying	Microstructure of emptied sample
36 min				
73 min				
109 min				
145 min				
182 min				

Appendix E6: Behaviour of the UHT+Homo sample with and without the addition of pepsin solution during the simulated gastric digestion. The images correspond to the behaviour in the stomach model right before the emptying, and examples of confocal microscopy images of the emptied aliquots in each gastric emptying (GE) point. The average of GE time was 36 min (GE1), 73 min (GE2), 109 min (GE3), 145 min (GE4) and 182 min (GE5). Red shows the lipid and green shows the protein

Gastric digestion time	UHT+Homo with pepsin		UHT+Homo without pepsin	
	Gastric behaviour before emptying	Microstructure of emptied sample	Gastric behaviour before emptying	Microstructure of emptied sample
36 min				
73 min				
109 min				
145 min				
182 min				

Appendix F

Appendix F1: The lipid content (% w/w) of initial (before digestion) and the gastric emptying points (GE1-GE5) in digestion with pepsin (black bar) and without pepsin (grey bar) for all milk samples. Each data point is the representation of one measurement. The values were corrected for the different gastric dilution in each point.
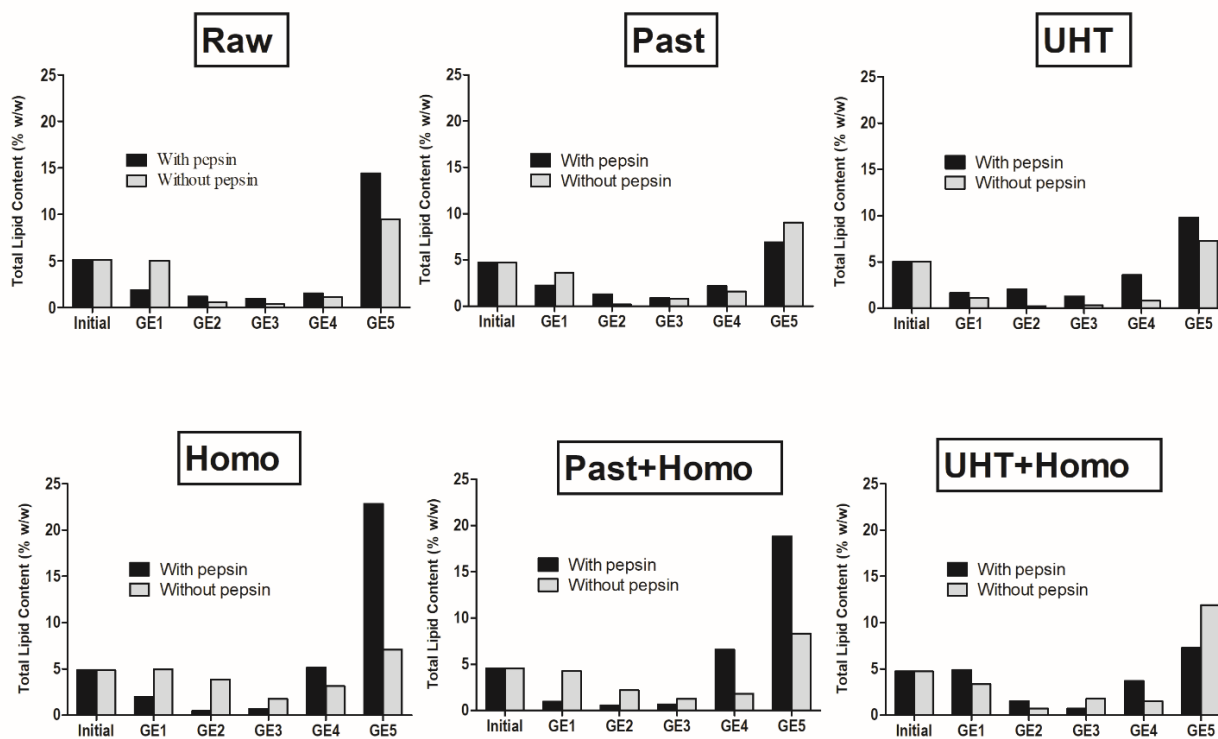
Appendix F2: The protein content (% w/w) of initial (before digestion) and the gastric emptying points (GE1-GE5) in digestion with pepsin (black bar) and without pepsin (grey bar) for all milk samples. Each data point is the representation of one measurement. The values were corrected for the different gastric dilution in each point.
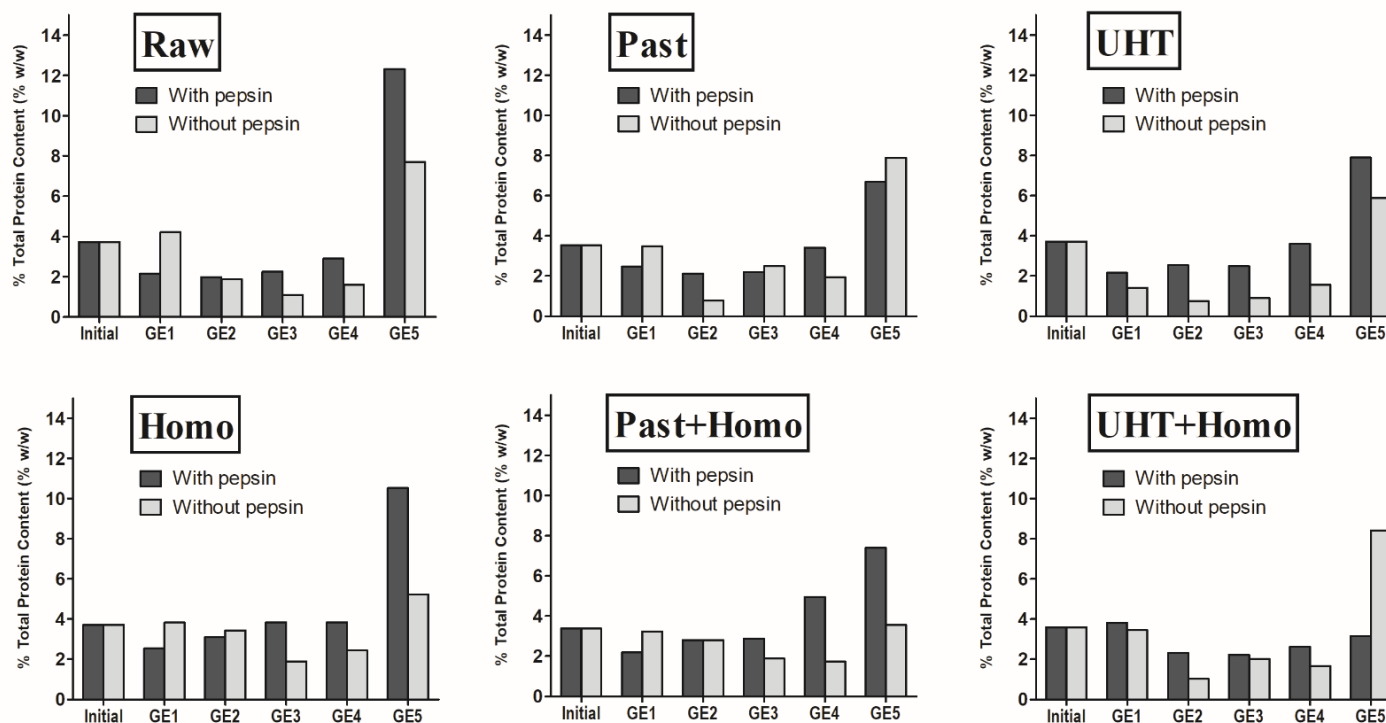
Appendix G

Appendix G1: SDS-PAGE (under reducing conditions) of the Raw sample with and without the inclusion of pepsin at initial (I) referred to before digestion and the gastric emptying points (GE1-GE5), and a molecular weight marker. The samples are labelled in the figure accordingly. The protein content in each sample was 0.1% w/w.
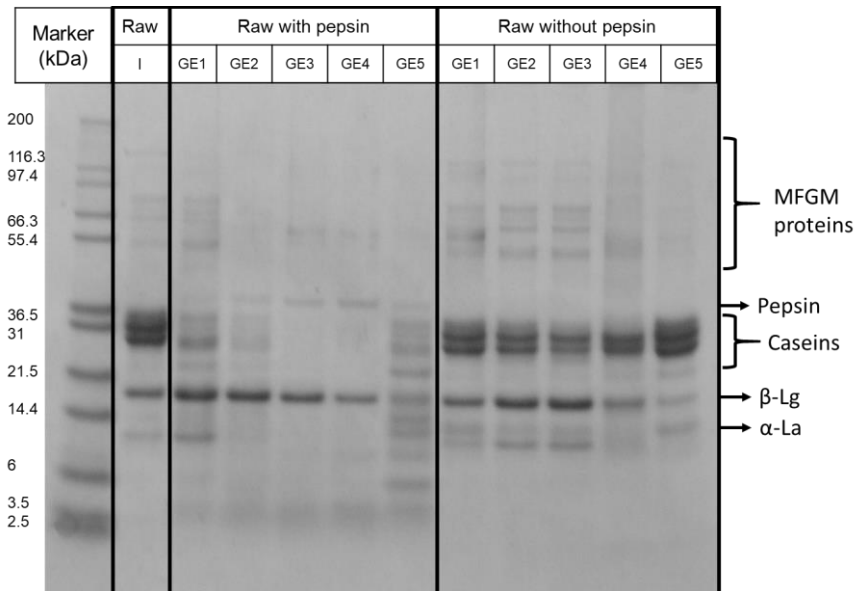
Appendix G2: SDS-PAGE (under reducing conditions) of the Homo sample with and without the inclusion of pepsin at initial (I) referred to before digestion and the gastric emptying points (GE1-GE5), and a molecular weight marker. The samples are labelled in the figure accordingly. The protein content in each sample was 0.1% w/w.

318
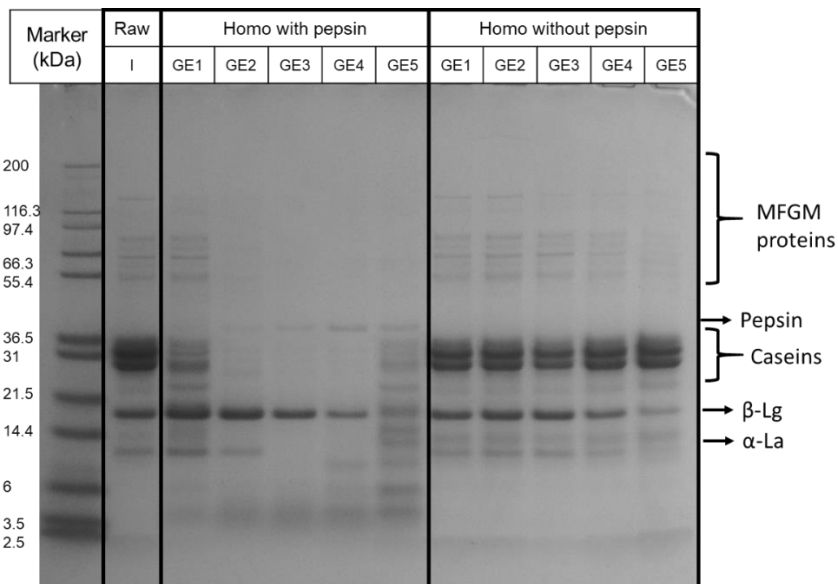
Appendix G3: SDS-PAGE (under reducing conditions) of the Past sample with and without the inclusion of pepsin at initial (I) referred to before digestion and the gastric emptying points (GE1-GE5), and a molecular weight marker. The samples are labelled in the figure accordingly. The protein content in each sample was 0.1% w/w.
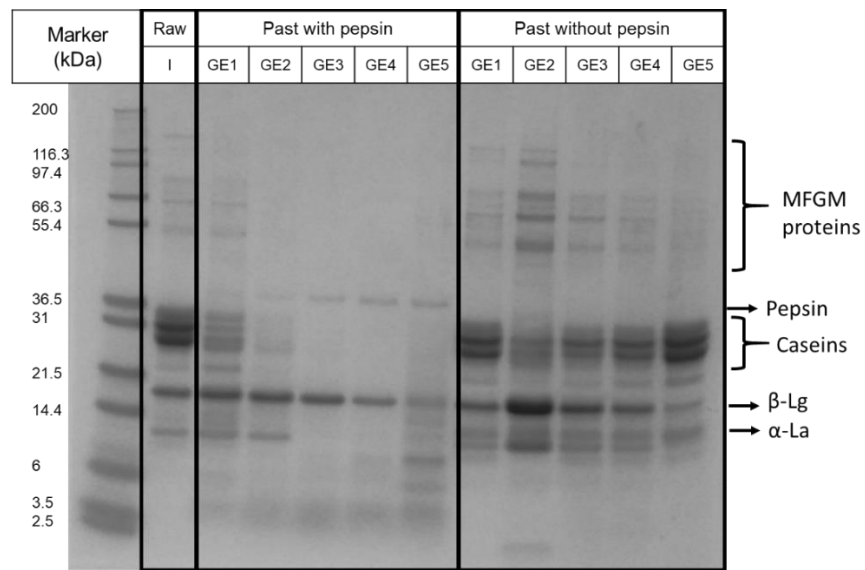
Appendix G4: SDS-PAGE (under reducing conditions) of the Past+Homo sample with and without the inclusion of pepsin at initial (I) referred to before digestion and the gastric emptying points (GE1-GE5), and a molecular weight marker. The samples are labelled in the figure accordingly. The protein content in each sample was 0.1% w/w.
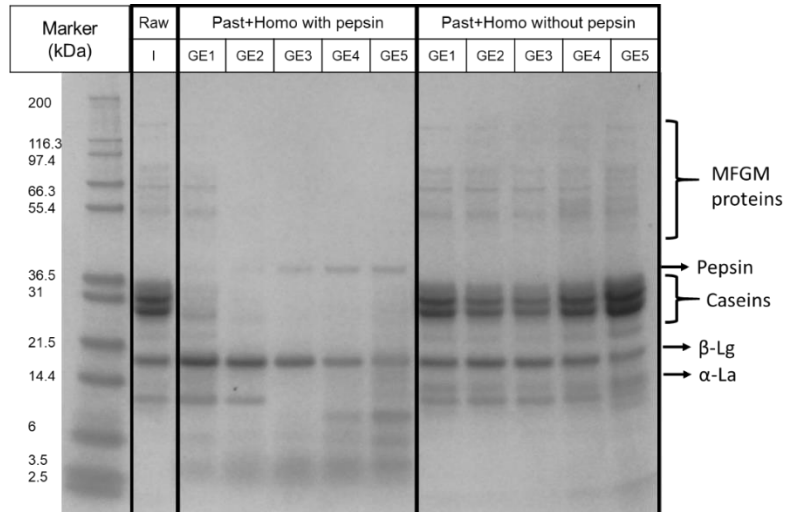
Appendix G5: SDS-PAGE (under reducing conditions) of the UHT sample with and without the inclusion of pepsin at initial (I) referred to before digestion and the gastric emptying points (GE1-GE5), and a molecular weight marker. The samples are labelled in the figure accordingly. The protein content in each sample was 0.1% w/w.
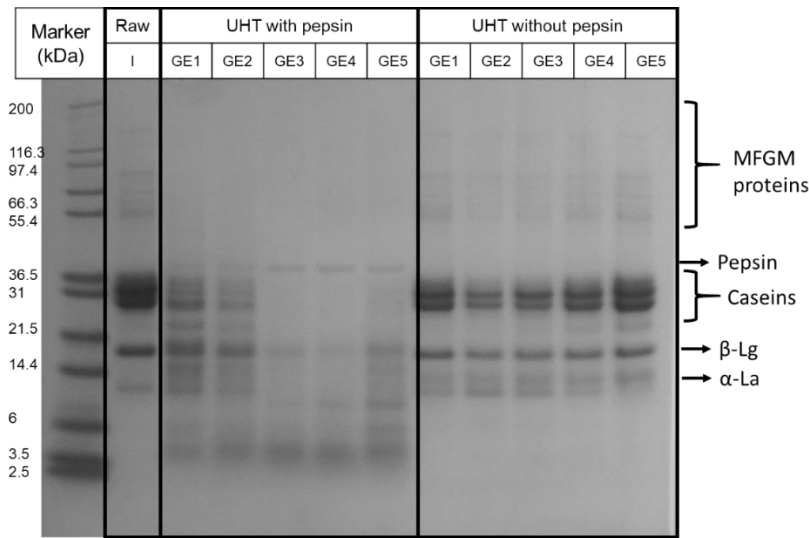
Appendix G6: SDS-PAGE (under reducing conditions) of the UHT+Homo sample with and without the inclusion of pepsin at initial (I) referred to before digestion and the gastric emptying points (GE1-GE5), and a molecular weight marker. The samples are labelled in the figure accordingly. The protein content in each sample was 0.1% w/w.
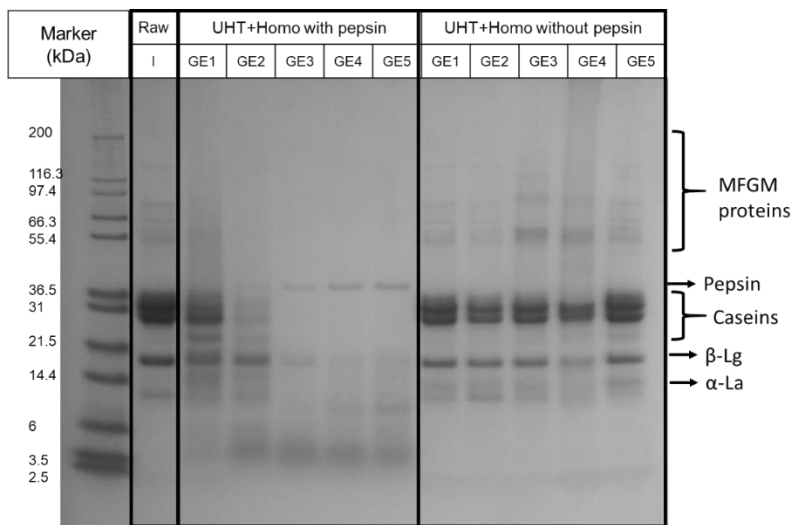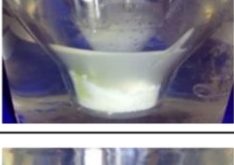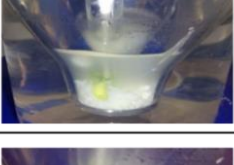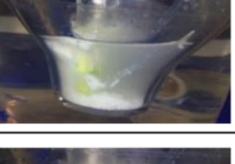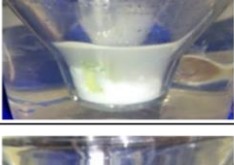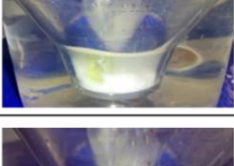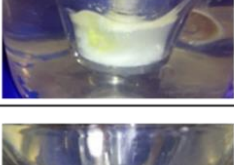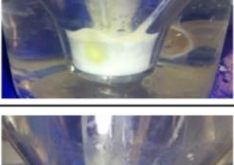
Appendix H

Amount of protein and lipid determined in all the samples at the digesta separated in A) serum and B) coagulum after 36 min of gastric digestion.
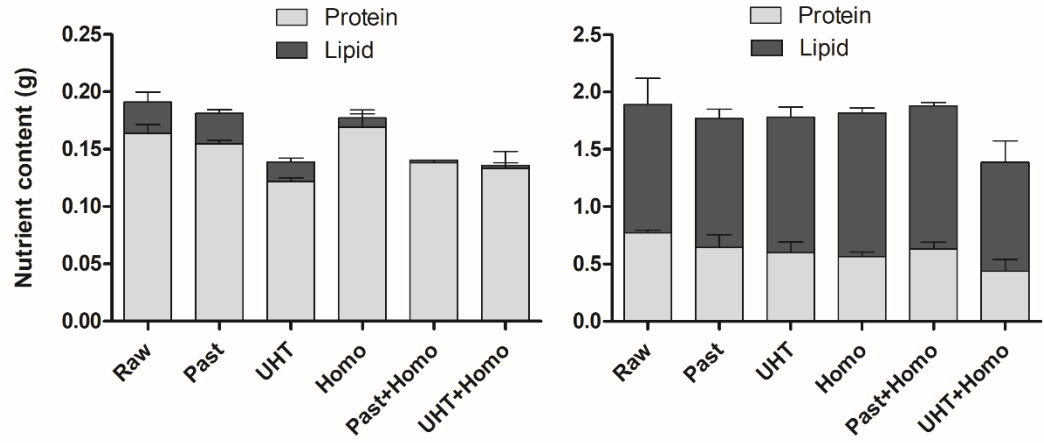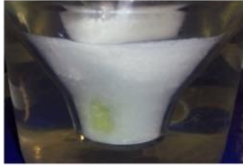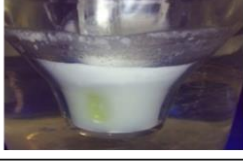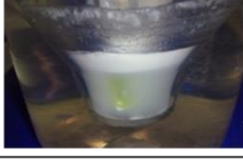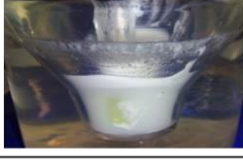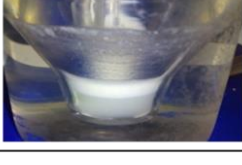
Appendix I

Appendix I1: Gastric behaviour of Semi-Solid sample at the different gastric digestion time points, using pepsin and gastric lipase, pepsin and no enzyme. The images were taken just before the emptying. Note: the yellow block corresponds to the pH probe.

GE time (min)	With Pepsin+ Lipase	With Pepsin	Without enzyme
5.9			
29			
50			
69.9			
89.5			
110.3			
131.9			
150.8			
171.4			

Appendix I2: Gastric behaviour of Liquid sample at the different gastric digestion time points, using pepsin and gastric lipase, pepsin and no enzyme. The images were taken just before the emptying. Note: the yellow block corresponds to the pH probe

GE time (min)	With Pepsin+ Lipase	With Pepsin	Without enzyme
7.1			
29.7			
50.1			
70.0			
89.4			
111.1			
132.4			
152.0			
171.8			

Appendix J

Profile of free fatty acids released from Liquid (A, C, E) and Semi-Solid (B, D, F) samples after 1 min (A, B), 30 min (C, D) and 60 min (E, F) of intestinal digestion. Data point represents means (n=3 for each meal) of mass percentage.